Reliability-Based Design of A Retaining Wall

by

JOHN SANG KIM

Dissertation submitted to the Faculty of the
Virginia Polytechnic Institute and State University
in partial fulfillment of the requirements for the degree of
Doctor of Philosophy in Civil Engineering

submitted to Advisory Committee

J. M. DUNCAN

R. A. HELLER

J. R. MARTIN

T. M. MURRAY

R. M. BARKER, Chair

CHARLES E. VIA, JR., DEPARTMENT OF CIVIL ENGINEERING
VIRGINIA POLYTECHNIC INSTITUTE AND STATE UNIVERSITY
BLACKSBURG, VA

April, 1995

Reliability-Based Design of A Retaining Wall

John S. Kim

Chairman: **Richard M. Barker**

Civil Engineering

(ABSTRACT)

A retaining wall is subject to various limit states such as sliding, overturning and bearing capacity, and it can fail by any one of them. Since a great deal of uncertainty is involved in the analysis of the limit states, the use of deterministic conventional safety factors may produce a misleading result.

The main objective of this study is to develop a procedure for the optimum design of a retaining wall by using the reliability theory. Typical gravity retaining walls with four different heights were selected in this study. The walls were designed first to satisfy the conventional design criteria, and later the safety indices inherent in the walls were computed by using Advanced First Order Second Moment method. With the safety indices the probabilities of failure for the three limit states were calculated and the probabilistically optimized design could be achieved by using the probability of failure. The influence of the coefficient of variation on the probability of failure was investigated. The ratios of base width to wall height which lead to the optimum design were obtained through a parametric study.

Acknowledgment

Sometimes it seems to be very hard to express my gratitude in a few words. When the language is not my mother tongue, it becomes twice harder. But, I will do my best.

First of all, a thousand thanks should be extended to Dr. R. M. Barker, who is not only my academic advisor but also the mentor of my life. Through the experience of working with him on a number of projects as well as the dissertation, I was enabled to broaden my knowledge and perspectives. The patience, honesty, humbleness and care that he has shown to me are beyond description. If someone asks me to show a Christian who lives up to what he says, I would not hesitate any more.

I would also like to express a special thanks to Dr. J. M. Duncan. Owing to his excellent lectures on foundation design and the experience of working with him on the NCHRP Project 24-4, I have a great confidence in the bridge substructure design that I have been involved at Virginia Department of Transportation since 1994. I also appreciate him for that he never fails to greet to his students.

I owe many thanks to Dr. R. A. Heller, who enabled me to open my eyes on the reliability theory with his wonderful lecture and helpful advice on the research. I still remember one of his jokes on the NORMAL distribution. I have been trying to figure out how the HELLER distribution would look like.

A special thanks should go to Dr. J. R. Martin for his willing mind to serve as a committee member when I had to substitute one of the members. I still remember his graduation speech that he made on his hooding ceremony at Burruss Hall, quoting from

the book, "All I need to know..., I learned them in the kindergarten." For some reason, one of the quotes that he made never disappear from my memory.

"Clean up your own mess." Well, I am trying harder than ever.

Before Virginia Tech sent me the admission letter, University of Oklahoma was one of a few graduate schools that issued early admission. I drove up to Oklahoma state from California to see Dr. T. M. Murray who used to be a professor in that institute. Due to schedule conflict, I could not meet him. A few weeks later, I came to VA Tech, and about one year later, Dr. Murray joined me at Tech.....hmm, to become one of my committee members (?). I am speechless, Dr. Murray.

I want to include Mrs. Ann Crate and Mrs. Mary R. McDonald in my list of giving thanks. Their heart-warming friendship made my staying at Civil Engineering department more pleasant and comfortable.

Part of the study was sponsored by Federal Highway Administration under the contract NCHRP Project 24-4. I appreciate co-workers, Dr. C. K. Tan, Dr. P. Ooi and Mr. R. J. Chen for their useful discussion and encouragement.

I want to thank my church members and K.C.C.C members who always encouraged me with their care and consistent prayer. I also want to deeply thank my parents for their sacrificial love and undying passion for their son's education. I would like to express my best gratitude to my wife, Eunice and my son, Jonathan. Without their long-suffering patience and unending support, I would not have finished this work.

Finally, I want to dedicate all of this to my Lord, Jesus Christ, who died and rose for me.

Table of Contents

CHAPTER 4 SAFETY INDEX OF CONVENTIONAL DESIGN

List of Figures

List of Tables

List of Notations

B	Base width
c	Cohesion
C	Cost of construction
CF	Cost of failure
d	Depth of
D_f	Footing depth
d_i	Depth factors in bearing capacity equation
e	Eccentricity
H	Height of wall
I_i	Inclination factors in bearing capacity equation
K_a	Earth pressure coefficient
N	Resultant of force
n	Ratio of height of resultant to wall height
N_i	Bearing capacity factors
P_a	Resultant of earth pressure
q	Inclination angle of the load
Q_{ult}	Ultimate bearing capacity force
q_{ult}	Ultimate bearing capacity pressure
R	Resistances
S	Loads
S.F.	Safety factor
S_i	Shape factors in bearing capacity equation

List of Notations (continued)

t	Width of top of wall
vol.	Volume of concrete mass
W_c	Weight of the concrete mass
x-bar	Distance of resultant measured from toe
x_o	Distance of resultant measured from toe
α	Cosine direction used in Advanced FOSM method
β	Safety index
δ_f	Friction angle between base and foundation soil
ϕ	Internal friction angle of backfill soil
ϕ_f	Internal frinction angle of foundation soil
γ	Unit weight of backfill soil
γ_c	Unit weight of concrete
μ	Coefficient of friction between base and foundation soil
μ_i	Mean values
σ_i	Standard deviation

Chapter 1
INTRODUCTION

1.1 GENERAL

A retaining wall is used to hold back an earth embankment or water in order to maintain an abrupt change in elevation. An abutment is a particular type of retaining wall which supports the end of a bridge superstructure.

A retaining wall and an abutment can be considered virtually the same in function and behavior. Some have said an abutment is nothing more than a retaining wall with a vertical load on top. When a retaining wall or an abutment is designed to resist the loads from an earth embankment or bridge superstructure, reaction pressures are developed across its foundation. The safety of the wall is determined by the capability of the foundation to resist these reaction forces. When a wall is founded on a spread footing on soil or rock, the bearing capacity and sliding resistance of the foundation materials and overturning stability must be determined. When a wall is supported on piles or drilled shafts, the axial and lateral load capacities must be determined.

The current design practices for abutments and retaining walls are reviewed in Chapter 2. This chapter presents a general overview of current design methods, earth pressure estimation, stability criteria, design procedures and other design considerations.

To provide background information and direction for the study, a questionnaire was developed and distributed to the departments of transportation of the fifty states and the District of Columbia. Its purpose was to gather information on bridge abutments and retaining wall that had experienced unsatisfactory performance. A similar survey was conducted forty-eight years ago by Peck et al (1948). Chapter 3 provides the detailed survey result and comparison with the former survey.

In the conventional design method, a safety factor has been used to measure the safety margin of a structure. However, the reliability-based design method invented a new terminology called 'safety index'. In the reliability theory, the safety index is used to estimate the probability of failure. The procedure to find the safety indices inherent in the conventional design criteria is illustrated in Chapter 4.

The traditional design optimization usually implies that the wall is designed to minimize the initial construction cost while satisfying the design criteria. Since the conventional design method does not directly consider the randomness of design parameters, the current optimization concept may be misleading. A true optimization in the long term may be obtained by considering not only the initial cost but also the cost of failure which can be estimated by the reliability method. Chapter 5 presents the detailed procedures on the optimized design and provides examples.

A parametric study has been performed to find the ratio of base width to wall height (B/H) which produces the probabilistically optimized design. Chapter 6 discusses on the procedure and the result in detail. Finally Chapter 7 concludes this study and provide a suggestion for the future study.

Chapter 2
LITERATURE REVIEW AND DESIGN CONSIDERATIONS

2.1 GENERAL

The current design practices for abutments and retaining walls are reviewed in this chapter. Types of retaining walls and abutments and the selection procedures are discussed. This chapter also presents a general overview of current design methods, estimation of earth pressures, stability criteria, design procedures, and other design considerations.

2.2 TYPES OF RETAINING WALLS AND ABUTMENTS

Retaining walls and abutments have many different types for various design needs. This section discusses several types of retaining walls and abutments, and a number of considerations for selecting the most suitable type of retaining walls or abutments.

2.2.1 Types of Retaining Walls

Retaining walls can be classified into two major categories: conventional retaining walls and alternative (or innovative) retaining walls. The conventional walls, such as gravity type of walls and reinforced concrete walls, have a long history of successful use. However, several different types of innovative walls have been developed during the last two decades and are used as alternatives for the conventional walls.

The conventional retaining walls can be subdivided to two principal types: gravity walls and cantilever walls. Gravity walls, as shown in Figure 2.1a, rely on the mass of wall to resist the retained earth and water behind the wall. Cantilever walls, as shown in Figure 2.1b, resist the forces exerted on them by flexural strength. When the wall is so high that cantilever walls are not economical, a counterfort or a buttressed reinforced concrete wall, as shown in Figures 2.1c and 2.1d, can be used.

A number of different types of alternative retaining walls have been developed in recent years. Munfakh (1990) classifies the alternative retaining walls into two major categories: walls retaining fill and walls supporting excavations. The first

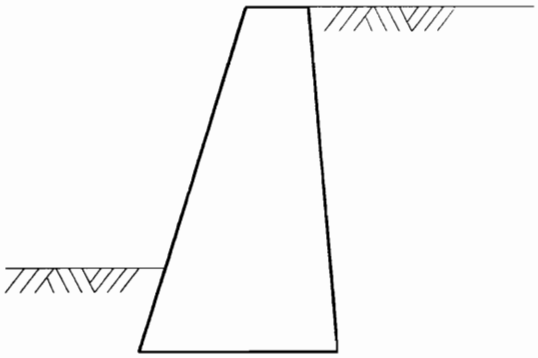

(a) Gravity Wall

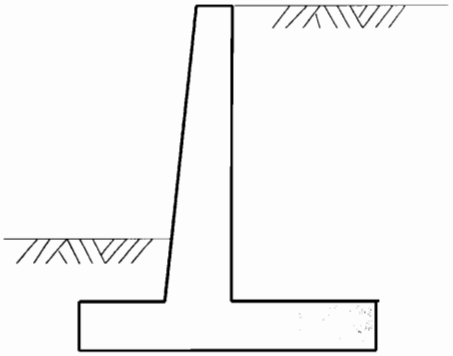

(b) Cantilever Wall

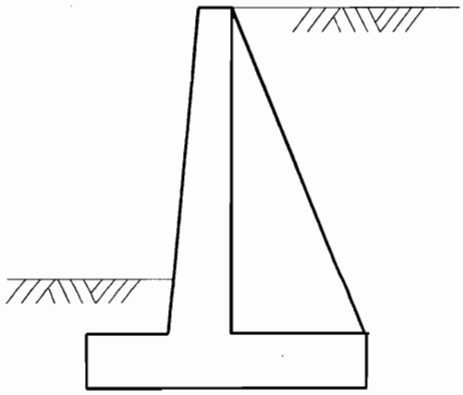

(c) Counterfort Wall

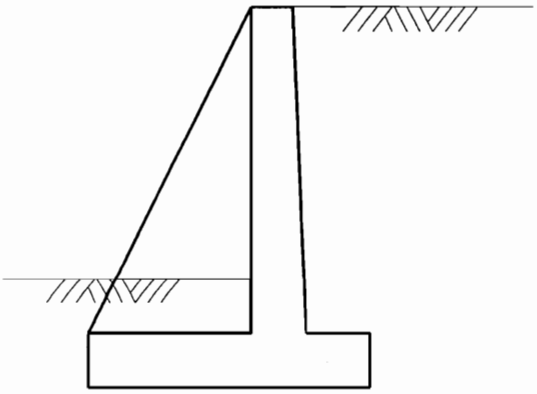

(d) Buttress Wall

Figure 2.1 Typical Gravity, Cantilever, Counterfort and Buttress Wall

category of alternative walls includes embankment-type mechanically stabilized walls (e.g., VSL retained earth, geotextile walls, geogrid walls, and welded wire walls) and modular gravity walls (e.g., criblock walls, Doublewals, gabion walls, and Evergreen walls). Some of the mechanically stabilized earth walls and a precast concrete modular gravity wall are illustrated in Figure 2.2. The second category of alternative walls are those that support excavations (e.g., soil nailing, reticulated micro piles, soil doweling, sheet piles, soldier piles, secant piles, and drilled shaft walls).

2.2.2 Types of Abutments

The 15th edition of the AASHTO bridge specifications (1992) divides abutments into four types: stub abutments, partial depth abutments, full depth abutments, and integral abutments. Peck et al (1974) classify bridge abutments in a different way: gravity abutments, U-abutments, Spill-through abutments, and pile-bent abutments. A gravity abutment with wing walls (Figure 2.3a) is an abutment which consists of a bridge seat, wingwalls, backwall, and footing. A U-abutment (Figure 2.3b) is an abutment whose wingwalls are perpendicular to the bridge seat. The spill-through abutment (Figure 2.3c) consists of a beam which supports the bridge seat, two or more columns supporting the beam, and a footing supporting

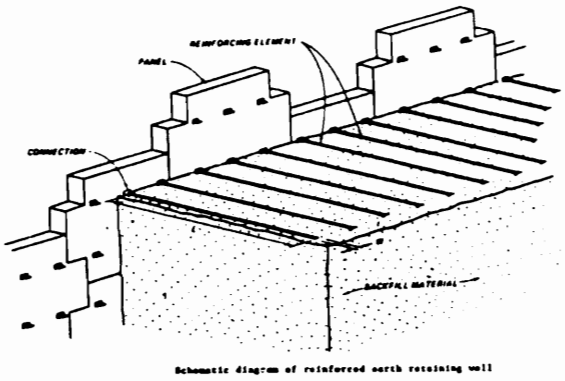

Schematic diagram of reinforced earth retaining wall

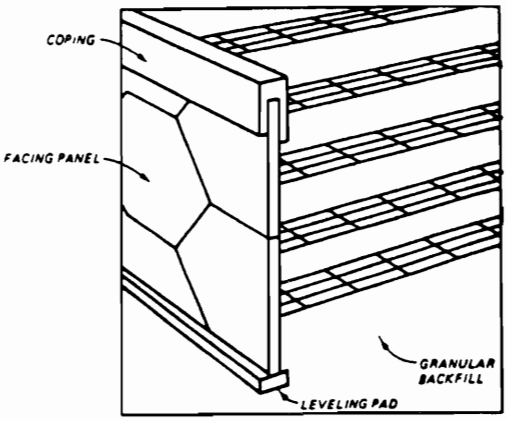

VSL retained earth retaining wall (adapted from VSL Corporation 1984)

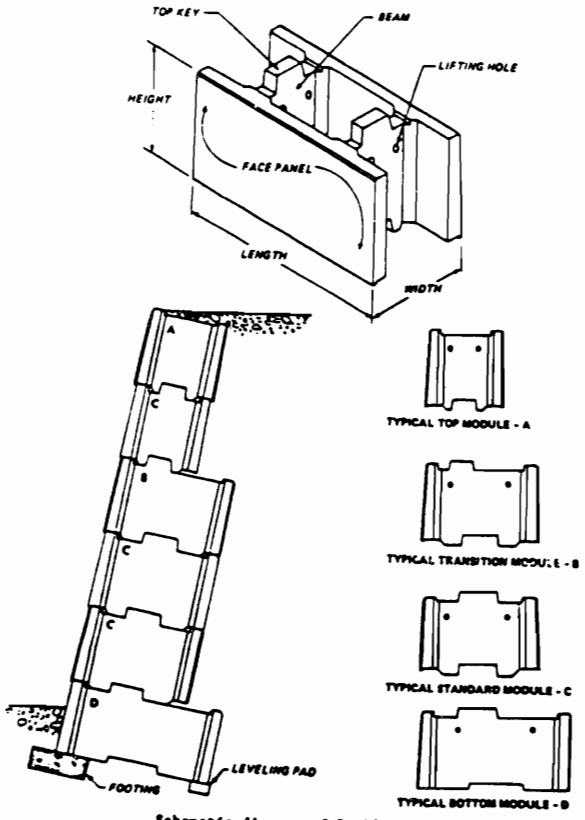

Schematic diagram of Doublewal retaining wall (after Doublewal Corporation 1984)

Figure 2.2 Mechanically Stabilized Earth Walls and Concrete Modular Wall (From Corps of Engineers, 1989)

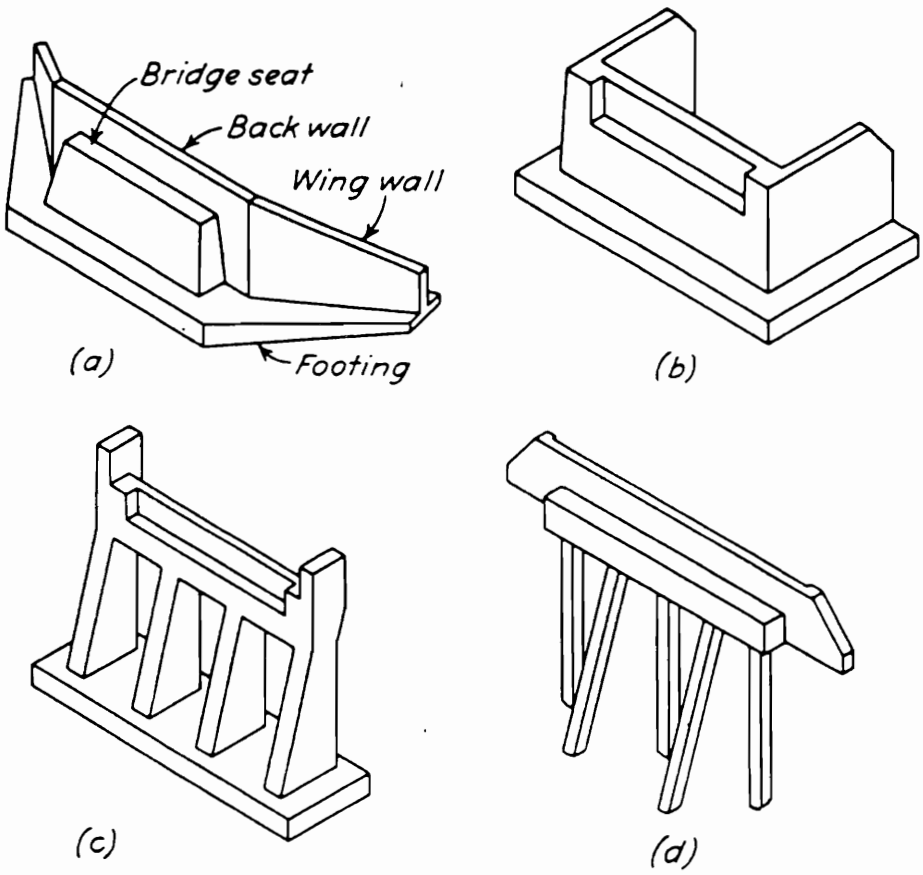

(*a*) Typical gravity abutment with wing walls. (*b*) U abutment. (*c*) Spill-through abutment. (*d*) Pile-bent abutment with stub wings.

Figure 2.3 Various Types of Abutments (From Peck et al, 1974)

the columns. The columns are embedded up to the bottom of the beam in the fill which extends on its natural slope in front of the abutment. The pile-bent abutment with stub wings (Figure 2.3d) is another type of spill-through abutment, in which a row of driven piles supports the beam.

2.2.3 Selection of Retaining Walls and Abutments

Selection of the most suitable type of retaining wall or abutment should be based on a number of considerations, including:

1. Construction and maintenance cost
2. Cut or fill earthwork situation
3. Traffic maintenance during construction
4. Construction period
5. Safety of construction workers
6. Availability and cost of backfill material
7. Superstructure depth
8. Size of wall
9. Horizontal and vertical alignment changes
10. Area of excavation
11. Aesthetics and similarity to adjacent structures
12. Previous experience with the type of wall or abutment being considered
13. Ease of access for inspection and maintenance
14. Anticipated life, loading conditions and acceptability of deformations.

Munfakh (1990) and Schnore (1990) have discussed the advantages and disadvantages of various types of walls and abutments. They present decision matrices which include many of the above factors. These tables can be very helpful in selecting the proper wall or abutment for particular site conditions.

2.3 OVERVIEW OF CURRENT DESIGN METHODS

The last three decades have seen a trend away from Allowable Stress Design (ASD) that incorporates factors of safety, and toward strength design methods that incorporate limit states and reliability concepts. Examples of strength design procedures are Load Factor Design (LFD), and Load and Resistance Factor Design (LRFD). The 15th edition of the AASHTO bridge specifications makes use of LFD as an alternative method for the design of superstructures. In 1994, AASHTO released a new specifications which incorporate the LRFD method for foundation design, so that engineers may use the same philosophy for design of foundations that is used for the superstructure.

2.3.1 Limit States

If retaining walls and abutments fail to satisfy their intended design functions, they are considered to reach "limit states". Limit states can be categorized into two types: Ultimate or Strength Limit States and Serviceability Limit States.

Ultimate Limit States

A retaining wall reaches an ultimate limit state when the strength of at least one of its components is fully mobilized or when the structure becomes unstable. In this ultimate limit state a retaining wall may experience serious distress and structural damage, both local and global. In addition, various failure modes in the soil that supports the wall can also be identified. These are also called ultimate limit states; they include bearing capacity failure, sliding, overturning, and overall instability.

Serviceability Limit States

A retaining wall experiences a serviceability limit state when it fails to perform its intended design function fully, due to excessive deformation or deterioration. Serviceability limit states include excessive total or differential settlement, lateral movement, fatigue, vibration, and cracking.

2.3.2 Design Methods

Allowable Stress Design (ASD)

Allowable Stress Design is a method which ensures safety by restricting values of stress obtained from elastic analysis to values that are not larger than some allowable values. Values of allowable stress are generally selected as some function of the yield strength of a material, and are determined by dividing the yield strength by a global factor of safety.

Since the ASD method uses deterministic values for loads and resistances, the random nature of the loads and resistances are not accounted for explicitly. The ASD method therefore does not consider the different degree of uncertainty for different types of loads; live load is treated the same as dead load, even though it usually has greater variation during the life of the structure and greater uncertainty. Another shortcoming of the ASD method is its inability to account rationally for uncertainties in the strengths of materials and the ultimate resistances of structural components.

Load Factor Design (LFD)

Load Factor Design is a strength design or limit state design method. Unlike ASD, this method takes into account the random nature of loads and resistances, and different levels of uncertainty for different types of load.

The design loads are obtained by multiplying the normally expected values, called "nominal" loads, by load factors typically larger than unity. The design strengths or resistances are calculated by multiplying nominal strengths by resistance factors, which have values smaller than unity. For an acceptable design, the factored resistance has to be greater than or equal to the strength demand resulting from the factored design loads for a particular limit state. A mathematical statement of LFD is given as:

$$\phi R_n \geq \text{Effect of } \sum \gamma_i Q_i \qquad (2.1)$$

where ϕ = performance factor,

R_n = nominal resistance,

γ_i = load factor for load component i,

Q_i = load component i.

In LFD the values of the load and performance factors are based on semi-quantitative considerations of probabilities, judgment, and previous experience with other design methods

Load and Resistance Factor Design (LRFD)

Load and Resistance Factor Design is also a strength design method and has the same design format as LFD (Eq. 2.1). However, the manner in which load and resistance factors are derived is different. LRFD formally utilizes reliability theory. Loads and resistances are considered as random variables, and are represented by their means and standard deviations. The load and resistance factors used in LRFD depend upon the value of the safety index, which is directly related to probability of failure. The safety index is chosen such that the probability of failure of a structure or foundation is small. Probability density functions for load and resistance are illustrated in Figure 2.4, and the relationship between safety index and probability of failure is presented Figure 2.5.

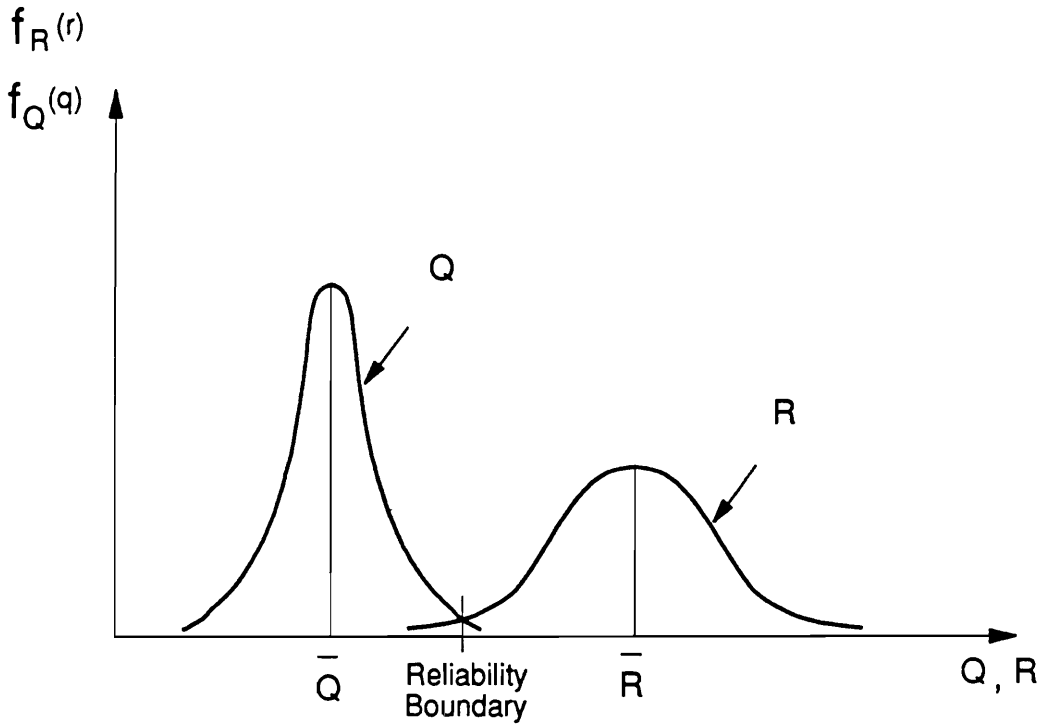

where

Q : Load

R : Resistance

$\bar{Q}$: Mean of Load

$\bar{R}$: Mean of Resistance

Figure 2.4 Probability Density Functions for Load and Resistance

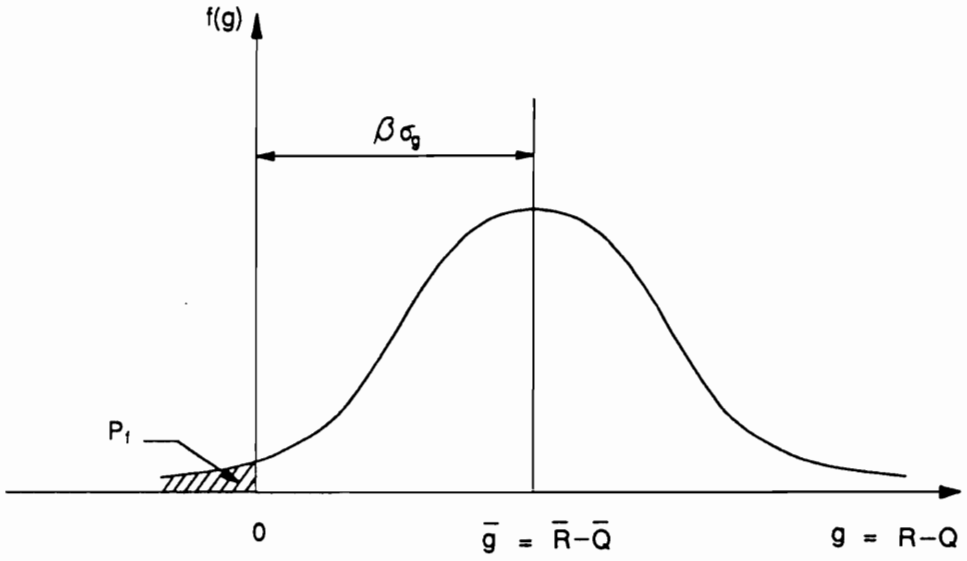

where

Q : Load

R : Resistance

$\bar{Q}$: Mean of Load

$\bar{R}$: Mean of Resistance

P_f: Probability of Failure

σ_g: Standard Deviation of g = $\sqrt{\sigma_R^2 + \sigma_Q^2}$

β: Safety Index = $\dfrac{\bar{g}}{\sigma_g}$

Figure 2.5 Definition of Safety Index

2.3.3 Safety Factors, Load Factors and Performance Factors

Safety Factors

In ASD, a global safety factor is used to ensure safety of a structure or foundation. Table 2.1 gives typical values of safety factors used in geotechnical engineering.

Load Factors

Load factors are applied to the loads to account for the uncertainties involved in the process of selecting loads and load effects. The load factors used in the 15th edition of the AASHTO bridge specifications (1992) are shown in Table 2.2.

Performance Factors

Performance factors are used to reduce various types of resistance to account for uncertainties in structural properties, soil properties, variability in workmanship, and inaccuracies in the design equations used to estimate the capacity. These factors are used for design at the ultimate limit state. Suggested values of performance factors for shallow foundations, for driven piles, and for drilled shafts are listed in Tables 2.3 to 2.5.

Table 2.1 Typical Safety Factors in Foundation Design
(After Meyerhof, 1984)

Failure Type	Item	Safety Factor *
Shearing	Earthworks	1.3 to 1.5
	Earth Retaining	
	Structures, Excavations	1.5 to 2.0
	Foundations	2.0 to 3.0
Seepage	Uplift, Heave	1.5 to 2.0
	Exit gradient, Piping	2.0 to 3.0

* The lower values are used when uncertainty in design is small and consequences of failure are minor; higher values are used when uncertainty in design is large and consequences of failure are major.

Table 2.2 Load Factors and Load Combinations of AASHTO Bridge Specifications (AASHTO, 1992)

Col. No.		1	2	3	3A	4	5	6	7	8	9	10	11	12	13	14	
			β FACTORS														
GROUP		γ	D	$(L+I)_n$	$(L+I)_p$	CF	E	B	SF	W	WL	LF	R+S+T	EQ	ICE	%	
SERVICE LOAD	I	1.0	1	1	0	1	β_E	1	1	0	0	0	0	0	0	100	
	IA	1.0	1	2	0	0	0	0	0	0	0	0	0	0	0	150	
	IB	1.0	1	0	1	1	β_E	1	1	0	0	0	0	0	0	**	
	II	1.0	1	0	0	0	1	1	1	1	0	0	0	0	0	125	
	III	1.0	1	1	0	1	β_E	1	1	0.3	1	1	0	0	0	125	
	IV	1.0	1	1	0	1	β_E	1	1	0	0	0	1	0	0	125	
	V	1.0	1	0	0	0	1	1	1	1	0	0	1	0	0	140	
	VI	1.0	1	1	0	1	β_E	1	1	0.3	1	1	1	0	0	140	
	VII	1.0	1	0	0	0	1	1	1	0	0	0	0	1	0	133	
	VIII	1.0	1	1	0	1	1	1	1	0	0	0	0	0	1	140	
	IX	1.0	1	0	0	0	1	1	1	1	0	0	0	0	1	150	
	X	1.0	1	1	0	0	β_E	0	0	0	0	0	0	0	0	100	Culvert
LOAD FACTOR DESIGN	I	1.3	β_D	1.67*	0	1.0	β_E	1	1	0	0	D	0	0	0		
	IA	1.3	β_D	2.20	0	0	0	0	0	0	0	0	0	0	0		
	IB	1.3	β_D	0	1	1.0	β_E	1	1	0	0	0	0	0	0		
	II	1.3	β_D	0	0	0	β_E	1	1	1	0	0	0	0	0		
	III	1.3	β_D	1	0	1	β_E	1	1	0.3	1	1	0	0	0		
	IV	1.3	β_D	1	0	1	β_E	1	1	0	0	0	1	0	0		
	V	1.25	β_D	0	0	0	β_E	1	1	1	0	0	1	0	0		
	VI	1.25	β_D	1	0	1	β_E	1	1	0.3	1	1	1	0	0		
	VII	1.3	β_D	0	0	0	β_E	1	1	0	0	0	0	1	0		
	VIII	1.3	β_D	1	0	1	β_E	1	1	0	0	0	0	0	1		
	IX	1.20	β_D	0	0	0	β_E	1	1	1	0	0	0	0	1		
	X	1.30	1	1.67	0	0	β_E	0	0	0	0	0	0	0	0		Culvert

Not Applicable

$(L + I)_n$ - Live load plus impact for AASHTO Highway H or HS loading

$(L + I)_p$ - Live load plus impact consistent with the overload criteria of the operation agency.

* 1.25 may be used for design of outside roadway beam when combination of sidewalk live load as well as traffic live load plus impact governs the design, but the capacity of the section should not be less than required for highway traffic live load only using a beta factor of 1.67. 1.00 may be used for design of deck slab with combination of loads as described in Article 3.24.2.2.

** Percentage = $\frac{\text{Maximum Unit Stress (Operating Rating)}}{\text{Allowable Basic Unit Stress}} \times 100$

For Service Load Design

% (Column 14) Percentage of Basic Unit Stress

No increase in allowable unit stresses shall be permitted for members or connections carrying wind loads only

β_E = 1.00 for vertical and lateral loads on all other structures.

For culvert loading specifications, see Article 6.2.

β_E = 1.0 and 0.5 for lateral loads on rigid frames (check both loadings to see which one governs). See Article 3.20.

For Load Factor Design

β_E = 1.3 for lateral earth pressure for retaining walls and rigid frames excluding rigid culverts.

β_E = 0.5 for lateral earth pressure when checking positive moments in rigid frames. This complies with Article 3.20.

β_E = 1.0 for vertical earth pressure

β_D = 0.75 when checking member for minimum axial load and maximum moment or maximum eccentricity ..... For

β_D = 1.0 when checking member for maximum axial load and minimum moment ..... Column Design

β_D = 1.0 for flexural and tension members

β_E = 1.0 for Rigid Culverts

β_E = 1.5 for Flexible Culverts

For Group X loading (culverts) the β_E factor shall be applied to vertical and horizontal loads.

Table 2.3 Performance Factors for Shallow Foundations (Barker et al, 1991)

Type of Limit State	Performance Factor
1. Bearing Capacity	
a. Sand	
Semi-empirical Procedure (SPT)	0.45
Semi-empirical Procedure (CPT)	0.55
Rational Method:	
using ϕ_f estimated from SPT	0.35
using ϕ_f estimated from CPT	0.45
b. Clay	
Semi-empirical Procedure (CPT)	0.50
Rational Method:	
using shear strength in lab tests	0.60
using shear strength from field vane tests	0.60
using shear strength estimated from CPT data	0.50
c, Rock	
Semi-empirical procedure	0.60
2. Sliding	
a. Precast concrete placed on sand:	
using ϕ_f estimated from SPT	0.90
using ϕ_f estimated from CPT	0.90
b. Concrete cast in place on sand:	
using ϕ_f estimated from SPT	0.80
using ϕ_f estimated from CPT	0.80
c. Clay (where shear strength is less than 0.5 times normal pressure)	
using shear strength in lab tests	0.85
using shear strength from field vane tests	0.85
using shear strength estimated from CPT data	0.80
d. Clay (where shear strength is greater than 0.5 times normal pressure)	0.85

Table 2.4 Performance Factors for Driven Piles
(Barker et al, 1991)

	Method / Soil / Condition		Performance Factor
Ultimate Bearing Capacity of Single Piles	Skin Friction	α - method	0.70
		β - method	0.50
		λ - method	0.55
	End Bearing	Clay (Skempton, 1951)	0.70
		Sand (Kulhawy, 1983)	
		ϕ_f from CPT	0.45
		ϕ_f from SPT	0.35
		Rock (Canadian Geotech. Society, 1985)	0.50
	Skin Friction and End Bearing	SPT - method	0.45
		CPT - method	0.55
		Load test	0.80
		Pile Driving Analyzer	0.70
Block Failure		Clay	0.65
Uplift Capacity of Single Piles		α - method	0.60
		β - method	0.40
		λ - method	0.45
		SPT - method	0.35
		CPT - method	0.45
		Load test	0.80
Group Uplift Capacity		Sand	0.55
		Clay	0.55

Table 2.5 Performance Factors for Drilled Shafts
(Barker et al, 1991)

	Method / Soil / Condition		Performance Factor
Ultimate Bearing Capacity of Single Drilled Shafts	Side Resistance in Clay	α - method (Reese & O'Neill)	0.65
		β - method (Stas & Kulhawy	0.50
	Base Resistance in Clay	Total Stress (Reese & O'Neill)	0.55
		Effective Stress (Stas & Kulhawy)	0.45
	Side Resistance in Sand	1) Touma & Reese 2) Meyerhof 3) Quiros & Reese 4) Reese & Wright 5) Reese & O'Neill	See Discussion in Section 4.2.2 (Barker et al. 1991)
	Base Resistance in Sand	1) Touma & Reese 2) Meyerhof 3) Quiros & Reese 4) Reese & Wright 5) Reese & O'Neill	See Discussion in Section 4.2.2 (Barker et al. 1991)
	Side Resistance in Rock	Carter & Kulhawy	0.55
		Horvath & Kenney	0.65
	Base Resistance in Rock	Canadian Foundation Engineering Method	0.65
		Pressuremeter Method	0.50
	Skin Friction and End Bearing	Load Test	0.80
Block Failure		Clay	0.65

Table 2.5 Performance Factors for Drilled Shafts (continued)

	Method / Soil / Condition		Performance Factor
Uplift Capacity of Single Drilled Shafts	Clay	α - method (Reese & O'Neill)	0.55
		β - method (Stas & Kulhawy)	0.40
		Belled Shafts (Reese & O'Neill)	0.50
	Sand	1) Touma & Reese 2) Meyerhof 3) Quiros & Reese 4) Reese & Wright 5) Reese & O'Neill	See Discussion in Section 4.2.2 (Barker et al. 1991)
	Rock	Carter & Kulhawy	0.45
		Horvath & Kenney	0.55
	Load Test		0.80
Group Uplift Capacity	Sand		0.55
	Clay		0.55

2.3.4 Design Loads and Load Combinations

Various combinations of different loads are used for the design of superstructures and foundations. These loads include dead load, live load, lateral earth pressure, wind load, earthquake load, ice load, and strain-related loads such as creep and shrinkage in concrete. The 15th edition AASHTO load factors and load combinations for ultimate limit states and serviceability limit states, which are given in Table 2.2, are expressed in the following format:

$$\text{Group } N = \gamma[\beta_D D + \beta_L(L+I) + \beta_C CF + \beta_E E + \beta_B B + \beta_{SF} SF + \beta_W W + \beta_{WL} WL + \beta_{LF} LF + \beta_R(R+S+T) + \beta_{EQ} EQ + \beta_{ICE} ICE] \quad (2.2)$$

where N = loading group number,

γ = load factor,

β = coefficient,

D = dead load,

L = live load,

I = impact due to live load,

E = earth pressure,

B = buoyancy,

W = wind load on structure,

WL = wind load on live load,

LF = longitudinal force from live load,

CF = centrifugal force,

R = rib shortening,

S = shrinkage,

T = temperature,

EQ = earthquake,

SF = stream flow pressure,

ICE = ice pressure.

2.3.5 Other Considerations

Backfill

Various types of soil can be used as backfill for walls and abutments. Free-draining soils such as clean sands and gravels are the most desirable materials for backfill. Clay soils cause many problems, including seasonal volume changes, slow drainage, settlement, creep movements, and cracks due to shrinkage. Shrinkage cracks that develop in clay may be filled with water so that the walls may be subject to unexpectedly high lateral pressures. Because of these disadvantages, clay soils are not recommended for backfill.

The backfill material should be compacted to minimize settlements due to self weight and surcharge loads. Compaction increases the lateral forces exerted on the wall, and these should be considered in design.

Drainage

One of the major reasons for unsatisfactory performance of retaining walls is an improperly designed or poorly constructed drainage systems. The main purpose of a drainage system is to prevent excessive water pressures from acting against the wall. Various types of drainage systems can be used based on the type of retaining wall, the type of backfill material, the ground water condition, and possible frost effects. An inclined drainage system is more effective than a vertical drainage system located at the back of the wall.

A drainage blanket or a prefabricated drainage composite can be used as drain material. Longitudinal drains within drainage blankets should be located at adequate intervals to convey the released water from behind the wall to a free exit. According to the Corps of Engineers (1989), even when a drainage system is used, walls should still have a sufficient factor of safety to account for the possibility that the drain system may not work properly.

Frost

Water in soil expands when it freezes and ice lenses may develop, resulting in frost heave in the frozen soil. Foundations should be built below the frost line to avoid possible frost damage. The maximum frost depth can be estimated from local experience, or from a frost-depth contour map.

Undermining of Abutments by Scour

Bridge abutments and piers in streams, flood plains, or adjacent to water are subject to undermining by scouring action. This scouring action has caused many bridge failures.

Three types of scour in a river are shown in Figure 2.6 (Sowers, 1962). The first type of scour (a) is due to the lateral shifting of the channel. Continuous scouring occurs at the outside of each bend in a meandering river due to higher velocity of the stream, while sedimentation occurs at the inside of each bend. The abutment close to the outside of a bend should be protected from undermining by placing concrete or asphaltic mats over the river bank or by founding the abutment below the greatest possible depth of scour.

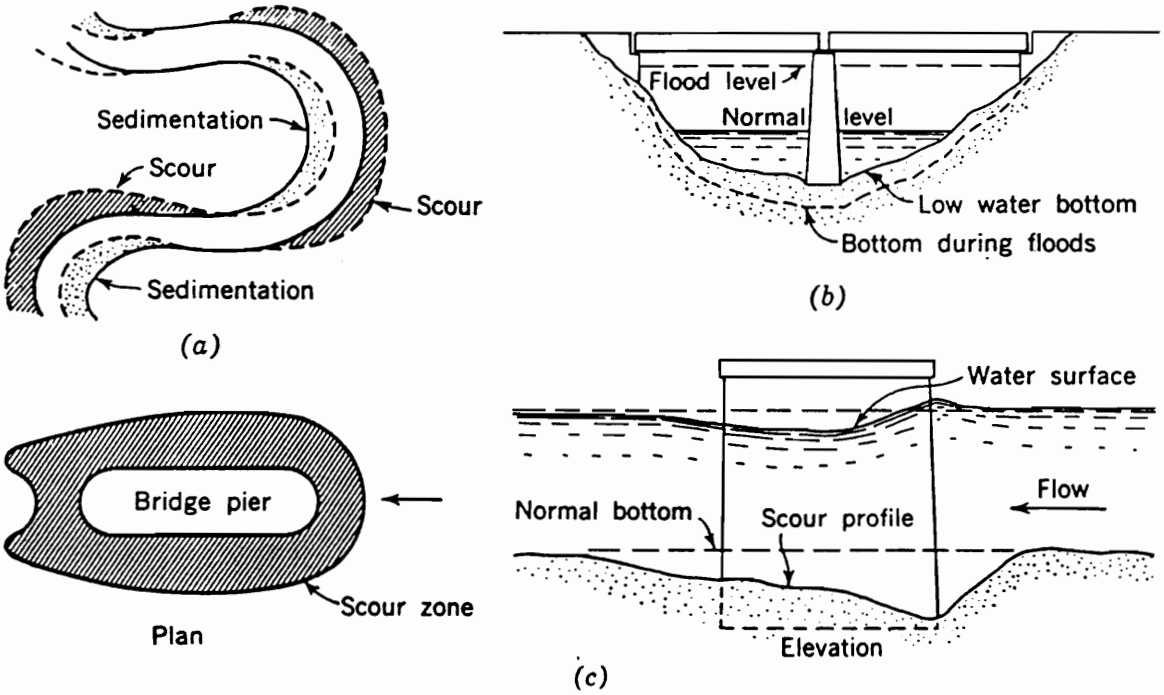

(a) Lateral Shift of a Stream caused by Bank Erosion and Deposition
(b) Normal Bottom Scour during Floods
(c) Accelerated Scour caused by a Bridge Pier

Figure 2.6 Forms of Scour in Rivers (From Sowers, 1962)

The second type of scour (b) is due to the erosion of the river bed which occurs during periods of high flow. High velocity flow moves heavy bed materials, so that the bed is lowered. The scouring action is especially large where the width of the flow path is narrow. In general, this normal scour is proportional to the rise in the water surface, and therefore the maximum depth of scour can be estimated by observation of the river bed during periods of high flow.

The third type of scour (c) is the localized and accelerated scour resulting from such obstructions as bridge piers which cause contraction of the channel cross section and generates higher velocity of flow. The depth of scour in this case depends on factors such as the configuration of the pier, the angle between the flow and the pier, the contraction of the waterway, and the volume of debris that may be caught by the bridge.

The above considerations indicate the difficulty of assigning fixed numbers to represent phenomenon that are highly variable. What is needed to represent their variability are formulations based on reliability theory.

2.4 RELIABILITY METHODS

Engineering design specifications have been formulated with the recognition of uncertainties that arise as a result of inherent variability of design parameters. Examples of design parameters that are variable in nature are loading and resistance. If the exact loads and load effects were known, safety could be obtained by supplying a capacity slightly larger than the applied loads. However, due to the many uncertainties involved in the actual circumstances, safety factors of two to four are often provided. These safety factors were selected based on experience, tradition or engineering judgment rather than based on a systematic analysis of uncertainties involved in design. As a result, the current design practice which uses the safety factors, applied only to the resistance, provides different level of safety for different loading conditions and different failure modes.

During the last three decades, research has been conducted on probability theory to systematically incorporate the uncertainties in engineering design. Examples of this research can be found in the literatures of Cornell (1969), Tang et al (1976), Ravindra et al (1978), and Ellingwood et al (1980). This research has resulted in a number of reliability-based design codes such as the Ontario Highway Bridge Design Code

(1983), the Danish Code of Practice for Foundation Engineering (1985) and American Institute of Steel Construction Specification (1986).

2.4.1 Probabilistic Design

In the probabilistic design, the design parameters are treated as random variables rather than deterministic constants. Safety is measured by the probability of reaching a particular limit state, which is defined as the probability that a system fails to perform its intended function. While the deterministic safety factor is based on past experience or intuitive judgment, the probability of failure can be computed from the distributions of the load and resistance. Even though the probabilistic method demands more complicated procedures than the deterministic method, it provides a more consistent level of safety for different structures and materials.

Based on the level of complexity involved in the probability theory used, the International Standards Organization (Oliphant, et al, 1988) categorized the design procedures into three groups:

1. Level I: Semi-probabilistic method
2. Level II: Approximate probabilistic method
3. Level III: Fully probabilistic method.

The Level III reliability method requires the exact shape of probability distributions of each random variables. Since the fully probabilistic method is too complex and the exact information about loads and resistance is hardly available, this method is not practical for the design of retaining walls or abutments.

The Level II method requires no knowledge of the exact probability distributions of the random variables but demands only the density functions of the load and resistance variables. In the Level II method, the load and resistance are statistically independent and the density functions can be approximated by an analysis of existing data. One of the approximate probabilistic methods is the first order second moment (FOSM) method, which uses the first two so-called moments, the mean and coefficient of variation. A Taylor series expansion is used to approximate the first two moments and only the first order terms in the series are considered. In this method the safety is measured by the reliability or safety index, β, which was previously defined in Figure 2.5. Now that it can be analyzed from the first two moments of the density function without knowing the exact shape of the distribution functions, this method is more advantageous and applicable to the design of walls and is utilized in this study.

The semi-probabilistic methods (Level I) represents safety by separate load and resistance factors, which are obtained from a second moment reliability analysis (Level II). Since this method is convenient and simple, most of the earlier reliability-based design code utilized its format.

2.4.2 Reliability Analysis

The level of reliability implied in a structure can be measured by a safety index or reliability index, β. The reliability analysis used in this study is for calculating the safety index based on a First Order Second Moment (FOSM) method. Before introducing this method a few general comments on reliability methods will be made.

In the general reliability model, the load, Q and the resistance, R are treated as random variables which may be represented by frequency distributions or probability density functions. As shown in Figure 2.4, safety is ensured when the effects of the load, Q is smaller than the resistance, R. However, due to their random variability, sometimes the load effect, Q exceeds the resistance, R. The possible chance that such a situation may occur is called the probability of failure and may be expressed as

$$p_f = P(R < Q) \tag{2.3}$$

If the exact probability density functions for R and Q are known and R and Q are statistically independent, then the probability of failure p_f can be obtained by

$$p_f = \int_0^\infty f_R(r)dr \cdot \int_0^\infty f_Q(q)dq \qquad (2.4)$$

or

$$p_f = \int_0^\infty F_R(r) \cdot f_Q(q)dq \qquad (2.5)$$

where $f_R(r)$ and $f_Q(q)$ are probability density functions for R and Q and $F_R(r)$ is the cumulative distribution function of R. Since the actual density functions of R and Q are often not available, approximate reliability methods such as the FOSM method should be used.

The Mean Value First Order Second Moment Method (MVFOSM)

In this method, a failure function or limit state function g() is used to represent the safety margin. If R and Q are assumed to be normally distributed, g() can be expressed as:

$$g() = R - Q \qquad (2.6)$$

For lognormally distributed R and Q, the limit state function, g() is written as:

$$g() = \ln(R) - \ln(Q) \qquad (2.7)$$

In both cases, failure occurs when g() is less than zero.

The probability of failure for normally distributed R and Q can be obtained by

$$p_f = 1 - F_u \cdot \left(\frac{\overline{R} - \overline{Q}}{\sqrt{\sigma_R^2 + \sigma_Q^2}} \right) \tag{2.8}$$

and for lognormally distributed R and Q,

$$p_f = 1 - F_u \left(\frac{\ln\left(\frac{\overline{R}}{\overline{Q}}\right)}{\sqrt{V_R^2 + V_Q^2}} \right) \tag{2.9}$$

where $\overline{R}$ and $\overline{Q}$ are mean values of R and Q,

σ_R and σ_Q are standard deviations of R and Q,

V_R and V_Q are coefficients of variations of R and Q (V_R and $V_Q < 0.3$),

$F_u()$ is the standard normal distribution function.

Another method to express the probability of failure is to use the safety or reliability index, β. As shown in Figure 2.5, the reliability index, β is the distance measured in standard deviations between the mean safety margin and the failure limit. For normally distributed R and Q, the reliability index can be calculated from

$$\beta = \frac{\overline{R} - \overline{Q}}{\sqrt{\sigma_R^2 + \sigma_Q^2}} \tag{2.10}$$

For lognormally distributed R and Q, the reliability index β is

$$\beta = \frac{\ln\left(\frac{\overline{R}}{\overline{Q}}\right)}{\sqrt{V_R^2 + V_Q^2}} \tag{2.11}$$

When R and Q are normally distributed, the reliability index has a useful relationship with the probability of failure as

$$\beta = F_u^{-1}(1 - p_f) \tag{2.12}$$

where $F_u^{-1}()$ is the inverse normal function.

When R and Q are not normally distributed, the reliability index provides an approximate probability of failure. Rosenblueth and Esteva (1972) found a consistent agreement between the reliability index and probability of failure and suggested the following relationship for lognormally distributed R and Q.

$$p_f = 460\, e^{(-4.3\beta)} \qquad 2 < \beta < 6 \tag{2.13}$$

Based on the above equation, Table 2.6 shows the relationship between reliability index and probability of failure.

Meyerhof (1976) conducted a study to compare safety factors with the reliability index for earth retaining structures, earthworks and foundations. The relationship between safety factors and the reliability index, and typical coefficients of variation are summarized in Table 2.7.

The limit state function formulated using the Mean Value First Order Second Moment (MVFOSM) method is linearlized at the mean values of the design variables rather than at a point on the failure surface. According to Hasofer and Lind (1974), MVFOSM method has two shortcomings. First, due to the linearlization at the mean values, considerable errors may occur when the limit state function is nonlinear. Second, the MVFOSM method is not consistent for equivalent formulations of the same physical problem. In other words, different values of the reliability index may be obtained for the same problem, depending on how the limit state equation is formulated.

Table 2.6 Relationship between Probability of Failure P_f and Reliability Index β

β	P_f	P_f	β
2.5	0.99×10^{-2}	10^{-1}	1.96
3.0	1.15×10^{-3}	10^{-2}	2.50
3.5	1.34×10^{-4}	10^{-3}	3.03
4.0	1.56×10^{-5}	10^{-4}	3.57
4.5	1.82×10^{-6}	10^{-5}	4.10
5.0	2.12×10^{-7}	10^{-6}	4.64
5.5	2.46×10^{-8}	10^{-7}	5.17

Table 2.7 Typical Reliability Indices for Geotechnical Facilities (after Meyerhof, 1976)

Facility	Typical c.o.v.	Typical Safety Factor	Typical Safety Index
Earth Retaining Structures	0.13	1.3 to 1.5	2.0 to 2.5
Earthworks	0.15	1.5 to 2.0	2.0 to 3.0
Offshore Foundations	0.20	1.5 to 2.0	1.5 to 2.5
Onshore Foundations	0.25	2.0 to 3.0	2.0 to 3.0

Advanced First Order Second Moment Methods

In order to overcome the shortcoming of the MVFOSM method, advanced FOSM methods have been developed by many researchers such as Diltlevsen (1974), Hasofer and Lind (1974), Rackwitz and Fiessler (1978), and Ellingwood et al (1980). Since the limit state function is linearlized at a point on the failure surface, a consistent reliability index can be obtained regardless how the limit state function is formulated.

In the Advanced FOSM method, the limit state function can be expressed in a general format as

$$g(X) = g(X_1, X_2, ..., X_n) = 0 \qquad (2.14)$$

where X_1, X_2, ..., X_n are design variables of the system.

The limit state function, g(X) can be considered geometrically as an n-dimensional surface which is the failure surface. The condition $g() > 0$ represents that the system is in the safe state and $g() < 0$ means that the system fails. Figure 2.7 illustrates an example with two variables.

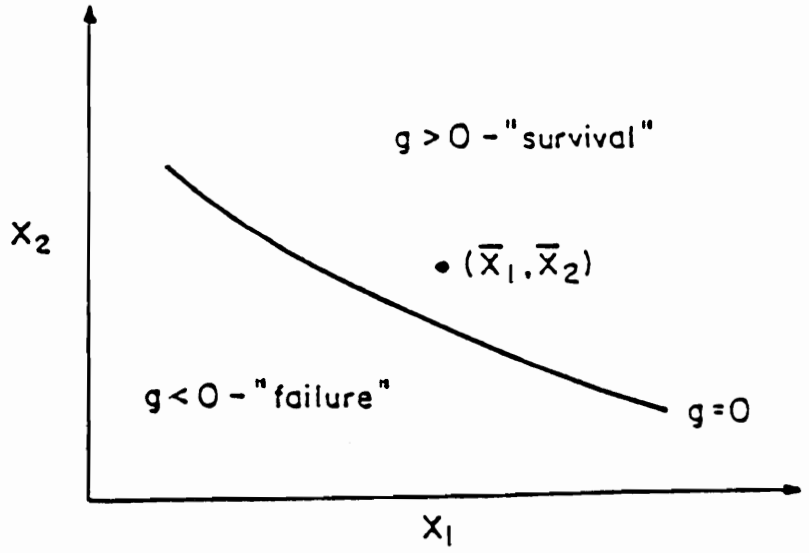

(a) Original coordinates

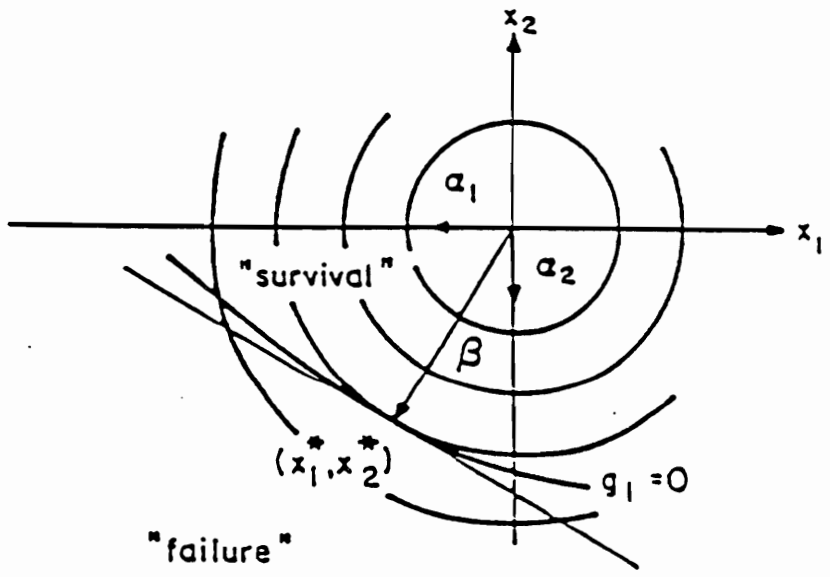

(b) Reduced coordinates

Figure 2.7 Safety Analysis of Two-variable Problem using the Advanced Method in Reduced and Original Coordinates

The first step in the reliability analysis is the transformation of the X_i variables to a space of reduced variables with zero mean and unit variance using

$$x_i = \frac{X_i - \overline{X}_i}{\sigma_{X_i}} \tag{2.15}$$

The limit state function in the reduced space is

$$g(x_1, x_2, \ldots, x_n) = 0 \tag{2.16}$$

As shown in Figure 2.7, the safety index is the shortest distance between the origin and the failure surface. The point $(x_1^*, x_2^*, \ldots, x_n^*)$ on the failure surface corresponding to this shortest distance is defined as design or checking point.

The design point can be obtained by solving the following equations simultaneously

$$\alpha_i = - \frac{\sigma_i \frac{\partial g}{\partial X_i}}{\sqrt{\Sigma \left(\sigma_i \frac{\partial g}{\partial X_i} \right)^2}} \tag{2.17}$$

$$x_i^* = - \alpha_i \cdot \beta \tag{2.18}$$

$$g(x_1^*, x_2^*, \ldots, x_n^*) = 0 \tag{2.19}$$

and finding the direction cosines, α_i that produce the smallest reliability index, β.

For random variables that are not normally distributed, Rackwitz and Fiessler (1978) developed the equivalent normalization method. With this method non-normal variables can be transformed into equivalent normal variables before solving equations 2.17 through 2.19.

Ellingwood et al (1980) suggested a systematic procedure to obtain the reliability index using the advanced FOSM method as follows:

Step 1: Define the proper limit state function, $g(X_1, X_2, \ldots, X_n) = 0$

where the $X_1, X_2, \ldots, X_n$ are the design random variables.

Step 2: Assume an initial value of reliability index, β.

Step 3: Assume the point at the mean values $(\overline{X}_1, \overline{X}_2, \ldots, \overline{X}_n)$ to be the initial design point $(X_1^*, X_2^*, \ldots, X_n^*)$ for the first iteration.

Step 4: If variables are non-normal, compute the mean value $(\overline{X}_i^N)$ and standard deviation (σ_i^N) of the equivalent normal distribution.

where $\overline{X}_i^N = X_i^* - \sigma_i^N \cdot \Phi^{-1}\left[F_{\overline{X}}(x_i^*)\right]$

$$\sigma_i^N = \frac{\varphi\left\{\Phi^{-1}\left[F_{\overline{x}}(x_i^*)\right]\right\}}{f_{\overline{X}}(x_i^*)}$$

Step 5: Compute the partial derivatives $\frac{\partial g}{\partial X_i}$, using the values at the design point

$(X_1^*, X_2^*, \ldots, X_n^*)$.

Step 6: Calculate the direction cosines using

$$\alpha_i = - \frac{\sigma^N{}_i \frac{\partial g}{\partial X_i}}{\sqrt{\sum \left(\sigma^N{}_i \frac{\partial g}{\partial X_i} \right)^2}}$$

Step 7: Find new design point values from

$$X_i^* = X_i^N + \alpha_i \beta \sigma_i^N$$

and repeat steps 4 to 7 until the estimates of the direction cosines α_i stabilize.

Step 8: Obtain the reliability index, β corresponding to $g(X_1^*, X_2^*, \ldots, X_n^*) = 0$.

Repeat steps 4 to 8 until the values of β converges with a designated tolerance. The probability of failure, P_f is $\Phi(-\beta)$.

2.5 METHODS OF ESTIMATING EARTH PRESSURES

This section is concerned with the considerations involved in estimating static earth pressures on retaining walls and abutments. Static earth pressures exerted on a retaining wall can be classified into at-rest, active and passive. The stresses at any point within a soil mass can be illustrated by Mohr circles, as shown in Figure 2.8, on coordinates which consist of effective normal stress, σ_v' and shear stress, τ.

The at-rest condition develops when any possible combinations of normal stresses and shear stresses in a soil mass are within the limiting envelope (the dotted half-circle in Figure 2.8).

Failure conditions, called states of limiting or plastic equilibrium may evolve as the maximum shear strength is fully mobilized. These states are known as active and passive conditions, and they occur when shear stresses reach the maximum possible values due to lateral extension or compression in a soil mass.

Each of these earth pressure states corresponds to different conditions with regard to the direction and the magnitude of wall movement, as discussed below.

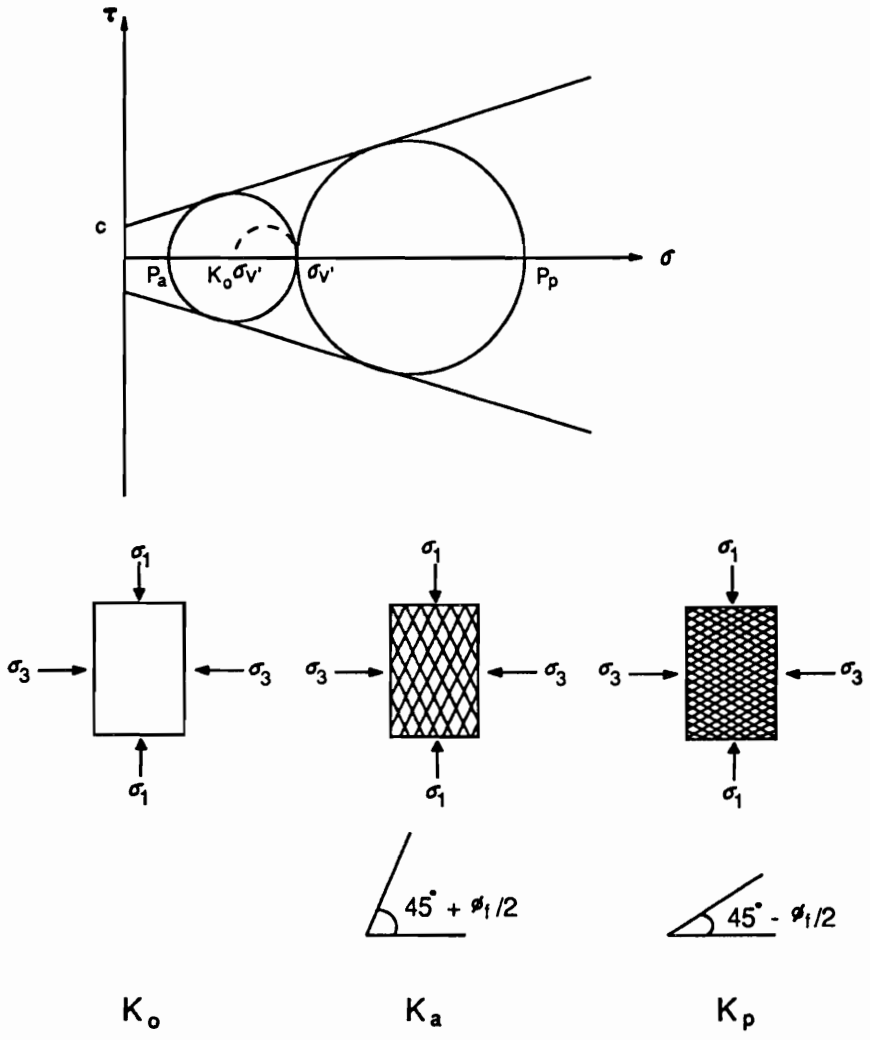

where P_a : Static active earth pressure force,

P_p: Static passive earth pressure force,

K_o: Coefficient of at-rest earth pressure

K_a: Coefficient of static active earth pressure

K_p: Coefficient of static passive earth pressure

c: Cohesion

Figure 2.8 Mohr's Circles for Earth Pressure Coefficients

2.5.1 At-Rest Earth Pressure

Walls that do not move, or that move very little, are acted on by at-rest earth pressures. At-rest pressures increase linearly with depth (see Figure 2.9) and can be expressed as:

$$p_h = K_o \cdot \gamma \cdot z \tag{2.19}$$

where p_h = at-rest pressure (force/length^2),

K_o = coefficient of lateral earth pressure at-rest,

γ = unit weight of soil (force/length^3);

for depths below water table use submerged unit-weight, γ',

z = depth below the surface of the fill (length).

For Normally Consolidated Soils

The coefficient, K_o for normally consolidated soils can be estimated by the following empirical correlation (Jaky, 1944):

$$K_o = 1 - \sin \phi' \tag{2.20}$$

where ϕ' = drained friction angle of soil (degrees).

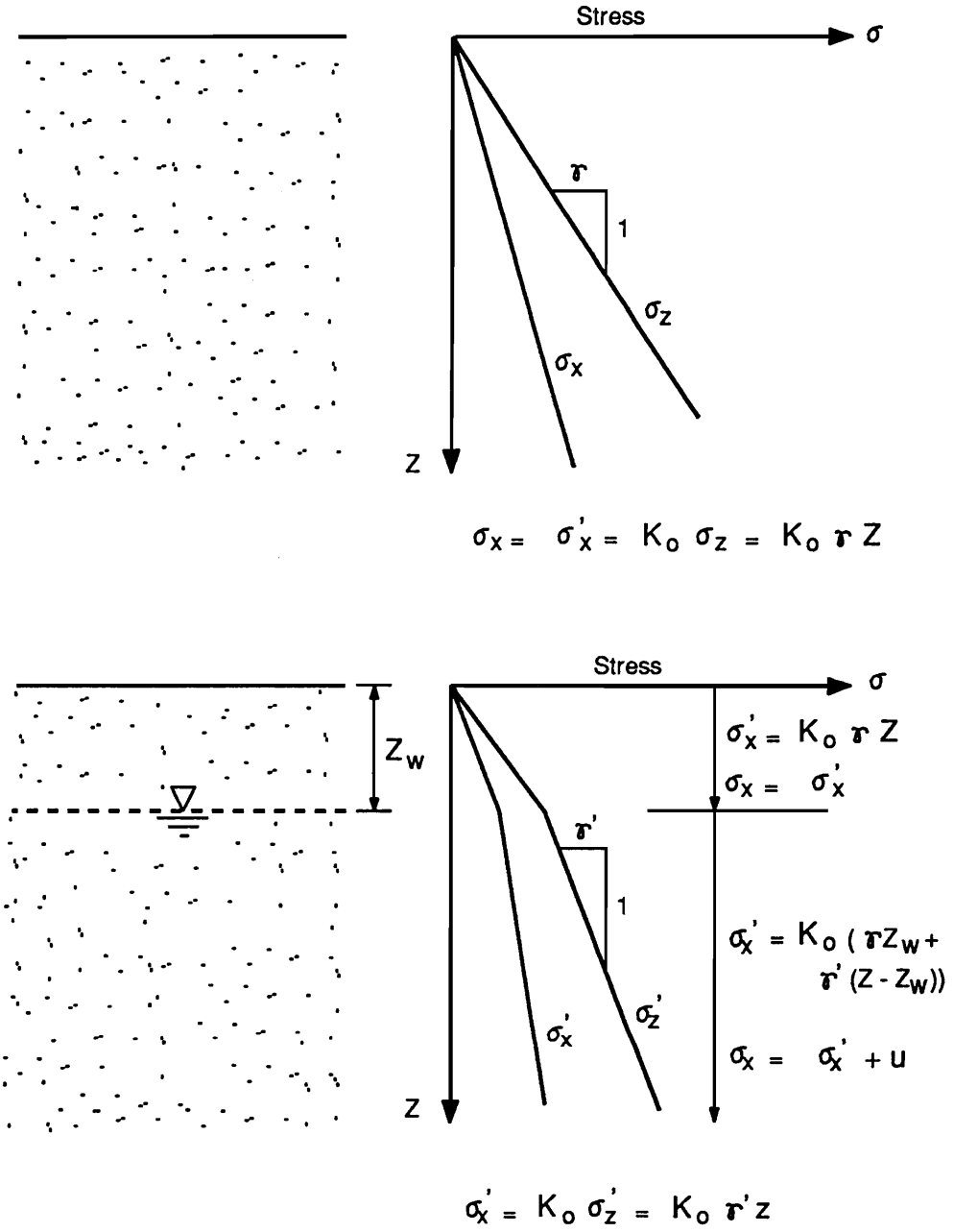

Figure 2.9 At-Rest Earth Pressure Distribution, Homogeneous Soil (After Clough and Duncan, 1991)

Since Eq. 2.20 is based on level backfills, the following equation for sloping backfills is recommended by the Danish Code (1978):

$$K_{oi} = K_o (1 + \sin i) \tag{2.21}$$

where $K_{oi} = K_o$ for sloping backfills,

K_o = coefficient of earth pressure at-rest for normally consolidated soils (Eq. 2.20),

i = the sloping angle of backfill (degrees).

For Overconsolidated Soils

Values of coefficient of at-rest earth pressure for overconsolidated soils can be estimated using the empirical relationship (Mayne and Kulhawy, 1982):

$$K_{ou} = K_o \cdot (OCR)^{\sin \phi'} \tag{2.22}$$

where K_{ou} = coefficient of at-rest earth pressure for overconsolidated soils,

K_o = coefficient of earth pressure at-rest for normally consolidated soils (Eq. 2.20),

ϕ' = drained friction angle of soil (degrees),

OCR = Over Consolidation Ratio, or maximum previous vertical pressure divided by current effective vertical pressure.

Typical values of K_{ou} corresponding to various values of OCR are presented in Table 2.8.

2.5.2 Wall Movements and Earth Pressures

The earth pressures that act on a wall vary with wall displacement. That is, when a retaining wall moves away from the backfill, the earth pressure decreases (active pressure) and when it moves toward the backfill, the earth pressure increases (passive pressure). Table 2.9, obtained through experimental data and finite element analyses (Clough and Duncan, 1991), gives approximate magnitudes of wall movements required to reach minimum active and maximum passive earth pressure conditions. Observations from the table can be summarized as follows (Clough and Duncan, 1991):

1. The required movements for the extreme conditions are approximately proportional to the wall height.
2. The movement required to reach the maximum passive pressure is about 10 times as great as that required to reach the minimum active pressure, for walls of the same height.
3. The movement required to reach the extreme conditions for dense and incompressible soils is smaller than those for loose and compressible soils.

Table 2.8 Typical Coefficients of Lateral Earth Pressure At-Rest (after Clough and Duncan, 1991)

Coefficient of Lateral Earth Pressure					
Soil Type	**ϕ_f (deg)**	**OCR = 1**	**OCR = 2**	**OCR = 5**	**OCR = 10**
Loose Sand	33.5	0.45	0.65	1.10	1.50
Medium Sand	36.5	0.40	0.60	1.05	1.55
Dense Sand	40.5	0.35	0.55	1.00	1.50
Silt	29.5	0.50	0.70	1.10	1.60
Lean Clay, CL	23.5	0.60	0.80	1.20	1.65
Highly Plastic Clay, CH	20.5	0.65	0.80	1.10	1.40

Table 2.9 Approximate Magnitudes of Movements Required to Reach Minimum Active and Maximum Passive Earth Pressure Conditions (after Clough and Duncan, 1991)

Type of Backfill	Values of Δ/H *	
	Active	Passive
Dense sand	0.001	0.01
Medium dense sand	0.002	0.02
Loose sand	0.004	0.04
Compacted silt	0.002	0.02
Compacted lean clay	0.01 **	0.05 **
compacted fat clay	0.01 **	0.05 **

* Δ = movement of top of wall required to reach minimum active or maximum passive pressure, by tilting or lateral translation

H = height of wall

** Under stress conditions close to the minimum active or maximum passive earth pressures, cohesive soils creep continually. The movements shown would produce active or passive pressures only temporarily. With time the movements would continue if pressures remain constant. If movement remains constant, active pressures will increase with time, approaching the at-rest pressure, and passive pressures will decrease with time, approaching values on the order of 40% of the maximum short-term passive pressure.

For any cohesionless backfill, conservative and simple guidelines for the maximum movements required to reach the extreme cases are provided by Clough and Duncan (1991). For example, for minimum active pressure the movement is no more than about 1 inch in 20 feet ($\Delta/H = 0.004$) and for maximum passive pressure about 1 inch in 2 feet ($\Delta/H = 0.04$).

As shown in Figure 2.10, the value of the earth pressure coefficient varies with wall displacement and eventually remains constant after sufficiently large displacements. The change of pressures also varies with the type of soils, i.e., the pressures in the dense sand change more quickly with wall movement.

The earth pressure coefficients shown in Figure 2.11 are for a backfill compacted to a medium dense condition. Compared with the values in Figure 2.10, the curve is shifted upward so that the required movement for the minimum active earth pressure is increased and the required movement for the maximum passive earth pressure is decreased. However, in spite of the effect of compaction, the conservative guidelines of 1 inch in 20 feet for active condition and 1 inch in 2 feet for passive condition still can be used to estimate the required movements for the extreme earth pressure conditions.

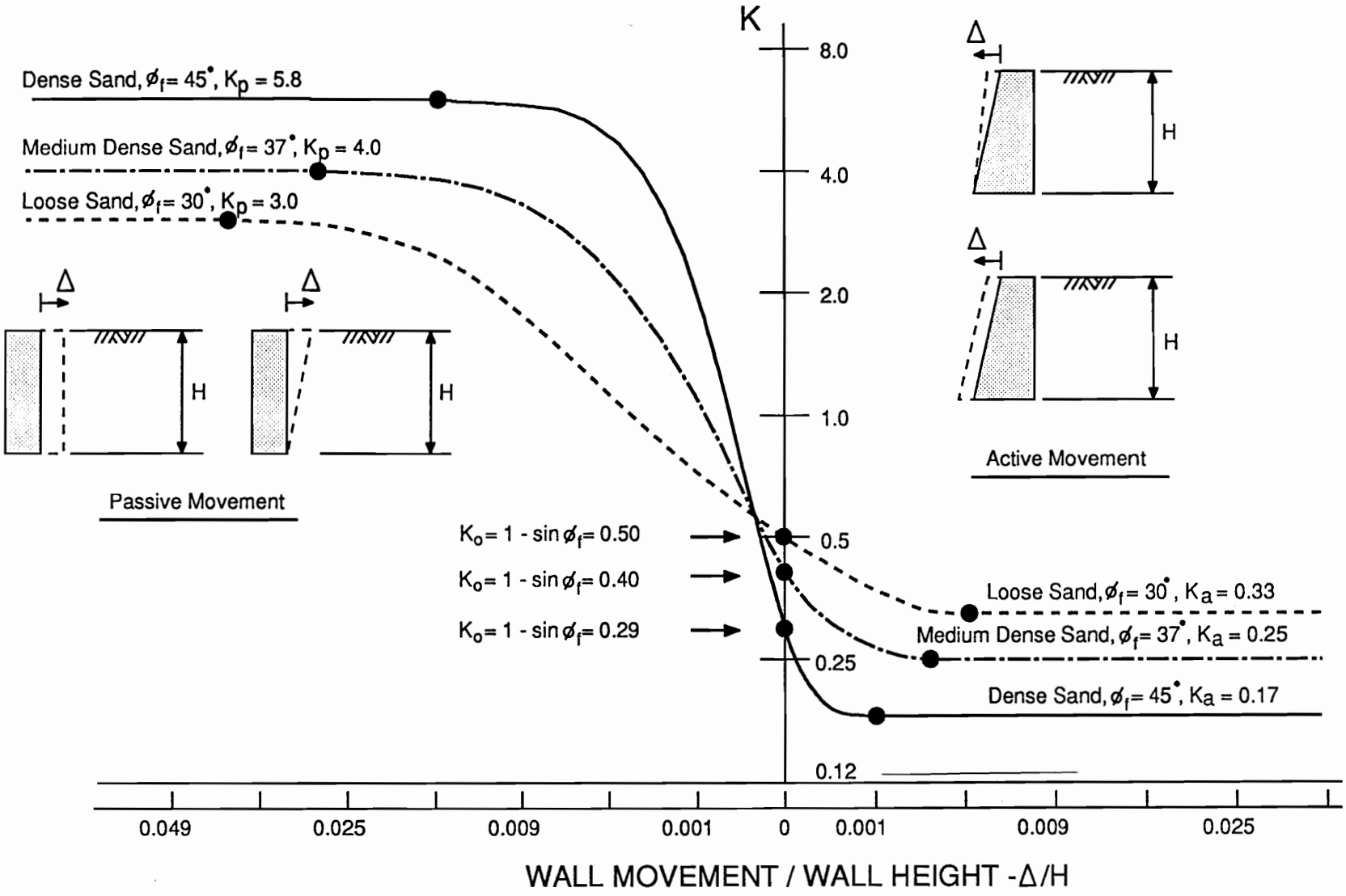

Figure 2.10 Relationship between Wall Movement and Earth Pressure
(After Clough and Duncan, 1991)

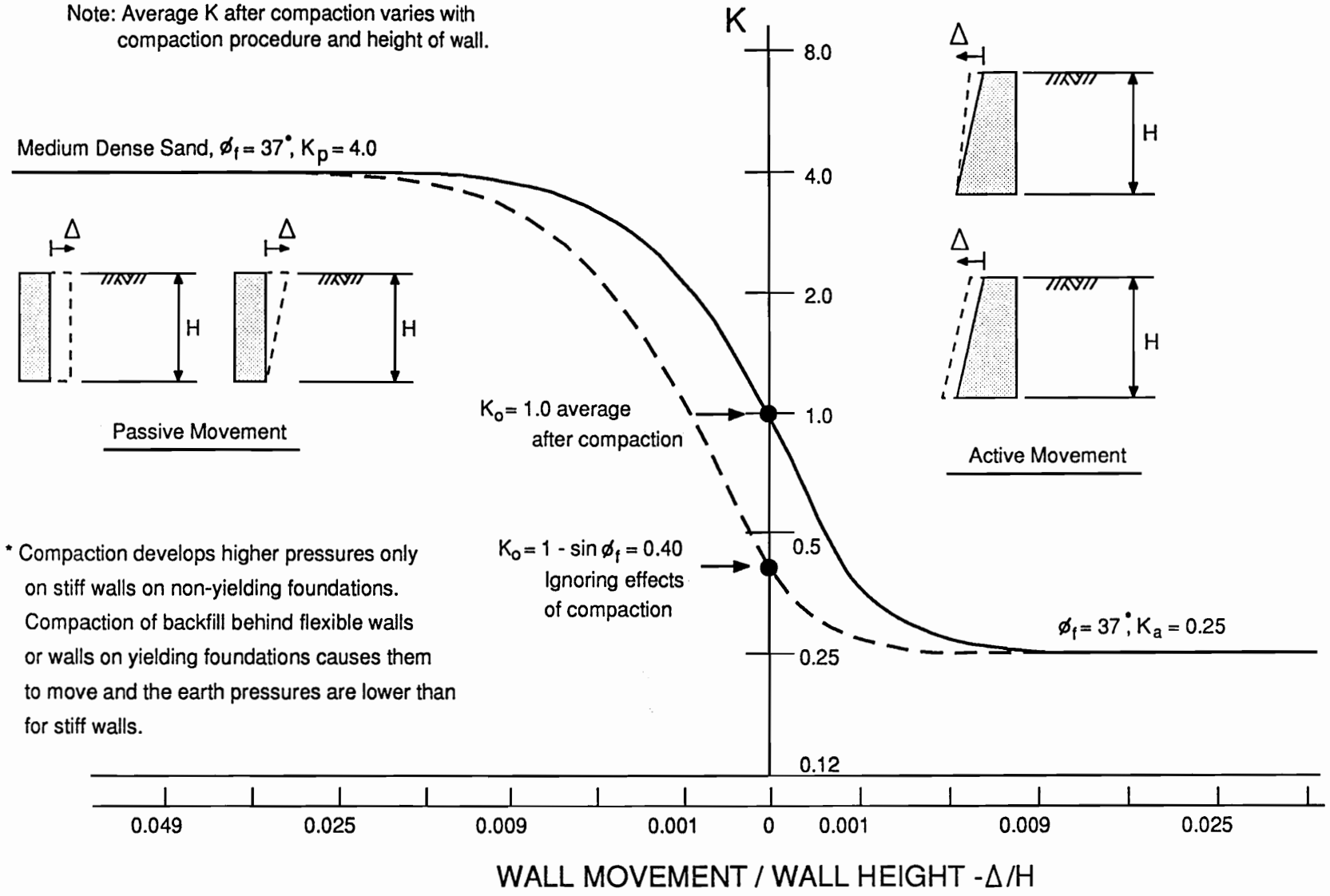

Figure 2.11 Relationship between Wall Movement and Earth Pressure for a Wall with Compacted Backfill (After Clough and Duncan, 1991)

2.5.3 Methods for Estimating K_a and K_p

Coulomb (1776) and Rankine (1856) developed simple methods for calculating the active and passive earth pressures exerted on retaining structures. Caquot and Kerisel (1948) developed the more generally applicable log spiral theory. Where the movements of walls are sufficiently large so that the shear strength of the backfill soil is fully mobilized, and where the strength properties of the backfill can be estimated with sufficient accuracy, these methods of calculation are useful for practical purposes.

Coulomb's trial wedge method can be used for irregular backfill configurations, and Rankine's theory and the log spiral analysis can be used for more regular configurations. Each of these methods will be discussed below.

2.5.4 Coulomb Theory

The Coulomb theory, the first rational solution to the earth pressure problem, is based on the concept that the lateral force exerted on a wall by the backfill can be evaluated by analysis of the equilibrium of a wedge-shaped mass of soil bounded by the back of the wall, the backfill surface, and a surface of sliding through the soil. The assumptions in this analysis are:

1. The surface of sliding through the soil is a straight line.
2. The full strength of the soil is mobilized to resist sliding (shear failure) through the soil.

Active Pressure

A graphical illustration for the mechanism of active failure according to the Coulomb theory is shown in Figure 2.12a. The active earth pressure force can be expressed as:

$$P_a = \frac{1}{2}\gamma H^2 \frac{\cos^2(\phi_f - \beta)}{\cos^2\beta \cdot \cos(\beta + \delta)\left[1 + \sqrt{\frac{\sin(\phi_f + \delta)\cdot\sin(\phi_f - i)}{\cos(\beta + \delta)\cdot\cos(\beta - i)}}\right]^2} \quad (2.23)$$

where P_a = active earth pressure force (force/length),

$= 1/2\ \gamma H^2 K_a$,

K_a = coefficient of active earth pressure

γ = unit weight of backfill soil (force/length^3),

H = wall height (length),

ϕ_f = the internal friction angle of soil (degrees),

β = the slope of stem face (degrees),

δ = the friction angle between wall and soil (degrees),

i = the slope of backfill surface (degrees).

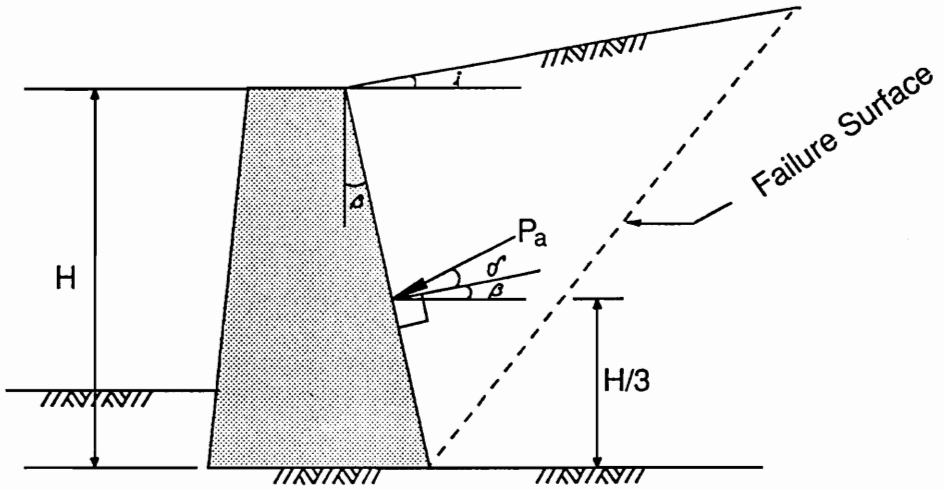

(a) Active Pressure Force

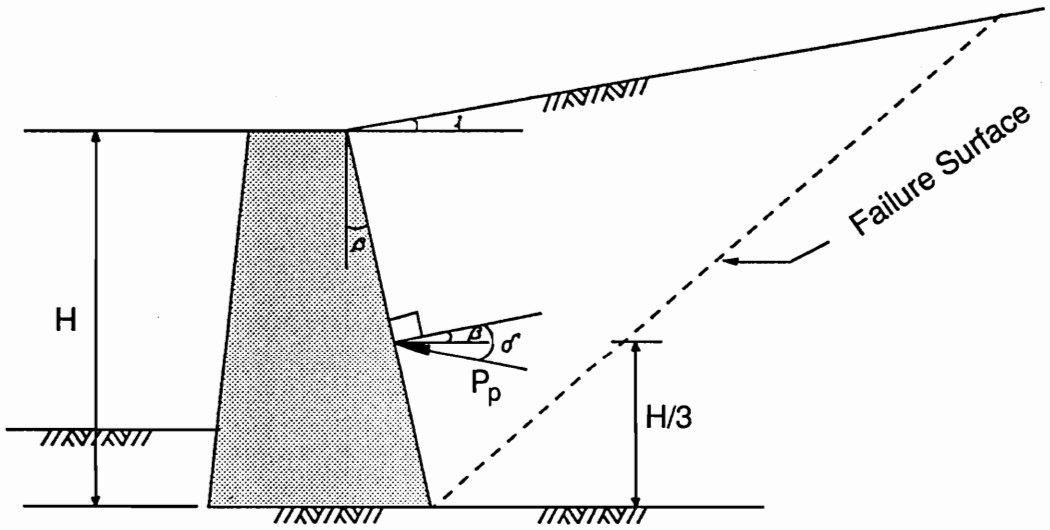

(b) Passive Pressure Force

Figure 2.12 Coulomb Theory for Active and Passive Earth Pressures

Passive Pressure

The Coulomb theory can be used to evaluate passive resistance, using the same basic assumptions. Figure 2.12b shows the failure mechanism for the passive case. The passive earth pressure force, P_p, can be expressed as follows:

$$P_p = \frac{1}{2}\gamma H^2 \frac{\cos^2(\phi_f + \beta)}{\cos^2\beta \cdot \cos(\beta - \delta)\left[1 - \sqrt{\frac{\sin(\phi_f + \delta)\cdot\sin(\phi_f + i)}{\cos(\beta - \delta)\cdot\cos(\beta - i)}}\right]^2} \quad (2.24)$$

The basic assumption in the Coulomb theory is that the surface of sliding is a plane. This assumption does not affect appreciably the accuracy for the active case. However, for the passive case, values of P_p calculated by the Coulomb theory can be much larger than can actually be mobilized, especially when the value of δ exceeds about half of ϕ_f.

Wall Friction

Friction between the wall and backfill has an important effect on the magnitude of earth pressures and an even more important effect on the direction of the earth pressure force. Table 2.10 presents values of the maximum possible wall friction angle for various wall materials and soil types.

Table 2.10 Ultimate Friction Factors, Friction Angles and Adhesion for Dissimilar Materials (From NAVFAC, 1982)

INTERFACE MATERIALS	FRICTION FACTOR tan δ	(1) FRICTION ANGLE, δ (degrees)
Mass concrete on the following foundation materials:		
- Clean sound rock	0.70	35
- Clean gravel, gravel-sand mixtures, coarse sand	0.55 to 0.60	29 to 31
- Clean fine to medium sand, silty medium to coarse sand, silty or clayey gravel	0.45 to 0.55	24 to 29
- Clean fine sand, silty or clayey fine to medium sand	0.35 to 0.45	19 to 24
- Fine sandy silt, nonplastic silt	0.30 to 0.35	17 to 19
- Very stiff and hard residual or preconsolidated clay	0.40 to 0.50	22 to 26
- Medium stiff and stiff clay and silty clay	0.30 to 0.35	17 to 19
(Masonry on foundation materials has same friction factors)		
Steel sheet piles against the following soils:		
- Clean gravel, gravel-sand mixtures, well-graded rock fill with spalls	0.40	22
- Clean sand, silty sand-gravel mixture, single size hard rock fill	0.30	17
- Silty sand, gravel or sand mixed with silt or clay	0.25	14
- Fine sandy silt, nonplastic silt	0.20	11

(1) δ = friction angle between two dissimilar materials.

Table 2.10 (Continued)

INTERFACE MATERIALS	FRICTION FACTOR tan δ	(1) FRICTION ANGLE, δ (degrees)
Formed concrete or concrete sheet piling against the following soils:		
- Clean gravel, gravel-sand mixtures, well-graded rock fill with spalls	0.40 to 0.50	22 to 26
- Clean sand, silty sand-gravel mixture, single size hard rock fill	0.30 to 0.40	17 to 22
- Silty sand, gravel or sand mixed with silt or clay	0.30	17
- Fine sandy silt, nonplastic silt	0.25	14
Various structural materials:		
- Masonry on masonry, igneous and metamorphic rocks:		
* Dressed soft rock on dressed soft rock	0.70	35
* Dressed hard rock on dressed soft rock	0.65	33
* Dressed hard rock on dressed hard rock	0.55	29
- Masonry on wood (cross grain)	0.50	26
- Steel on stee at sheet pile interlocks	0.30	17

INTERFACE MATERIALS	SOIL COHESION, c (psf)	ADHESION, c_a (psf)
Very soft cohesive soil	(0 - 250)	0 - 250
Soft cohesive soil	(250 - 500)	250 - 500
Medium stiff cohesive soil	(500 - 1,000)	500 - 750
Stiff cohesive soil	(1,000 - 2,000)	750 - 950
Very stiff cohesive soil	(2,000 - 4,000)	950 - 1,300

2.5.5 Rankine Theory

The Rankine theory is applicable to conditions where the wall friction angle (δ) is equal to the slope of the backfill surface (i). As in the case of the Coulomb theory, it is assumed that the strength of the soil is fully mobilized.

Active Pressure

The active earth pressure considered in the Rankine theory is illustrated in Figure 2.13a for a level backfill condition. The coefficient of active earth pressure, K_a, can be expressed as:

$$K_a = \cos i \frac{\cos i - \sqrt{\cos^2 i - \cos^2 \phi_f}}{\cos i + \sqrt{\cos^2 i - \cos^2 \phi_f}} \qquad (2.25)$$

When the ground surface is horizontal, i.e. when $i = 0$, K_a can be expressed as:

$$K_a = \frac{1 - \sin \phi_f}{1 + \sin \phi_f} \qquad (2.26)$$

The active earth pressure, P_a, can be expressed as:

$$P_a = K_a \gamma z - 2c\sqrt{K_a} \qquad (2.27)$$

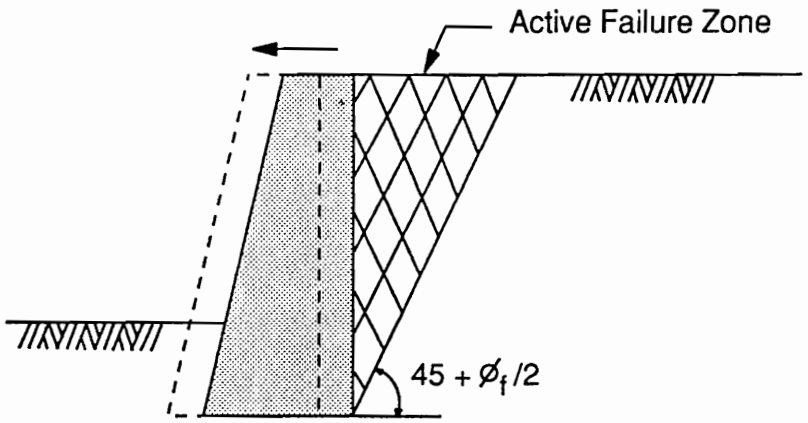

(a) Frictionless Wall Moves away from Backfill

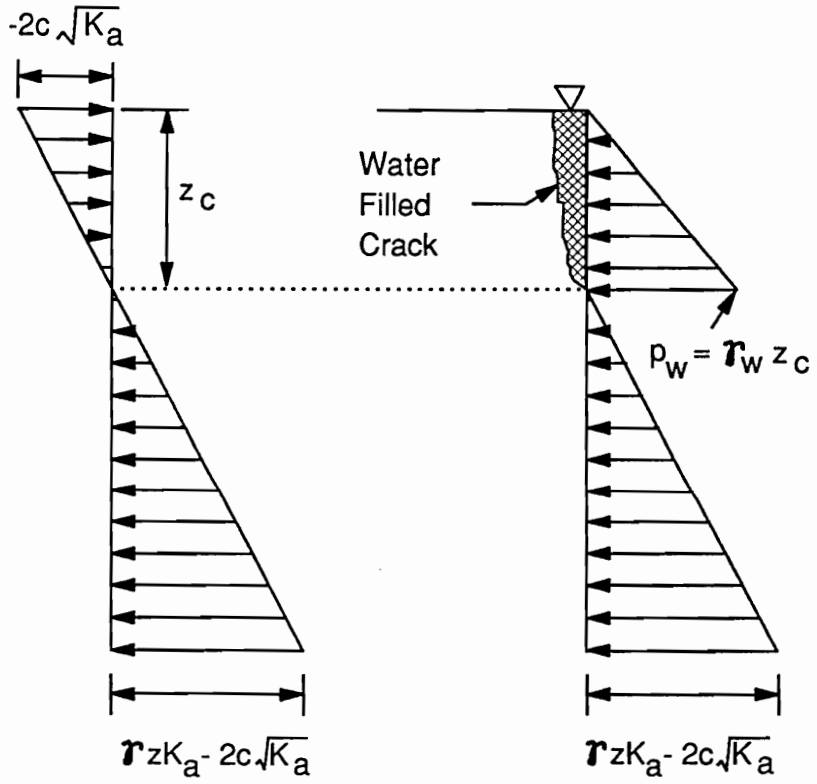

(b) Theoretical Active Pressure Distribution

(c) Water-Filled Crack In Tension Zone

Figure 2.13 Active Pressure, Frictionless Wall (After Clough and Duncan, 1991)

where P_a = the active pressure (force/length^2),

K_a = the active pressure coefficient,

γ = the unit weight of soil (force/length^3),

c = the cohesion (force/length^2),

z = the depth below the ground surface (length).

The variation of active pressure with depth is linear, as shown in Figure 2.13b. If the backfill is cohesive, the soil is theoretically in a tension zone down to a depth of $2 \cdot c/\gamma \cdot (K_a)^{1/2}$. However, a tension crack is likely to develop in that zone, and may be filled with water, so that hydrostatic pressure will be exerted on the wall, as shown in Figure 2.13c.

Passive Pressure

The Rankine theory can also be applied to passive pressure conditions. The passive earth pressure coefficient (K_p) can be expressed as:

$$K_p = \cos i \frac{\cos i + \sqrt{\cos^2 i - \cos^2 \phi_f}}{\cos i - \sqrt{\cos^2 i - \cos^2 \phi_f}} \qquad (2.28)$$

When the ground surface is horizontal, K_p can be expressed as:

$$K_p = \frac{1 + \sin \phi_f}{1 - \sin \phi_f} \tag{2.29}$$

The passive pressure at depth z can be expressed as:

$$P_p = K_p \gamma z + 2c\sqrt{K_p} \tag{2.30}$$

where P_p = the passive pressure (force/length^2),

K_p = the passive pressure coefficient.

2.5.6 Log Spiral Analysis

The failure surface in most cases is more closely approximated by a log spiral than a straight line, as shown in Figure 2.14. Active and passive pressure coefficients, K_a and K_p obtained from analyses using log spiral surfaces are listed in Tables 2.11 and 2.12 (Caquot and Kerisel, 1948). Values of K_a and K_p for walls with level backfill and vertical stem are also shown in Figure 2.15. These values are also based on the log spiral analyses performed by Caquot and Kerisel.

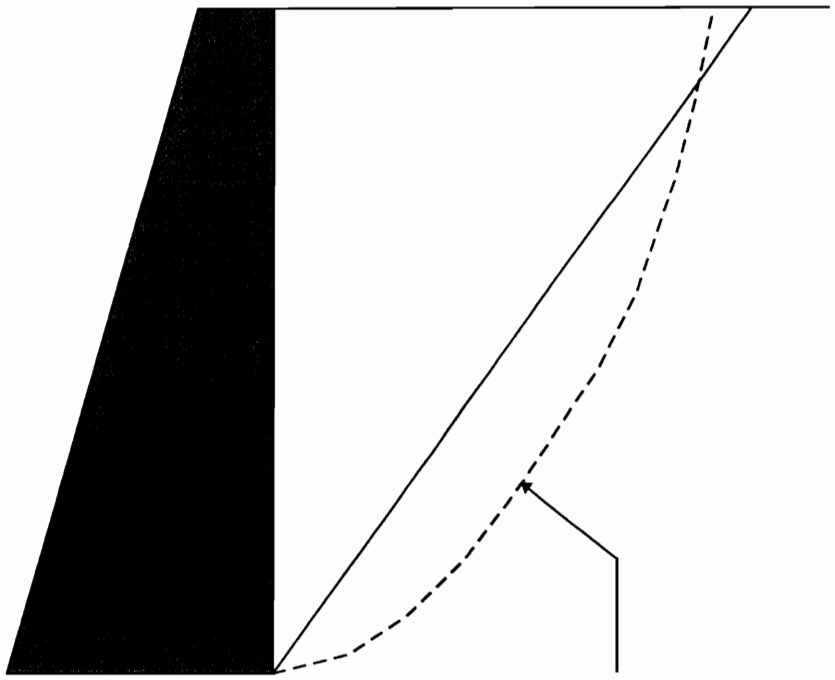

Figure 2.14 Comparison of Log Spiral and Straight Line Failure Surfaces for Active Conditions (From Clough and Duncan, 1991)

Table 2.11 Values of K_a for Log Spiral Failure Surface (After Caquot and Kerisel, 1948)

δ °	i °	β °	ϕ_f °					
			20	25	30	35	40	45
0	-15	-10	0.37	0.30	0.24	0.19	0.14	0.11
		0	0.42	0.35	0.29	0.24	0.19	0.16
		10	0.45	0.39	0.34	0.29	0.24	0.21
	0	-10	0.42	0.34	0.27	0.21	0.16	0.12
		0	0.49	0.41	0.33	0.27	0.22	0.17
		10	0.55	0.47	0.40	0.34	0.28	0.24
	15	-10	0.55	0.41	0.32	0.23	0.17	0.13
		0	0.65	0.51	0.41	0.32	0.25	0.20
		10	0.75	0.60	0.49	0.41	0.34	0.28
ϕ_f	-15	-10	0.31	0.26	0.21	0.17	0.14	0.11
		0	0.37	0.31	0.26	0.23	0.19	0.17
		10	0.41	0.36	0.31	0.27	0.25	0.23
	0	-10	0.37	0.30	0.24	0.19	0.15	0.12
		0	0.44	0.37	0.30	0.26	0.22	0.19
		10	0.50	0.43	0.38	0.33	0.30	0.26
	15	-10	0.50	0.37	0.29	0.22	0.17	0.14
		0	0.61	0.48	0.37	0.32	0.25	0.21
		10	0.72	0.58	0.46	0.42	0.35	0.31

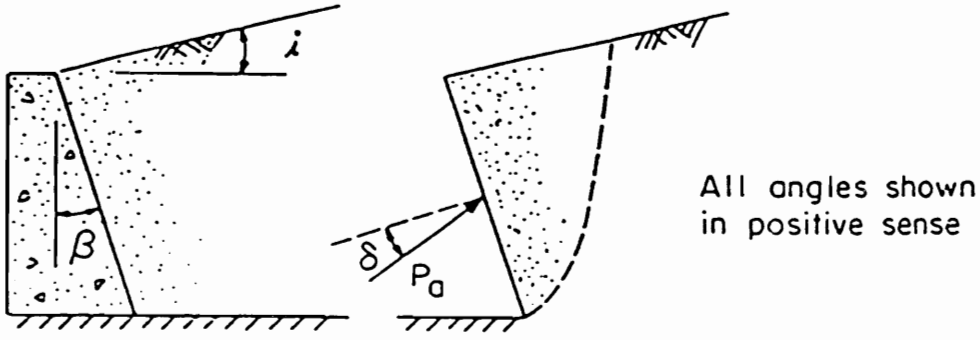

Table 2.12 Values of K_p for Log Spiral Failure Surface (After Caquot and Kerisel, 1948)

δ	i	β	ϕ_f					
			20	25	30	35	40	45
		-10	1.32	1.66	2.05	2.52	3.09	3.95
	-15	0	1.09	1.33	1.56	1.82	2.09	2.48
		10	0.87	1.03	1.17	1.30	1.33	1.54
		-10	2.33	2.96	3.82	5.00	6.68	9.20
0	0	0	2.04	2.46	3.00	3.69	4.59	5.83
		10	1.74	1.89	2.33	2.70	3.14	3.69
		-10	3.36	4.56	6.30	8.98	12.2	20.0
	15	0	2.99	3.86	5.04	6.72	10.4	12.8
		10	2.63	3.23	3.97	4.98	6.37	8.2
		-10	1.95	2.90	4.39	6.97	11.8	22.7
	-15	0	1.62	2.31	3.35	5.04	7.99	14.3
		10	1.29	1.79	2.50	3.58	5.09	8.86
		-10	3.45	5.17	8.17	13.8	25.5	52.9
$-\phi_f$	0	0	3.01	4.29	6.42	10.2	17.5	33.5
		-10	2.57	3.50	4.98	7.47	12.0	21.2
		-10	4.95	7.95	13.5	24.8	50.4	11.5
	15	0	4.42	6.72	10.8	18.6	39.6	73.6
		10	3.88	5.62	8.51	13.8	24.3	46.9

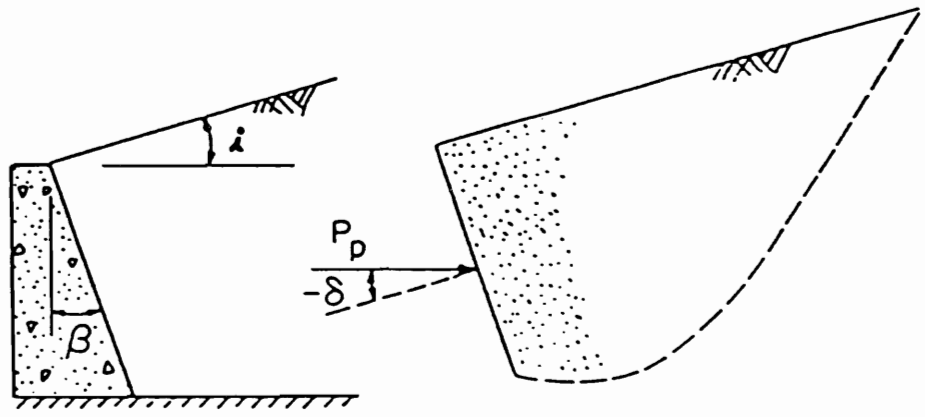

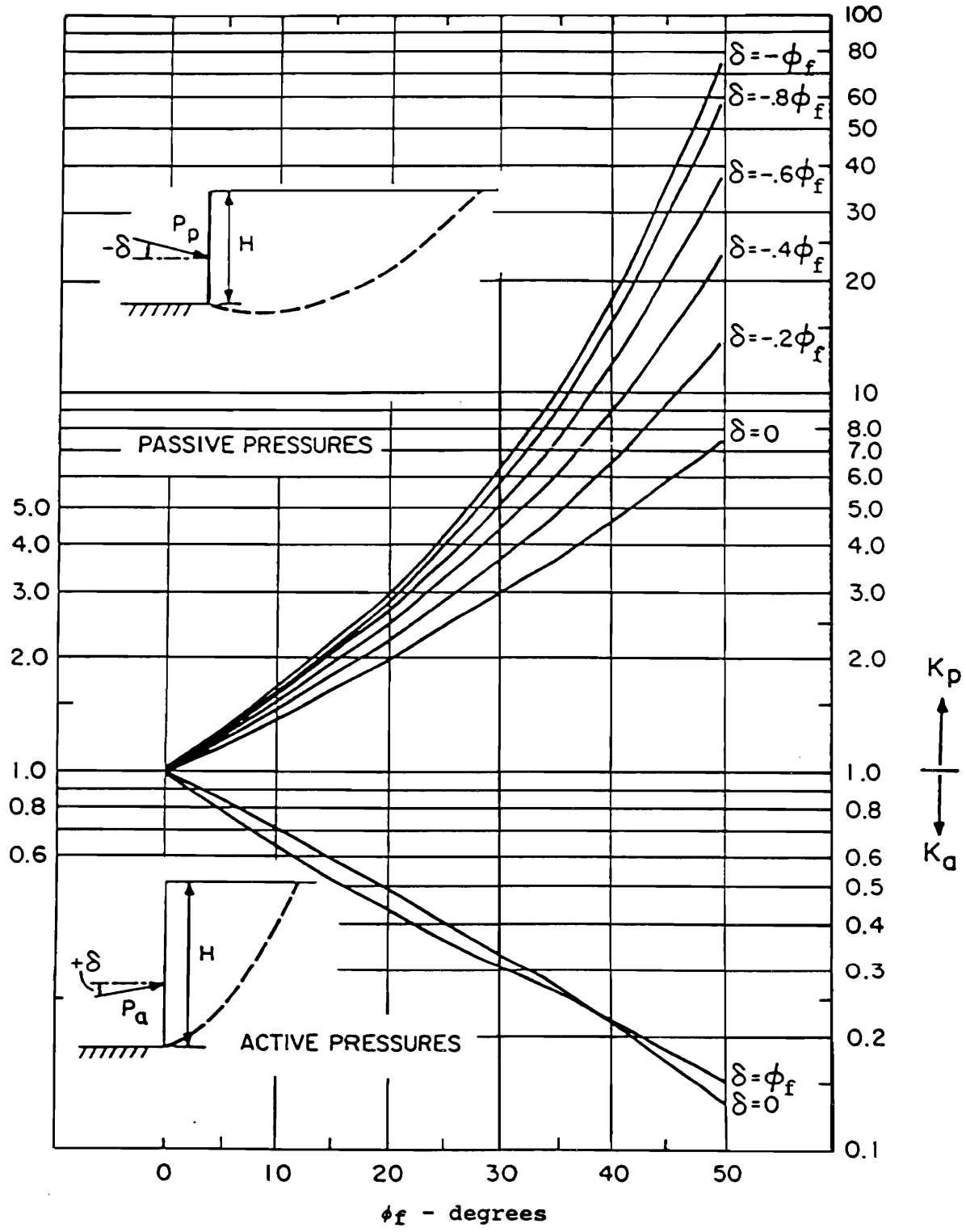

Figure 2.15 Active and Passive Pressure Coefficients for Vertical Wall and Horizontal Backfill - Based on Log Spiral Failure Surfaces (After Caquot and Kerisel, 1948)

2.5.7 Selection of Earth Pressure Coefficients

Selecting a proper earth pressure coefficient is essential for a successful wall design. A number of methods previously discussed can be used to decide the magnitude of the coefficients.

An alternative method is to use a hydrostatic fluid pressure which is equivalent to the product of an earth pressure coefficient and the unit weight of the soil. A decision on what type of earth pressure coefficient should be used is based on the direction and the magnitude of the wall movement. Table 2.9, Figure 2.10 and Figure 2.11 can be useful in this procedure.

The New Zealand Ministry of Works and Development (N.Z.M.W.D., 1979) has recommended the following static earth pressure coefficients for use in design:

1. Counterfort or gravity walls founded on rock or piles : K_o
2. Cantilever walls less than 16 ft high founded on rock or piles : $0.5 (K_o + K_a)$
3. Cantilever walls higher than 16 ft or any wall founded on a spread footing : K_a

N.Z.M.W.D. (1979) also recommended that K_o should be used for the types of abutments that are not mentioned above. Earth pressures on integral abutments or framed abutments may be higher than active due to thermal movements of the bridge superstructure.

2.5.8 Location of Horizontal Resultant

In conventional designs and analyses, the horizontal resultant is assumed to be located at one third of total height from the bottom of the wall. However, several experimental tests performed by many researchers including Terzaghi (1934), Clausen and Johansen (1972), and Sherif et al (1982) have shown that the point of application is above the lower third point.

According to a study by Duncan et al (1990), Terzaghi found that the resultant was applied at 0.40H to 0.45H from the bottom of the wall, where H is the total height of the wall. Clausen and Johansen found the same range of locations as Terzaghi's, and Sherif et al recommended 0.42H for a wall in static active condition. However, Duncan et al (1990) suggested that the location of the resultant should be assumed to be 0.40H above the bottom of the wall.

2.5.9 Equivalent Fluid Pressure

Equivalent fluid pressures provide a convenient means of estimating design earth pressures, especially when the backfill material is a clayey soil.

The lateral earth pressure at depth z can be expressed as:

$$p_h = \gamma_{eq} \cdot z \qquad (2.31)$$

where p_h = lateral earth pressure (force/length^2),

γ_{eq} = equivalent fluid unit weight (force/length^3);
unit weight of a fluid that would exert the same pressure as the backfill soil,

z = depth below the surface of backfill (length).

Some typical equivalent fluid unit weights and corresponding pressure coefficients are presented in Table 2.13. These are appropriate for use in designing walls up to about 20 ft in height. Values are presented for at-rest condition and for walls that can tolerate movements of 1 inch in 20 ft, and for level and sloped backfill.

2.6 EFFECT OF SURCHARGES

When vertical loads act on a surface of the backfill near a retaining wall or an abutment, the lateral and vertical earth pressure used for the design of the wall should be increased.

Table 2.13 Coefficients and Unit Weights for Equivalent Fluid Pressure (From Clough and Duncan, 1991)

Type of Soil	Equivalent Fluid Unit Weights and Pressure Coefficients							
	Level Backfill				Backfill 2(H) on 1(V)			
	At-Rest		Δ/H = 1/240		At-Rest		Δ/H = 1/240	
	γ_{eq} (pcf)	K	γ_{eq} (pcf)	K	γ_{eq} (pcf)	K	γ_{eq} (pcf)	K
Loose Sand or Gravel	55	0.45	40	0.35	65	0.55	50	0.45
Medium Dense Sand or Gravel	50	0.40	35	0.25	60	0.50	45	0.35
Dense Sand or Gravel	45	0.35	30	0.20	55	0.45	40	0.30
Compacted Silt (ML)	60	0.50	40	0.35	70	0.60	50	0.45
Compacted Clay (CL)	70	0.60	45	0.40	80	0.70	55	0.50
Lean Compacted Fat Clay (CH)	80	0.65	55	0.50	90	0.75	65	0.60

$P_h = \gamma_{eq}\, z + K\, q_s$

where γ_{eq} = equivalent fluid unit weight,

z = depth below ground surface,

K = horizontal earth pressure coefficient,

q_s = uniform surcharge pressure.

2.6.1 Uniform Surcharge Load

A surcharge load uniformly distributed over a large ground surface area increases both the vertical and the lateral pressures. The increase in the vertical pressure, Δp_v is the same as the applied surcharge pressure, q_s. That is,

$$\Delta p_v = q_s \tag{2.32}$$

and the amount of increase in the lateral pressure, Δp_h is

$$\Delta p_h = K \cdot q_s \tag{2.33}$$

where K = an earth pressure coefficient (dimensionless),

K = K_a for active pressure,

K = K_o for at-rest condition,

K = K_p for passive pressure.

Because the applied area is infinitely large, the increases in both vertical and horizontal pressures are constant over the height of the wall. Therefore, the horizontal resultant force due to a surcharge load is located at mid-height of the wall.

2.6.2 Point Load, Line Load, and Strip Load

The theory of elasticity can be used to estimate the increased earth pressures induced by various types of surcharge loads. Equations for earth pressures due to point loads, line loads, and strip loads are presented in Figure 2.16.

2.7 LIMIT STATES AND DESIGN CRITERIA

2.7.1 Limit States

Retaining walls and abutments are subject to various limit states or types of failure, as illustrated in Figure 2.17. Failures can occur within soils or the structural members. Sliding failure (Figure 2.17a) occurs when the lateral earth pressure exerted on the wall exceeds the frictional sliding capacity of the wall. If the bearing pressure is larger than the capacity of the foundation soil or rock, bearing failure (Figure 2.17b) results. Deep-seated sliding failure (Figure 2.17c) may develop in clayey soils. Structural failure (Figure 2.17d) also should be checked.

2.7.2 Design Criteria

For design purposes, retaining walls on spread footings can be classified into three categories (Duncan et al., 1990):

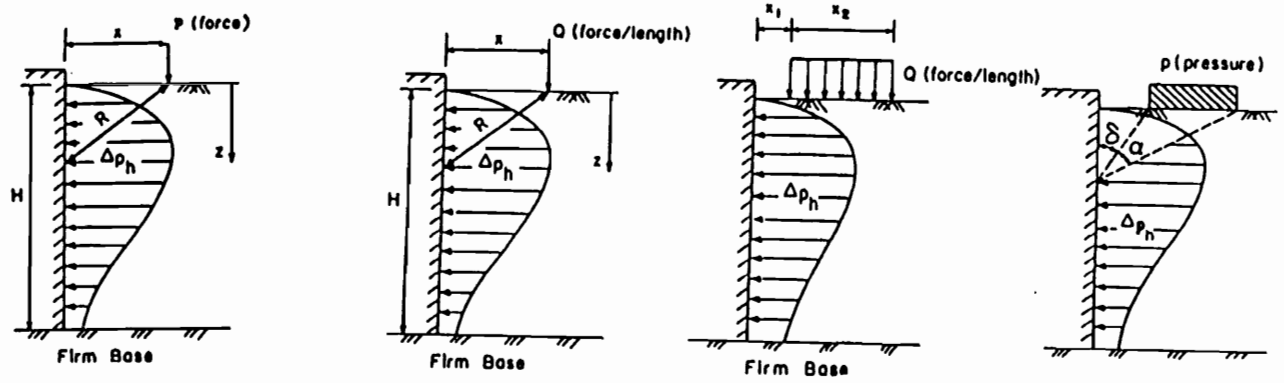

(a) Point Load

(b) Infinitely long line load parallel to wall

(c) Finite line load perpendicular to wall

(d) Uniformly loaded strip parallel to wall

$$\Delta p_h = \frac{P}{\pi R^2}\left[\frac{3zx^2}{R^3} - \frac{R(1-2\nu)}{R+z}\right]$$

$$\Delta p_h = \frac{4Q}{\pi}\frac{x^2 z}{R^4}$$

$$\Delta p_h = \frac{Q}{\pi z}\left(\frac{1}{\left[1+\left(\frac{z}{x_2}\right)^2\right]^{3/2}} - \frac{1-2\nu}{\left[1+\left(\frac{z}{x_2}\right)^2\right]^{1/2}+\frac{z}{x_2}} - \frac{1}{\left[1+\left(\frac{z}{x_1}\right)^2\right]^{3/2}} + \frac{1-2\nu}{\left[1+\left(\frac{z}{x_1}\right)^2\right]^{1/2}+\frac{z}{x_1}}\right)$$

$$\Delta p_h = \frac{2p}{\pi}\left[\alpha - \sin\alpha\cos(\alpha+2\delta)\right]$$

where ν = Poisson's ratio.

α in radian

Figure 2.16 Earth Pressure due to Point Loads, Line Loads and Strip Loads (From Clough and Duncan, 1991)

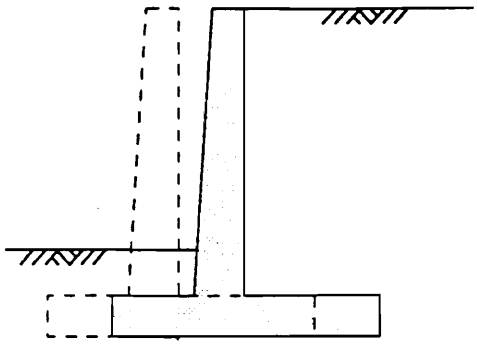

(a) Sliding Failure

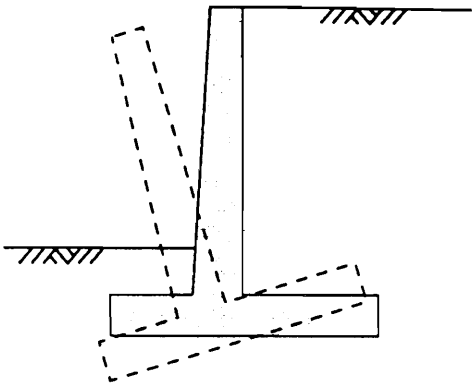

(b) Bearing Failure Associated with Overturning

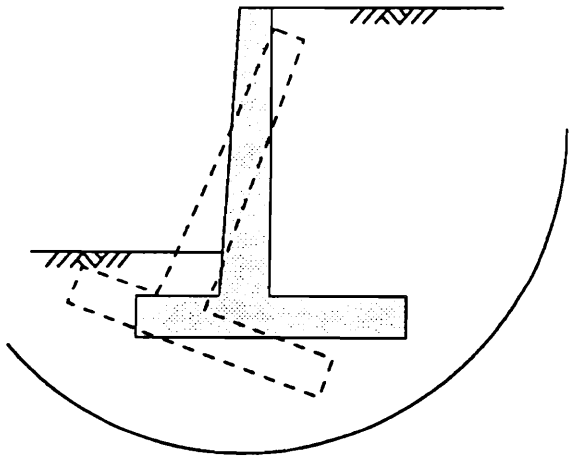

(c) Deep-seated Sliding Failure

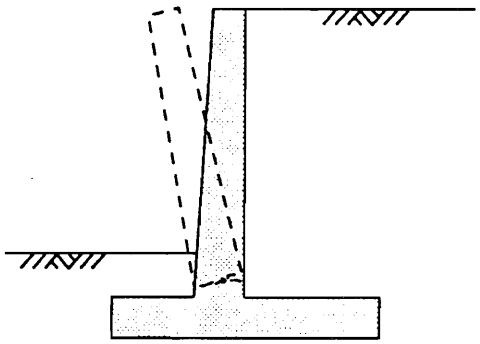

(d) Structural Failure

Figure 2.17 Failure Modes for Retaining Walls

1. walls with clayey soils in the backfill or foundation,
2. walls with granular backfills and foundations of sand or gravel,
3. walls with granular backfills and foundations on rock.

For each category, design procedures and stability criteria for the ASD method and the LFD method are summarized in Figures 2.18 through 2.20. The uniform pressure distributions shown in the figures are based on the method presented by Meyerhof (1953). Gravity walls are used in the figures, but the procedures and criteria are equally applicable to semi-gravity, cantilever, and other types of retaining walls or abutments that develop similar foundation pressures when subjected to lateral forces.

2.8 DESIGN PROCEDURES

In both ASD and LFD, a series of steps must be followed to obtain a satisfactory design. These are:

1. Select preliminary proportions of the wall.
2. Determine loads and earth pressures.
3. Calculate magnitude of reaction forces on base.

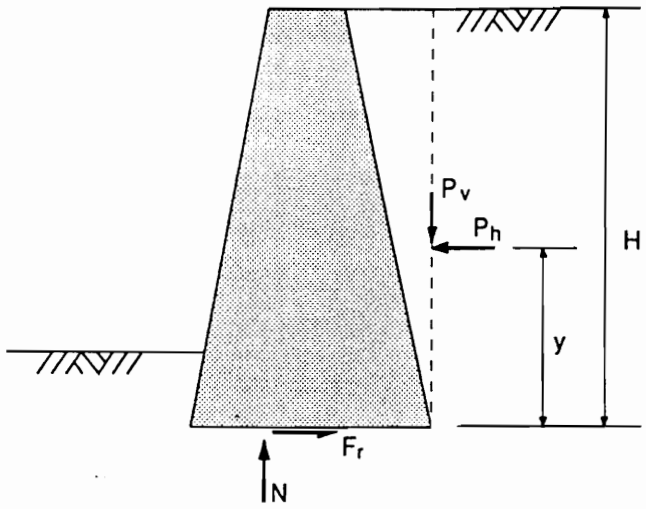

Earth Loads:

P_v and P_h based on experience, with allowance for creep

$y = 0.4\ H$

Stability Criteria:

ASD Method

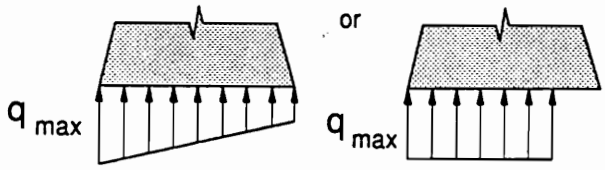

(1) N within middle third of base

(2) $R_I q_{ult} / FS \geq q_{max\ (unfactored)}$

(3) Safe against sliding:

$F_r / FS \geq P_h$ (unfactored)

(4) Settlement within tolerable limits

(5) Safe against deep-seated foundation failure.

LFD Method

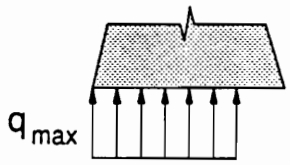

(1) N within middle half of base

(2) $\phi R_I q_{ult} \geq q_{u\ max}$

(3) Safe against sliding:

$\phi_s F_r \geq \Sigma \gamma_i P_{hi}$

(4) Settlement within tolerable limits

(5) Safe against deep-seated foundation failure.

Figure 2.18 Earth Loads and Stability Criteria for Walls with Clayey Soils in the Backfill or Foundation (After Duncan et al, 1990)

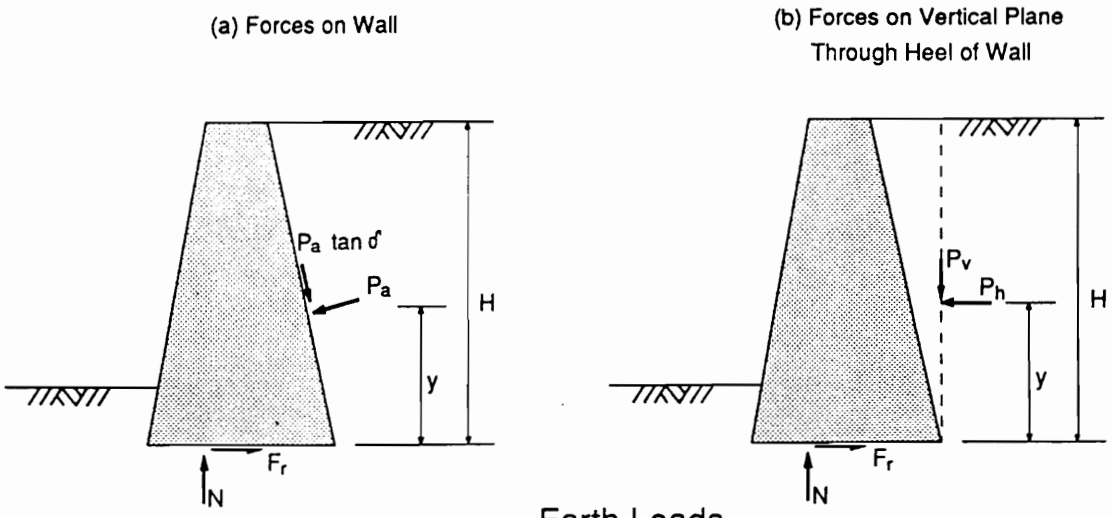

Earth Loads

P_a and P_h calculated using Coulomb active earth pressure theory
δ or P_a estimated using judgement, with allowance for movement of backfill relative to wall.
$y = 0.4\ H$

Stability Criteria

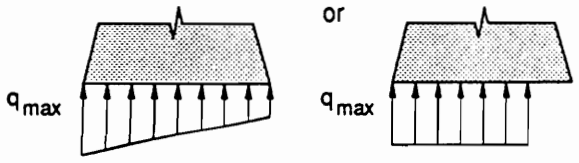

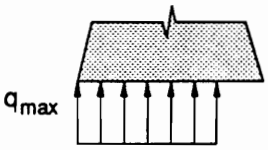

(1) N within middle third of base

(2) $R_I\, q_{ult} / FS \geq q_{max\ (unfactored)}$

(3) Safe against sliding:

$F_r / FS \geq P_{h\ (unfactored)}$

(4) Settlement within tolerable limits

(1) N within middle half of base

(2) $\phi R_I\, q_{ult} \geq q_{u\,max}$

(3) Safe against sliding:

$\phi_s F_r \geq \Sigma r_i P_{h_i}$

(4) Settlement within tolerable limits

Figure 2.19 Earth Loads and Stability Criteria for Walls with Granular Backfills or Foundations on Sand or Gravel (After Duncan et al, 1990)

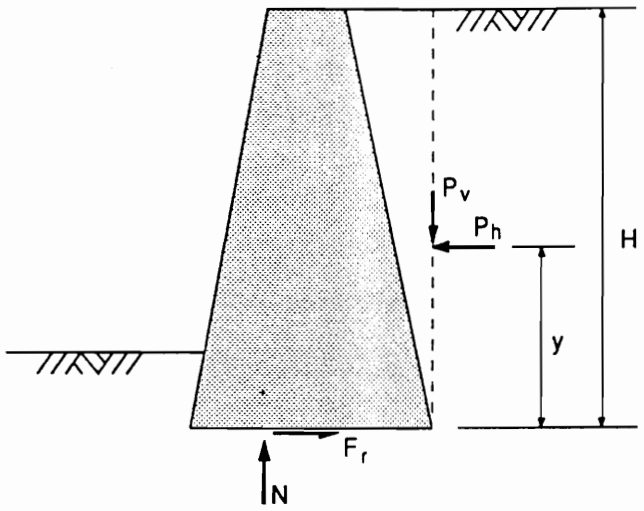

Earth Loads

P_h based on at-rest pressure

K_o : refer to Table 4.6

P_v estimated using judgement

$y = 0.4\ H$

Stability Criteria

ASD Method

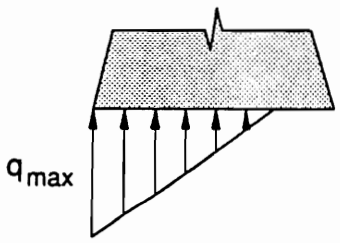

(1) N within middle half of base

(2) $R_I\ q_{ult} / FS \geq q_{max\ (unfactored)}$

(3) Safe against sliding

$F_r / FS \geq P_{h\ (unfactored)}$

LFD Method

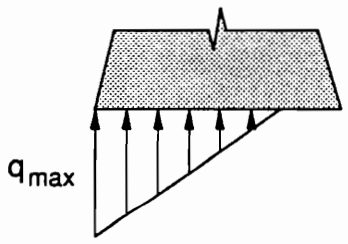

(1) N within middle three quarters of base

(2) $\phi R_I\ q_{ult} \geq q_{u\ max}$

(3) Safe against sliding

$\phi_s\ F_r \geq \Sigma \gamma_i\ P_{h_i}$

Figure 2.20 Earth Loads and Stability Criteria for Walls with Granular Backfills and Foundations on Rock (After Duncan et al, 1990)

4. Check stability and safety criteria:

    (a) location of normal component of reactions

    (b) adequacy of bearing pressure

    (c) safety against sliding.

5. Revise proportions of wall and repeat steps 2 through 4 until stability criteria are satisfied and then check:

    (a) settlement within tolerable limits

    (b) safety against deep-seated foundation failure.

6. If proportions become unreasonable, consider a foundation supported on driven piles or drilled shafts.

7. Compare economics of completed design with other wall systems.

2.8.1 Step 1. Preliminary Proportions

Figure 2.21 shows commonly used dimensions for a gravity retaining wall and a cantilever wall. These proportions can be used when scour is not a concern to obtain dimensions for a first trial.

2.8.2 Step 2. Loads and Earth Pressures

Design loads for a retaining wall or an abutment are obtained by using group load combinations described in Table 2.2. Methods for calculating earth pressures

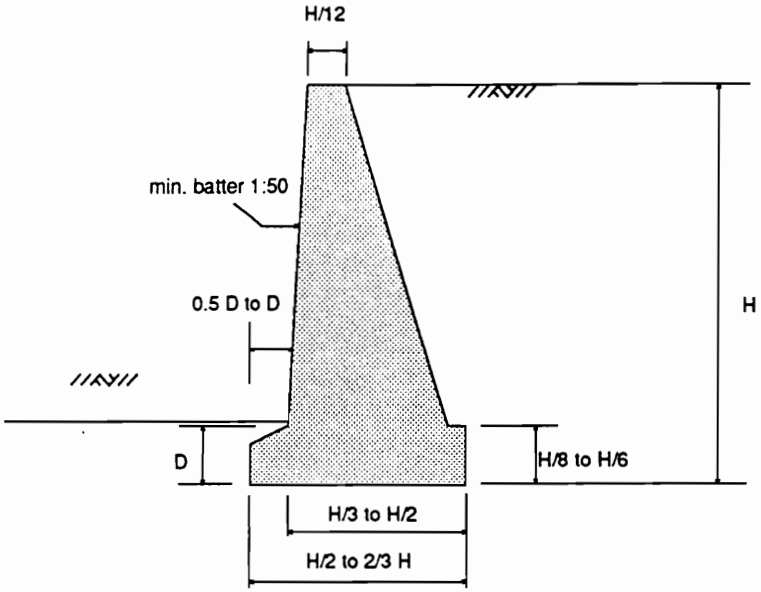

(a) Mass Concrete Wall

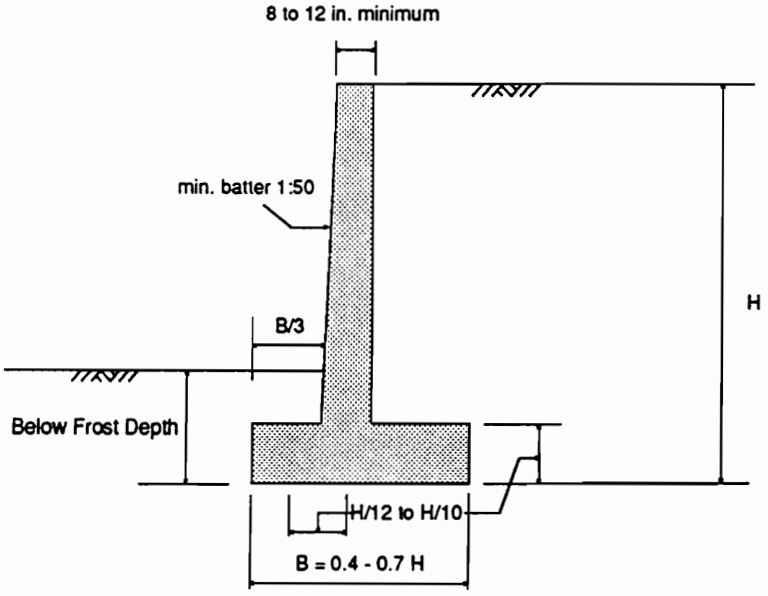

(b) Cantilever Wall

Figure 2.21 Preliminary Dimensions for Gravity Walls and Cantilever Walls (After Clayton and Milititsky, 1986)

exerted on the wall are discussed in Section 2.5. The use of equivalent fluid pressures presented in Table 2.13 gives satisfactory earth pressures if conditions are not unusual.

2.8.3 Step 3. Reaction Forces on Base

Figure 2.22 illustrates a typical cantilever wall subjected to various loads causing reaction forces which are normal to the base (N) and tangent to the base (F_r). These reaction forces are determined by simple statics for each load combination being investigated.

2.8.4 Step 4. Stability Criteria

(a) The location of the resultant on the base is determined by balancing moments about the toe of the wall. The criteria for foundations on soil for the location of the resultant is that it must lie within the middle one third for ASD and the middle half for LFD. This criterion replaces the check on the ratio of stabilizing moment to overturning moment. For foundations on rock, the acceptable location of the resultant has a greater range than for foundations on soil (see Figure 2.20).

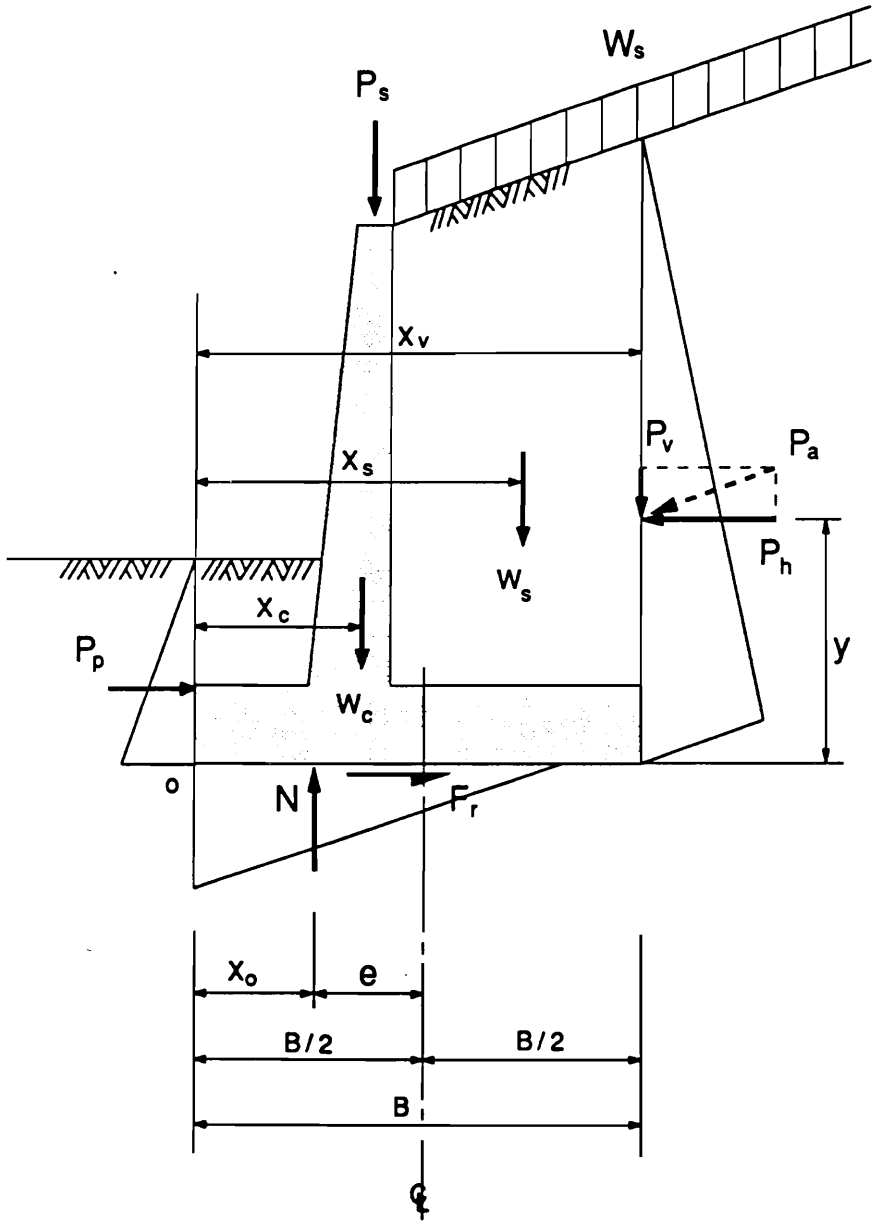

Figure 2.22 Forces on a Typical Retaining Wall or Abutment

As shown in Figure 2.22, the location of the resultant, X_o, is obtained by:

$$X_o = \frac{\text{Summation of moments about point o}}{N} \qquad (2.34)$$

where N = the vertical resultant force (force/length).

The eccentricity of the resultant, e, with respect to the centerline of the base is:

$$e = \frac{B}{2} - X_o \qquad (2.35)$$

where B = base width (length).

(b) Safety against bearing failure is obtained by applying a safety factor to the ultimate bearing capacity in the ASD method or by applying a performance factor to the ultimate bearing capacity in the LFD method. The ultimate bearing capacity can be calculated from in situ tests or semi-empirical procedures as presented in an engineering manual for shallow foundations (Barker et al., 1991).

Safety against bearing failure is checked by:

$$\text{In ASD:} \quad R_I \, q_{ult} \; / \; FS \geq q_{max} \tag{2.36}$$

$$\text{In LFD:} \quad \phi \, R_I \, q_{ult} \geq q_{umax} \tag{2.37}$$

where q_{ult} = ultimate bearing capacity (force/length^2),

R_I = reduction factor due to inclined loads,

FS = factor of safety,

ϕ = performance factor,

q_{max} = maximum bearing pressure due to unfactored loads (force/length^2),

q_{umax} = maximum bearing pressure due to factored loads (force/length^2).

Shape of Bearing Pressure Distribution

The shape of the bearing pressure distribution for soil foundations can be treated as a triangle, a trapezoid or a rectangle, and for rock foundations treated as a triangle or a trapezoid (see Figures 2.18 through 2.20). Therefore, the resultant, N, will pass through the centroid of a triangular or trapezoidal stress distribution or the middle of a uniformly distributed stress block, as illustrated in Figure 2.23.

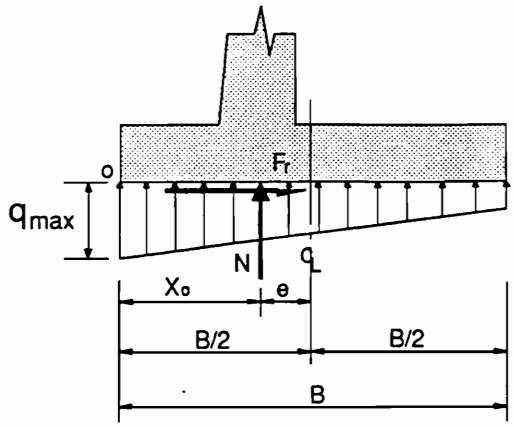

(a) Trapezoidal Distribution

$$q_{max} = \frac{N}{B} + \frac{6\,N\,e}{B^2}$$

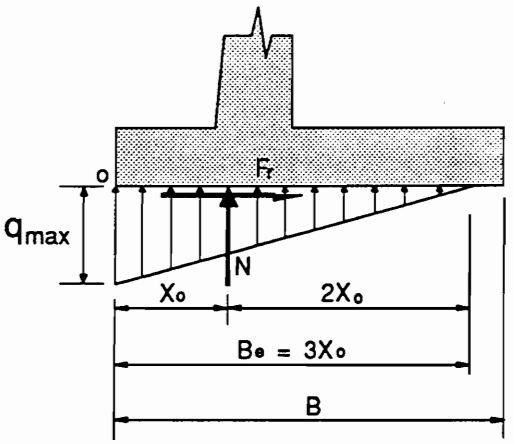

(b) Triangular Distribution

$$q_{max} = \frac{2\,N}{3\,X_o}$$

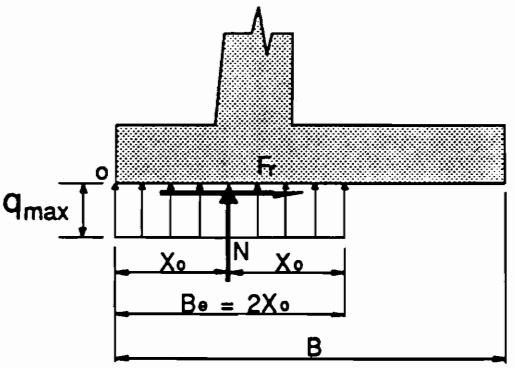

(c) Rectangular Distribution

$$q_{max} = \frac{N}{2\,X_o}$$

Figure 2.23 Various Shapes of Stress Distributions and Maximum Bearing Pressures

Maximum Bearing Pressure

The following equations are used to compute the maximum soil pressures, q_{max} and q_{umax} (both indicated as $q_{(u)max}$, where (u) is not present in ASD), per unit length of a rigid footing.

For a triangular shape of bearing pressure:

(i) when the resultant is within the middle third of base:

$$q_{(u)max} = \frac{N_{(u)}}{B} - \frac{6\,N_{(u)}\,e}{B^2} \qquad (2.38)$$

(ii) when the resultant is outside of the middle third of base:

$$q_{(u)max} = \frac{2\,N_{(u)}}{3\,X_o} \qquad (2.39)$$

For a uniform distribution of bearing pressure:

$$q_{(u)max} = \frac{N_{(u)}}{2\,X_o} \tag{2.40}$$

where $N_{(u)}$ = unfactored (factored) vertical resultant (force/length),

X_o = location of the resultant measured from toe (length),

e = eccentricity of $N_{(u)}$ (length).

(c) Sliding stability is checked in the ASD method by satisfying the following criteria:

$$\frac{F_r}{FS} \geq P_h \tag{2.41}$$

where FS = 1.5 for sands and 2.0 for clays whose shear strength is less than 0.5 times the normal pressure,

F_r = frictional resistance (force/length) or,

$= N \cdot \tan \delta_b + c_a \cdot B_e$,

N = resultant on base required for vertical equilibrium (force/length),

δ_b = friction angle between base and soil (degrees)

$= \phi_f$ of base soil for cast-in-place concrete, or

= the values given in Table 2.10,

c_a = adhesion (force/length^2),

c = cohesion of the base soil (force/length^2),

B_e = effective length of base in compression (length),

P_h = horizontal earth pressure force causing sliding (force/length).

In the LFD method, sliding stability is checked by

$$\phi_s F_{ru} \geq \sum \gamma_i P_{hi} \tag{2.42}$$

where $F_{ru} = N_u \cdot \tan \delta_b + c_a \cdot B_e$,

N_u = factored vertical resultant (force/length),

ϕ_s = performance factor for sliding

(values given in Table 2.3),

γ_i = load factor for force component i,

$= \gamma\beta_i$ shown in Table 2.2,

P_{hi} = horizontal earth pressure force i causing sliding (force/length).

As shown in Figure 2.22, the lateral pressure, P_h causes the wall to slide and is resisted by friction and adhesion between the base and foundation soil. According to the proposed revision to the AASHTO Specifications prepared by D'Appolonia (1989), the passive earth pressure, P_p generated by the soil in front of the wall may be included to resist sliding if it is ensured that the soil in front of the wall will exist permanently, for example, if the wall is embedded deeply below a covering

such as a sidewalk or pavement. When passive earth pressure is used, a safety factor of 2.0 or larger is recommended by Lambe and Whitman (1969). However, sliding failure occurs in many cases before the passive earth pressure is fully mobilized. Therefore, it is safer to ignore the effect of the passive earth pressure.

2.8.5 Step 5. Revise Proportions

When the preliminary wall dimensions are found inadequate, the wall dimensions should be adjusted by a trial and error method. A sensitivity study done by the authors shows that the stability can be improved by varying the location of the wall stem, the base width, and the wall height. Some suggestions for correcting each stability or safety problem are presented as follows:

Bearing Failure or Eccentricity Criterion Not Satisfied

1. Increase the base width.
2. Relocate the wall stem moving it toward the heel.
3. Minimize P_h by replacing a clayey backfill with granular material or by reducing pore water pressures behind the wall stem with a well-designed drainage system.

4. Provide an adequately designed reinforced concrete approach slab supported at one end by the abutment so that no horizontal pressure due to live load surcharge need be considered.

Sliding Stability Criterion Not Satisfied

1. Increase the base width.
2. Minimize P_h as described above.
3. Use an inclined base (heel side down) to increase horizontal resistance.
4. Provide an adequately designed approach slab as mentioned above.
5. Use a shear key*.

* The main function of a shear key is to generate additional passive soil pressure to increase sliding resistance. The considerations discussed earlier concerning the amount of displacement required to mobilize passive earth pressure are also important with regard to the resistance that can be achieved through the use of a key. Depending on local experience or job conditions, the design engineer must decide whether some passive earth pressure should be included or not.

Settlement and Overall Stability Check

Once the proportions of the wall have been selected to satisfy the bearing pressure, eccentricity and sliding criteria, then the requirements on settlement and overall slope stability must be checked.

(a) Settlement should be checked for walls founded on compressible soils to ensure that the predicted settlement is less than the settlement that the wall or structure it supports can tolerate. The magnitude of settlement can be estimated using the methods described in Engineering Manual for Shallow Foundations (Barker et al., 1991). For a determination of the allowable settlement, refer to the Engineering Manual for Estimating Tolerable Movements of Bridges (Barker et al., 1991).

(b) The overall stability of slopes with regard to the most critical sliding surface should be evaluated if the wall is underlain by weak soil. This check is based on limiting equilibrium methods which employ the modified Bishop, simplified Janbu or Spenser analysis. This subject is discussed in a number of design manuals and papers including NAVFAC DM-7.1 (1982a) and a manual by the Corps of Engineers (1989), and will not be covered in this study.

2.8.6 Step 6. Consider Deep Foundations

Driven piles and drilled shafts can be used when the configuration of the wall is unreasonable or uneconomical. Engineering manuals for driven piles and drilled shafts (Barker et al., 1991) may be consulted with regard to design of deep foundations to withstand vertical and lateral loads.

2.8.7 Step 7. Compare with Alternative Wall Systems

When a design is completed, it should be compared with other types of walls that may result in a more economical design. Detail information can be found in Section 2.2.1 and Section 10 of a manual by the Corps of Engineers (1989).

Chapter 3
SURVEY OF FAILURES

3.1 INTRODUCTION

A survey was conducted by Peck et al. (1948) in 1945 to obtain information on bridge abutments and retaining walls that had experienced unsatisfactory performance. The questionnaire was distributed to the chief engineers of 77 railroads in the United States and Canada.

A similar questionnaire was developed by the author in 1993 and sent to the departments of transportation of the fifty states and the District of Columbia to gather similar information for highway bridge abutments and retaining walls. This was done to determine if additional parameters should be included in the study of limit states for retaining walls. The survey results compared with the results of the previous one, provide a valuable source of new information for two reasons:

(a) The previous survey was conducted for railroad bridges. The results may be different for highway bridge abutments and walls because vehicle loads and design standards are different.

(b) After forty-eight years, another type of failure trend, which was not detected previously, may now exist.

3.2 SURVEY BY PECK ET AL. IN 1945

In the survey by Peck et al. (1948) about fifty-two percent of the engineers surveyed responded and thirty-one percent reported no significant problems with the behavior of abutments and retaining walls. The remaining twenty-one percent reported some incidence of unsatisfactory experience with walls and abutments. Based on their survey results and the fact that about eighty percent of the surveyed individuals reported no problem or did not reply, Peck, et al. made a conclusion that a majority of abutment and wall designs could be considered successful. A companion conclusion was that the present design methods were probably conservative.

As presented in Figure 3.1a, the height of unsatisfactory abutments and retaining walls ranges from 5 ft to 60 ft and average height was about 25 ft. As shown in Figure 3.1b, the majority of the abutments and walls reported as having failed or performed in an unsatisfactory manner moved forward six to twelve inches. The survey result suggested that movements less than about three inches could be considered practically normal and tolerable.

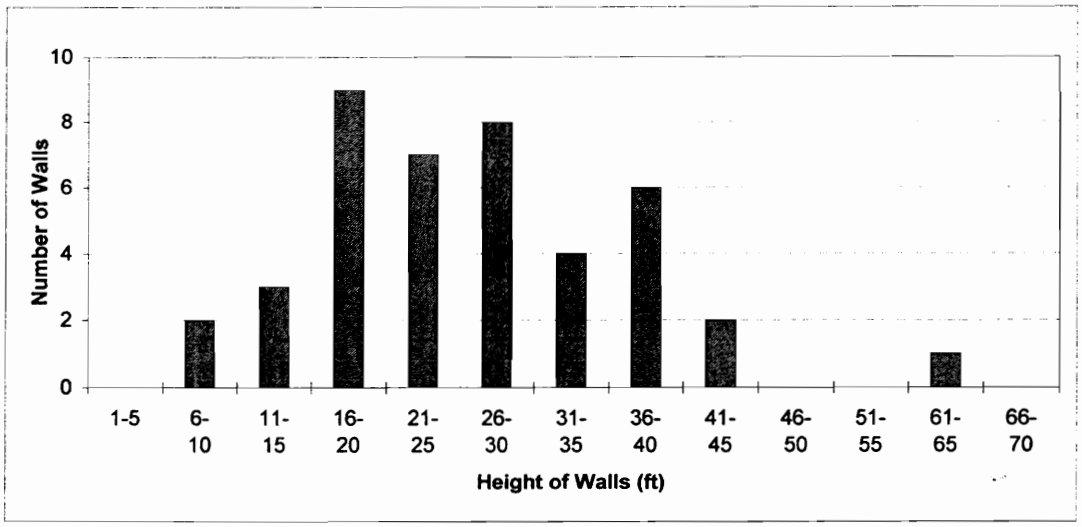

(a) Height of Walls and Abutments Reported

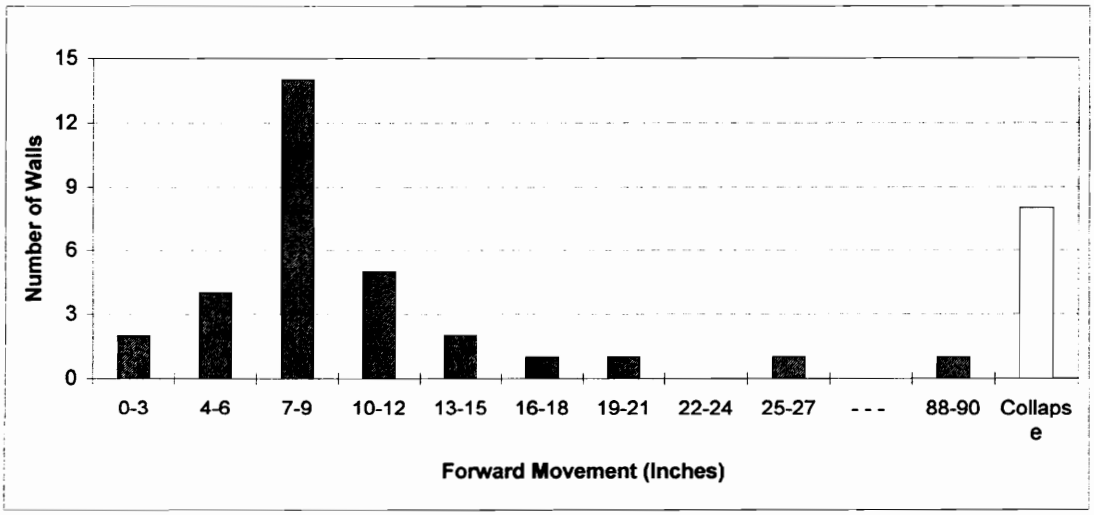

(b) Reported Movement of Walls and Abutments

Figure 3.1 Height and Movement of Walls and Abutments (Peck et al., 1948)

In Figure 3.2a, the walls are categorized according to the type of movement that they experienced. More than half of the walls experienced a progressive outward or tilting movement.

Figure 3.2b classifies the foundation and backfill materials of the wall which experienced progressive outward or tilting movement. All of the walls subjected to progressive movement were either backfilled with clay or founded on clay, and in most cases clay was used in both. According to Peck et al., the walls founded on clay or backfilled with clay probably have a lower safety factor than conventionally believed. No failures were reported for walls founded on sand or rock and backfilled with granular material. This result may indicate that the conventional design methods for such walls must be quite conservative.

3.3 SURVEY CONDUCTED IN 1993

In the survey conducted for this study, thirty-seven responses out of fifty-one requests have been received, which is a return of seventy-three percent. Among thirty-seven responses, five indicated that records were not available and eleven reported no failure. The remaining twenty-one (40%) reported a number of cases of unsatisfactory behavior of walls. The cover letter and the questionnaire are attached in the appendix. The states responded are summarized in Figure 3.3.

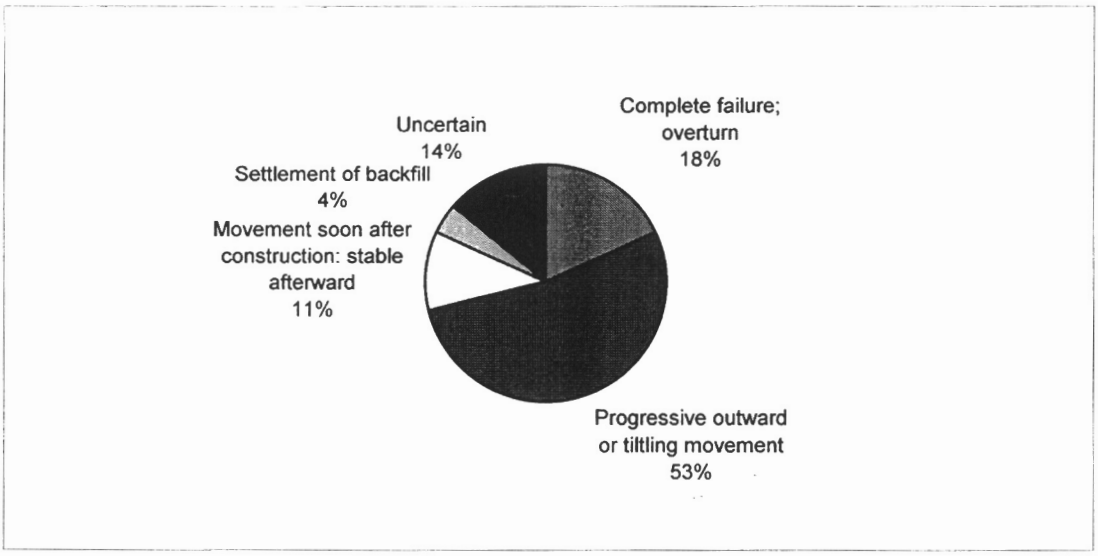

(a) Types of Unsatisfactory Behavior

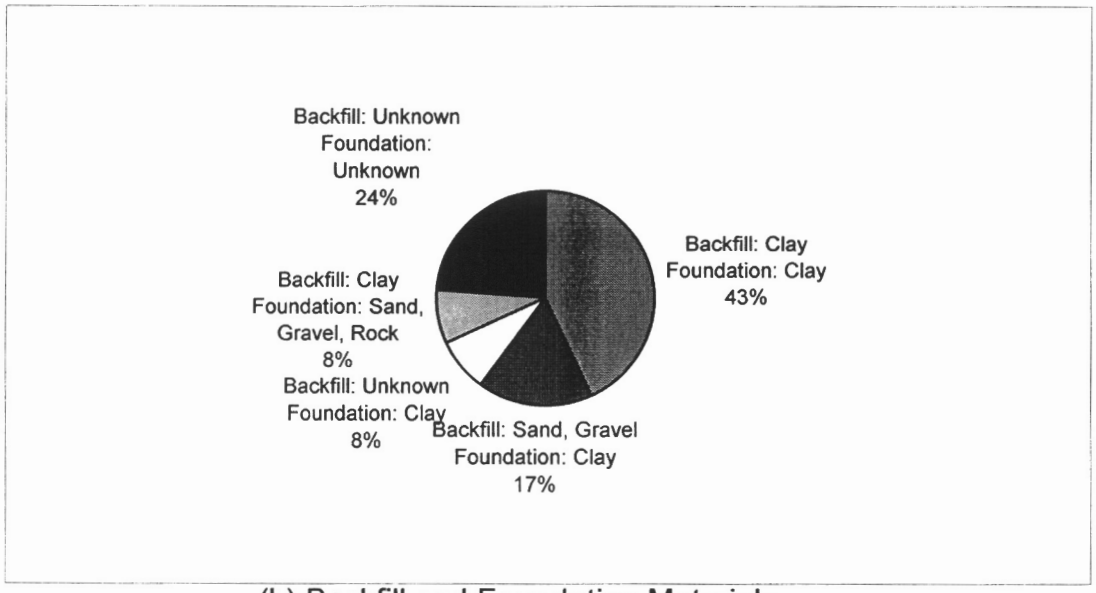

(b) Backfill and Foundation Materials
Walls Subject to Progressive Outward Movement

Figure 3.2 Types of Unsatisfactory Behavior and
Backfill and Foundation Materials (Peck, et al., 1948)

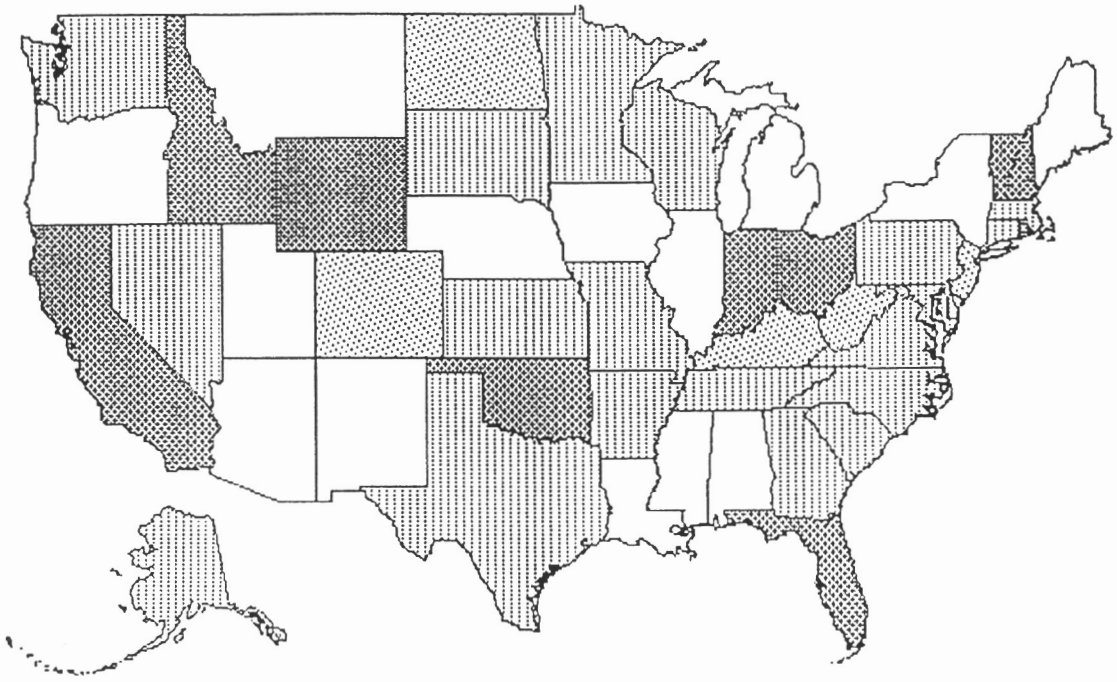

Records Unavailable (5): CO, KY, ND, NJ, WV

No Failure Occured (11): CA, DC, FL, ID, IN, NH, OH, OK, RI, VT, WY

Failure Occured (21): AK, AR, CT, DE, GA, KS, MA, MD, MN, MS, NC, NV, NY, PA, SC, SD, TN, TX, VA, WA, WI

Total 37 out of 51 responded.

Figure 3.3 States Responding to the Survey

About 125 walls and abutments which failed completely or experienced undesirable movements were reported by the twenty-one states. The detailed information on these structures is summarized in Table 3.1. Some of the responses were not complete and limited to local jurisdiction rather than state wide. The table displays height of walls, type of footings, type of backfill and foundation materials, amount of movement, and type of unsatisfactory behavior.

Table 3.2 summarizes the total number of bridges and walls in each jurisdiction and an estimate of the probability of failure. The total number of bridges listed is that given by the states in response to the questionnaire. In many cases this did not agree with the number given in National Bridge Inventory (1992).

The actual probability of failure for abutments was obtained by dividing the total number of failed abutments (FAN) by total number of abutments reported (TAN). Because states often did not indicate whether one abutment or both abutments failed, it has been assumed that if one abutment fails this constitutes a bridge failure. The actual probability of failure for retaining walls was also calculated by dividing the total number of failed retaining walls (FWN) by total number of

Table 3.1 Summary of Responses

State	Wall or Abut	Height (ft)	Footing Type	Soil Type		Amount of Movement (in.)				Type of Unsatisfactory Behavior
				Backfill	Found.	For ward	Back ward	Down ward	Up ward	
AK	W	18	spread	S	C	6		4		PG
	W	18	spread	S	C	3		2		SB
AR	W	15	spread	U	R	12				PG
	W	10	spread	U	R	10				PG
	W	20	pile	U	U	12				PG
CT	A	U	U	U	U					UN
	A	U	U	U	U					UN
	W	U	U	U	U					UN
	W	U	U	U	U					UN
	W	U	U	U	U					UN
	W	U	U	U	U					UN
DE	A	U	spread	U	U	6				PG
GA	W	15	spread	S	U					PG
KS	W	25	spread	C	C	5				PG
	W	20	spread	S	S					SB
	W	12	spread	S	C	TF				PG
	W	20	spread	S	C					SB
MA	W	U	spread	C	C	15				PG
MD	A	11	spread	U	U	2.5				MS
	A	U	spread	U	U			1.8		MS
	A	6	pile	S	C	3				MS
	A	18	spread	S	C			0.25		MS
	A	U	spread	U	U			0.25		MS
MN	W	13.5	spread	U	U					SB
	A	16	spread	U	U	2.5				PG
	A	13	pile	U	U	6				PG
	A	10	pile	S	C			42		SB
	A	12	pile	S	S	6				PG
	A	12	pile	S	C	7				PG
	A	9	pile	S	C			24		PG
	A	9	pile	S	C			18		SB
	A	30	pile	S	U	1.75				MS
	A	16	pile	U	U	2.5				PG
MS	W	25	spread	S	U			2		SB
	W	25	spread	S	C			5		SB
	W	25	spread	S	C			5		SB
	W	32	spread	S	C	19		10		PG
	W	18	spread	S	C	5				PG

Where A: Abutment
W: Wall
U: Unknown

S: Sand
C: Clay
R: Rock

PG: Progressive Outward or Tilting
MS: Move Soon after Construction; Stable Later
SB: Settlement of Backfill
OT: Complete Failure - Overturning
ST: Complete Failure - Structural Failure
UN: Uncertain

Table 3.1 - continued

State	Wall or Abut	Height (ft)	Footing Type	Soil Type		Amount of Movement (in.)				Type of Unsatisfactory Behavior
				Backfill	Found.	For ward	Back ward	Down ward	Up ward	
NC	A	10	pile	U	U	TF		48		ST
NV	A	30	pile	C	C	4				PG
	A	6	spread	S	R					PG
	W	40	pile	S	S	8				PG
	W	14	spread	S	S	12				PG
	W	10	spread	S	S	22				PG
	W	16	spread	S	S	TF				OT
	W	8	spread	S	S	TF				OT
	W	10	spread	S	S	12				MS
NY	A	U	spread	U	U	12				PG
	A	U	spread	U	U	12				PG
	A	U	spread	U	U	24				PG
	A	U	U	U	U	12				PG
	A	U	spread	U	U	6				PG
	A	U	pile	C	C	TF				PG
	A	U	spread	S	C	6				PG
	W	U	spread	U	U	12				PG
	A	22	spread	U	U	TF				ST
PA	A	23	spread	S	R	2				PG
	A	25	spread	S	S	1.5				PG
	W	U	spread	U	U					UN
	W	U	spread	U	U					UN
	W	U	spread	U	U					UN
SC	W	10	spread	C	C	TF		TF		ST
SD	A	16	spread	S	S					MS
	A	5	pile	C	C	12			6	PG
	A	14	pile	C	C	TF				PG
	A	U	pile	C	C	TF				PG
	A	U	pile	C	C	TF				PG
	A	14	pile	C	C	TF				PG
	A	5	pile	C	C	TF				PG
	A	6	pile	C	C	8				PG
	A	6	pile	C	C	8				PG
	A	6	pile	C	C	8				PG
	A	6	pile	S	S	6				PG
	A	6	pile	S	S	6				PG
	A	6	pile	S	S	6				PG
	A	4	pile	C	S	4				PG
	A	4	pile	C	S	4				PG
	W	30	spread	S	S					MS
	W	30	spread	S	R			6		MS
	W	10	spread	S	S					MS
	W	U	spread	C	C					PG
	W	10	spread	S	C	TF			24	UN
	W	15	spread	C	C	24				PG

Table 3.1 - continued

State	Wall or Abut	Height (ft)	Footing Type	Soil Type		Amount of Movement (in.)				Type of Unsatisfactory Behavior
				Backfill	Found.	For ward	Back ward	Down ward	Up ward	
TN	A	U	U	U	U					PG
	A	U	U	U	U					SB
	A	U	U	U	U					ST
	W	U	U	U	U					PG
	W	U	U	U	U					SB
	W	U	U	U	U					ST
TX	W	29	spread	C	C	TF				MS
VA Bristol	A	U	U	U	U			6		MS
	A	U	U	U	U			8		MS
	A	U	U	U	U			6		MS
	A	U	U	U	U			8		MS
	A	U	U	U	U	6				UN
	A	U	U	U	U	5.5				PG
VA Salem	A	9	spread	U	R	7		1		PG
	A	4	spread	U	U			12		OT
	A	5	spread	U	U	5				PG
	A	5	spread	U	U					OT
	A	7	spread	U	U			10		UN
	A	5	spread	U	U			4		UN
VA Suffolk	A	U	pile	U	U			8		PG
	A	U	pile	U	U			12		PG
	A	U	pile	U	U		3			PG
	A	U	pile	U	U	2				MS
	A	U	pile	U	U		1.5			MS
	W	U	pile	U	U	12				MS
	W	U	pile	U	U	3				MS
VA Staunton	A	15	spread	S	C	15		30		PG
	A	15	spread	S	C	15		30		PG
	A	18	spread	S	C	12		24		PG
	A	18	spread	S	C	12		24		PG
	A	18	spread	S	C	12		24		PG
	A	18	spread	S	C	12		24		PG
	A	11	pile	S	C	3				MS
VA Nova	W	16	spread	U	U	2				MS
	W	20	spread	U	U	3				SB
	W	18	spread	U	U	1.5				MS
WA	W	25	spread	S	R	2				MS
	W	15	spread	S	R	2				MS
	W	27	spread	S	R	TF				OT
	W	24	spread	C	R	12				MS
WI	W	20	U	U	U					PG
	A	U	U	U	U					MS

Table 3.2 Probability of Failure of the Reported Walls and Abutments

	State	Abutments			Retaining Walls			Both
		Total No. of Bridges, **TAN**	Total No. of Failed Abuts, **FAN**	Prob. of Failure, **FAN / TAN**	Total No. of Walls, **TWN**	Total No. of Failed Walls, **FWN**	Prob. of Failure, **FWN / TWN**	**FN / TN**
No Failure Reported	CA	11650	0	0	47	0	0	0
	D.C.	280	0	0	102	0	0	0
	FL	5611	0	0	287	0	0	0
	ID	1700	0	0	100	0	0	0
	IN	5562	0	0	120	0	0	0
	NH	3549	0	0	NA	0	-	-
	OH	14946	0	0	NA	0	-	-
	OK	6800	0	0	NA	0	-	-
	RI	750	0	0	200	0	0	0
	VA, Rich.	2250	0	0	25	0	0	0
	VT	2700	0	0	NA	0	-	-
	WY	2800	0	0	NA	0	-	-
Failure Reported	AK	740	0	0	50	2	4.00E-02	2.53E-03
	AR	6500	0	0	200	3	1.50E-02	4.48E-04
	CT	4000	2	5.00E-04	250	4	1.60E-02	1.41E-03
	DE	1222	1	8.18E-04	NA	-	-	-
	GA	14500	0	0	2000	1	5.00E-04	6.06E-05
	KS	5000	0	0	500	5	1.00E-02	9.09E-04
	MA	4500	0	0	NA	-	-	-
	MD	2400	5	2.08E-03	NA	-	-	-
	MN	3000	9	3.00E-03	NA	-	-	-
	MS	5700	0	0	50	4	8.00E-02	6.96E-04
	NC	16970	1	5.89E-05	NA	-	-	-
	NV	887	2	2.25E-03	200	6	3.00E-02	7.36E-03
	NY	NA	-	-	NA	-	-	-
	PA	NA	-	-	NA	-	-	-
	SC	9000	0	0	NA	-	-	-
	SD	2000	15	7.50E-03	NA	-	-	-
	TN	18700	3	1.60E-04	NA	-	-	-
	TX	48000	0	0	2000	1	5.00E-04	2.00E-05
	VA, Bristol	1852	6	3.24E-03	NA	-	-	-
	VA, Nova	1739	0	0	500	3	6.00E-03	1.34E-03
	VA, Salem	2150	6	2.79E-03	NA	-	-	-
	VA, Staunton	2400	7	2.92E-03	300	0	0.00E+00	2.59E-03
	VA, Suffolk	1170	5	4.27E-03	100	2	2.00E-02	5.51E-03
	WA	3100	0	0	5000	4	8.00E-04	4.94E-04
	WI	13000	1	7.69E-05	300	1	3.33E-03	1.50E-04
Total		**227128**	**63**	**2.77E-04**	**12331**	**36**	**2.92E-03**	**4.13E-04**

retaining walls which has been reported (TWN). The overall probability of failure was obtained by dividing the total number of failed abutments and retaining walls (FN) by the total number of abutments and retaining walls reported (TN). Based on the data reported by the states, the probability of failure of abutments appears to be about 4 in 10,000 while the probability of failure of retaining walls is about 3 in 1000.

Figure 3.4 classifies the unsatisfactory walls and abutments based on their height. The average heights of the abutments and the retaining walls were 11.9 ft and 19.0 ft, respectively. The height of the abutments and walls combined, ranges from 4 ft to 40 ft and the average height is about 15.2 ft.

As shown in Figure 3.5, where failure occurred in retaining walls, spread footings were more frequent than pile foundations while in abutments slightly more pile foundations than spread footings were reported. The combined result indicates that more spread footings than pile foundations were among the reported walls which experienced undesirable behavior. Apparently, unsatisfactory behavior can occur even if pile foundations are used.

Height (ft)	Abut	Wall	Combined
1-5	8	0	8
6-10	14	7	21
11-15	9	8	17
16-20	8	11	19
21-25	3	6	9
26-30	2	4	6
31-35	0	1	1
36-40	0	1	1
Avg. ht.	11.9	19.0	15.2
sum	44	38	82

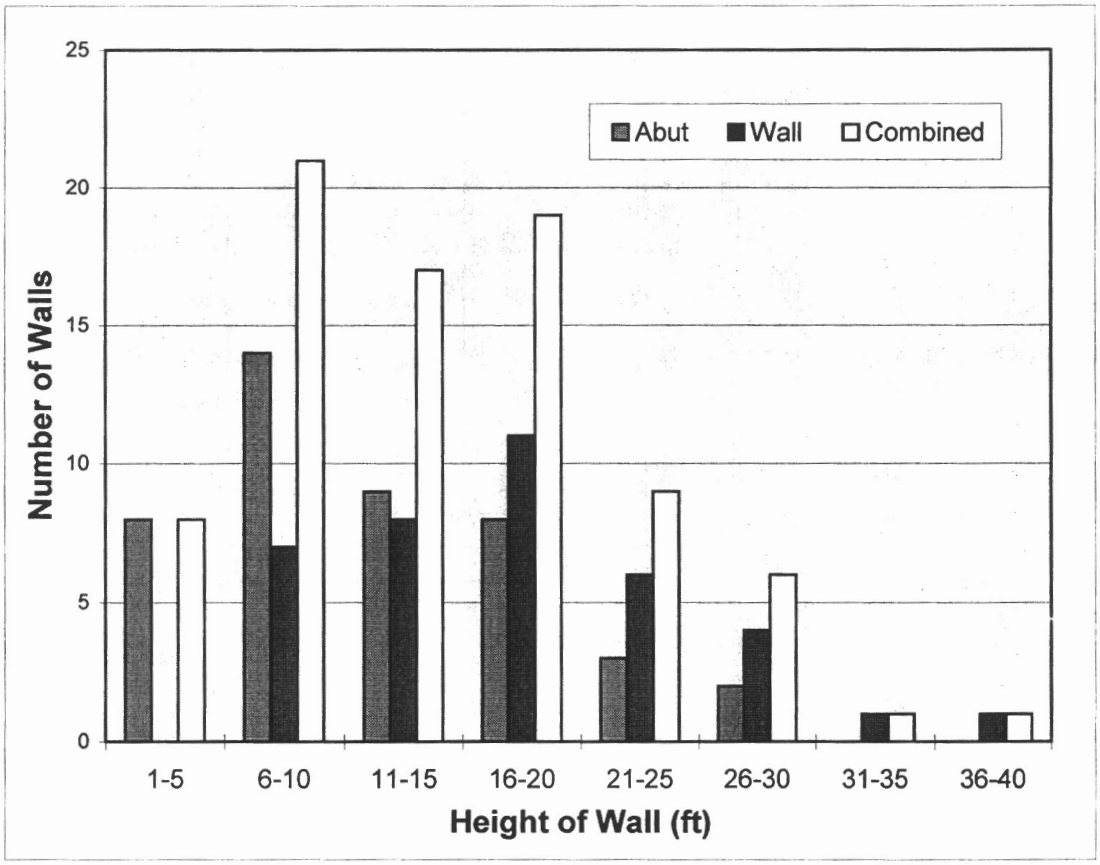

Figure 3.4 Reported Heights of Unsatisfactory Walls and Abutments

	Abut	Wall	Combined
spread	28	40	68
pile	32	4	36
unknown	13	8	21

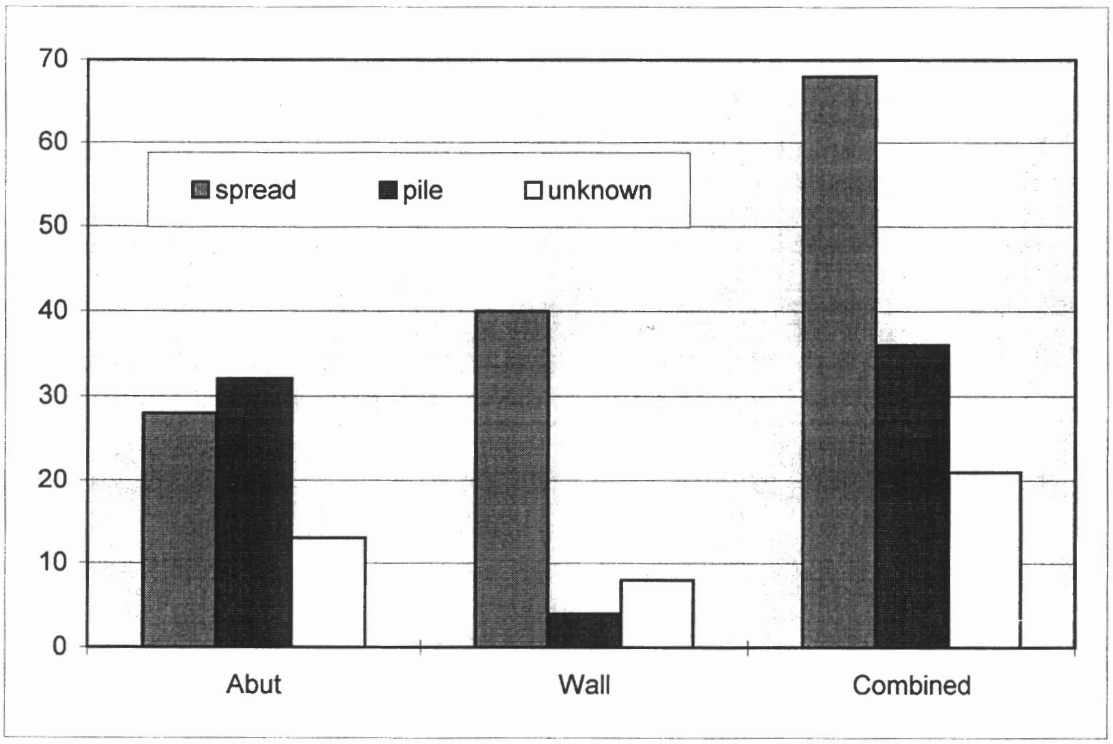

Figure 3.5 Types of Footings Under Unsatisfactory Walls and Abutments

Figure 3.6 presents the magnitude of forward movement that the unsatisfactory walls and abutments experienced. As previously shown in Peck et al.'s survey results, the magnitude of the forward movement of a majority of the walls considered unsatisfactory ranged from 6 to 12 inches. In the 1993 survey the average movement considered unsatisfactory is 7 inches for abutments and 9 inches for walls. Using the average heights of abutments and retaining walls from Figure 3.4, the Δ/H ratios become 0.05 to 0.04, respectively. Walls are considered by those who responded as complete failures if they move more than 2 ft.

As shown in Figure 3.7, the abutments and the walls are categorized according to the type of movements that they experienced. The most common type of behavior appears to be the progressive outward or tilting movement (50 %). The trend is more severe in abutments than in retaining walls as shown in Figure 3.8. The percentages of progressive outward movement are 61 % for abutments and 35 % for retaining walls. It is reported that about 8 % failed completely either by structural failure or by overturning. It can be observed that a considerable number of unsatisfactory walls were founded on piles. This result may imply that the use of piles does not necessarily eliminate the excessive movement of the walls.

Movement (in.)	Abut	Wall	Combined
1-3	9	7	16
4-6	14	3	17
7-9	5	1	6
10-12	8	8	16
13-15	2	1	3
16-18	0	0	0
19-21	0	1	1
22-24	1	2	3
- - -			
Collapse	8	7	15
Avg. in.	7.3	9.3	8.1
No. of Walls	47	30	77

- excluding failures

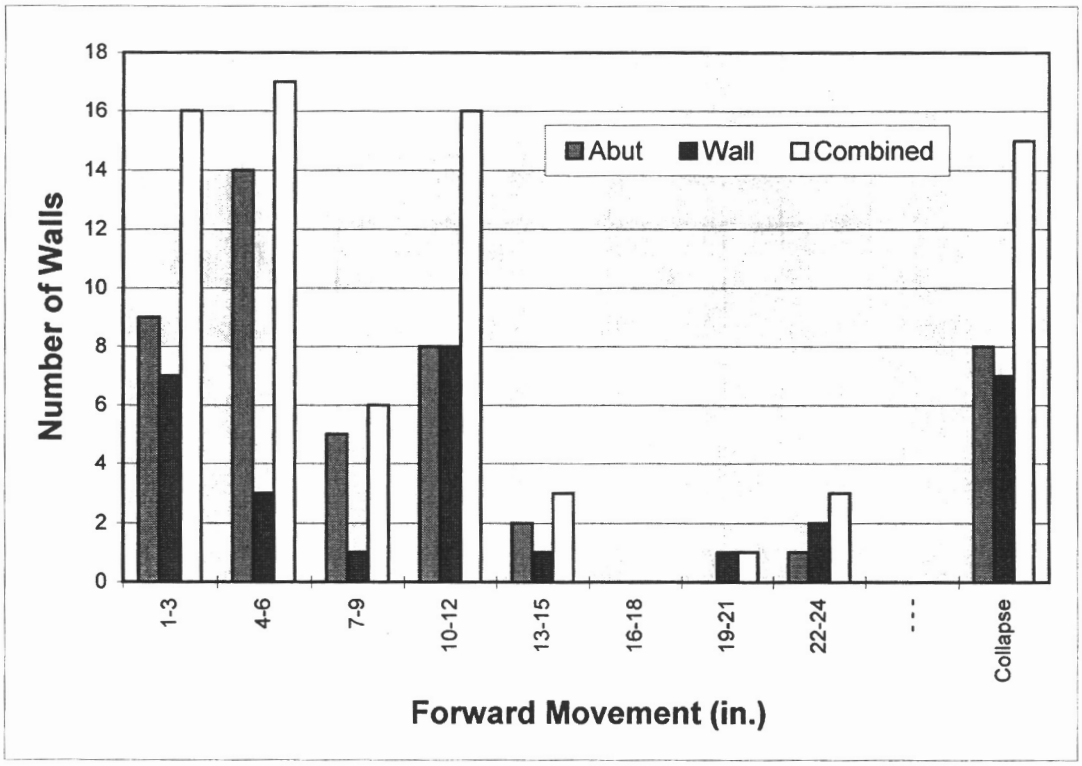

Figure 3.6 Forward Movement of Unsatisfactory Walls and Abutments

	PG	MS	SB	UN	OT	ST	sum
Pile	26	7	2	0	0	1	36
Spread	32	15	8	6	5	2	68
Unknown	5	5	2	7	0	2	21
Total	63	27	12	13	5	5	125

where PG: Progressive Outward or Tiliting Movement
MS: Movement Soon After Construction; Stable Afterward
SB: Settlement Under Backfill
UN: Uncertain
OT: Complete Failure - Overturning
ST: Complete Failure - Structural Failure

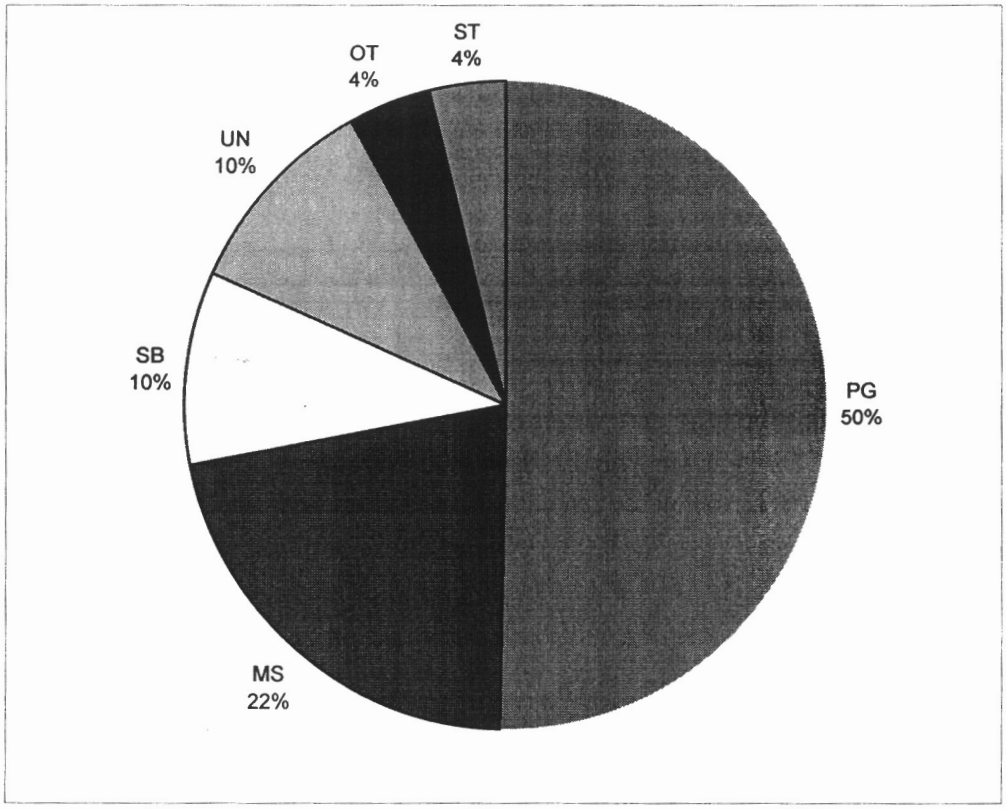

Figure 3.7 Type of Unsatifactory Behavior - Combined

	PG	MS	SB	UN	OT	ST
Abut	45	15	3	5	2	3
Wall	18	12	9	8	3	2

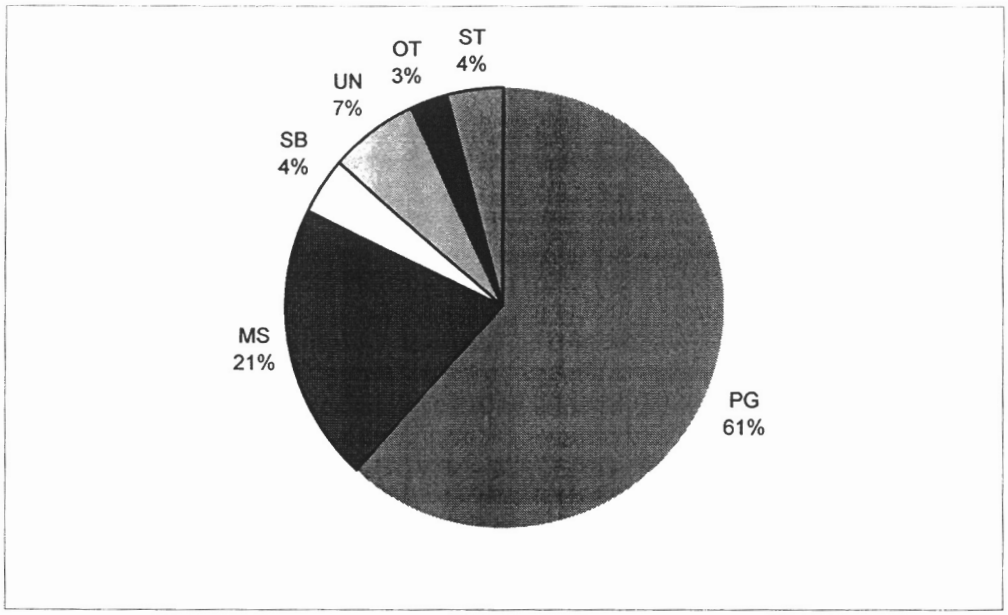

(a) Abutments

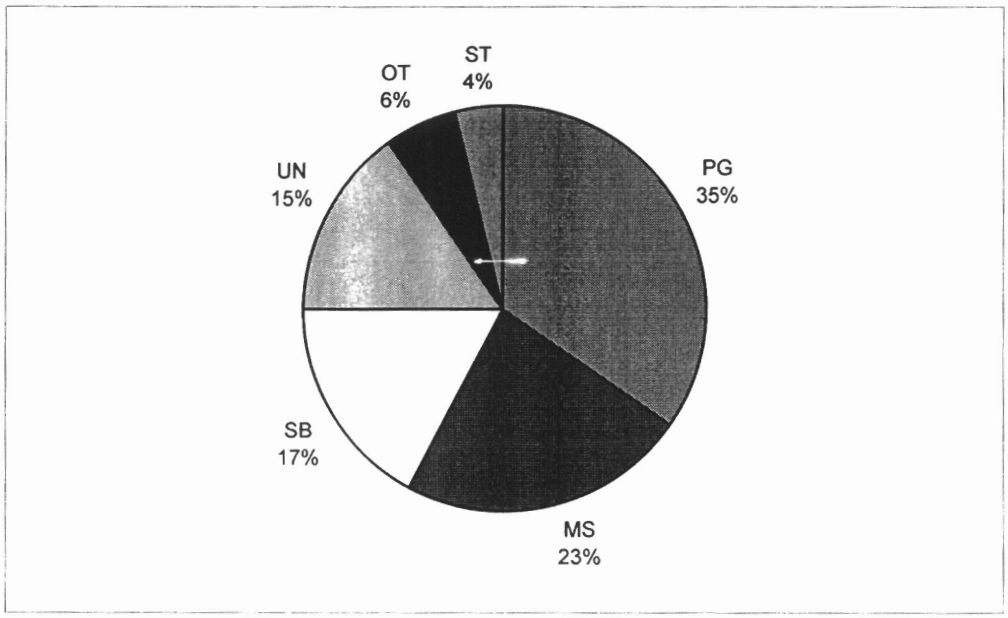

(b) Retaining Walls

Figure 3.8 Type of Unsatifactory Behavior - Abutments and Walls

Figure 3.9 presents the type of foundation and backfill materials of all of the walls that experienced unsatisfactory behavior described in Figure 3.7. Unlike the previous survey results, a considerable number of walls backfilled with sand and founded on sand or rock were reported to experience unsatisfactory behavior. It is observed that such walls experienced various failures with almost the same percentage as the walls associated with clay. For convenient comparison with Figure 3.2, Figure 3.10 was created as a subset of Figure 3.7. It shows the foundation and backfill materials of the walls which experienced progressive outward or tilting movements.

3.4 COMPARISON

Table 3.3 presents a summary of both surveys. Comparing the two indicates that 48 years elapsed between surveys and that different bridge types were surveyed. The 1993 survey received more responses. In the railroad survey 21 % of those surveyed reported problems while in the highway survey 41 % of those surveyed reported some problems. Average height of railroad walls reported was higher than the average height of highway walls. Tolerable movement for railroad walls was 3 inches and 2 inches for highway walls.

	Backfill: clay Foundation: clay	Backfill: sand, gravel Foundation: clay	Backfill: sand, gravel Foundation: sand, gravel, rock	Backfill: clay Foundation: sand, gravel, rock	Backfill: unknown Foundation: unknown
Number of Case	17	23	21	3	61
Percent	14	18	17	2	49

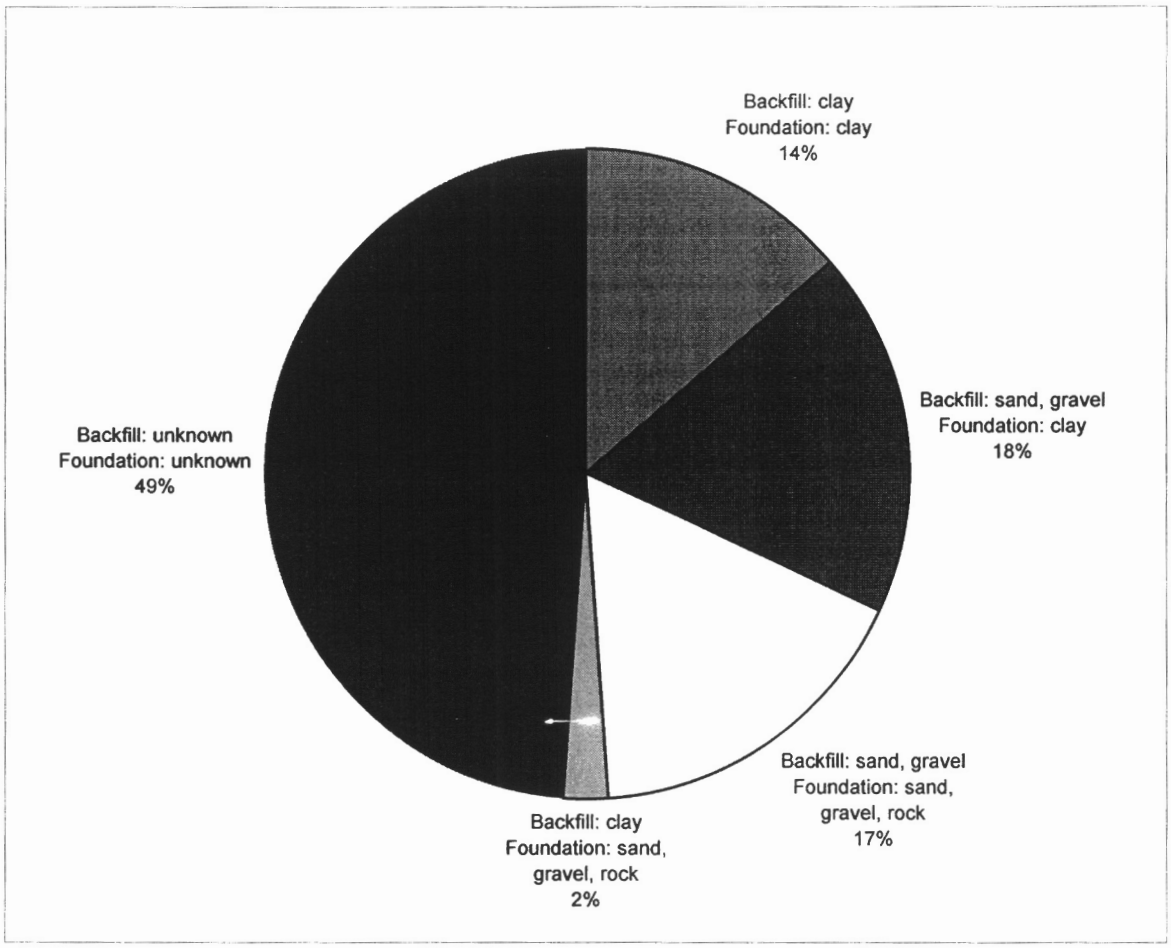

Figure 3.9 Materials of Backfill and Foundation (Overall)

	Backfill: clay Foundation: clay	Backfill: sand, gravel Foundation: clay	Backfill: sand, gravel Foundation: sand, gravel, rock	Backfill: clay Foundation: sand, gravel, rock	Backfill: unknown Foundation: unknown
Number of Case	15	13	10	2	23
Percent	24	21	16	3	36

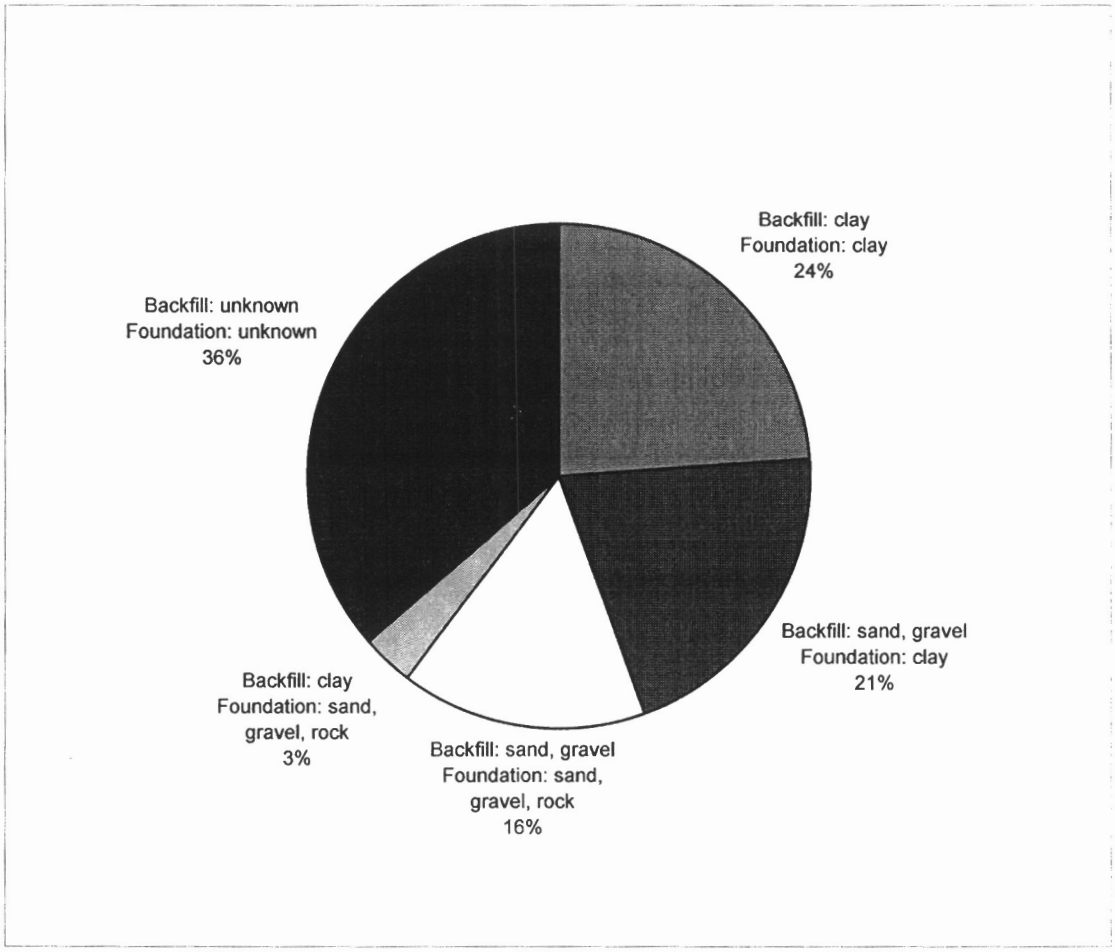

Figure 3.10 Backfill and Foundation Materials
(Walls subject to Progressive Outward Movement)

Table 3.3 Comparison of Railroad Survey and Highway Survey

	Comparison	Railroad Survey	Highway Survey
1	Survey Year	1945	1993
2	Bridge Type Surveyed	Railroad Bridges	Highway Bridges
3	Total Number of Requests	77	51
4	Total Number of Responses	40 (52%)	37 (73%)
5	No Significant Problems Reported Among Responses	24 (31%)	11 (22%)
6	Some Indication of Problems	16 (21%)	21 (41%)
7	No Problem or No Response	61 (79%)	30 (59%)
8	Height of Walls (combined)	5 ft - 60 ft	4 ft - 40 ft
9	Avg. Height of Walls	25 ft (combined)	15 ft (combined) 12 ft (abut), 19 ft (wall)
10	Most Frequent Forward Movement	6 in. - 12 in.	4 in. - 6 in.
11	Tolerable Movement	up to 3 in. (Δ/H = 0.010)	up to 2 in. (Δ/H = 0.011)
12	Progressive Outward or Tilting	53% (combined)	50% (combined) 61% (abut), 35% (wall)
13	Material of Walls Subject to Progressive Outward or Tilting	All associated with clay either backfilled with or founded on	Considerable number of walls associated with sand
14	Conclusion from No.13	Lower safety margin for clay than sand	Similar safety margin for sand and clay

The highway survey results show that abutments are much more sensitive than retaining walls to progressive outward movement. However, the ratios of tolerable movement to wall height in both surveys are almost identical ($\Delta/H = 0.01$).

Since the 1945 survey, one could speculate that designers were aware that the factor of safety was greater in granular soils than in clay soils and took measures to reduce the conservatism. As a result, the 1993 survey indicates an almost equal percentage of unsatisfactory behavior in granular and clay soils. On the other hand, the reverse might be true, i.e., the safety factor applied to designs in clay soils may have been increased. In any event, the result is that more unsatisfactory behavior in sand, gravel and rock has been reported in 1993 for highway bridges than that given for railroad bridges in 1945.

Chapter 4
SAFETY INDEX OF CONVENTIONAL DESIGN

4.1 GENERAL

This chapter presents the procedure for obtaining safety indices inherent in gravity retaining walls. The walls are initially designed according to a conventional, deterministic design method (ASD) and then analyzed by the reliability method (Advanced FOSM) for the estimation of the safety indices. Gravity retaining walls are taken as examples because there is general agreement on the mathematical analysis to evaluate soil pressures against the wall. For the purpose of presentation, three limit states are considered: Sliding, Overturning, and Bearing Capacity. Safety factors used in the ASD method are 1.5 for sliding, 2.0 for overturning and a minimum of 2.5 for bearing capacity. The heights of the gravity walls evaluated for each limit state are 5 ft, 10 ft, 20 ft and 30 ft. For each height of the wall, the top thickness and base width of the wall are adjusted by trial and error to closely match the desired safety factors for each failure mode. As Meyerhof (1976) presented, typical safety indices of 2.0 to 3.0 are anticipated from this study for earth retaining structures when the safety factors are 1.5 to 2.0.

4.2 ANALYSIS CONSIDERATIONS

A definition sketch of a typical gravity retaining wall, showing dimensions and soil properties, is given in Figure 4.1. The basic random variables for a retaining wall analysis used in this study are the unit weight of the backfill soil (γ), the internal friction angle of the backfill (ϕ), the internal friction angle of the foundation soil (ϕ_f), the friction angle between foundation soil and footing base (δ_f), and the unit weight of concrete (γ_c). The wall dimensions such as base width (B), top thickness (t) and wall height (H) are assumed to be deterministic. It is reasonable to assume that all the random variables are statistically independent of each other.

4.2.1 Reliability Considerations

To avoid confusion and inaccurate results, it is recommended that the limit state function, g() be expressed in terms of the basic random variables rather than in an abbreviated format. For example, g() for the sliding limit state can be expressed in a shortened format as

$$g() = W_c \cdot \mu - P_a = 0 \qquad (4.1)$$

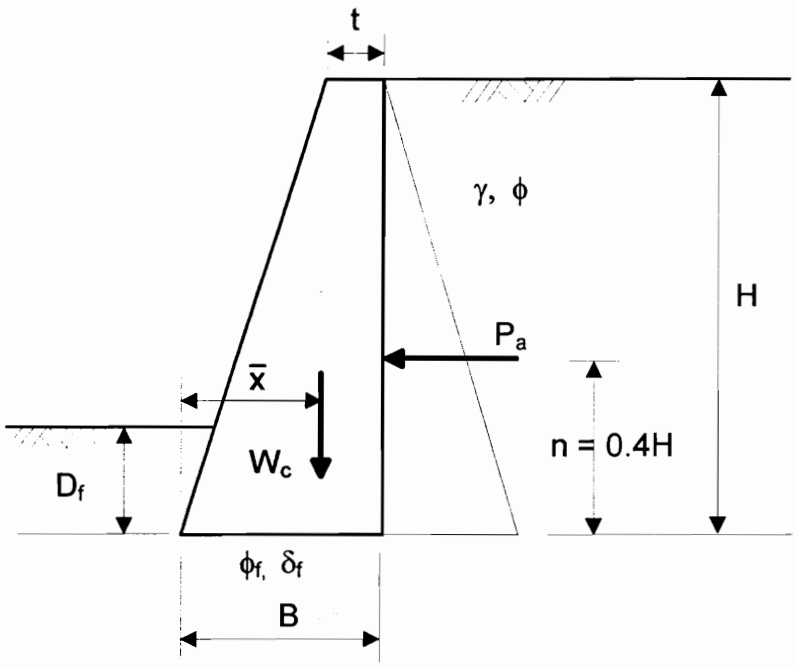

Figure 4.1 A Typical Gravity Retaining Wall

where W_c = weight of the concrete mass = vol. * γ_c

vol. = volume of concrete mass

γ_c = unit weight of concrete

μ = coefficient of friction between base and foundation soil = tan δ_f

δ_f = friction angle between base and foundation soil

P_a = resultant of earth pressure = $\frac{1}{2} \gamma H^2 K_a$

γ = unit weight of backfill soil

H = height of wall

K_a = earth pressure coefficient from Rankine theory

$= \frac{1 - \sin\phi}{1 + \sin\phi}$ or $\tan^2(\frac{\pi}{4} - \frac{\phi}{2})$

In this case, additional calculation procedures for obtaining the mean and standard deviation for W_c, μ, and P_a should be provided and a careful follow-up should also be made throughout the whole procedure. For this reason, the limit state functions used hereafter will be expressed in terms of the basic random variables, despite their lengthy formats. Therefore, the previous limit state function for sliding (Eq. 4.1) should be restated as

$$g() = \text{vol.} \cdot \gamma_c \cdot \tan\delta_f - \frac{1}{2} \gamma H^2 \tan^2(\frac{\pi}{4} - \frac{\phi}{2}) = 0 \qquad (4.2)$$

4.2.2 Methods and Theories Used to Estimate Forces

Rankine theory is adopted in this study to estimate the earth pressure generated by the backfill. The resultant of the horizontal earth pressure is assumed to apply at 0.4 H measured from the base of the wall.

The methods currently practiced to predict the ultimate bearing capacity are based on the superposition method suggested by Terzaghi (1943). During the following years several investigators have developed their modified methods to estimate the ultimate bearing capacity. A typical equation for the ultimate bearing capacity of the shallow foundations can be expressed as

$$q_{ult} = 0.5\,\gamma\,B\,N_\gamma\,S_\gamma\,d_\gamma\,I_\gamma + \gamma\,D_f\,N_q\,S_q\,d_q\,I_q + c\,N_c\,S_c\,d_c\,I_c \qquad (4.3)$$

where γ = unit weight of soil

B = footing width

D_f = footing depth

c = cohesion

N_i = bearing capacity factors

S_i = shape factors

d_i = depth factors

I_i = inclination factors

Table 4.1 shows various expressions for bearing capacity factors and other factors proposed by Meyerhof, Hansen, and Caquot and Kerisel. The bearing capacity factors, N_γ and N_q, for each equation are graphed in Figure 4.2 and Figure 4.3. As shown in the figures, Terzaghi's equation estimates the ultimate bearing capacity too conservatively and is dropped from further consideration. The following example is given to compare the ultimate bearing capacities estimated by the three equations in Table 4.1.

Example 4.1

Estimate the ultimate bearing capacity using equations in Table 4.1.

Given conditions: $\phi_f = 39$ deg, $\gamma = 110$ pcf, $H = 5.962$ kips, $V = 16.931$ kips,
$B = 9.25$ ft, $B_e = 6.278$ ft, $L = 50$ ft, $D_f = 3$ ft, $\theta = 19.4$ deg,
$n = 1.23$ (for Caquot & Kerisel's equation, from AASHTO)

	Meyerhof	Hansen	Caquot & Kerisel
$N_q * (S_q * d_q * I_q)$	42.573	26.245	37.691
$N_\gamma * (S_\gamma * d_\gamma * I_\gamma)$	21.122	15.015	32.419
q_{ult}	**63.69**	**41.26**	**70.11**

Considering that the current AASHTO specifications adopted the equation suggested by Caquot and Kerisel, it is reasonable to select Meyerhof's equation, which predicts the ultimate bearing capacity neither too high nor too low.

Table 4.1 Comparison of the Various Bearing Capacity Factors

	Meyerhof	Hansen	Caquot & Kerisel
N_q	$e^{\pi \tan\phi} \cdot \tan^2\left(45+\frac{\phi}{2}\right)$	$e^{\pi \tan\phi} \cdot \tan^2\left(45+\frac{\phi}{2}\right)$	$e^{\pi \tan\phi} \cdot \tan^2\left(45+\frac{\phi}{2}\right)$
N_γ	$(N_q - 1) * \tan(1.4\phi)$	$1.5(N_q - 1) * \tan\phi$	$2(N_q + 1) * \tan\phi$
I_q	$\left(1-\frac{\theta}{90}\right)^2$	$\left(1-0.5\left(\frac{H}{V}\right)\right)^5$	$\left(1-\frac{H}{(V + BLc\cot\phi)}\right)^n$
I_γ	$\left(1-\frac{\theta}{\phi}\right)^2$	$\left(1-0.7\left(\frac{H}{V}\right)\right)^5$	$\left(1-\frac{H}{(V + BLc\cot\phi)}\right)^{n+1}$
S_q	$1+0.1\frac{B}{L}\left[\tan^2\left(45+\frac{\phi}{2}\right)\right]$	$1+\left(\frac{B}{L}\right)\sin\phi$	$1+\left(\frac{B}{L}\right)\tan\phi$
S_γ	$1+0.1\frac{B}{L}\left[\tan^2\left(45+\frac{\phi}{2}\right)\right]$	$1-0.4\left(\frac{B}{L}\right)$	$1-0.4\left(\frac{B}{L}\right)$
d_q	$1+0.3\frac{D_f}{B_e}$	$1+2\tan\phi\,(1-\sin\phi)^2\frac{D_f}{B_e}$	1.0
d_γ	1.0	1.0	1.0

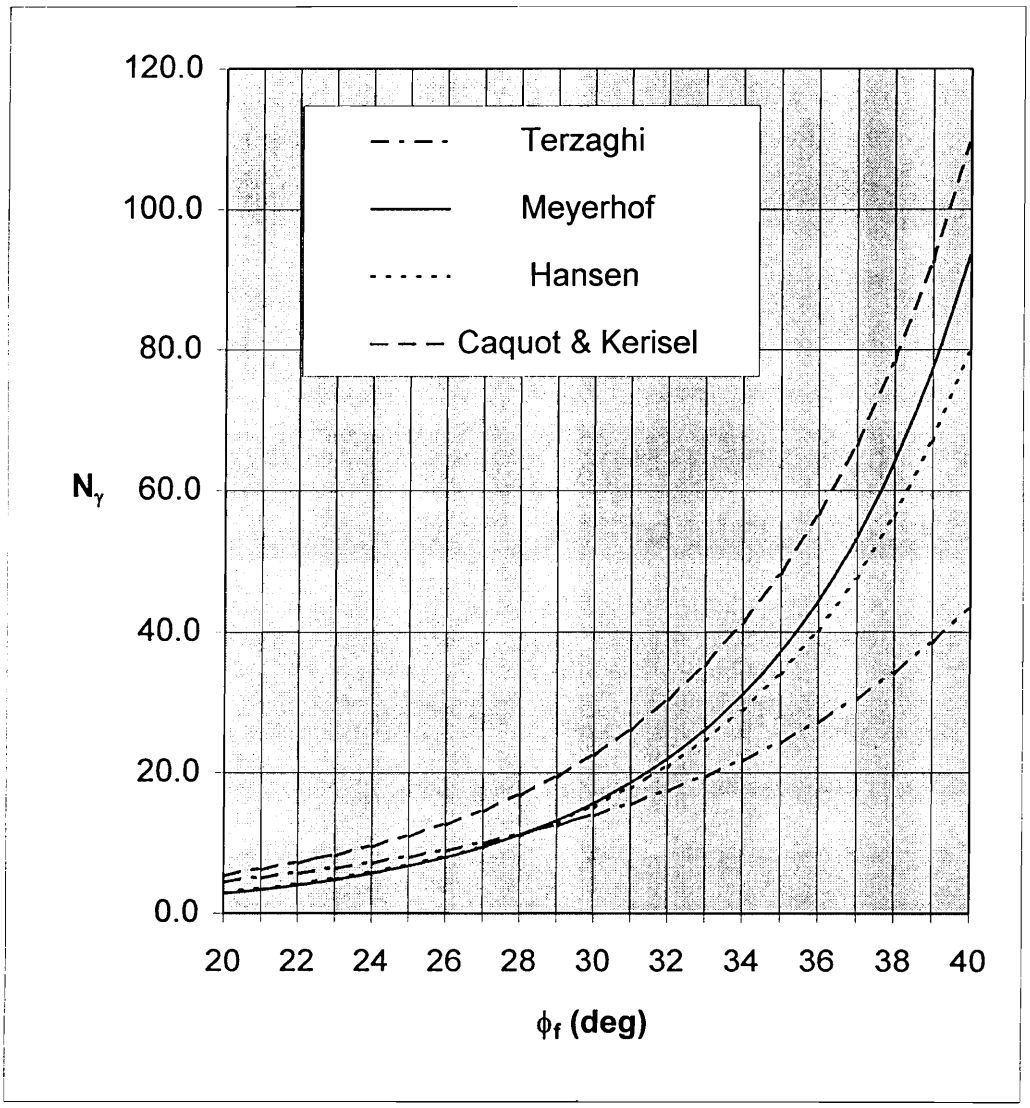

Figure 4.2 Various N_γ Values

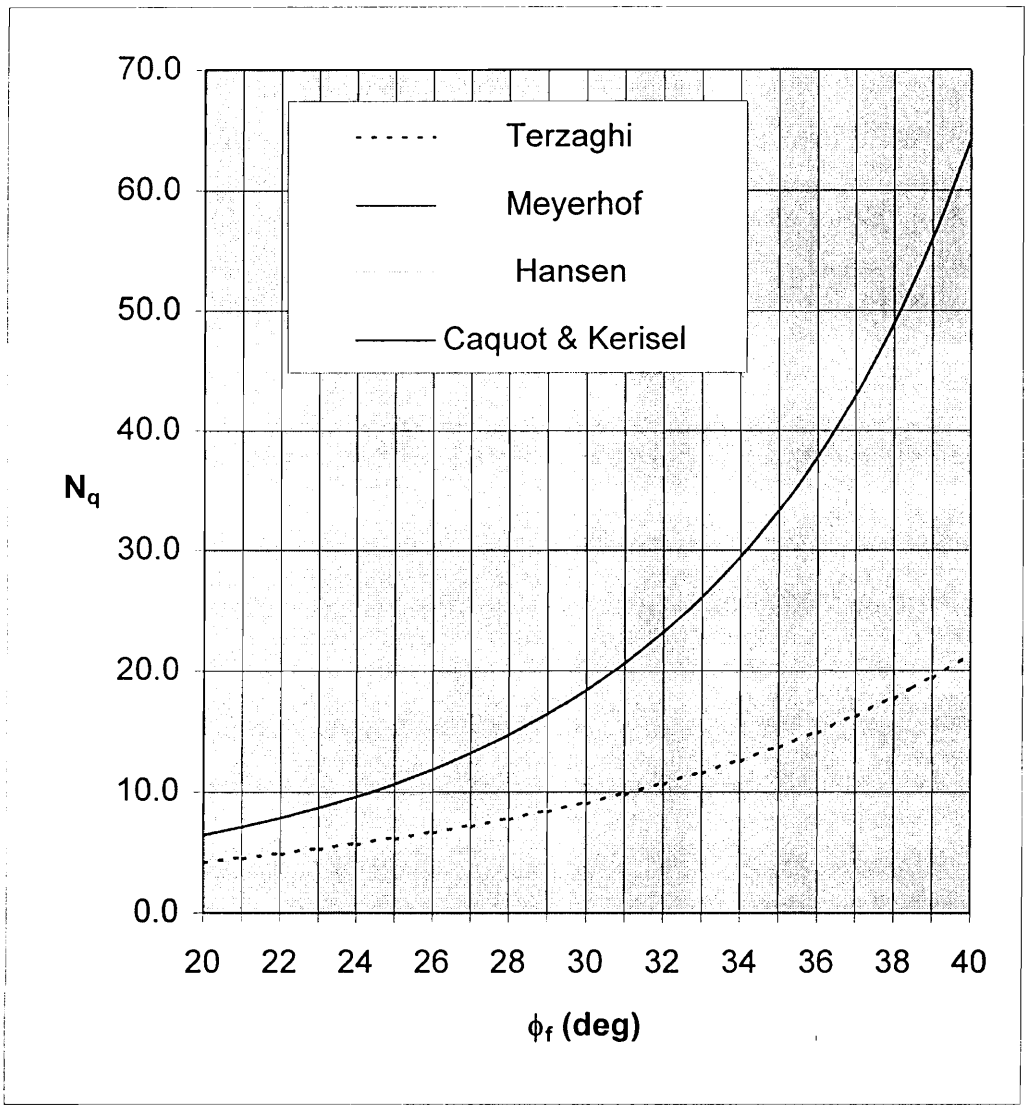

* N_q values of Meyerhof, Hansen, and Caquot & Kerisel are identical.

Figure 4.3 Various N_q Values

4.3 A Detailed Illustration of the Procedures

To illustrate the procedures, the gravity wall presented in Figure 4.1 will be used. For a given set of design parameters, the wall dimensions (t and B) are determined to closely satisfy all the ASD stability criteria of a retaining wall. Once the wall is optimized with the conventional design method, a safety index for each limit state will be obtained with the Advanced FOSM method. The sliding limit state is chosen to present the details of the procedure. For more convenient and systematic analysis, a spreadsheet program named EXCEL is employed in this study.

4.3.1 Given Conditions for the Sliding Limit State Example

Wall dimensions and soil conditions of the design example are as follows:

Wall	Height = 10 ft
	Unit weight of concrete (γ_c) = 150 pcf
Backfill	Internal friction angle of backfill (ϕ) = 35 deg.
	Unit weight of backfill soil (γ) = 110 pcf
Foundation Soil	Internal friction angle of foundation soil (ϕ_f) = 35 deg.
	Friction angle between base and foundation soil (δ_f) = 30 deg.
	Depth of soil in front of the wall (D_f) = 3.0 ft

4.3.2 Conventionally Optimized Design

The following calculations illustrate the steps necessary to obtain an optimized conventional design.

Step 1. Select Preliminary Proportion of the Wall

From the recommendation of Clayton and Mililitsky(Fig. 2.21),

t = H / 12 = 0.83 ft

B = H/3 to H/2 = 3.3 ft to 5.0 ft

After a number of trials, the following dimensions were found to closely satisfy all of the ASD criteria.

t = 0.75 ft and B = 4.6 ft

Step 2. Determine Loads and Earth Pressure Forces

(1) Earth Pressure Force: $P_a = \frac{1}{2} K_a \gamma H^2$

K_a = 0.271 Rankine,

P_a = 1.490 kips/ft

h = 0.4 H = 4.0 ft

(2) Concrete Weight

vol. = 26.75 cu. ft

W_c = 4.013 kips/ft (N = W_c = 4.013 kips/ft)

$\bar{x}$ = 3.032 ft from the toe

Step 3. Calculate Reaction Forces (For details, refer to Figure 2.23)

Trapezoidal Distribution	Rectangular Distribution
$q_{max} = \frac{N}{B}(1 + \frac{6e}{B})$	$q_{max} = \frac{N}{2 x_o}$
= 1.730 ksf	= 1.298 ksf

Where $x_o = \frac{W_c \cdot \bar{x} - P_a \cdot h}{N}$ = 1.546 ft

Step 4. Check Stability and Safety Criteria

(1) Eccentricity Check:

$e = B/2 - x_o =$ **0.754** < $e_{max} = B/6 =$ **0.767** **o.k.**

(2) Sliding Check:

$$S.F. = \frac{N \tan \delta_f}{P_a} =$$ **1.55** > **1.50** **o.k.**

(3) Overturning Check:

$$S.F. = \frac{W_c \cdot \bar{x}^{\,\mathcal{L}_c}}{p_a \cdot h} =$$ **2.04** > **2.0** **o.k.**

(4) Bearing Capacity Check: (using Meyerhof 's Equation)

$$Q_{ult} = \tfrac{1}{2}\gamma(B - 2e)^2 \left(1 - \frac{\theta}{\phi_f}\right)^2 N_\gamma + \gamma D_f \left(1 - \frac{\theta}{90}\right)^2 (B - 2e)\left(1 + 0.3\frac{D_f}{B - 2e}\right) N_q$$

where $B - 2e =$ 3.092 ft

θ = Arctan (H/V) = 20.38 deg.

$N_\gamma =$ 34.61

$N_q =$ 31.69

Thus, $Q_{ult} =$ 10.13 kips/ft

$q_{ult} = Q_{ult} / (B-2e) =$ 3.276 ksf

$S.F. = q_{ult} / q_{max} =$ **2.52** > **2.50** **o.k.**

(based on rational theory)

4.3.3 Find the Safety Index Value

Step 1. Formulate the Limit State Function

$$g() = vol \cdot \gamma_c \cdot \tan \delta_f - \frac{1}{2} \cdot \gamma \cdot \left(\frac{1 - \sin \phi}{1 + \sin \phi} \right) \cdot H^2 = 0$$

Step 2. Prepare Statistical Data for Design Variables

Values below are from Hoeg and Murarka (1974).

Var.	μ	σ	δ	Bias
γ_c	0.158	0.0158	0.100	1.05
δ_f	0.524	0.0524	0.100	1.0
γ	0.110	0.0110	0.100	1.0
ϕ	0.611	0.0524	0.086	1.0

where

μ = mean value

σ = standard deviation

δ = covariance = μ/σ

Bias = mean / nominal

Step 3. Obtain Partial Derivatives for Each Random Variable

For the first trial, use mean values.

$$\frac{\partial g}{\partial \gamma_c} = a \cdot \tan \delta_f$$

$$\frac{\partial g}{\partial \delta_f} = a \cdot \gamma_c \cdot \sec^2 \delta_f$$

$$\frac{\partial g}{\partial \gamma} = -b \cdot \frac{1 - \sin \phi}{1 + \sin \phi}$$

$$\frac{\partial g}{\partial \phi} = 2b \cdot \gamma \cdot \frac{\cos \phi}{(1 + \sin \phi)^2}$$

where $a = vol. = 26.8 \ ft^3$

$b = \frac{1}{2} H^2 = 50.0 \ ft^2$

Step 4. Obtain Direction Cosines

$$\Delta = \sqrt{\left(\sigma_{\gamma_c}\frac{\partial g}{\partial \gamma_c}\right)^2 + \left(\sigma_{\delta_f}\frac{\partial g}{\partial \delta_f}\right)^2 + \left(\sigma_{\gamma}\frac{\partial g}{\partial \gamma}\right)^2 + \left(\sigma_{\phi}\frac{\partial g}{\partial \phi}\right)^2}$$

$$\alpha_{\gamma_c} = -\frac{\sigma_{\gamma_c}\frac{\partial g}{\partial \gamma_c}}{\Delta}$$

$$\alpha_{\delta_f} = -\frac{\sigma_{\delta_f}\frac{\partial g}{\partial \delta_f}}{\Delta}$$

$$\alpha_{\gamma} = -\frac{\sigma_{\gamma}\frac{\partial g}{\partial \gamma}}{\Delta}$$

$$\alpha_{\phi} = -\frac{\sigma_{\phi}\frac{\partial g}{\partial \phi}}{\Delta}$$

Step 5. Find the New Design Point

$$\gamma_c^* = \mu_{\gamma_c} + \alpha_{\gamma_c}\cdot\sigma_{\gamma_c}\cdot\beta$$
$$\delta_f^* = \mu_{\delta_f} + \alpha_{\delta_f}\cdot\sigma_{\delta_f}\cdot\beta$$
$$\gamma^* = \mu_{\gamma} + \alpha_{\gamma}\cdot\sigma_{\gamma}\cdot\beta$$
$$\phi^* = \mu_{\phi} + \alpha_{\phi}\cdot\sigma_{\phi}\cdot\beta$$

Step 6. Substitute the new design point into the Limit State Function and Solve for β

$$g() = a\cdot\gamma_c^*\cdot\tan\delta_f^* - b\cdot\gamma^*\cdot\left(\frac{1-\sin\phi^*}{1+\sin\phi^*}\right) = 0$$

Step 7. Repeat Step 3 through Step 6 until β ***Value Converges***

4.3.4 Iteration Procedure to Obtain the β Value

To illustrate Step 7, a detailed breakdown of Step 3 through Step 6 are given below.

1st Trial with Mean Values

Step 3. Obtain the Partial Derivatives

$\frac{\partial g}{\partial \gamma_c}$	$\frac{\partial g}{\partial \delta_f}$	$\frac{\partial g}{\partial \gamma}$	$\frac{\partial g}{\partial \phi}$
15.44	5.618	-13.55	3.639

Step 4. Calculate the Direction Cosines

$\sigma_{\gamma c}\frac{\partial g}{\partial \gamma_c}$	$\sigma_{\delta f}\frac{\partial g}{\partial \delta_f}$	$\sigma_{\gamma}\frac{\partial g}{\partial \gamma}$	$\sigma_{\phi}\frac{\partial g}{\partial \phi}$
0.2432	0.2941	-0.149	0.191

$\Delta = 0.452$

$\alpha_{\gamma c}$	$\alpha_{\delta f}$	α_{γ}	α_{ϕ}
-0.538	-0.651	0.330	-0.42

Step 5. Find the New Design Point

$$\gamma_c^* = \mu_{\gamma_c} + \alpha_{\gamma_c} \cdot \sigma_{\gamma_c} \cdot \beta = 0.139$$

$$\delta_f^* = \mu_{\delta_f} + \alpha_{\delta_f} \cdot \sigma_{\delta_f} \cdot \beta = 0.449$$

$$\gamma^* = \mu_{\gamma} + \alpha_{\gamma} \cdot \sigma_{\gamma} \cdot \beta = 0.118$$

$$\phi^* = \mu_{\phi} + \alpha_{\phi} \cdot \sigma_{\phi} \cdot \beta = 0.563$$

Step 6. Substitute New Design Point into g() and Solve for β

$$g() = a \cdot \gamma_c^* \cdot \tan \delta_f^* - b \cdot \gamma^* \cdot \left(\frac{1 - \sin \phi^*}{1 + \sin \phi^*} \right) = 0$$

$\beta_1 = 2.179$

2nd Trial with Results from 1st Trial

Step 3. Obtain the Partial Derivatives

$\frac{\partial g}{\partial \gamma_c}$	$\frac{\partial g}{\partial \delta_f}$	$\frac{\partial g}{\partial \gamma}$	$\frac{\partial g}{\partial \phi}$
12.90	4.584	-15.21	4.241

Step 4. Calculate the Direction Cosines

$\sigma_{\gamma c}\frac{\partial g}{\partial \gamma_c}$	$\sigma_{\delta f}\frac{\partial g}{\partial \delta_f}$	$\sigma_{\gamma}\frac{\partial g}{\partial \gamma}$	$\sigma_{\phi}\frac{\partial g}{\partial \phi}$
0.2032	0.2400	-0.1673	0.2220

$\Delta = 0.420$

$\alpha_{\gamma c}$	$\alpha_{\delta f}$	α_{γ}	α_{ϕ}
-0.484	-0.572	0.399	-0.529

Step 5. Find the New Design Point

$$\gamma_c^* = \mu_{\gamma_c} + \alpha_{\gamma_c} \cdot \sigma_{\gamma_c} \cdot \beta = 0.141$$

$$\delta_f^* = \mu_{\delta_f} + \alpha_{\delta_f} \cdot \sigma_{\delta_f} \cdot \beta = 0.459$$

$$\gamma^* = \mu_{\gamma} + \alpha_{\gamma} \cdot \sigma_{\gamma} \cdot \beta = 0.119$$

$$\phi^* = \mu_{\phi} + \alpha_{\phi} \cdot \sigma_{\phi} \cdot \beta = 0.551$$

Step 6. Substitute New Design Point into g() and Solve for β

$$g() = a \cdot \gamma_c^* \cdot \tan \delta_f^* - b \cdot \gamma^* \cdot \left(\frac{1 - \sin \phi^*}{1 + \sin \phi^*} \right) = 0$$

$\beta_2 = 2.151$

3rd Trial with Results from 2nd Trial

Step 3. Obtain the Partial Derivatives

$\frac{\partial g}{\partial \gamma_c}$	$\frac{\partial g}{\partial \delta_f}$	$\frac{\partial g}{\partial \gamma}$	$\frac{\partial g}{\partial \phi}$
13.227	4.697	-15.63	4.382

Step 4. Calculate the Direction Cosines

$\sigma_{\gamma c}\frac{\partial g}{\partial \gamma_c}$	$\sigma_{\delta f}\frac{\partial g}{\partial \delta_f}$	$\sigma_{\gamma}\frac{\partial g}{\partial \gamma}$	$\sigma_{\phi}\frac{\partial g}{\partial \phi}$
0.2083	0.2459	-0.1719	0.2294

$\Delta = 0.431$

$\alpha_{\gamma c}$	$\alpha_{\delta f}$	α_{γ}	α_{ϕ}
-0.483	-0.570	0.398	-0.532

Step 5. Find the New Design Point

$$\gamma_c^* = \mu_{\gamma_c} + \alpha_{\gamma_c} \cdot \sigma_{\gamma_c} \cdot \beta = 0.141$$

$$\delta_f^* = \mu_{\delta_f} + \alpha_{\delta_f} \cdot \sigma_{\delta_f} \cdot \beta = 0.459$$

$$\gamma^* = \mu_{\gamma} + \alpha_{\gamma} \cdot \sigma_{\gamma} \cdot \beta = 0.119$$

$$\phi^* = \mu_{\phi} + \alpha_{\phi} \cdot \sigma_{\phi} \cdot \beta = 0.551$$

Step 6. Substitute New Design Point into g() and Solve for β

$$g() = a \cdot \gamma_c^* \cdot \tan \delta_f^* - b \cdot \gamma^* \cdot \left(\frac{1 - \sin \phi^*}{1 + \sin \phi^*} \right) = 0$$

$\beta_3 = 2.151$

4th Trial with Results from 3rd Trial

Step 3. Obtain the Partial Derivatives

$\frac{\partial g}{\partial \gamma_c}$	$\frac{\partial g}{\partial \delta_f}$	$\frac{\partial g}{\partial \gamma}$	$\frac{\partial g}{\partial \phi}$
13.233	4.699	-15.64	4.384

Step 4. Calculate the Direction Cosines

$\sigma_{\gamma c}\frac{\partial g}{\partial \gamma_c}$	$\sigma_{\delta f}\frac{\partial g}{\partial \delta_f}$	$\sigma_{\gamma}\frac{\partial g}{\partial \gamma}$	$\sigma_{\phi}\frac{\partial g}{\partial \phi}$
0.2084	0.2461	-0.1720	0.2295

$\Delta = 0.432$

$\alpha_{\gamma c}$	$\alpha_{\delta f}$	α_{γ}	α_{ϕ}
-0.483	-0.570	0.399	-0.532

Step 5. Find the New Design Point

$$\gamma_c^* = \mu_{\gamma_c} + \alpha_{\gamma_c} \cdot \sigma_{\gamma_c} \cdot \beta = 0.158$$

$$\delta_f^* = \mu_{\delta_f} + \alpha_{\delta_f} \cdot \sigma_{\delta_f} \cdot \beta = 0.524$$

$$\gamma^* = \mu_{\gamma} + \alpha_{\gamma} \cdot \sigma_{\gamma} \cdot \beta = 0.110$$

$$\phi^* = \mu_{\phi} + \alpha_{\phi} \cdot \sigma_{\phi} \cdot \beta = 0.611$$

Step 6. Substitute New Design Point into g() and Solve for β

$$g() = a \cdot \gamma_c^* \cdot \tan \delta_f^* - b \cdot \gamma^* \cdot \left(\frac{1 - \sin \phi^*}{1 + \sin \phi^*} \right) = 0$$

$\beta_4 = 2.151$ Stop iteration at the 4th Trial.

Thus,

$$\beta = 2.15$$

4.4 SLIDING LIMIT STATE

Using the procedure presented in Section 4.3, analyses for various heights of the wall are provided in this section. The limit state function for sliding can be expressed as

$$g() = R - S$$

$$= (\text{vol.} \cdot \gamma_c) - \left(\frac{1}{2}\gamma \cdot \frac{1-\sin\phi}{1+\sin\phi} \cdot H^2\right)$$

$$= (a \cdot \gamma_c) - \left(b \cdot \gamma \cdot \frac{1-\sin\phi}{1+\sin\phi}\right)$$

where $a = \text{vol.}$

$$b = \frac{1}{2}H^2$$

Statistical data (from Hoeg and Murarka, 1974) for random variables are as below:

Var.	μ	σ	δ	Bias
γ_c	0.158	0.0158	0.10	1.05
δ_f	0.524	0.0524	0.10	1.00
γ	0.110	0.011	0.10	1.00
ϕ	0.6109	0.0524	0.086	1.00

The results of the iteration process for each height of wall are presented in the following sections.

4.4.1 Sliding Limit State - 5 ft High Wall

Conventional (ASD) Optimized Design:
S.F. = 1.57 t = 0.42 ft B = 2.28 ft D_f = 1.73 ft

Safety Index by Advanced FOSM Method:

		γ_c	δ_f	γ	ϕ	Δ	β
Mean, μ		0.158	0.524	0.110	0.611		
Std. Deviation, σ		0.0158	0.0524	0.0110	0.0524		
1st Iteration	$\frac{\partial g}{\partial x_i}$	3.897	1.4180	-3.387	0.9097		
	$\sigma_{x_i}\frac{\partial g}{\partial x_i}$	0.0614	0.7420	-0.0373	0.0476	0.114	
	α_{x_i}	-0.5400	-0.6530	0.3280	-0.419		2.230
	x_i^*	0.1390	0.447	0.1180	0.5620		
2nd Iteration	$\frac{\partial g}{\partial x_i}$	3.2390	1.1510	-3.8095	1.0628		
	$\sigma_{x_i}\frac{\partial g}{\partial x_i}$	0.0510	0.0602	-0.0419	0.0556	0.105	
	α_{x_i}	-0.4850	-0.5720	0.3980	-0.529		2.199
	x_i^*	0.1410	0.458	0.1200	0.5500		
3rd Iteration	$\frac{\partial g}{\partial x_i}$	3.3250	1.1800	-3.9182	1.0996		
	$\sigma_{x_i}\frac{\partial g}{\partial x_i}$	0.0524	0.0618	-0.0431	0.0576	0.108	
	α_{x_i}	-0.4830	-0.5710	0.3980	-0.531		2.191
	x_i^*	0.1410	0.458	0.1200	0.5500		
4th Iteration	$\frac{\partial g}{\partial x_i}$	3.3290	1.1820	-3.9194	1.0995		
	$\sigma_{x_i}\frac{\partial g}{\partial x_i}$	0.0524	0.0619	-0.0431	0.0576	0.108	
	α_{x_i}	-0.4840	-0.5710	0.3980	-0.531		2.191
	x_i^*	0.1410	0.458	0.1200	0.5500		

4.4.2 Sliding Limit State - 10 ft High Wall

Conventional (ASD) Optimized Design:
S.F. = 1.55 t = 0.75 ft B = 4.6 ft D_f = 2.67 ft

Safety Index by Advanced FOSM Method:

		γ_c	δ_f	γ	ϕ	Δ	β
Mean, μ		0.158	0.524	0.110	0.611		
Std. Deviation, σ		0.0158	0.0524	0.0110	0.0524		
1st Iteration	$\frac{\partial g}{\partial x_i}$	15.4440	5.6180	-13.5495	3.6390		
	$\sigma_{x_i}\frac{\partial g}{\partial x_i}$	0.2432	0.2941	-0.1490	0.1905	0.452	
	α_{x_i}	-0.5380	-0.6510	0.3300	-0.422		2.179
	x_i^*	0.1390	0.449	0.1180	0.5630		
2nd Iteration	$\frac{\partial g}{\partial x_i}$	12.9000	4.5840	-15.2096	4.2406		
	$\sigma_{x_i}\frac{\partial g}{\partial x_i}$	0.2032	0.2400	-0.1673	0.2220	0.420	
	α_{x_i}	-0.4840	-0.5720	0.3990	-0.529		2.151
	x_i^*	0.1410	0.459	0.1190	0.5510		
3rd Iteration	$\frac{\partial g}{\partial x_i}$	13.2270	4.6970	-15.6262	4.3817		
	$\sigma_{x_i}\frac{\partial g}{\partial x_i}$	0.2083	0.2459	-0.1719	0.2294	0.431	
	α_{x_i}	-0.4830	-0.5700	0.3980	-0.532		2.151
	x_i^*	0.1410	0.459	0.1190	0.5510		
4th Iteration	$\frac{\partial g}{\partial x_i}$	13.2330	4.6990	-15.6380	4.3840		
	$\sigma_{x_i}\frac{\partial g}{\partial x_i}$	0.2084	0.2461	-0.1720	0.2295	0.432	
	α_{x_i}	-0.4830	-0.5700	0.3990	-0.532		2.151
	x_i^*	0.1410	0.459	0.1190	0.5510		

4.4.3 Sliding Limit State - 20 ft High Wall

Conventional (ASD) Optimized Design:
S.F. = 1.55 t = 1.5 ft B = 9.2 ft D_f = 3.93 ft

Safety Index by Advanced FOSM Method:

		γ_c	δ_f	γ	ϕ	Δ	β
Mean, μ		0.158	0.524	0.110	0.611		
Std. Deviation, σ		0.0158	0.0524	0.0110	0.0524		
1st Iteration	$\frac{\partial g}{\partial x_i}$	61.7760	22.4800	-54.1980	14.5556		
	$\sigma_{x_i}\frac{\partial g}{\partial x_i}$	0.9730	1.1765	-0.5962	0.7621	1.808	
	α_{x_i}	-0.5380	-0.6510	0.3300	-0.422		2.179
	x_i^*	0.1390	0.449	0.1180	0.5630		
2nd Iteration	$\frac{\partial g}{\partial x_i}$	51.5980	18.3350	-60.8385	16.9623		
	$\sigma_{x_i}\frac{\partial g}{\partial x_i}$	0.8127	0.9600	-0.6692	0.8881	1.679	
	α_{x_i}	-0.4840	-0.5720	0.3990	-0.529		2.151
	x_i^*	0.1410	0.459	0.1190	0.5510		
3rd Iteration	$\frac{\partial g}{\partial x_i}$	52.9060	18.7890	-62.5048	17.5266		
	$\sigma_{x_i}\frac{\partial g}{\partial x_i}$	0.8333	0.9838	-0.6876	0.9177	1.725	
	α_{x_i}	-0.4830	-0.5700	0.3980	-0.532		2.151
	x_i^*	0.1410	0.459	0.1190	0.5510		
4th Iteration	$\frac{\partial g}{\partial x_i}$	52.9310	18.7970	-62.5521	17.5360		
	$\sigma_{x_i}\frac{\partial g}{\partial x_i}$	0.8337	0.9842	-0.6881	0.9182	1.726	
	α_{x_i}	-0.4830	-0.5700	0.3990	-0.532		2.151
	x_i^*	0.1410	0.459	0.1190	0.5510		

4.4.4 Sliding Limit State - 30 ft High Wall

Conventional (ASD) Optimized Design:
S.F. = 1.57 t = 2.5 ft B = 13.7 ft D_f = 4.0 ft

Safety Index by Advanced FOSM Method:

		γ_c	δ_f	γ	ϕ	Δ	β
Mean, μ		0.158	0.524	0.110	0.611		
Std. Deviation, σ		0.0158	0.0524	0.0110	0.0524		
1st Iteration	$\frac{\partial g}{\partial x_i}$	140.296	51.0300	-121.946	32.7510		
	$\sigma_{x_i}\frac{\partial g}{\partial x_i}$	2.2097	2.6719	-1.3414	1.7148	4.094	
	α_{x_i}	-0.5400	-0.6530	0.3280	-0.419		2.221
	x_i^*	0.1390	0.448	0.1180	0.5620		
2nd Iteration	$\frac{\partial g}{\partial x_i}$	116.694	41.4530	-137.080	38.2365		
	$\sigma_{x_i}\frac{\partial g}{\partial x_i}$	1.8379	2.1705	-1.5079	2.0021	3.791	
	α_{x_i}	-0.4850	-0.5730	0.3980	-0.528		2.191
	x_i^*	0.1410	0.458	0.1200	0.5500		
3rd Iteration	$\frac{\partial g}{\partial x_i}$	119.761	42.5150	-140.971	39.5559		
	$\sigma_{x_i}\frac{\partial g}{\partial x_i}$	1.8862	2.2261	-1.5507	2.0711	3.900	
	α_{x_i}	-0.4840	-0.5710	0.3980	-0.531		2.191
	x_i^*	0.1410	0.458	0.1200	0.5500		
4th Iteration	$\frac{\partial g}{\partial x_i}$	119.821	42.5350	-141.084	39.5784		
	$\sigma_{x_i}\frac{\partial g}{\partial x_i}$	1.8872	2.2271	-1.5519	2.0723	3.902	
	α_{x_i}	-0.4840	-0.5710	0.3980	-0.531		2.191
	x_i^*	0.1410	0.458	0.1200	0.5500		

4.4.5 Summary of Safety Indices for Sliding Limit State

The trend of convergence in the safety index of the sliding limit state is shown in Figure 4.4.

The safety indices for sliding limit state are summarized in Table 4.2. It can be observed that the safety indices are virtually identical to each other throughout the various wall heights.

Table 4.2 Safety Indices for Sliding Limit State

H (ft)	B (ft)	t (ft)	Safety Factor	Safety Index
5	2.28	0.42	1.57	**2.19**
10	4.60	0.75	1.55	**2.15**
20	9.20	1.50	1.55	**2.15**
30	13.70	2.50	1.57	**2.19**

5 ft wall

β1	2.230
β2	2.199
β3	2.191
β4	2.191

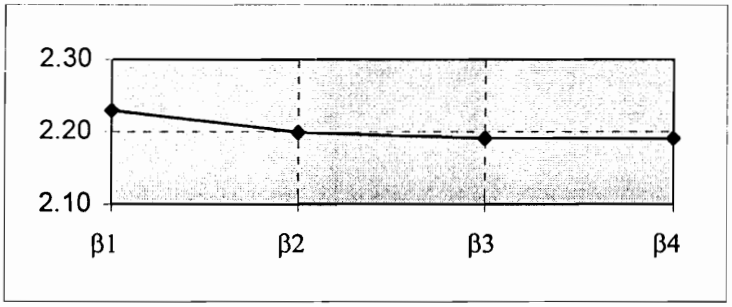

10 ft wall

β1	2.179
β2	2.151
β3	2.151
β4	2.151

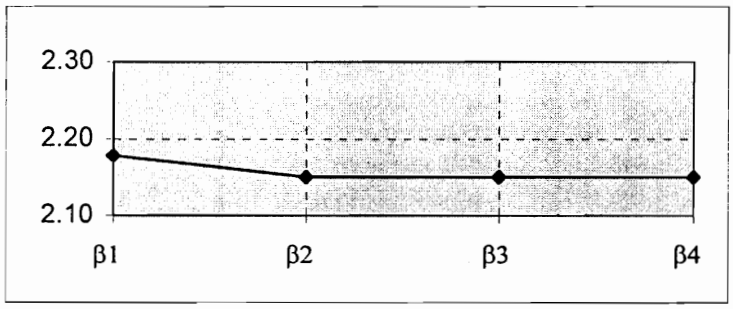

20 ft wall

β1	2.179
β2	2.151
β3	2.151
β4	2.151

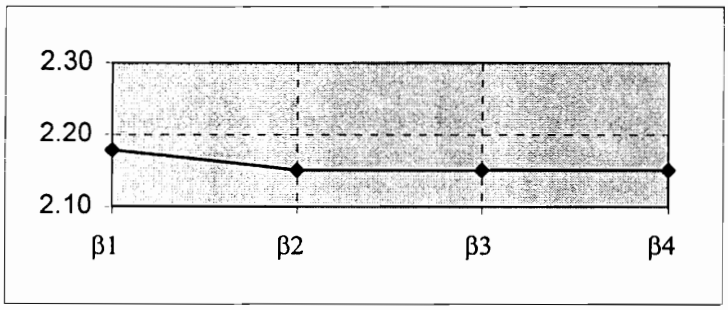

30 ft wall

β1	2.221
β2	2.191
β3	2.191
β4	2.191

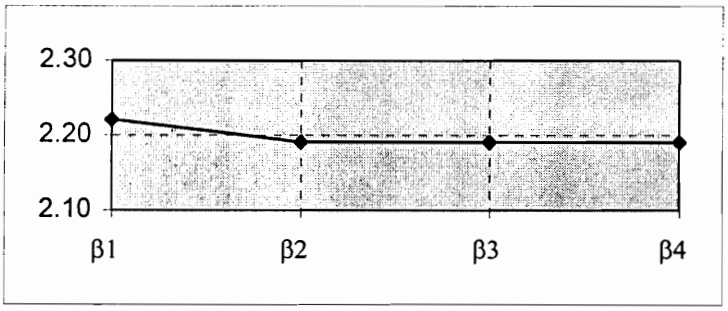

Figure 4.4 The Trend of Convergence in β of Sliding Limit State

4.5 OVERTURNING LIMIT STATE

Using the similar procedure described in Section 4.3, analyses of the overturning limit state for various heights of the wall are provided in this section. The limit state function for overturning can be expressed as

$$
\begin{aligned}
g() &= R - S \\
&= \left(\text{vol.} \cdot \gamma_c \cdot \bar{x}\right) - \left(\frac{1}{2}\gamma \cdot \frac{1-\sin\phi}{1+\sin\phi} \cdot H^2 \cdot (n \cdot H)\right) \\
&= a \cdot \gamma_c - b \cdot \gamma \cdot \frac{1-\sin\phi}{1+\sin\phi} \cdot n
\end{aligned}
$$

where $a = \bar{x} \cdot \text{vol.}$

$$b = \frac{1}{2}H^3$$

Statistical data (from Hoeg and Murarka, 1974) for random variables are as below:

Var.	μ	σ	δ	Bias
γ_c	0.158	0.0158	0.10	1.05
ϕ	0.6109	0.0524	0.086	1.00
γ	0.110	0.011	0.10	1.00
n	0.40	0.04	0.10	1.00

The results of the iteration process for each height of wall are presented in the following sections.

4.5.1 Overturning Limit State - 5 ft High Wall

Conventional (ASD) Optimized Design:
S.F. = 2.04 t = 0.42 ft B = 2.28 ft D_f = 1.73 ft

Safety Index by Advanced FOSM Method:

		γ_c	δ_f	γ	ϕ	Δ	β
Mean, μ		0.158	0.611	0.110	0.400		
Std. Deviation, σ		0.0158	0.0524	0.0110	0.0400		
1st Iteration	$\frac{\partial g}{\partial x_i}$	10.113	1.820	-6.775	-1.863		
	$\sigma_{x_i}\frac{\partial g}{\partial x_i}$	0.1593	0.0953	-0.0745	-0.0745	0.123	
	α_{x_i}	-0.7460	-0.4460	0.3490	0.349		3.658
	x_i^*	0.1146	0.526	0.1240	0.4510		
2nd Iteration	$\frac{\partial g}{\partial x_i}$	10.113	2.681	-9.350	-2.571		
	$\sigma_{x_i}\frac{\partial g}{\partial x_i}$	0.1593	0.1404	-0.1028	-0.1028	0.257	
	α_{x_i}	-0.6190	-0.5450	0.4000	0.4		3.581
	x_i^*	0.1226	0.509	0.1257	0.4570		
3rd Iteration	$\frac{\partial g}{\partial x_i}$	10.113	2.839	-9.860	-2.712		
	$\sigma_{x_i}\frac{\partial g}{\partial x_i}$	0.1593	0.1486	-0.1085	-0.1085	0.266	
	α_{x_i}	-0.5980	-0.5580	0.4070	0.4070		3.579
	x_i^*	0.1238	0.506	0.1260	0.4580		
4th Iteration	$\frac{\partial g}{\partial x_i}$	10.113	2.863	-9.935	-2.732		
	$\sigma_{x_i}\frac{\partial g}{\partial x_i}$	0.1593	0.1499	-0.1093	-0.1093	0.268	
	α_{x_i}	-0.5950	-0.5600	0.4080	0.4080		3.579
	x_i^*	0.1240	0.506	0.1261	0.4580		

4.5.2 Overturning Limit State - 10 ft High Wall

Conventional (ASD) Optimized Design:
S.F. = 2.04 t = 0.75 ft B = 4.6 ft D_f = 2.67 ft

Safety Index by Advanced FOSM Method:

		γ_c	δ_f	γ	ϕ	Δ	β
Mean, μ		0.158	0.611	0.110	0.400		
Std. Deviation, σ		0.0158	0.0524	0.0110	0.0400		
1st Iteration	$\frac{\partial g}{\partial x_i}$	81.096	14.556	-54.198	-14.905		
	$\sigma_{x_i}\frac{\partial g}{\partial x_i}$	1.2773	0.7621	-0.5962	-0.5962	1.710	
	α_{x_i}	-0.7470	-0.4460	0.3490	0.349		3.658
	x_i^*	0.1145	0.525	0.1240	0.4510		
2nd Iteration	$\frac{\partial g}{\partial x_i}$	81.096	21.461	-74.842	-20.581		
	$\sigma_{x_i}\frac{\partial g}{\partial x_i}$	1.2773	1.1237	-0.8233	-0.8233	2.061	
	α_{x_i}	-0.6200	-0.5450	0.3990	0.399		3.592
	x_i^*	0.1224	0.508	0.1258	0.4570		
3rd Iteration	$\frac{\partial g}{\partial x_i}$	81.096	22.735	-78.950	-21.711		
	$\sigma_{x_i}\frac{\partial g}{\partial x_i}$	1.2773	1.1904	-0.8684	-0.8684	2.135	
	α_{x_i}	-0.5980	-0.5580	0.4070	0.407		3.590
	x_i^*	0.1237	0.506	0.1261	0.4580		
4th Iteration	$\frac{\partial g}{\partial x_i}$	81.096	22.932	-79.552	-21.877		
	$\sigma_{x_i}\frac{\partial g}{\partial x_i}$	1.2773	1.2007	-0.8751	-0.8751	2.146	
	α_{x_i}	-0.5950	-0.5600	0.4080	0.4080		3.590
	x_i^*	0.1238	0.506	0.1261	0.4590		

4.5.3 Overturning Limit State - 20 ft High Wall

Conventional (ASD) Optimized Design:
S.F. = 2.04 t = 1.5 ft B = 9.2 ft D_f = 3.93 ft

Safety Index by Advanced FOSM Method:

		γ_c	δ_f	γ	ϕ	Δ	β
Mean, μ		0.158	0.611	0.110	0.400		
Std. Deviation, σ		0.0158	0.0524	0.0110	0.0400		
1st Iteration	$\frac{\partial g}{\partial x_i}$	648.767	116.450	-433.584	-119.236		
	$\sigma_{x_i}\frac{\partial g}{\partial x_i}$	10.2181	6.0972	-4.7694	-4.7694	13.678	
	α_{x_i}	-0.7470	-0.4460	0.3490	0.349		3.658
	x_i^*	0.1145	0.525	0.1240	0.4510		
2nd Iteration	$\frac{\partial g}{\partial x_i}$	648.767	171.690	-598.732	-164.651		
	$\sigma_{x_i}\frac{\partial g}{\partial x_i}$	10.2181	8.9894	-6.5860	-6.5860	16.492	
	α_{x_i}	-0.6200	-0.5450	0.3990	0.399		3.592
	x_i^*	0.1224	0.508	0.1258	0.4570		
3rd Iteration	$\frac{\partial g}{\partial x_i}$	648.767	181.880	-631.594	-173.688		
	$\sigma_{x_i}\frac{\partial g}{\partial x_i}$	10.2181	9.5233	-6.9475	-6.9475	17.077	
	α_{x_i}	-0.5980	-0.5580	0.4070	0.407		3.590
	x_i^*	0.1237	0.506	0.1261	0.4580		
4th Iteration	$\frac{\partial g}{\partial x_i}$	648.767	183.450	-636.409	-175.013		
	$\sigma_{x_i}\frac{\partial g}{\partial x_i}$	10.2181	9.6055	-7.0005	-7.0005	17.167	
	α_{x_i}	-0.5950	-0.5600	0.4080	0.4080		3.590
	x_i^*	0.1238	0.506	0.1261	0.4590		

4.5.4 Overturning Limit State - 30 ft High Wall

Conventional (ASD) Optimized Design:
S.F. = 2.04 t = 2.5 ft B = 13.7 ft D_f = 4.0 ft

Safety Index by Advanced FOSM Method:

		γ_c	δ_f	γ	ϕ	Δ	β
Mean, μ		0.158	0.611	0.110	0.400		
Std. Deviation, σ		0.0158	0.0524	0.0110	0.0400		
1st Iteration	$\frac{\partial g}{\partial x_i}$	2188.150	393.010	-1463.35	-402.420		
	$\sigma_{x_i}\frac{\partial g}{\partial x_i}$	34.4634	20.5780	-16.0968	-16.0968	46.145	
	α_{x_i}	-0.7460	-0.4460	0.3490	0.349		3.654
	x_i^*	0.1146	0.526	0.1240	0.4510		
2nd Iteration	$\frac{\partial g}{\partial x_i}$	2188.150	579.320	-2020.39	-555.607		
	$\sigma_{x_i}\frac{\partial g}{\partial x_i}$	34.4634	30.3330	-22.2243	-22.2243	55.639	
	α_{x_i}	-0.6190	-0.5450	0.3990	0.3990		3.589
	x_i^*	0.1225	0.508	0.1258	0.4570		
3rd Iteration	$\frac{\partial g}{\partial x_i}$	2188.150	613.670	-2131.11	-586.054		
	$\sigma_{x_i}\frac{\partial g}{\partial x_i}$	34.4634	32.1318	-23.4422	-23.4422	57.613	
	α_{x_i}	-0.5980	-0.5580	0.4070	0.4070		3.587
	x_i^*	0.1237	0.506	0.1261	0.4580		
4th Iteration	$\frac{\partial g}{\partial x_i}$	2188.150	618.960	-2147.31	-590.510		
	$\sigma_{x_i}\frac{\partial g}{\partial x_i}$	34.4634	32.4085	-23.6204	-23.6204	57.913	
	α_{x_i}	-0.5950	-0.5600	0.4080	0.4080		3.587
	x_i^*	0.1239	0.506	0.1261	0.4590		

4.5.5 Summary of Safety Indices for Overturning Limit State

The trend of convergence in the safety index of the overturning limit state is shown in Figure 4.5.

The safety indices for overturning limit state are summarized in Table 4.3. Just like the sliding limit state cases, it is observed that the safety indices are almost same each other for different heights of the wall.

Table 4.3 Safety Indices for Overturning Limit State

H (ft)	**B** (ft)	**t** (ft)	**Safety Factor**	**Safety Index**
5	2.28	0.42	2.04	**3.58**
10	4.60	0.75	2.04	**3.59**
20	9.20	1.50	2.04	**3.59**
30	13.70	2.50	2.04	**3.59**

5 ft wall

β1	3.658
β2	3.581
β3	3.579
β4	3.579

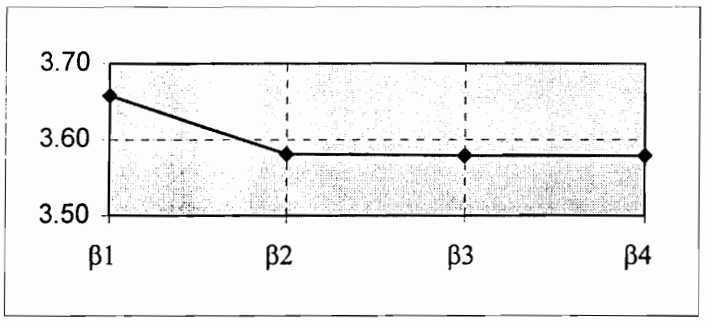

10 ft wall

β1	3.658
β2	3.592
β3	3.590
β4	3.590

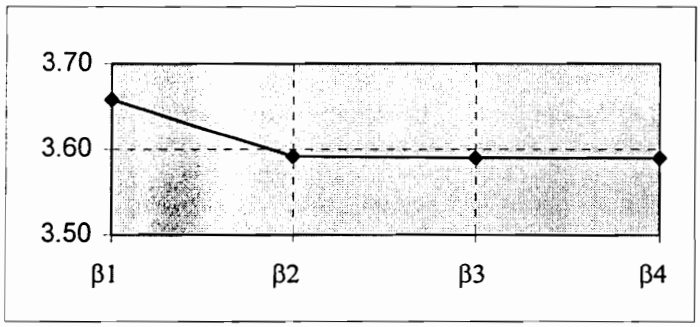

20 ft wall

β1	3.658
β2	3.590
β3	3.590
β4	3.590

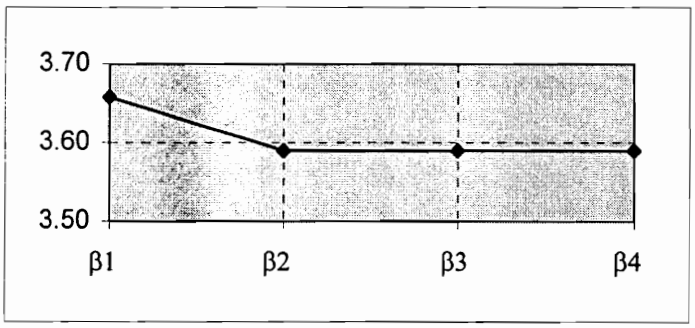

30 ft wall

β1	3.654
β2	3.589
β3	3.587
β4	3.587

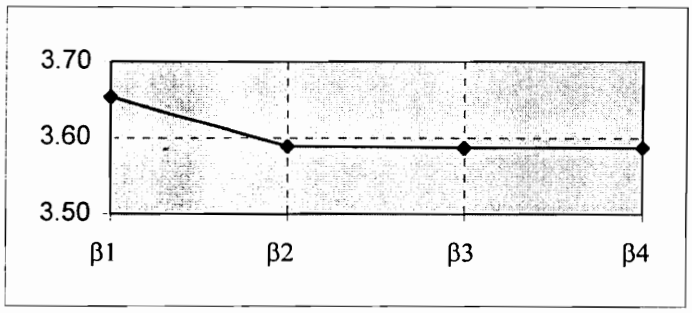

Figure 4.5 The Trend of Convergence in β of Overturning Limit State

4.6 BEARING CAPACITY LIMIT STATE

Unlike the two previous limit states, the procedures for the bearing limit state are so complicated that it is difficult to program the long equation in one cell of the spreadsheet and it is hard to verify the result. Therefore, the whole process will be subdivided into several small calculation units, named Modules, for the purpose of convenient programming. Another personal computer software, MATHEMATICA is employed to verify the result. This math-oriented program has a feature to generate the symbolic partial derivatives as well as the numerical values for each partial derivative. The procedure for analyzing the bearing capacity limit state will be detailed in the following sections.

4.6.1 Limit State Function for Bearing Capacity

The limit state function for bearing capacity can be expressed as

$$g() = R - S = q_{ult} - q_{max} = 0 \tag{4.6}$$

Using Meyerhof's equation and rectangular shape of pressure distribution,

$$q_{ult} = \gamma \cdot x_o \cdot \left(1 - \frac{\theta}{\phi_f}\right)^2 \cdot N_\gamma + \gamma \cdot D_f \cdot \left(1 - \frac{\theta}{90}\right)^2 \cdot \left(1 + 0.3\frac{D_f}{2x_o}\right) \cdot N_q \tag{4.7}$$

$$q_{max} = \frac{W_c}{2x_o} = \left(\frac{vol.}{2}\right) \cdot \left(\frac{\gamma_c}{x_o}\right) \tag{4.8}$$

where

$$\begin{cases} x_o = \bar{x} - \dfrac{P \cdot n \cdot H}{\text{vol.} \cdot \gamma_c} \\ \theta = \text{Arctan}\left(\dfrac{P}{\text{vol.} \cdot \gamma_c}\right) \\ P = \dfrac{1}{2}\gamma \cdot H^2 \cdot \tan^2\left(\dfrac{\pi}{4} - \dfrac{\phi}{2}\right) \\ N_q = e^{\pi \tan\phi_f} \cdot \tan^2\left(\dfrac{\pi}{4} + \dfrac{\phi_f}{2}\right) \\ N_\gamma = \left(N_q - 1\right) \cdot \tan\left(1.4\phi_f\right) \end{cases} \tag{4.9}$$

By substituting Eq. 4.9 into Eq. 4.6, the limit state function for bearing capacity is fully expanded in terms of the basic random variables as

$$g() = \gamma \cdot \left(\bar{x} - \frac{\frac{1}{2}\gamma \cdot H^2 \cdot \tan^2\left(\frac{\pi}{4} - \frac{\phi}{2}\right) \cdot n \cdot H}{\text{vol.} \cdot \gamma_c} \right) \cdot$$

$$\left(1 - \frac{\text{Arctan}\left(\dfrac{\frac{1}{2}\gamma \cdot H^2 \cdot \tan^2\left(\frac{\pi}{4} - \frac{\phi}{2}\right)}{\text{vol.} \cdot \gamma_c} \right)}{\phi_f} \right)^2 \cdot \left(e^{\pi \tan\phi} \cdot \tan^2\left(\frac{\pi}{4} + \frac{\phi}{2}\right) - 1 \right) \cdot \tan\left(1.4\phi_f\right)$$

$$+ \gamma \cdot D_f \cdot \left(1 + 0.3 \frac{D_f}{2\left(\bar{x} - \frac{\frac{1}{2}\gamma \cdot H^2 \cdot \tan^2\left(\frac{\pi}{4} - \frac{\phi}{2}\right) \cdot n \cdot H}{\text{vol.} \cdot \gamma_c} \right)} \right) \cdot$$

$$\left(1 - \frac{\text{Arctan}\left(\frac{\frac{1}{2}\gamma \cdot H^2 \cdot \tan^2\left(\frac{\pi}{4} - \frac{\phi}{2}\right)}{\text{vol.} \cdot \gamma_c} \right)}{90} \right)^2 \cdot \left(e^{\pi \tan\phi} \cdot \tan^2\left(\frac{\pi}{4} + \frac{\phi_f}{2}\right) \right)$$

$$- \left(\frac{\text{vol.}}{2}\right) \cdot \frac{\gamma_c}{\left(\bar{x} - \frac{\frac{1}{2}\gamma \cdot H^2 \cdot \tan^2\left(\frac{\pi}{4} - \frac{\phi}{2}\right) \cdot n \cdot H}{\text{vol.} \cdot \gamma_c} \right)} \qquad (4.10)$$

Since the limit state function is too complex to handle, it is advantageous to subdivide g() into several manageable sizes and express the function using not only the *basic* random variables but also the *intermediate* random variables which are in Eq. 4.9. (For lack of a better term, they will be referred to as the *intermediate* random variables.)

When q_{ult} (Eq. 4.7) can be expressed as $q_{ult} = B_\gamma + B_q$

then, $g() = B_\gamma + B_q - q_{max} = 0$

where $$B_\gamma = \gamma \cdot x_o \cdot \left(1 - \frac{\theta}{\phi_f}\right)^2 \cdot N_\gamma$$

$$B_q = \gamma \cdot D_f \cdot \left(1 - \frac{\theta}{90}\right)^2 \cdot \left(1 + 0.3\frac{D_f}{2x_o}\right) \cdot N_q$$

4.6.2 Algorithm of Analysis

g() is a function of the five basic random variables (γ, γ_c, n, ϕ, ϕ_f). It is, therefore, required to obtain the partial derivatives for each random variables as follows:

$$\frac{\partial g}{\partial \gamma} = \frac{\partial B_\gamma}{\partial \gamma} + \frac{\partial B_q}{\partial \gamma} - \frac{\partial q_{max}}{\partial \gamma}$$

$$\frac{\partial g}{\partial \gamma_c} = \frac{\partial B_\gamma}{\partial \gamma_c} + \frac{\partial B_q}{\partial \gamma_c} - \frac{\partial q_{max}}{\partial \gamma_c}$$

$$\frac{\partial g}{\partial n} = \frac{\partial B_\gamma}{\partial n} + \frac{\partial B_q}{\partial n} - \frac{\partial q_{max}}{\partial n}$$

$$\frac{\partial g}{\partial \phi} = \frac{\partial B_\gamma}{\partial \phi} + \frac{\partial B_q}{\partial \phi} - \frac{\partial q_{max}}{\partial \phi}$$

$$\frac{\partial g}{\partial \phi_f} = \frac{\partial B_\gamma}{\partial \phi_f} + \frac{\partial B_q}{\partial \phi_f} - \frac{\partial q_{max}}{\partial \phi_f}$$

Since B_γ, B_q and q_{max} are functions of all basic random variables, five partial derivatives for each term should be provided. The partial derivatives for B_γ, B_q and q_{max} are fully expanded in terms of the basic random variables (γ, γ_c, n, ϕ, ϕ_f) and the intermediate random variables (x_o, θ, P, N_γ, N_q). The partial derivatives of the intermediate random variables also should be expressed in terms of the basic random variables. All the procedures are subdivided into several modules for convenient analysis and summarized in Tables 4.4 through 4.8. Application of theses modules in the determination of the safety index for a 30 ft wall are illustrated in Example 4.2.

Example 4.2

Using the procedure in Section 4.3 and the modules in the Table 4.4, the safety index is found for a wall with the following conditions.

Given conditions:

Wall height = 30 ft,

Unit weight of concrete = 150 pcf,

Internal friction angle of bacfill = 35 deg,

Unit weight of backfill soil = 110 pcf,

Internal friction angle of foundation soil = 37 deg.

Table 4.4 Modules used in the Spreadsheet Program

Module I	$\gamma_c^*,\ \gamma^*,\ n^*,\ \phi^*,\ \phi_f^*$
Module II	$P(\gamma,\phi),\quad \frac{\partial P}{\partial \gamma},\ \frac{\partial P}{\partial \phi},$ $N_q(\phi_f),\quad \frac{\partial N_q}{\partial \phi_f},$ $N_\gamma(\phi_f),\quad \frac{\partial N_\gamma}{\partial \phi_f},$ $\theta(\gamma,\phi,\gamma_c),\quad \frac{\partial \theta}{\partial \gamma},\ \frac{\partial \theta}{\partial \phi},\ \frac{\partial \theta}{\partial \gamma_c},$ $x_o(\gamma,\phi,n,\gamma_c),\quad \frac{\partial x_o}{\partial \gamma},\ \frac{\partial x_o}{\partial \phi},\ \frac{\partial x_o}{\partial n},\ \frac{\partial x_o}{\partial \gamma_c}$
Module III	$\frac{\partial B_\gamma}{\partial \gamma_c},\ \frac{\partial B_\gamma}{\partial \gamma},\ \frac{\partial B_\gamma}{\partial n},\ \frac{\partial B_\gamma}{\partial \phi},\ \frac{\partial B_\gamma}{\partial \phi_f},$ $\frac{\partial B_q}{\partial \gamma_c},\ \frac{\partial B_q}{\partial \gamma},\ \frac{\partial B_q}{\partial n},\ \frac{\partial B_q}{\partial \phi},\ \frac{\partial B_q}{\partial \phi_f},$ $\frac{\partial q_{max}}{\partial \gamma_c},\ \frac{\partial q_{max}}{\partial \gamma},\ \frac{\partial q_{max}}{\partial n},\ \frac{\partial q_{max}}{\partial \phi},\ \frac{\partial q_{max}}{\partial \phi_f}$
Module IV	$\frac{\partial g}{\partial \gamma_c},\ \frac{\partial g}{\partial \gamma},\ \frac{\partial g}{\partial n},\ \frac{\partial g}{\partial \phi},\ \frac{\partial g}{\partial \phi_f}$
Module V	$\frac{\partial g}{\partial \gamma_c}\cdot\sigma_{\gamma_c},\ \frac{\partial g}{\partial \gamma}\cdot\sigma_\gamma,\ \frac{\partial g}{\partial n}\cdot\sigma_n,\ \frac{\partial g}{\partial \phi}\cdot\sigma_\phi,\ \frac{\partial g}{\partial \phi_f}\cdot\sigma_{\phi_f}$ $\Delta=\sqrt{\Sigma\left(\frac{\partial g}{\partial x_i}\cdot\sigma_{x_i}\right)^2}$ $\alpha_{\gamma_c},\ \alpha_\gamma,\ \alpha_n,\ \alpha_\phi,\ \alpha_{\phi_f}$
Module VI	$\gamma_c^*,\ \gamma^*,\ n^*,\ \phi^*,\ \phi_f^*$
Module VII	$g() = B_\gamma + B_q - q_{max} = 0$

Table 4.5 Partial Derivatives in Module II (continued over)

$P(\gamma, \phi)$	$P = \frac{1}{2}\gamma \cdot H^2 \cdot \tan^2\left(\frac{\pi}{4} - \frac{\phi}{2}\right)$ $\frac{\partial P}{\partial \gamma} = \frac{1}{2} H^2 \cdot \tan^2\left(\frac{\pi}{4} - \frac{\phi}{2}\right) = \frac{P}{\gamma}$ $\frac{\partial P}{\partial \phi} = \frac{1}{2}\gamma \cdot H^2 \cdot \tan^2\left(\frac{\pi}{4} - \frac{\phi}{2}\right) \cdot \sec^2\left(\frac{\pi}{4} - \frac{\phi}{2}\right)$
$N_q(\phi_f)$	$N_q = e^{\pi \tan\phi_f} \tan^2\left(\frac{\pi}{4} + \frac{\phi_f}{2}\right)$ $\frac{\partial N_q}{\partial \phi_f} = \frac{e^{\pi \tan\phi_f} \tan^2\left(\frac{\pi}{4} + \frac{\phi_f}{2}\right)}{\left(\cos\frac{\phi_f}{2} - \sin\frac{\phi_f}{2}\right)^4}$
$N_\gamma(\phi_f)$	$N_\gamma = \left(e^{\pi \tan\phi_f} \tan^2\left(\frac{\pi}{4} + \frac{\phi_f}{2}\right) - 1\right) \cdot \tan(1.4\phi_f)$ $\frac{\partial N_\gamma}{\partial \phi_f} = \frac{e^{\pi \tan\phi_f}(\pi + 2\cos\phi_f)}{\left(\cos\frac{\phi_f}{2} - \sin\frac{\phi_f}{2}\right)^4} \cdot \tan(1.4\phi_f)$ $+ \ 1.4\sec^2(1.4\phi_f) \cdot \left(e^{\pi \tan\phi_f} \tan^2\left(\frac{\pi}{4} + \frac{\phi_f}{2}\right) - 1\right)$
$\theta(\gamma, \phi, \gamma_c)$	$\theta = \arctan\left(\frac{P}{\text{vol.}\cdot\gamma_c}\right)$ $\frac{\partial \theta}{\partial \gamma} = \frac{1}{1 + \left(\frac{P}{\text{vol.}\cdot\gamma_c}\right)} \cdot \left(\frac{1}{\text{vol.}\cdot\gamma_c}\right) \cdot \frac{\partial P}{\partial \gamma} = \frac{P \cdot \text{vol.}\cdot\gamma_c}{\gamma\left(P^2 + (\text{vol.}\cdot\gamma_c)^2\right)}$ $\frac{\partial \theta}{\partial \phi} = \frac{(\text{vol.}\cdot\gamma_c)^2}{(\text{vol.}\cdot\gamma_c)^2 + P^2} \cdot \frac{1}{\text{vol.}} \cdot \frac{\partial P}{\partial \phi} = -\frac{\text{vol.}\cdot\gamma_c}{(\text{vol.}\cdot\gamma_c)^2 + P^2} \cdot \frac{\partial P}{\partial \phi}$ $\frac{\partial \theta}{\partial \gamma_c} = \frac{(\text{vol.}\cdot\gamma_c)^2}{(\text{vol.}\cdot\gamma_c)^2 + P^2} \cdot \frac{P}{\text{vol.}} \cdot \left(\frac{-1}{\gamma_c^2}\right) = -\frac{\text{vol.}\cdot P}{(\text{vol.}\cdot\gamma_c)^2 + P^2}$

Table 4.5 Partial Derivatives in Module II (continued)

$x_o(\gamma, \phi, n, \gamma_c)$	$x_o = \bar{x} - \frac{P \cdot n \cdot H}{vol. \cdot \gamma_c}$ $\frac{\partial x_o}{\partial \gamma} = -\frac{\partial P}{\partial \gamma} \cdot \frac{n \cdot H}{vol. \cdot \gamma_c}$ $\frac{\partial x_o}{\partial \phi} = -\frac{\partial P}{\partial \phi} \cdot \frac{n \cdot H}{vol. \cdot \gamma_c}$ $\frac{\partial x_o}{\partial n} = -\frac{P \cdot H}{vol. \cdot \gamma_c}$ $\frac{\partial x_o}{\partial \gamma_c} = \frac{P \cdot n \cdot H}{vol. \cdot \gamma_c^2}$

Table 4.6 Partial Derivatives of B_γ in Module III

$B_\gamma(\gamma_c, \gamma, x_o, \theta, \phi_f)$	$B_\gamma = \gamma \cdot x_o \cdot \left(1 - \frac{\theta}{\phi_f}\right)^2 \cdot N_\gamma$
	$\frac{\partial B_\gamma}{\partial \gamma_c} = \gamma \cdot \left(1 - \frac{\theta}{\phi_f}\right)\left(\left(1 - \frac{\theta}{\phi_f}\right) \cdot \frac{\partial x_o}{\partial \gamma_c} - \frac{2x_o}{\phi_f} \cdot \frac{\partial \theta}{\partial \gamma_c}\right) \cdot N_\gamma$
	$\frac{\partial B_\gamma}{\partial \gamma} = \left(1 - \frac{\theta}{\phi_f}\right)^2 N_\gamma \left(x_o + \gamma \frac{\partial x_o}{\partial \gamma}\right) - \left(1 - \frac{\theta}{\phi_f}\right) N_\gamma \left(\frac{2\gamma x_o}{\phi_f} \cdot \frac{\partial \theta}{\partial \gamma}\right)$
	$\frac{\partial B_\gamma}{\partial n} = \gamma \cdot \frac{\partial x_o}{\partial n}\left(1 - \frac{\theta}{\phi_f}\right)^2 N_\gamma$
	$\frac{\partial B_\gamma}{\partial \phi} = \gamma \cdot N_\gamma \left(1 - \frac{\theta}{\phi_f}\right)\left(\left(1 - \frac{\theta}{\phi_f}\right) \cdot \frac{\partial x_o}{\partial \phi} - \frac{2x_o}{\phi_f} \cdot \frac{\partial \theta}{\partial \phi}\right)$
	$\frac{\partial B_\gamma}{\partial \phi_f} = \gamma \cdot x_o \cdot \left(1 - \frac{\theta}{\phi_f}\right)\left(\left(1 - \frac{\theta}{\phi_f}\right) \cdot \frac{\partial N_\gamma}{\partial \phi_f} + \frac{2\theta}{\phi_f^2} \cdot \frac{\partial \theta}{\partial \phi_f} N_\gamma\right)$

Table 4.7 Partial Derivatives of B_q in Module III

$B_q(\gamma_c, \gamma, x_o, \theta, \phi_f)$	$B_q = \gamma \cdot D_f \cdot \left(1-\frac{2\theta}{\pi}\right)^2 \left(1+0.15\frac{D_f}{x_o}\right) \cdot N_q$
	$\frac{\partial B_q}{\partial \gamma_c} = -\gamma \cdot D_f \cdot \left(1-\frac{2\theta}{\pi}\right) \cdot N_q \cdot \left(\frac{4}{\pi}\frac{\partial \theta}{\partial \gamma_c}\left(1+0.15\frac{D_f}{x_o}\right)+\left(1-\frac{2\theta}{\pi}\right)\left(0.15\frac{D_f}{x_o^2}\frac{\partial x_o}{\partial \gamma_c}\right)\right)$
	$\frac{\partial B_q}{\partial \gamma} = D_f \cdot \left(1-\frac{2\theta}{\pi}\right) \cdot N_q \cdot \left(\left(1+0.15\frac{D_f}{x_o}\right)\left(1-\frac{2\theta}{\pi}-\frac{4\gamma}{\pi}\frac{\partial \theta}{\partial \gamma}\right)-\left(1-\frac{2\theta}{\pi}\right)\left(0.15\frac{D_f}{x_o^2}\frac{\partial x_o}{\partial \gamma}\right)\right)$
	$\frac{\partial B_q}{\partial n} = -0.15\frac{\gamma \cdot D_f^2}{x_o^2}\left(1-\frac{2\theta}{\pi}\right)^2 \cdot N_q \cdot \frac{\partial x_o}{\partial n}$
	$\frac{\partial B_q}{\partial \phi} = -\gamma \cdot D_f \cdot \left(1-\frac{2\theta}{\pi}\right) \cdot N_q \cdot \left(\frac{4}{\pi}\frac{\partial \theta}{\partial \phi}\left(1+0.15\frac{D_f}{x_o}\right)+\left(1-\frac{2\theta}{\pi}\right)\left(0.15\frac{D_f}{x_o^2}\frac{\partial x_o}{\partial \phi}\right)\right)$
	$\frac{\partial B_q}{\partial \phi_f} = \gamma \cdot D_f \cdot \left(1-\frac{2\theta}{\pi}\right)^2 \cdot \left(1+0.15\frac{D_f}{x_o}\right)\frac{\partial N_q}{\partial \phi_f}$

Table 4.8 Partial Derivatives of q_{max} in Module III

$q_{max}(\gamma_c, \gamma, x_o, \theta, \phi_f)$	$q_{max} = \frac{vol.}{2}\frac{\gamma_c}{x_o}$
	$\frac{\partial q_{max}}{\partial \gamma_c} = \left(\frac{vol.}{2x_o}\right)\left(1 - \frac{\gamma_c}{x_o}\frac{\partial x_o}{\partial \gamma_c}\right)$
	$\frac{\partial q_{max}}{\partial \gamma} = -\left(\frac{vol.}{2x_o}\right)\left(\frac{\gamma_c}{x_o^2}\right)\left(\frac{\partial x_o}{\partial \gamma}\right)$
	$\frac{\partial q_{max}}{\partial n} = -\left(\frac{vol.}{2x_o}\right)\left(\frac{\gamma_c}{x_o^2}\right)\left(\frac{\partial x_o}{\partial n}\right)$
	$\frac{\partial q_{max}}{\partial \phi} = -\left(\frac{vol.}{2x_o}\right)\left(\frac{\gamma_c}{x_o^2}\right)\left(\frac{\partial x_o}{\partial \phi}\right)$
	$\frac{\partial q_{max}}{\partial \phi_f} = 0$

Example 4.2 (continued)

Using a similar procedure to that described in Section 4.3.2, the wall dimensions are determined as follows:

For a safety factor of 2.5, $t = 2.5$ ft, $B = 13.7$ ft and $D_f = 4.0$ ft.

The statistical data (from Hoeg and Murarka, 1974) for the random variables are as follows:

	μ	σ	δ	Bias
γ_c	0.1575	0.0158	0.100	1.05
γ	0.110	0.011	0.100	1.00
n	0.400	0.040	0.100	1.00
ϕ (rad)	0.6109	0.0524	0.086	1.00
ϕ_f (rad)	0.6458	0.0646	0.100	1.00

An actual analysis printout of the spreadsheet program (EXCEL) for the first iteration process is presented in Figure 4.6. Each cell of the spreadsheet is programmed with the equations described in Tables 4.5 to 4.8. As shown in Figure 4.6, Module I contains the basic random variables which begin with the mean values in the first iteration. In Module II, the intermediate random variables

BEAR-30.XLS

(i) 1st Iteration with Mean Values

Mod I

γ_c	γ	n	ϕ	ϕ_f
0.1575	0.1100	0.4000	0.6109	0.6458

Mod II

P	$dP/d\gamma$	$dP/d\phi$
13.41	121.95	-32.75

N_q	$dN_q/d\phi_f$
42.92	318.89

N_γ	$dN_\gamma/d\phi_f$
53.27	558.69

θ	$d\theta/d\gamma_c$	$d\theta/d\gamma$	$d\theta/d\phi$
0.34	-1.98186	2.84	-0.76

x_o	$dx_o/d\gamma_c$	$dx_o/d\gamma$	dx_o/dn	$dx_o/d\phi$
4.80	26.70	-38.23	-10.51	10.27

Mod III

$B\gamma$	$dB\gamma/d\gamma_c$	$dB\gamma/d\gamma$	$dB\gamma/dn$	$dB\gamma/d\phi$	$dB\gamma/d\phi_f$
6.42	118.25	-110.91	-14.08	45.47	89.11

Bq	$dBq/d\gamma_c$	$dBq/d\gamma$	dBq/dn	$dBq/d\phi$	$dBq/d\phi_f$
13.11	34.00	70.45	3.19	13.08	97.37

qx	$dqx/d\gamma_c$	$dqx/d\gamma$	dqx/dn	$dqx/d\phi$	$dqx/d\phi_f$
3.99	3.13	31.77	8.74	-8.53	0.00

Mod IV

$dg/d\gamma_c$	$dg/d\gamma$	dg/dn	$dg/d\phi$	$dg/d\phi_f$
149.12	-72.22	-19.62	67.08	186.48

Mod V

$s_{\gamma c}$	s_γ	s_n	s_ϕ	$s_{\phi f}$
2.3487	-0.7945	-0.7849	3.5123	12.0422

where $s_i = \sigma_i * dg/dx_i$

Δ =	12.811

$\alpha_{\gamma c}$	α_γ	α_n	α_ϕ	$\alpha_{\phi f}$
-0.183	0.062	0.061	-0.274	-0.940

where $\alpha_i = s_i/\Delta$

Mod VI

$\gamma_c^* = \mu_{\gamma_c} + \alpha_{\gamma_c} \cdot \sigma_{\gamma_c} \cdot \beta =$ 0.1501

$\gamma^* = \mu_\gamma + \alpha_\gamma \cdot \sigma_\gamma \cdot \beta =$ 0.1118

$n^* = \mu_n + \alpha_n \cdot \sigma_n \cdot \beta =$ 0.4063

$\phi^* = \mu_\phi + \alpha_\phi \cdot \sigma_\phi \cdot \beta =$ 0.5739

$\phi_f^* = \mu_{\phi_f} + \alpha_{\phi_f} \cdot \sigma_{\phi_f} \cdot \beta =$ 0.4895

Mod VII

P*	Nq*	Nγ*	θ*	x_o*
14.90	14.80	11.28	0.39	4.02

Bγ	Bq	qx
0.22	4.31	4.53

g() = Br + Bq - qx = 0

β1 =	2.5741

Figure 4.6 An Analysis Printout of the Spreadsheet Program (EXCEL)

and their partial derivatives are calculated. MATHEMATICA is used to verify the values in Module III. For the purpose of illustration, actual printouts of the analysis for B_γ, B_q and q_{max}, and their partial derivatives are presented in Figures 4.7 to 4.9. Both results from EXCEL and MATHEMATICA are almost identical, which ensures the reliability of the analysis using the spreadsheet program.

The procedures from Module IV to Module VII are similar to the one described in Section 4.3. In the following sections, which illustrate the procedure for determining the bearing capacity limit state, the calculations for the first three modules have not been shown.

```
P=0.5 r H^2 (Tan[3.141593/4-phi/2])^2

Nq=Exp[3.141593 Tan[phif]](Tan[3.141593/4+phif/2])^2

Nr=(Nq-1) Tan[1.4 phif]

tt=ArcTan[P/vol/rc]

xnut= xbar-P n H/vol/rc
%6 Br=r xnut (1-tt/phif)^2 Nr
%7 D[Br,rc]
%8 D[Br,r]
%9 D[Br,n]
%10 D[Br,phi]
%11 D[Br,phif]

rc=0.158
r=0.11
n=0.4
phi=0.611
phif=0.646
H=30
xbar=9.005
vol=243

N[%6]=6.510597091280503
N[%7]=118.6365639393581
N[%8]=-111.2180001012553
N[%9]=-14.17106338428107
N[%10]=45.77012059583467
N[%11]=90.1466218676526
```

Figure 4.7 Bγ and the Partial Derivatives Calculated from MATHMATICA

```
P=0.5 r H^2 (Tan[3.141593/4-phi/2])^2

Nq=Exp[3.141593 Tan[phif]](Tan[3.141593/4+phif/2])^2

Nr=(Nq-1) Tan[1.4 phif]

tt=ArcTan[P/vol/rc]

xnut= xbar-P n H/vol/rc

%8 Bq=r Df (1-2 tt/3.141593)^2 (1+0.15 Df/xnut) Nq
%9 D[Bq,rc]
%10 D[Bq,r]
%11 D[Bq,n]
%12 D[Bq,phi]
%13 D[Bq,phif]

rc=0.158
r=0.11
n=0.4
phi=0.611
phif=0.646
H=30
xbar=9.005
vol=243
Df=4

N[%8]=13.14619692378608
N[%9]=33.9232808254072
N[%10]=70.78471412156129
N[%11]=3.171225928271034
N[%12]=13.08764012399172
N[%13]=97.7015325809832
```

Figure 4.8 B_q and the Partial Derivatives Calculated from MATHMATICA

```
P=0.5 r H^2 (Tan[3.141593/4-phi/2])^2

Nq=Exp[3.141593 Tan[phif]](Tan[3.141593/4+phif/2])^2

Nr=(Nq-1) Tan[1.4 phif]

tt=ArcTan[P/vol/rc]

xnut= xbar-P n H/vol/rc

%6 qx=vol/2 rc/xnut
%7 D[qx,rc]
%8 D[qx,r]
%9 D[qx,n]
%10 D[qx,phi]
%11 D[qx,phif]

rc=0.158
r=0.11
n=0.4
phi=0.611
phif=0.646
H=30
xbar=9.005
vol=243
Df=4

N[%6]=3.987
N[%7]=3.264
N[%8]=31.563
N[%9]=8.6800
N[%10]=-8.477
N[%11]=0
```

Figure 4.9 q_{max} and the Partial Derivatives Calculated from MATHMATICA

4.6.3 Bearing Capacity Limit State - 5 ft High Wall

Conventional (ASD) Optimized Design:

S.F. = 2.51 t = 0.42 ft B = 2.28 ft D_f = 1.73 ft

Safety Index by Advanced FOSM Method:

		γ_c	γ	n	ϕ	ϕ_f	Δ	β
Mean, μ		0.158	0.110	0.400	0.541	0.593		
Std. Deviation, σ		0.0158	0.0110	0.040	0.0524	0.0593		
1st Iteration	$\frac{\partial g}{\partial x_i}$	18.650	13.510	-0.110	8.800	39.360		
	$\sigma_{x_i}\frac{\partial g}{\partial x_i}$	0.2938	0.1486	-0.0045	0.4608	2.3358	2.403	
	α_{x_i}	-0.1220	-0.0620	0.0020	-0.1920	-0.972		5.00
	x_i^*	0.1479	0.1066	0.4004	0.5607	0.3050		
2nd Iteration	$\frac{\partial g}{\partial x_i}$	1.780	-2.480	-1.630	2.350	3.810		
	$\sigma_{x_i}\frac{\partial g}{\partial x_i}$	0.0281	-0.0273	-0.0650	0.1232	0.2263	0.269	
	α_{x_i}	-0.1050	0.1020	0.2420	-0.4590	-0.843		4.36
	x_i^*	0.1503	0.1149	0.4421	0.5065	0.3762		
3rd Iteration	$\frac{\partial g}{\partial x_i}$	10.370	-13.570	-4.520	6.370	6.870		
	$\sigma_{x_i}\frac{\partial g}{\partial x_i}$	0.1633	-0.1493	-0.1810	0.3333	0.4078	0.599	
	α_{x_i}	-0.2720	0.2490	0.3020	-0.5560	-0.68		4.00
	x_i^*	0.1403	0.1210	0.4483	0.4944	0.4320		
4th Iteration	$\frac{\partial g}{\partial x_i}$	37.020	-42.960	-12.630	16.620	12.580		
	$\sigma_{x_i}\frac{\partial g}{\partial x_i}$	0.5831	-0.4725	-0.5050	0.8705	0.7468	1.461	
	α_{x_i}	-0.3990	0.3230	0.3460	-0.5960	-0.511		3.82
	x_i^*	0.1335	0.1236	0.4529	0.4915	0.4774		

5th Iteration	$\frac{\partial g}{\partial x_i}$	119.20	-128.70	-36.40	45.80	26.70		
	$\sigma_{x_i}\frac{\partial g}{\partial x_i}$	1.900	-1.400	-1.500	2.400	1.600	3.988	
	α_{x_i}	-0.4710	0.3550	0.3650	-0.6020	-0.397		3.77
	x_i^*	0.1296	0.1247	0.4550	0.4922	0.5047		
6th Iteration	$\frac{\partial g}{\partial x_i}$	344.340	-357.75	-100.09	122.930	60.970		
	$\sigma_{x_i}\frac{\partial g}{\partial x_i}$	5.4233	-3.9352	-4.0040	6.4367	3.6182	10.75	
	α_{x_i}	-0.5050	0.3660	0.3730	-0.5990	-0.337		3.75
	x_i^*	0.1277	0.1251	0.4560	0.4931	0.5184		
7th Iteration	$\frac{\partial g}{\partial x_i}$	992.03	-940.69	-262.23	318.33	145.48		
	$\sigma_{x_i}\frac{\partial g}{\partial x_i}$	14.522	-10.348	-10.489	16.668	8.633	27.93	
	α_{x_i}	-0.5200	0.3700	0.3760	-0.5970	-0.309		3.75
	x_i^*	0.1268	0.1253	0.4563	0.4937	0.5246		
8th Iteration	$\frac{\partial g}{\partial x_i}$	2426.87	-2455.9	-683.69	825.73	363.47		
	$\sigma_{x_i}\frac{\partial g}{\partial x_i}$	38.223	-27.015	-27.350	43.235	21.569	72.62	
	α_{x_i}	-0.5260	0.3720	0.3770	-0.5950	-0.297		3.75
	x_i^*	0.1264	0.1253	0.4565	0.4939	0.5273		

Therefore, the final safety index value is

$\beta = 3.75$

4.6.4 Bearing Capacity Limit State - 10 ft High Wall

Conventional (ASD) Optimized Design:

S.F. = 2.51 t = 0.75 ft B = 4.6 ft D_f = 2.67 ft

Safety Index by Advanced FOSM Method:

		γ_c	γ	n	ϕ	ϕ_f	Δ	β
Mean, μ		0.158	0.110	0.400	0.541	0.593		
Std. Deviation, σ		0.0158	0.0110	0.040	0.0524	0.0593		
1st Iteration	$\frac{\partial g}{\partial x_i}$	41.370	8.830	-2.440	19.090	71.910		
	$x_i \frac{\partial g}{\partial x_i}$	0.6515	0.0972	-0.0976	0.9995	4.3927	4.554	
	x_i	-0.1430	-0.0210	0.0210	-0.2190	-0.965		4.19
	x_i^*	0.1481	0.1090	0.4036	0.5627	0.3640		
2nd Iteration	$\frac{\partial g}{\partial x_i}$	5.200	-7.060	-3.560	5.310	8.220		
	$x_i \frac{\partial g}{\partial x_i}$	0.0818	-0.0776	-0.1424	0.2780	0.5024	0.602	
	x_i	-0.1360	0.1290	0.2370	-0.4620	-0.834		3.75
	x_i^*	0.1495	0.1153	0.4355	0.5202	0.4197		
3rd Iteration	$\frac{\partial g}{\partial x_i}$	18.290	-23.710	-7.970	11.300	12.700		
	$x_i \frac{\partial g}{\partial x_i}$	0.2881	-0.2608	-0.3188	0.5917	0.7757	1.098	
	x_i	-0.2630	0.2380	0.2900	-0.5390	-0.707		3.58
	x_i^*	0.1427	0.1194	0.4416	0.5098	0.4563		
4th Iteration	$\frac{\partial g}{\partial x_i}$	40.720	-48.680	-14.870	19.980	17.590		
	$x_i \frac{\partial g}{\partial x_i}$	0.6413	-0.5355	-0.5947	1.0462	1.0747	1.817	
	x_i	-0.3530	0.2950	0.3270	-0.5760	-0.591		3.50
	x_i^*	0.1380	0.1213	0.4458	0.5054	0.4844		

5th Iteration	$\frac{\partial g}{\partial x_i}$	73.730	-83.880	-24.560	31.960	23.660		
	$x_i \frac{\partial g}{\partial x_i}$	1.1613	-0.9227	-0.9825	1.6733	1.4453	2.838	
	x_i	-0.4090	0.3250	0.3460	-0.5900	-0.509		3.47
	x_i^*	0.1352	0.1224	0.4480	0.5038	0.5030		
6th Iteration	$\frac{\partial g}{\partial x_i}$	110.77	-122.30	-35.19	44.88	29.70		
	$x_i \frac{\partial g}{\partial x_i}$	1.7446	-1.3453	-1.4076	2.3499	1.8144	3.956	
	x_i	-0.4410	0.3400	0.3560	-0.5940	-0.459		3.46
	x_i^*	0.1335	0.1229	0.4492	0.5033	0.5140		

Therefore, the final safety index value is

$$\beta = \mathbf{3.46}$$

4.6.5 Bearing Capacity Limit State - 20 ft High Wall

Conventional (ASD) Optimized Design:

S.F. = 2.50 t =1.5 ft B = 9.2 ft D_f = 3.93 ft

Safety Index by Advanced FOSM Method:

		γ_c	γ	n	ϕ	ϕ_f	Δ	β
Mean, μ		0.158	0.110	0.400	0.541	0.593		
Std. Deviation, σ		0.0158	0.0110	0.040	0.0524	0.0593		
1st Iteration	$\frac{\partial g}{\partial x_i}$	90.71	-15.95	-9.01	41.24	132.71		
	$\sigma_{x_i}\frac{\partial g}{\partial x_i}$	1.4286	-0.1754	-0.3602	2.1595	8.3386	8.741	
	α_{x_i}	-0.1630	0.0200	0.0410	-0.2470	-0.954		3.37
	x_i^*	0.1488	0.1107	0.4056	0.5673	0.4264		
2nd Iteration	$\frac{\partial g}{\partial x_i}$	14.510	-19.490	-7.700	12.200	18.460		
	$\sigma_{x_i}\frac{\partial g}{\partial x_i}$	0.2285	-0.2144	-0.3082	0.6386	1.1598	1.395	
	α_{x_i}	-0.1640	0.1540	0.2210	-0.4580	-0.831		3.12
	x_i^*	0.1495	0.1153	0.4275	0.5361	0.4655		
3rd Iteration	$\frac{\partial g}{\partial x_i}$	31.920	-41.390	-13.590	20.080	24.380		
	$\sigma_{x_i}\frac{\partial g}{\partial x_i}$	0.5028	-0.4553	-0.5436	1.0513	1.5319	2.051	
	α_{x_i}	-0.2450	0.2220	0.2650	-0.5130	-0.747		3.06
	x_i^*	0.1457	0.1175	0.4324	0.5288	0.4847		
4th Iteration	$\frac{\partial g}{\partial x_i}$	47.850	-59.340	-18.580	26.350	28.080		
	$\sigma_{x_i}\frac{\partial g}{\partial x_i}$	0.7536	-0.6527	-0.7434	1.3796	1.7643	2.562	
	α_{x_i}	-0.2940	0.2550	0.2900	-0.5390	-0.689		3.04
	x_i^*	0.1434	0.1185	0.4353	0.5251	0.4968		

5th Iteration	$\frac{\partial g}{\partial x_i}$	61.100	-73.940	-22.610	31.360	30.880		
	$\sigma_{x_i}\frac{\partial g}{\partial x_i}$	0.9624	-0.8133	-0.9044	1.6422	1.9404	2.978	
	α_{x_i}	-0.3230	0.2730	0.3040	-0.5510	-0.652		3.03
	x_i^*	0.1421	0.1191	0.4368	0.5233	0.5041		
6th Iteration	$\frac{\partial g}{\partial x_i}$	70.88	-84.54	-25.54	34.98	32.83		
	$\sigma_{x_i}\frac{\partial g}{\partial x_i}$	1.1164	-0.9299	-1.0214	1.8317	2.0628	3.281	
	α_{x_i}	-0.3400	0.2830	0.3110	-0.5580	-0.629		3.03
	x_i^*	0.1413	0.1194	0.4377	0.5223	0.5086		

Therefore, the final safety index value is

$$\beta = \mathbf{3.03}$$

4.6.6 Bearing Capacity Limit State - 30 ft High Wall

Conventional (ASD) Optimized Design:

S.F. = 2.50 t = 2.5 ft B = 13.7 ft D_f = 4.0 ft

Safety Index by Advanced FOSM Method:

		γ_c	γ	n	ϕ	ϕ_f	Δ	β
Mean, μ		0.158	0.110	0.400	0.541	0.593		
Std. Deviation, σ		0.0158	0.0110	0.040	0.0524	0.0593		
1st Iteration	$\frac{\partial g}{\partial x_i}$	149.12	-72.22	-19.62	67.08	186.48		
	$x_i \frac{\partial g}{\partial x_i}$	2.3487	-0.7945	-0.7849	3.5123	12.042	12.81	
	x_i	-0.1830	0.0620	0.0610	-0.2740	-0.94		2.57
	x_i^*	0.1501	0.1118	0.4063	0.5739	0.4895		
2nd Iteration	$\frac{\partial g}{\partial x_i}$	31.400	-42.170	-12.760	22.010	32.670		
	$x_i \frac{\partial g}{\partial x_i}$	0.4946	-0.4639	-0.5103	1.1525	2.1097	2.549	
	x_i	-0.1940	0.1820	0.2000	-0.4520	-0.828		2.45
	x_i^*	0.1500	0.1149	0.4196	0.5529	0.5150		
3rd Iteration	$\frac{\partial g}{\partial x_i}$	47.950	-62.610	-18.250	29.340	38.220		
	$x_i \frac{\partial g}{\partial x_i}$	0.7552	-0.6887	-0.7299	1.5360	2.4679	3.167	
	x_i	-0.2380	0.2170	0.2300	-0.4850	-0.779		2.43
	x_i^*	0.1484	0.1158	0.4224	0.549	0.5232		
4th Iteration	$\frac{\partial g}{\partial x_i}$	55.610	-71.230	-20.630	32.350	40.080		
	$x_i \frac{\partial g}{\partial x_i}$	0.8758	-0.7835	-0.8252	1.6941	2.5883	3.410	
	x_i	-0.2570	0.2300	0.2420	-0.4970	-0.759		2.43
	x_i^*	0.1477	0.1161	0.4235	0.5476	0.5265		

5th Iteration	$\frac{\partial g}{\partial x_i}$	59.010	-75.020	-21.670	33.670	40.870		
	$x_i \frac{\partial g}{\partial x_i}$	0.9294	-0.8253	-0.8670	1.7629	2.6393	3.517	
	x_i	-0.2640	0.2350	0.2470	-0.5010	-0.75		2.43
	x_i^*	0.1474	0.1163	0.4240	0.547	0.5279		

Therefore, the final safety index value is

$$\beta = \mathbf{2.43}$$

4.6.7 Summary of Safety Indices for Bearing Capacity Limit State

The trend of convergence in the safety index of the bearing capacity limit state is shown in Figure 4.10.

The safety indices for bearing capacity limit state are summarized in Table 4.9. Unlike the two previous cases, it is observed that the safety indices differ from each other for different heights of the wall.

Table 4.9 Safety Indices for Bearing Capacity Limit State

H (ft)	B (ft)	t (ft)	Safety Factor	Safety Index
5	2.50	0.42	2.51	**3.75**
10	4.60	0.75	2.51	**3.46**
20	9.20	1.50	2.50	**3.03**
30	13.70	2.50	2.50	**2.43**

5 ft wall

β1	5.000
β2	4.360
β3	4.000
β4	3.820
β5	3.770
β6	3.750
β7	3.750
β8	3.750

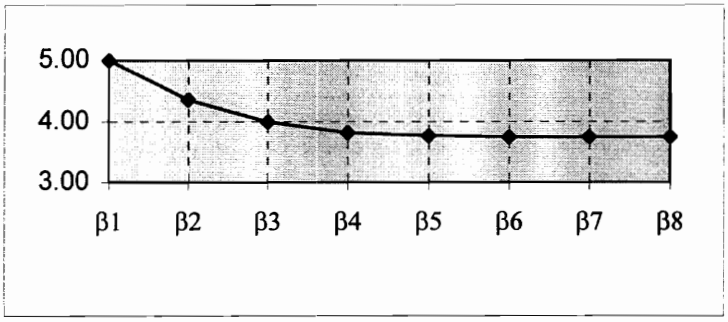

10 ft wall

β1	4.190
β2	3.752
β3	3.581
β4	3.499
β5	3.468
β6	3.457

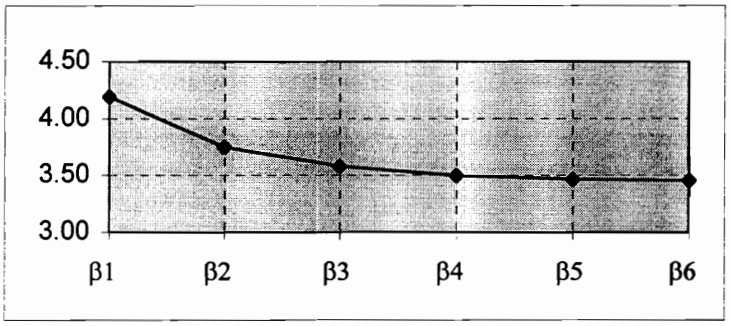

20 ft wall

β1	3.368
β2	3.118
β3	3.060
β4	3.040
β5	3.033
β6	3.031

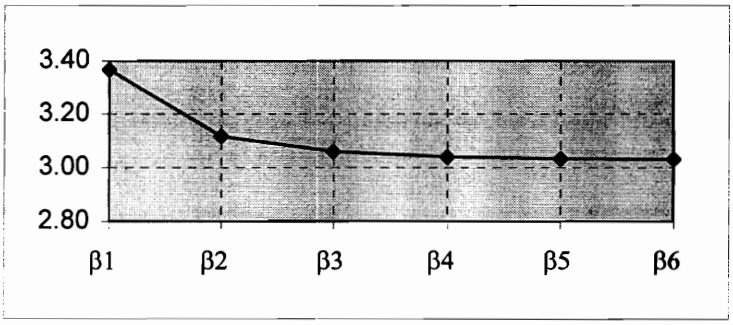

30 ft wall

β1	2.574
β2	2.448
β3	2.435
β4	2.433
β5	2.432

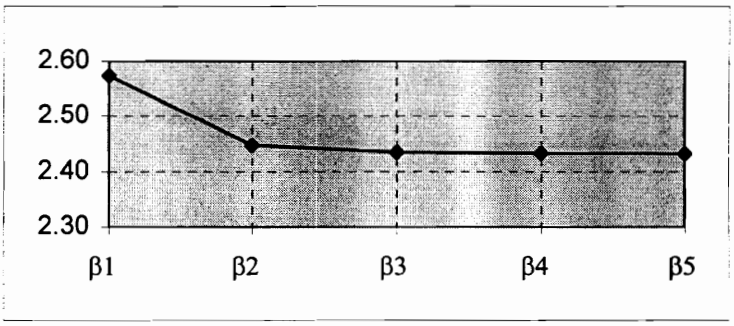

Figure 4.10 The Trend of Convergence in β of Bearing Capacity Limit State

4.7 SUMMARY AND DISCUSSION

Safety indices for sliding, overturning and bearing capacity limit states are summarized in Table 4.10. For the height of 5 ft, 10 ft, 20 ft and 30 ft, the wall dimensions, t and B were adjusted to closely match all the conventional design criteria. When this goal was not achieved simply by changing t and B, additional design parameters such as ϕ_f and D_f were modified. Since ϕ_f and D_f have effect only on the bearing capacity, it is convenient to change t and B first to satisfy the sliding and overturning criteria and then later modify ϕ_f and D_f to fine tune the bearing capacity criterion.

As shown in Table 4.10, the safety indices for the sliding and overturning limit states are consistent throughout the various wall heights. However, for the bearing capacity limit state, different safety indices are estimated for different wall heights. It is observed that the higher the wall height, the lower the safety indices which means a less reliable system. The internal friction angle of the foundation soil (ϕ_f) is found to be the cause of the phenomenon. The bearing capacity limit state analysis is very sensitive to the value of ϕ_f, but it has no effect on the other limit states. This friction angle, ϕ_f, is the only basic random variable that was modified mainly to satisfy the bearing capacity criterion. As the wall height increases, more

Table 4.10 Summary of Analysis for Three Limit States

	H (ft)	5	10	20	30
Design Parameters	B (ft)	2.28	4.60	9.20	13.70
	t (ft)	0.42	0.75	1.50	2.50
	D_f (ft)	1.73	2.67	3.93	4.00
	ϕ_f (deg)	34.0	35.0	36.0	37.0
	ϕ (deg)	35.0	35.0	35.0	35.0
	δ_f (deg)	30.0	30.0	30.0	30.0
	γ (kcf)	0.11	0.11	0.11	0.11
	γ_c (kcf)	0.15	0.15	0.15	0.15
	n	0.4	0.4	0.4	0.4
Sliding	SF	1.57	1.55	1.55	1.57
	β	**2.19**	**2.15**	**2.15**	**2.19**
Overturning	SF	2.04	2.04	2.04	2.04
	β	**3.58**	**3.59**	**3.59**	**3.59**
Bearing	SF	2.51	2.51	2.50	2.50
	β	**3.75**	**3.46**	**3.03**	**2.43**
B/H Ratio		**0.456**	**0.460**	**0.460**	**0.457**

solid foundation material with high friction angle is required. With a fixed coefficient of variance (COV, $\delta = \sigma / \mu$), the value of the standard deviation becomes larger as the mean value increases. In other words, as the internal friction angle of the foundation soil (ϕ_f) increases, the standard deviation increases, which means that the dispersion is greater. When the dispersion is greater, the safety index is smaller.

The last line in Table 4.10 is the B/H ratio of the wall dimensions selected to satisfy all of the conventional ASD limit states simultaneously. These values are nearly constant (0.46) for all wall heights.

Chapter 5
OPTIMIZED DESIGN

5.1 GENERAL

The conventional design optimization of a retaining wall usually implies that the wall is designed to minimize the initial construction cost while satisfying all the design criteria. Since the conventional design method does not directly consider the randomness (or dispersion) of design parameters but uses the deterministic values, the current optimization concept may be misleading.

In an effort to optimize the wall with a more rational concept, the costs of failure as well as the initial construction cost are included in the total expected cost of the wall. The probability of failure is employed to estimate the cost of failure. The following sections will discuss the probability of failure, the probable costs of failure and total expected construction costs.

5.2 PROBABILITY OF FAILURE

When a safety index is obtained by the procedures described in Chapter 4, the probability of failure (P_f) can be calculated using the standardized normal distribution function as,

$$P_f = \Phi(-\beta) = 1 - \Phi(\beta) \tag{5.1}$$

where $\Phi(x)$ is the standardized normal distribution function, i.e.,

$$\Phi(x) = \frac{1}{\sqrt{2\pi}} \int_{-\infty}^{x} \exp\left(-\frac{1}{2}y^2\right) dy \tag{5.2}$$

For example, if the random variables are normally distributed and the safety index, $\beta = 2.19$, then $P_f = 1 - \Phi(2.19) = 1 - 0.985738 = 1.43 \times 10^{-2}$. In a similar manner, the probability of failures for the three limit states discussed in the previous chapter are computed and summarized in Table 5.1.

Table 5.1 Safety Indices and Probability of Failure for the Three Limit States

H (ft)	Sliding		Overturning		Bearing	
	β	P_f (x 10^{-4})	β	P_f (x 10^{-4})	β	P_f (x 10^{-4})
5	2.19	143	3.58	1.72	3.75	0.1
10	2.15	157	3.59	1.65	3.46	2.7
20	2.15	157	3.59	1.65	3.03	12.2
30	2.19	143	3.59	1.65	2.43	75.5

If the random variables are lognormally distributed, an approximate equation suggested by Esteva and Rosenblueth(1972) can be used as

$$P_f = 460\, e^{(-4.3\beta)} \qquad 2 < \beta < 6 \qquad (5.3)$$

According to Hoeg and Murarka (1974), the results from the normal distribution and log-normal distribution are quite similar when the coefficient of variance (COV) is less than 0.2 and the probabilities of failure computed based on normal distribution would be valid for log-normally distributed random variables.

As shown in Table 5.1, the probabilities of failure calculated for the sliding limit state are the highest among the three limit states, which can be anticipated from the use of the smallest safety factor. However, the probabilities of the bearing failure are relatively high in spite of the largest safety factor among the three limit states.

As revealed in the survey conducted for this study, many of the unsatisfactory walls have experienced the bearing capacity failure or excessive settlements. It might occur due to a reason that the bearing capacity factors, N_γ and N_q, are very strong functions of the internal friction angle of the foundation soil, ϕ_f, and it is difficult to estimate the value of ϕ_f with enough accuracy. For example, the safety

factor of the bearing capacity in a 30 ft high wall described in Chapter 4 can jump from 2.5 to 4.0 by a small change of ϕ_f from 35 degree to 37 degree.

Another possible reason that the probabilities of the bearing failure are relatively high can be found in the strong influence of the standard deviation to the bearing capacity. As mentioned in the previous chapter, the values of ϕ_f were adjusted to match the required safety factor for bearing capacity (2.5). With the fixed COV value of 0.1, the standard deviation (σ) varies from 3.4 degree to 3.7 degree when the values of ϕ_f varies from 34 degree (for 5 ft wall) to 37 degree (for 30 ft wall). The probabilities of failure in the bearing capacity in Table 5.1 range from 1.03×10^{-5} to 7.55×10^{-3}. The difference of 0.3 degree in the standard deviation produced a more than seven hundred times higher probability of failure.

A parametric study was conducted for a 20 ft high wall to investigate the effect of various COV values for the different parameters. One COV value for each design parameter was changed at a time while the other four values remained the same. The results are presented in Table 5.2. Based on the typical COV values suggested by many investigators including Singh (1972), Schultze (1972) and Harr (1977), three different COV values of 0.05, 0.10 and 0.15 were employed for each random variable in the parametric study.

Table 5.2 Sensitivity of Coefficient of Variation

For H = 20 ft high

Var.	μ	σ	cov	Sliding		Overturning		Bearing	
				β	p_f ($x10^{-4}$)	β	p_f ($x10^{-4}$)	β	p_f ($x10^{-4}$)
ϕ_f	36 (deg)	1.80	**0.05**	2.151	**157.4**	3.590	**1.65**	3.293	**4.96**
		3.60	**0.10**	2.151	**157.4**	3.590	**1.65**	3.030	**12.20**
		5.40	**0.15**	2.151	**157.4**	3.590	**1.65**	2.332	**98.50**
ϕ	35 (deg)	1.75	**0.05**	2.386	**85.16**	4.030	**0.28**	3.394	**3.45**
		3.50	**0.10**	2.049	**202.30**	3.403	**3.33**	2.867	**20.70**
		5.25	**0.15**	1.712	**434.50**	2.802	**25.39**	2.345	**95.10**
γ_c	157.5 (lb)	7.88	**0.05**	2.352	**93.4**	4.119	**0.20**	3.148	**8.22**
		15.75	**0.10**	2.151	**157.4**	3.590	**1.65**	3.030	**12.20**
		23.63	**0.15**	1.876	**303.3**	2.945	**16.20**	2.709	**33.70**
γ	110 (lb)	5.50	**0.05**	2.298	**107.8**	3.855	**0.58**	3.127	**8.83**
		11.00	**0.10**	2.151	**157.4**	3.590	**1.65**	3.030	**12.20**
		16.50	**0.15**	1.972	**243.1**	3.285	**5.10**	2.867	**20.70**
n	0.4	0.02	**0.05**	2.151	**157.4**	3.855	**0.58**	3.152	**8.10**
		0.04	**0.10**	2.151	**157.4**	3.590	**1.65**	3.030	**12.20**
		0.06	**0.15**	2.151	**157.4**	3.285	**5.10**	2.849	**21.90**
δ_f	30 (deg)	1.50	**0.05**	2.455	**70.5**	3.590	**1.65**	3.030	**12.20**
		3.00	**0.10**	2.151	**157.4**	3.590	**1.65**	3.030	**12.20**
		4.50	**0.15**	1.802	**357.7**	3.590	**1.65**	3.030	**12.20**

With this parametric study, it can be observed from Table 5.2 how much an individual design parameter can affect the probability of failure of each limit state. For example, the internal friction angle of foundation soil, ϕ_f, is very influential to the bearing capacity but has no effect on the sliding or overturning limit state. The design parameter n has no influence on the sliding limit state, while the friction angel, δ_f, affects the sliding limit state only.

For each COV value, the probability of failure is calculated, and the minimum and maximum probabilities of failure are summarized in Table 5.3.

Table 5.3 Overall Minimum and Maximum Probabilities of Failure

	Min. P_f ($x10^{-4}$)	Max. P_f ($x10^{-4}$)	Max. P_f / Min. P_f
Sliding	70.5	434.5	6
Overturning	0.2	25.4	127
Bearing	3.45	98.5	29

Figures 5.1 to 5.3 illustrate the influence of the design parameters on the probability of failure of each limit state. The random variables are omitted from the graph if a change in COV values has no effect on the probability of failure.

As shown in Table 5.3, the ratio of the maximum P_f to the minimum P_f of the sliding limit state is lower than the other two limit states, even though the sliding limit state produces the largest probability of failure. On the contrary, the overturning limit state has the smallest probability of failure, while it has the highest ratio of the maximum P_f to the minimum P_f. In other words, the overturning limit state is the most sensitive to the change in COV values, while the sliding limit state is the least sensitive.

The internal friction angle of the backfill, ϕ, is proven to be the most sensitive random variable which affects all three limit states. The bearing capacity limit state is influenced by the internal friction angle of the foundation soil, ϕ_f, with almost same degree of sensitivity as the internal friction angle of the backfill, ϕ. The unit weight of the backfill appears to be the least influential random variable to all three limit states.

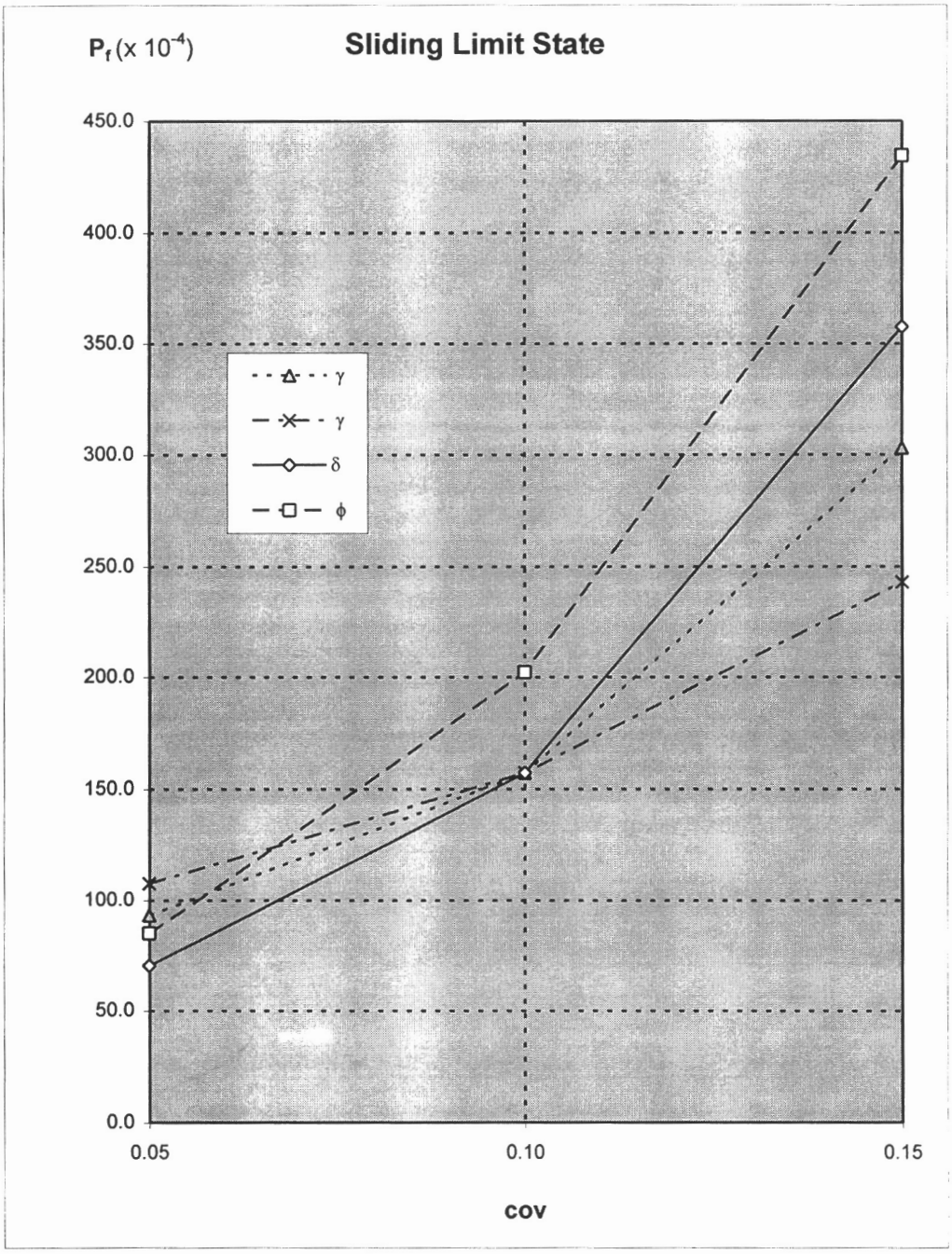

Figure 5.1 Probability of Failure for Sliding Limit State

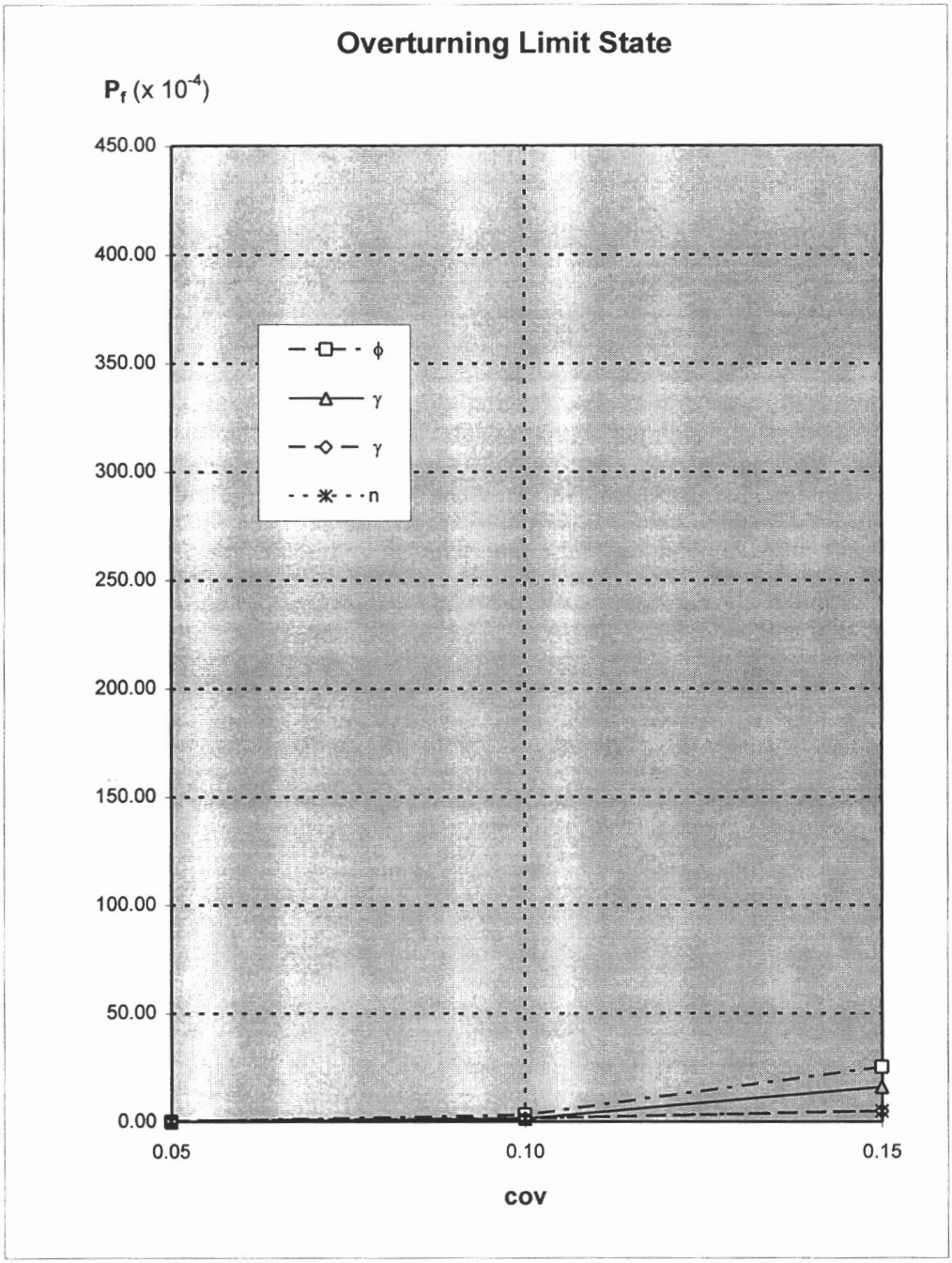

Figure 5.2 Probability of Failure for Overturning Limit State

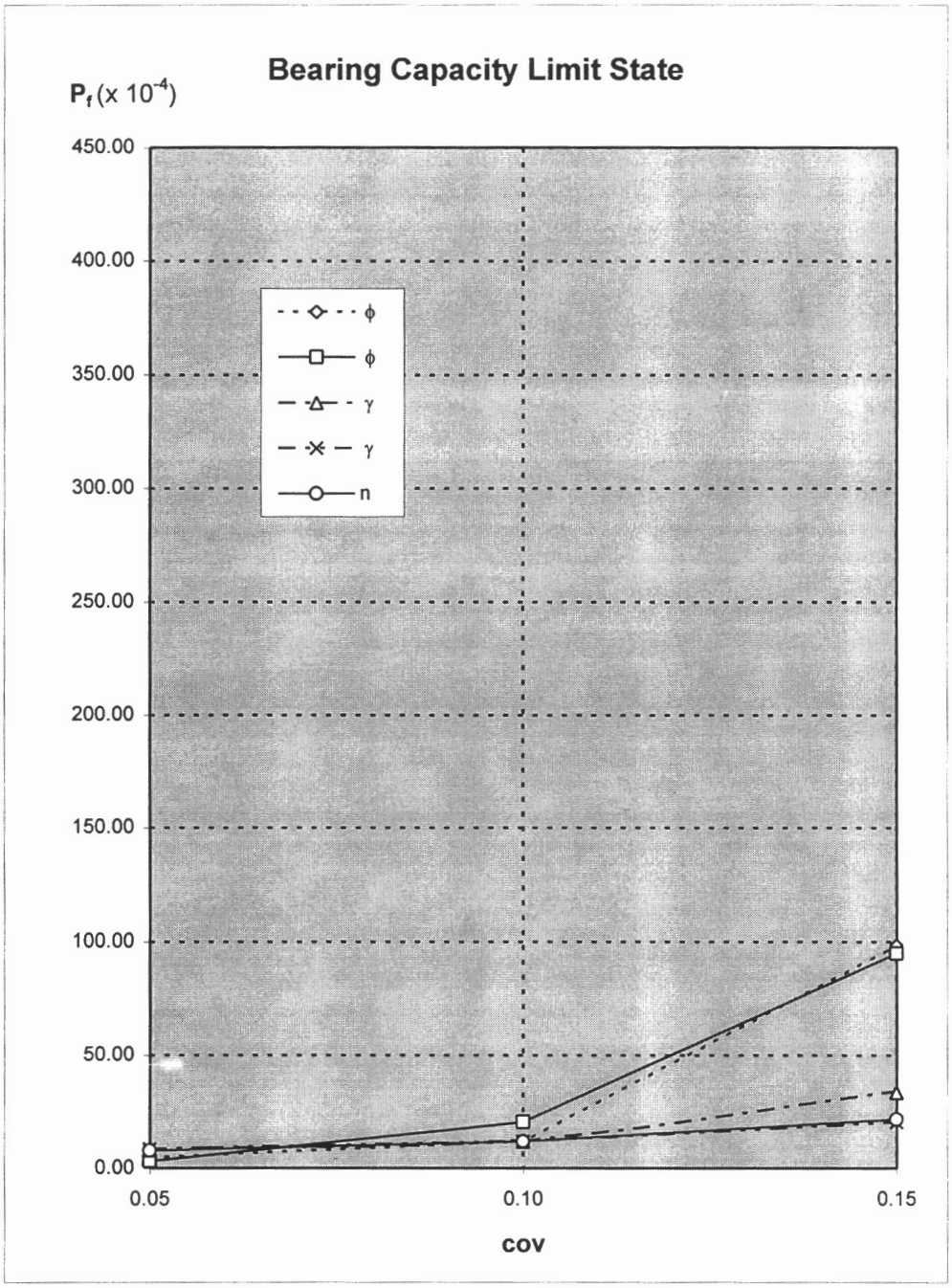

Figure 5.3 Probability of Failure for Bearing Capacity Limit State

5.3 OPTIMIZATION

To achieve a probabilistically optimized design, costs of failure must be estimated. The cost of failure, CF, may be expressed as a factor, η, multiplied by the cost of construction, C.

$$CF = \eta * C \tag{5.4}$$

The total expected cost, E, is the sum of the construction cost and the probable cost of failure of each limit state, i.e.,

$$E = C + \Sigma P_{fi} * \eta_i * C = C (1 + \Sigma P_{fi} * \eta_i) \tag{5.5}$$

where P_{fi} is the probability of failure of limit state i and η_i is the relative cost factor of limit state i.

To obtain relative values for the total cost of a design, the construction cost is assumed to be proportional to the volume of concrete in the wall and the volume of compacted backfill. The natural ground behind the wall is assumed to be excavated with a slope of 45 degree and later filled with the compacted backfill material. The unit price of concrete is set equal to six times that of the compacted backfill material. The relative cost factors for sliding, overturning and bearing are assumed to be one, five and three times the cost of construction, respectively.

For purpose of illustration, an example is provided as follows.

Example 5.1 Three cases of 20 ft high walls designed with different base width will be investigated to find the optimum design. The construction cost and the total expected cost for each case will be compared. The quantities of probability of failure for each mode are selected by the procedure described in Chapter 4 and the previous section. For this example problem, relative values of the construction cost are used. Actual construction costs could be obtained by multiplying the relative construction cost by a constant dollar value. However, for the purpose of determining the base width with the minimum total cost, the use of relative construction costs are satisfactory.

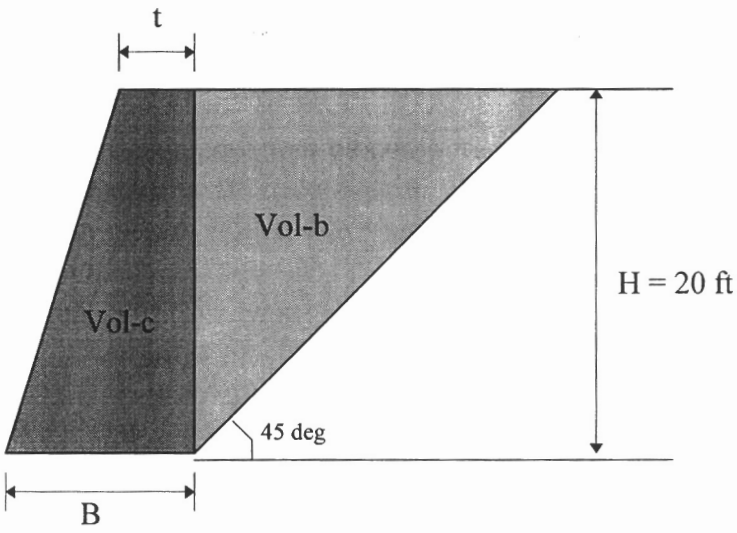

where Vol-c = Volume of Concrete = 1/2 (t + B)*H

Vol-b = Volume of Backfill = 1/2 H^2

C = Relative Construction Cost = 6 (Vol-c) + Vol-b

The probabilities of failure for each case are tabulated as below.

Case No.	t (ft)	B (ft)	P_f (x 10^{-4})		
			Sliding	Over	Bearing
1	1.5	8.5	100	110	200
2	1.5	9.5	25	2	100
3	1.5	10.5	5	0.01	20

The construction cost, C, for Case 1 can be estimated as

$$C = 6\,(0.5\,(t + B)*H) + 1/2\,H^2$$

$$= 6\,(0.5\,(1.5 + 8.5) * 20) + 0.5 * 20^2$$

$$= 600 + 200 = 800$$

The probable cost of failure, that is $P_f * CF$, for each limit state in Case 1 can be calculated as

$$P_{f\text{-}slid} * CF = P_{f\text{-}slid} * \eta_{slid} * C = (100 \times 10^{-4}) * (1.0) * (800) = 8.0$$

$$P_{f\text{-}over} * CF = P_{f\text{-}over} * \eta_{over} * C = (110 \times 10^{-4}) * (5.0) * (800) = 44.0$$

$$P_{f\text{-}bear} * CF = P_{f\text{-}bear} * \eta_{bear} * C = (200 \times 10^{-4}) * (3.0) * (800) = 48.0$$

The total expected cost, E, for Case 1 can be obtained as

$$E = C + \Sigma P_{fi} * \eta_i * C = 800 + (8.0 + 44.0 + 48.0) = 900.0$$

The construction cost and the total expected cost for all three cases are tabulated below.

Case No.	t	B	Construct. Cost, C	P_f * CF			Total Expected Cost, E
				Sliding	Over	Bearing	
1	1.5	8.5	800	8.0	44.0	48.0	900.0
2	**1.5**	**9.5**	**860**	**2.2**	**0.9**	**25.8**	**888.8**
3	1.5	10.5	920	0.5	0.0	5.5	926.0

Even though Case 1 produces the smallest construction cost, Case 2 results in the minimum total expected cost. Therefore, Case 2 is selected as the probabilistic optimum design.

The procedure of the optimum design can be summarized as

1. Define the random variables of the wall.
2. Determine a trial design and calculate the construction cost.
3. Estimate the probabilies of failure for each limit state.
4. Repeat steps 2 and 3 for various prospective designs.
5. Define the failure costs for each limit state.
6. Calculate the total cost for each prospective design.

A more thorough parametric study to find the ratio of B/H which leads to the reliabilistic optimum design will be discussed in the following chapter.

Chapter 6
RELIABILITY-BASED DESIGN FOR OPTIMUM B/H

6.1 GENERAL

The procedure to select the reliabilistic optimum design of a gravity wall will be discussed in this chapter. Four different heights of a gravity wall (5 ft, 10 ft, 20 ft and 30 ft) were investigated in this study. Forty-two cases with various top and base widths for four different wall heights were evaluated to find the reliabilistic optimum design.

The sensitivity of the wall dimensions to the safety factor and safety index were observed through a parametric study. The detailed procedure to find the ratio of the wall base to the wall height (B/H) that produces the probabilistic optimum design will be discussed. Since a large number of computations were involved, especially in the calculation to obtain safety indices, a computer program was developed by employing the program language, Visual Basic, and the spread sheet program, EXCEL.

6.2 SENSITIVITY STUDY

Forty-two cases with various top and base widths for four different heights of the gravity wall were investigated to observe the influence of the geometric change of the wall on the safety factor and safety index. For each case, the safety factors and the safety indices of the three limit states were calculated using the method described in Chapter 4. The results are summarized in Tables 6.1 to 6.4.

Each table consists of six groups assorted by the top width, t. Each group has seven base widths, B, which vary with a fixed increment. In Table 6.1, for example, the top width varies from 0.5 ft to 1.75 ft with an increment of 0.25 ft and the base width changes from 1.5 ft to 3.0 ft with 0.25 ft increment. The top and base widths given in Case 43 of each table are the dimensions taken from Table 4.10, where the top and base widths were adjusted to closely match the conventional design criteria.

6.2.1 Influence of t and B to Safety Factor and Safety Index

To observe the sensitivity of the top and base widths, the safety factors and the safety indices of the forty-two cases for each wall height are graphed in Figures 6.1 to 6.4. For the safety factors, the bearing limit state appears to be the most sensitive to the change of the base width, and the sliding limit state proves to be

Table 6.1 Safety Factors and Safety Indices for 5 ft High Wall

Group No.	Case No.	t (ft)	B (ft)	S.F.			β		
				Sliding	Over	Bear	Sliding	Over	Bear
I	1	0.50	1.50	1.16	0.96	0.17	0.88	0.06	0.64
	2	0.50	1.75	1.31	1.28	0.65	1.40	1.38	1.90
	3	0.50	2.00	1.45	1.64	1.45	1.86	2.55	2.82
	4	0.50	2.25	1.60	2.03	2.53	2.27	3.58	3.75
	5	0.50	2.50	1.74	2.47	3.85	2.64	4.48	4.62
	6	0.50	2.75	1.89	2.96	5.36	2.99	5.28	5.51
	7	0.50	3.00	2.03	3.48	7.01	3.30	5.97	6.04
II	8	0.75	1.50	1.31	1.04	0.35	1.40	0.40	1.00
	9	0.75	1.75	1.45	1.37	0.96	1.86	1.72	2.23
	10	0.75	2.00	1.60	1.75	1.84	2.27	2.87	3.10
	11	0.75	2.25	1.74	2.17	2.97	2.64	3.88	4.02
	12	0.75	2.50	1.89	2.63	4.29	2.99	4.76	4.97
	13	0.75	2.75	2.03	3.13	5.77	3.30	5.53	5.48
	14	0.75	3.00	2.18	3.68	7.37	3.59	6.20	5.94
III	15	1.00	1.50	1.45	1.09	0.53	1.86	0.63	1.24
	16	1.00	1.75	1.60	1.45	1.21	2.27	1.97	2.46
	17	1.00	2.00	1.74	1.85	2.14	2.64	3.12	3.31
	18	1.00	2.25	1.89	2.29	3.27	2.99	4.12	4.25
	19	1.00	2.50	2.03	2.77	4.57	3.30	4.99	5.08
	20	1.00	2.75	2.18	3.29	6.01	3.59	5.74	5.53
	21	1.00	3.00	2.32	3.86	7.56	3.85	6.39	5.83
IV	22	1.25	1.50	1.60	1.12	0.66	2.27	0.76	1.36
	23	1.25	1.75	1.74	1.50	1.39	2.64	2.14	2.51
	24	1.25	2.00	1.89	1.92	2.33	2.99	3.30	3.45
	25	1.25	2.25	2.03	2.38	3.45	3.30	4.30	4.38
	26	1.25	2.50	2.18	2.88	4.72	3.59	5.17	5.02
	27	1.25	2.75	2.32	3.43	6.12	3.85	5.91	5.42
	28	1.25	3.00	2.47	4.02	7.62	4.10	6.54	5.71
V	29	1.50	1.50	1.74	1.13	0.74	2.64	0.81	1.43
	30	1.50	1.75	1.89	1.53	1.49	2.99	2.23	2.48
	31	1.50	2.00	2.03	1.97	2.42	3.30	3.43	3.52
	32	1.50	2.25	2.18	2.45	3.52	3.59	4.44	4.37
	33	1.50	2.50	2.32	2.98	4.76	3.85	5.31	4.92
	34	1.50	2.75	2.47	3.54	6.11	4.10	6.05	5.29
	35	1.50	3.00	2.61	4.15	7.56	4.34	6.67	5.58
VI	36	1.75	1.50	1.89	1.12	0.78	2.99	0.76	1.39
	37	1.75	1.75	2.03	1.54	1.52	3.30	2.27	2.46
	38	1.75	2.00	2.18	2.00	2.44	3.59	3.50	3.50
	39	1.75	2.25	2.32	2.51	3.51	3.85	4.54	4.27
	40	1.75	2.50	2.47	3.05	4.70	4.10	5.41	4.78
	41	1.75	2.75	2.61	3.64	6.01	4.34	6.15	5.16
	42	1.75	3.00	2.76	4.27	7.41	4.55	6.77	5.45
	43	**0.42**	**2.28**	**1.57**	**2.04**	**2.51**	**2.19**	**3.58**	**3.75**

Table 6.2 Safety Factors and Safety Indices for 10 ft High Wall

Group No.	Case No.	t (ft)	B (ft)	S.F.			β		
				Sliding	Over	Bear	Sliding	Over	Bear
I	1	0.50	3.50	1.16	1.16	0.30	0.88	0.94	1.12
	2	0.50	4.00	1.31	1.50	0.95	1.40	2.13	2.14
	3	0.50	4.50	1.45	1.88	1.97	1.86	3.20	3.11
	4	0.50	5.00	1.60	2.30	3.31	2.27	4.14	3.98
	5	0.50	5.50	1.74	2.76	4.93	2.64	4.97	4.85
	6	0.50	6.00	1.89	3.26	6.75	2.99	5.70	5.34
	7	0.50	6.50	2.03	3.81	8.73	3.30	6.33	5.62
II	8	1.00	3.50	1.31	1.28	0.59	1.40	1.38	1.44
	9	1.00	4.00	1.45	1.64	1.39	1.86	2.55	2.49
	10	1.00	4.50	1.60	2.03	2.51	2.27	3.58	3.42
	11	1.00	5.00	1.74	2.47	3.89	2.64	4.48	4.28
	12	1.00	5.50	1.89	2.96	5.50	2.99	5.28	4.92
	13	1.00	6.00	2.03	3.48	7.29	3.30	5.97	5.29
	14	1.00	6.50	2.18	4.05	9.21	3.59	6.57	5.55
III	15	1.50	3.50	1.45	1.37	0.86	1.86	1.72	1.72
	16	1.50	4.00	1.60	1.75	1.75	2.27	2.87	2.75
	17	1.50	4.50	1.74	2.17	2.91	2.64	3.88	3.65
	18	1.50	5.00	1.89	2.63	4.31	2.99	4.76	4.41
	19	1.50	5.50	2.03	3.13	5.89	3.30	5.53	4.89
	20	1.50	6.00	2.18	3.68	7.63	3.59	6.20	5.22
	21	1.50	6.50	2.32	4.27	9.49	3.85	6.77	5.47
IV	22	2.00	3.50	1.60	1.45	1.08	2.27	1.97	1.90
	23	2.00	4.00	1.74	1.85	2.02	2.64	3.12	2.92
	24	2.00	4.50	1.89	2.29	3.19	2.99	4.12	3.78
	25	2.00	5.00	2.03	2.77	4.56	3.30	4.99	4.41
	26	2.00	5.50	2.18	3.29	6.11	3.59	5.74	4.83
	27	2.00	6.00	2.32	3.86	7.79	3.85	6.39	5.14
	28	2.00	6.50	2.47	4.47	9.60	4.10	6.93	5.39
V	29	2.50	3.50	1.74	1.50	1.23	2.64	2.14	1.99
	30	2.50	4.00	1.89	1.92	2.18	2.99	3.30	3.00
	31	2.50	4.50	2.03	2.38	3.34	3.30	4.30	3.80
	32	2.50	5.00	2.18	2.88	4.68	3.59	5.17	4.35
	33	2.50	5.50	2.32	3.43	6.18	3.85	5.91	4.75
	34	2.50	6.00	2.47	4.02	7.82	4.10	6.54	5.05
	35	2.50	6.50	2.61	4.64	9.56	4.34	7.07	5.30
VI	36	3.00	3.50	1.89	1.53	1.30	2.99	2.23	2.00
	37	3.00	4.00	2.03	1.97	2.24	3.30	3.43	3.00
	38	3.00	4.50	2.18	2.45	3.38	3.59	4.44	3.74
	39	3.00	5.00	2.32	2.98	4.69	3.85	5.31	4.26
	40	3.00	5.50	2.47	3.54	6.14	4.10	6.05	4.65
	41	3.00	6.00	2.61	4.15	7.72	4.34	6.67	4.96
	42	3.00	6.50	2.76	4.80	9.41	4.55	7.18	5.20
	43	**0.75**	**4.60**	**1.55**	**2.04**	**2.51**	**2.15**	**3.59**	**3.46**

Table 6.3 Safety Factors and Safety Indices for 20 ft High Wall

Group No.	Case No.	t (ft)	B (ft)	S.F.			β		
				Sliding	Over	Bear	Sliding	Over	Bear
I	1	1.00	7.00	1.16	1.16	0.26	0.88	0.94	0.70
	2	1.00	8.00	1.31	1.50	0.91	1.40	2.14	1.78
	3	1.00	9.00	1.45	1.88	1.96	1.86	3.20	2.72
	4	1.00	10.00	1.60	2.30	3.39	2.27	4.14	3.53
	5	1.00	11.00	1.74	2.76	5.12	2.64	4.97	4.13
	6	1.00	12.00	1.89	3.26	7.11	2.99	5.70	4.54
	7	1.00	13.00	2.03	3.81	9.30	3.30	6.33	4.83
II	8	1.50	7.00	1.23	1.22	0.39	1.15	1.18	0.90
	9	1.50	8.00	1.38	1.57	1.12	1.63	2.35	1.95
	10	1.50	9.00	1.53	1.96	2.24	2.07	3.40	2.86
	11	1.50	10.00	1.67	2.39	3.69	2.46	4.32	3.62
	12	1.50	11.00	1.82	2.86	5.44	2.82	5.13	4.16
	13	1.50	12.00	1.96	3.37	7.41	3.15	5.84	4.54
	14	1.50	13.00	2.11	3.93	9.57	3.45	6.46	4.82
III	15	2.00	7.00	1.31	1.28	0.51	1.40	1.38	1.06
	16	2.00	8.00	1.45	1.64	1.32	1.86	2.55	2.10
	17	2.00	9.00	1.60	2.03	2.48	2.27	3.58	2.98
	18	2.00	10.00	1.74	2.47	3.96	2.64	4.48	3.68
	19	2.00	11.00	1.89	2.96	5.70	2.99	5.28	4.18
	20	2.00	12.00	2.03	3.48	7.65	3.30	5.97	4.53
	21	2.00	13.00	2.18	4.05	9.78	3.59	6.57	4.81
IV	22	2.50	7.00	1.38	1.33	0.64	1.63	1.56	1.20
	23	2.50	8.00	1.53	1.70	1.50	2.07	2.72	2.21
	24	2.50	9.00	1.67	2.10	2.69	2.46	3.73	3.06
	25	2.50	10.00	1.82	2.56	4.18	2.82	4.63	3.72
	26	2.50	11.00	1.96	3.05	5.91	3.15	5.41	4.18
	27	2.50	12.00	2.11	3.58	7.84	3.45	6.09	4.52
	28	2.50	13.00	2.25	4.16	9.94	3.72	6.67	4.79
V	29	3.00	7.00	1.45	1.37	0.76	1.86	1.72	1.31
	30	3.00	8.00	1.60	1.75	1.65	2.27	2.87	2.30
	31	3.00	9.00	1.74	2.17	2.87	2.64	3.88	3.12
	32	3.00	10.00	1.89	2.63	4.35	2.99	4.76	3.73
	33	3.00	11.00	2.03	3.13	6.07	3.30	5.53	4.18
	34	3.00	12.00	2.18	3.68	7.98	3.59	6.20	4.51
	35	3.00	13.00	2.32	4.27	10.04	3.86	6.77	4.78
VI	36	3.50	7.00	1.53	1.41	0.86	2.07	1.85	1.39
	37	3.50	8.00	1.67	1.80	1.78	2.46	3.00	2.37
	38	3.50	9.00	1.82	2.23	3.01	2.82	4.00	3.16
	39	3.50	10.00	1.96	2.70	4.49	3.15	4.88	3.74
	40	3.50	11.00	2.11	3.22	6.19	3.45	5.64	4.16
	41	3.50	12.00	2.25	3.77	8.07	3.72	6.30	4.49
	42	3.50	13.00	2.40	4.37	10.10	3.98	6.85	4.76
	43	**1.50**	**9.20**	**1.55**	**2.04**	**2.50**	**2.15**	**3.59**	**3.03**

Table 6.4 Safety Factors and Safety Indices for 30 ft High Wall

Group No.	Case No.	t (ft)	B (ft)	S.F.			β		
				Sliding	Over	Bear	Sliding	Over	Bear
I	1	1.00	11.00	1.16	1.23	0.29	0.88	1.18	0.53
	2	1.00	12.00	1.26	1.45	0.72	1.23	1.97	1.22
	3	1.00	13.00	1.36	1.69	1.36	1.56	2.71	1.83
	4	1.00	14.00	1.45	1.95	2.22	1.86	3.38	2.37
	5	1.00	15.00	1.55	2.23	3.26	2.14	4.01	2.81
	6	1.00	16.00	1.65	2.53	4.48	2.40	4.58	3.18
	7	1.00	17.00	1.74	2.85	5.86	2.64	5.11	3.49
II	8	1.50	11.00	1.21	1.27	0.38	1.06	1.35	0.67
	9	1.50	12.00	1.31	1.50	0.85	1.40	2.14	1.34
	10	1.50	13.00	1.40	1.75	1.54	1.71	2.86	1.93
	11	1.50	14.00	1.50	2.01	2.43	2.00	3.52	2.44
	12	1.50	15.00	1.60	2.30	3.49	2.27	4.14	2.87
	13	1.50	16.00	1.69	2.60	4.73	2.52	4.70	3.23
	14	1.50	17.00	1.79	2.92	6.10	2.76	5.22	3.52
III	15	2.00	11.00	1.26	1.31	0.47	1.23	1.51	0.78
	16	2.00	12.00	1.36	1.55	0.99	1.56	2.28	1.44
	17	2.00	13.00	1.45	1.80	1.71	1.86	3.00	2.02
	18	2.00	14.00	1.55	2.07	2.62	2.14	3.65	2.51
	19	2.00	15.00	1.65	2.36	3.70	2.40	4.26	2.92
	20	2.00	16.00	1.74	2.67	4.94	2.64	4.82	3.26
	21	2.00	17.00	1.84	2.99	6.32	2.88	5.33	3.54
IV	22	2.50	11.00	1.31	1.35	0.56	1.40	1.66	0.88
	23	2.50	12.00	1.40	1.59	1.12	1.71	2.42	1.53
	24	2.50	13.00	1.50	1.85	1.87	2.00	3.13	2.09
	25	2.50	14.00	1.60	2.12	2.80	2.27	3.78	2.57
	26	2.50	15.00	1.69	2.42	3.90	2.52	4.37	2.96
	27	2.50	16.00	1.79	2.73	5.14	2.76	4.92	3.29
	28	2.50	17.00	1.89	3.06	6.51	2.99	5.43	3.57
V	29	3.00	11.00	1.36	1.39	0.66	1.56	1.79	0.97
	30	3.00	12.00	1.45	1.64	1.24	1.86	2.55	1.61
	31	3.00	13.00	1.55	1.90	2.02	2.14	3.25	2.15
	32	3.00	14.00	1.65	2.18	2.96	2.40	3.89	2.61
	33	3.00	15.00	1.74	2.47	4.06	2.64	4.48	3.00
	34	3.00	16.00	1.84	2.79	5.31	2.88	5.02	3.31
	35	3.00	17.00	1.94	3.13	6.67	3.09	5.52	3.58
VI	36	3.50	11.00	1.40	1.43	0.75	1.71	1.91	1.05
	37	3.50	12.00	1.50	1.68	1.36	2.00	2.66	1.67
	38	3.50	13.00	1.60	1.94	2.15	2.27	3.36	2.21
	39	3.50	14.00	1.69	2.23	3.11	2.52	4.00	2.65
	40	3.50	15.00	1.79	2.53	4.21	2.76	4.58	3.02
	41	3.50	16.00	1.89	2.85	5.45	2.99	5.12	3.33
	42	3.50	17.00	1.99	3.19	6.82	3.20	5.61	3.60
	43	**2.50**	**13.70**	**1.57**	**2.04**	**2.50**	**2.19**	**3.59**	**2.43**

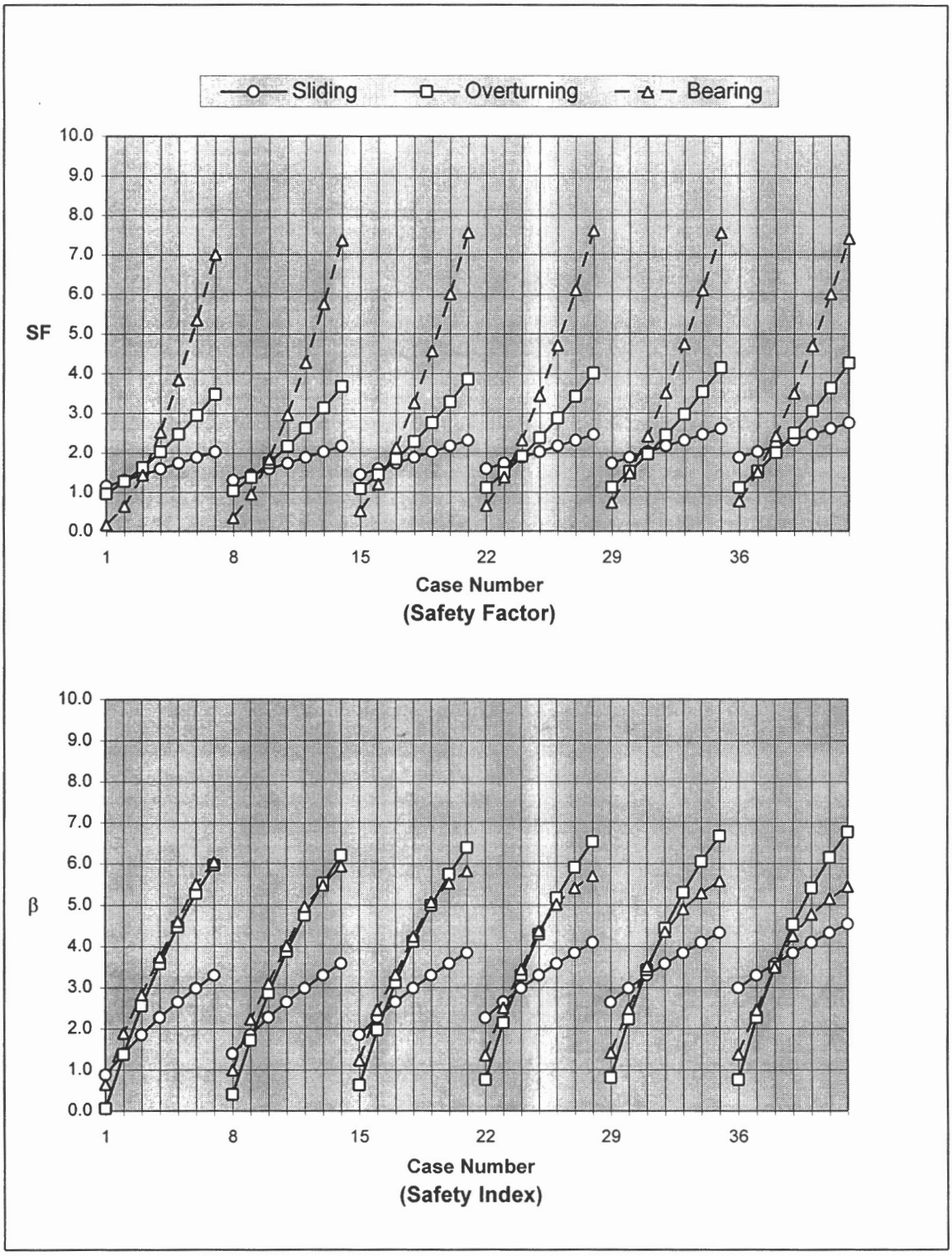

Figure 6.1 Safety Factors and Safety Indices of the Three Limit States for 5 ft Wall

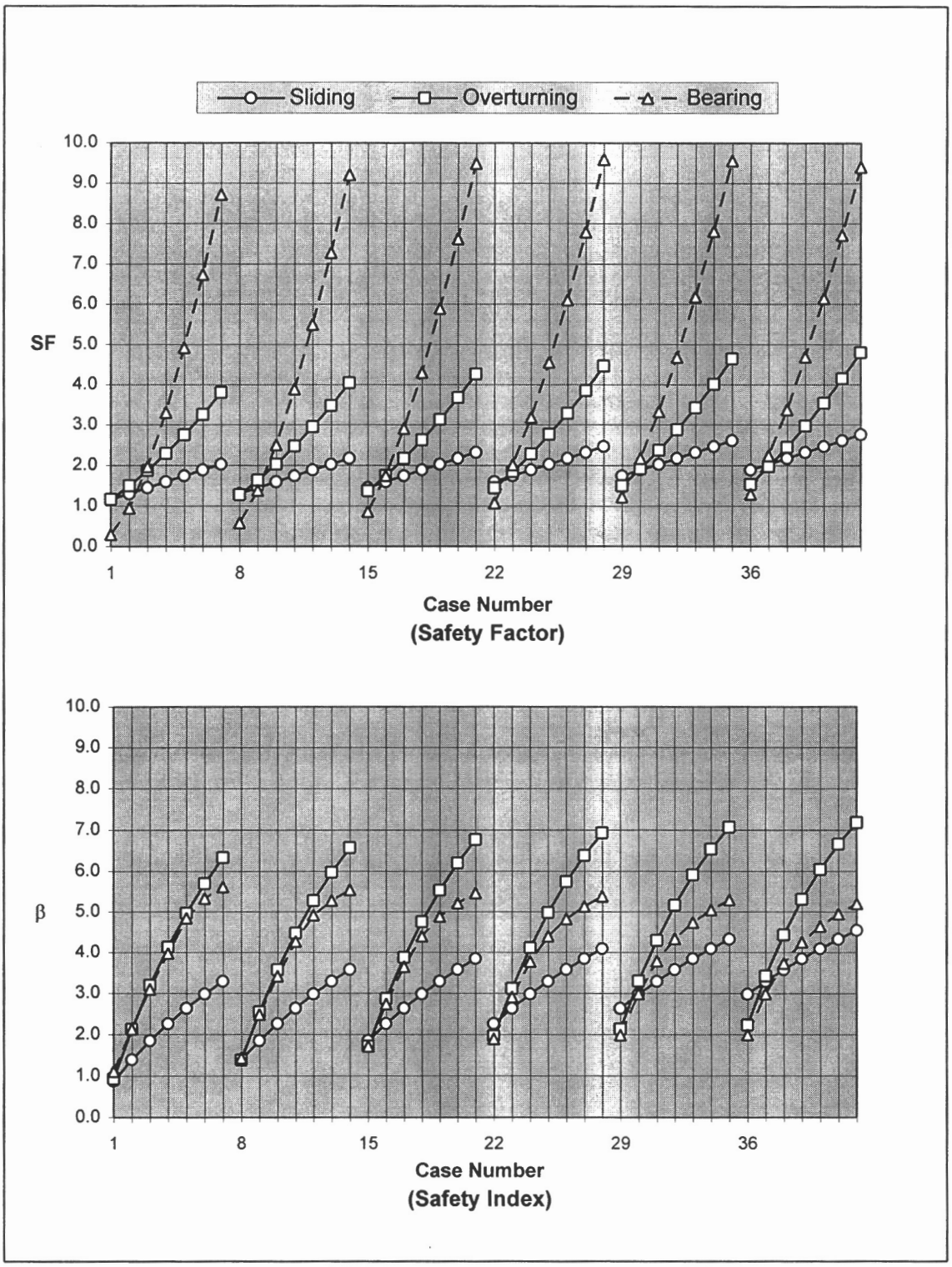

Figure 6.2 Safety Factors and Safety Indices of the Three Limit States for 10 ft Wall

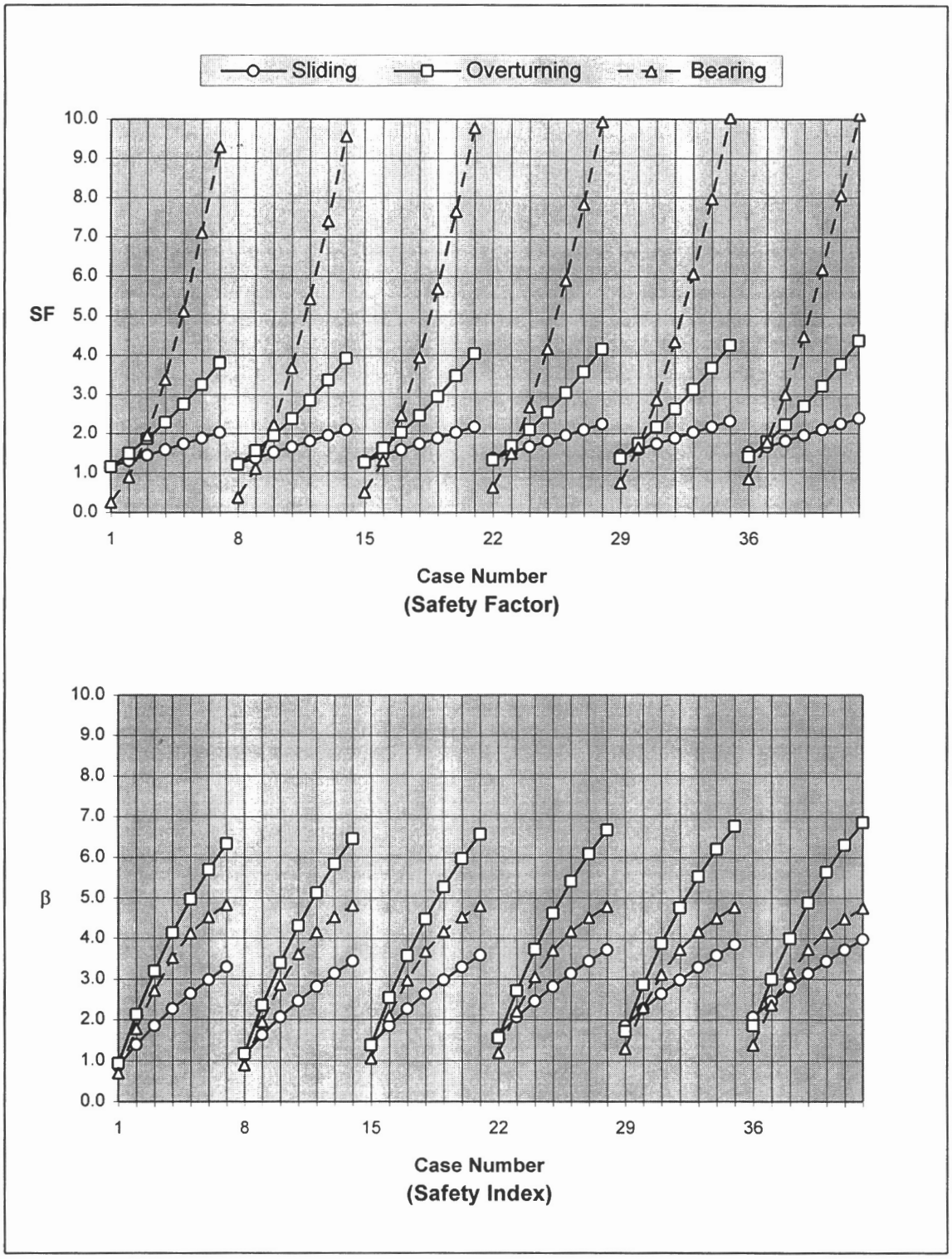

Figure 6.3 Safety Factors and Safety Indices of the Three Limit States for 20 ft Wall

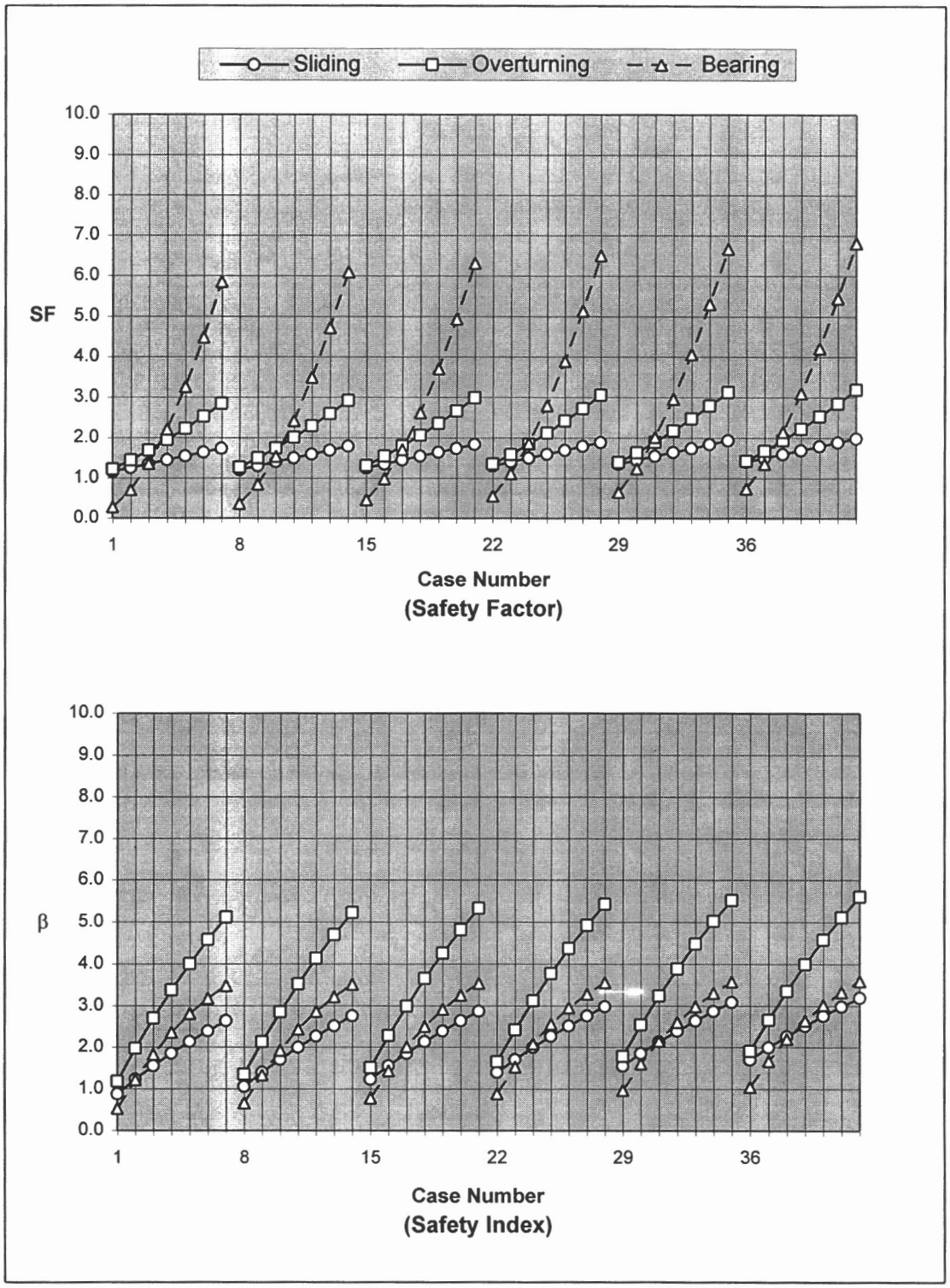

Figure 6.4 Safety Factors and Safety Indices of the Three Limit States for 30 ft Wall

the least influenced. For the safety indices, the overturning limit state is the most sensitive and the sliding limit state is the least affected.

The change of top width does not appear to significantly influence the safety factors or the safety indices compared to the base width. Since the influence of the top width is insignificant, it is recommended to set the top width first and then determine the base width in the actual design of the wall. For the purpose of convenient construction, the top width should be at least H/12. The top widths of Case 43 in Tables 6.1 to 6.4 are close to H/12.

6.2.2 Safety Factor vs. Safety Index

The smooth transition of the graphs in Figures 6.1 to 6.4 can be an evidence that the analysis results are reliable. As the base width increases, the safety indices as well as the safety factors are observed to increase. However, it is found that the gradient of the two values in this study are different from one limit state to another. For example, the safety factors of the bearing limit state in Figure 6.2 respond more sharply to the base width change (SF = 0.3 to 9.5) than the corresponding safety indices (β = 1.1 to 5.5). The opposite result occurs in the overturning limit state, i.e., the safety indices (β = 0.9 to 7.2) react more sensitively than the safety factors (SF = 1.2 to 4.8). In the bearing limit state, the

safety index corresponding to a safety factor of 9.5 is found to be 5.5, but in the overturning limit state the safety index corresponding to a safety factor of 4.8 proves to be 7.2. Consequently, there is no proportional relationship between the safety factors and the safety indices. In other words, a statement that a safety factor of 2.5 in a system is equivalent to a safety index of 3.0 may be misleading. Some investigators such as Meyerhof (1976) provided a table that compares the typical safety factors and the safety indices (Table 2.7), which may incorrectly lead one to believe that there is a certain relationship between the two values.

6.3 SELECTION OF OPTIMUM DESIGN

A probabilistically optimized design can be achieved by using the procedures described in Chapter 5. The same 42 combinations of t and B as described in Section 6.2 were evaluated and the results are summarized in Tables 6.5 to 6.8. The tables provide the information on the safety factors of the three limit states, the ratios of B to H, the construction costs, the probable failure costs and the total costs for each combination of t and B. As discussed in Chapter 5, the construction cost (C) is proportional to the volume of concrete in the wall and the volume of compacted backfill. The cost of failure (CF) is determined by multiplying the relative cost factors (η_i) by the construction cost. The probable failure cost of each

Table 6.5 Selection of Optimum Design for 5 ft High Wall

η		
Sliding	Over	Bear
1	5	3

Group No.	Case No.	t	B	S.F.			B/H	C	P_f * CF			Total Cost
				Sliding	Over	Bear			Sliding	Over	Bear	
I	1	0.50	1.50	1.16	0.96	0.17	0.300	42.5	8.05	101.17	33.11	184.83
	2	0.50	1.75	1.31	1.28	0.65	0.350	46.3	3.75	19.38	4.02	73.40
	3	0.50	2.00	1.45	1.64	1.45	**0.400**	**50.0**	**1.58**	**1.35**	**0.36**	**53.29**
	4	0.50	2.25	1.60	2.03	2.53	0.450	53.8	0.62	0.05	0.01	54.43
	5	0.50	2.50	1.74	2.47	3.85	0.500	57.5	0.24	0.00	0.00	57.74
	6	0.50	2.75	1.89	2.96	5.36	0.550	61.3	0.09	0.00	0.00	61.34
	7	0.50	3.00	2.03	3.48	7.01	0.600	65.0	0.03	0.00	0.00	65.03
II	8	0.75	1.50	1.31	1.04	0.35	0.300	46.3	3.75	79.68	22.12	151.80
	9	0.75	1.75	1.45	1.37	0.96	0.350	50.0	1.58	10.68	1.92	64.18
	10	0.75	2.00	1.60	1.75	1.84	**0.400**	**53.8**	**0.62**	**0.55**	**0.16**	**55.08**
	11	0.75	2.25	1.74	2.17	2.97	0.450	57.5	0.24	0.02	0.00	57.76
	12	0.75	2.50	1.89	2.63	4.29	0.500	61.3	0.09	0.00	0.00	61.34
	13	0.75	2.75	2.03	3.13	5.77	0.550	65.0	0.03	0.00	0.00	65.03
	14	0.75	3.00	2.18	3.68	7.37	0.600	68.8	0.01	0.00	0.00	68.76
III	15	1.00	1.50	1.45	1.09	0.53	0.300	50.0	1.59	66.09	16.25	133.92
	16	1.00	1.75	1.60	1.45	1.21	0.350	53.8	0.62	6.56	1.12	62.06
	17	1.00	2.00	1.74	1.85	2.14	**0.400**	**57.5**	**0.24**	**0.26**	**0.08**	**58.08**
	18	1.00	2.25	1.89	2.29	3.27	0.450	61,3	0.09	0.01	0.00	61.34
	19	1.00	2.50	2.03	2.77	4.57	0.500	65.0	0.03	0.00	0.00	65.03
	20	1.00	2.75	2.18	3.29	6.01	0.550	68.8	0.01	0.00	0.00	68.76
	21	1.00	3.00	2.32	3.86	7.56	0.600	72.5	0.00	0.00	0.00	72.50
VI	22	1.25	1.50	1.60	1.12	0.66	0.300	53.8	0.63	60.10	14.02	128.49
	23	1.25	1.75	1.74	1.50	1.39	0.350	57.5	0.24	4.65	1.04	63.43
	24	1.25	2.00	1.89	1.92	2.33	**0.400**	**61.3**	**0.09**	**0.15**	**0.05**	**61.54**
	25	1.25	2.25	2.03	2.38	3.45	0.450	65.0	0.03	0.00	0.00	65.04
	26	1.25	2.50	2.18	2.88	4.72	0.500	68.8	0.01	0.00	0.00	68.76
	27	1.25	2.75	2.32	3.43	6.12	0.550	72.5	0.00	0.00	0.00	72.50
	28	1.25	3.00	2.47	4.02	7.62	0.600	76.3	0.00	0.00	0.00	76.25
V	29	1.50	1.50	1.74	1.13	0.74	0.300	57.5	0.24	60.08	13.28	131.10
	30	1.50	1.75	1.89	1.53	1.49	0.350	61.3	0.09	3.94	1.20	66.48
	31	1.50	2.00	2.03	1.97	2.42	**0.400**	**65.0**	**0.03**	**0.10**	**0.04**	**65.17**
	32	1.50	2.25	2.18	2.45	3.52	0.450	68.8	0.01	0.00	0.00	68.76
	33	1.50	2.50	2.32	2.98	4.76	0.500	72.5	0.00	0.00	0.00	72.50
	34	1.50	2.75	2.47	3.54	6.11	0.550	76.3	0.00	0.00	0.00	76.25
	35	1.50	3.00	2.61	4.15	7.56	0.600	80.0	0.00	0.00	0.00	80.00
VI	36	1.75	1.50	1.89	1.12	0.78	0.300	61.3	0.09	68.49	15.17	144.99
	37	1.75	1.75	2.03	1.54	1.52	0.350	65.0	0.03	3.77	1.35	70.15
	38	1.75	2.00	2.18	2.00	2.44	**0.400**	**68.8**	**0.01**	**0.08**	**0.05**	**68.89**
	39	1.75	2.25	2.32	2.51	3.51	0.450	72.5	0.00	0.00	0.00	72.51
	40	1.75	2.50	2.47	3.05	4.70	0.500	76.3	0.00	0.00	0.00	76.25
	41	1.75	2.75	2.61	3.64	6.01	0.550	80.0	0.00	0.00	0.00	80.00
	42	1.75	3.00	2.76	4.27	7.41	0.600	83.8	0.00	0.00	0.00	83.75
	43	**0.42**	**2.28**	**1.57**	**2.04**	**2.51**	**0.456**	**53.0**	**0.76**	**0.05**	**0.01**	**53.82**

Table 6.6 Selection of Optimum Design for 10 ft High Wall

η		
Sliding	Over	Bear
1	5	3

Group No.	Case No.	t	B	S.F.			B/H	C	P_f * CF			Total Cost
				Sliding	Over	Bear			Sliding	Over	Bear	
I	1	0.50	3.50	1.16	1.16	0.30	0.350	170.0	32.21	148.10	66.99	417.31
	2	0.50	4.00	1.31	1.50	0.95	0.400	185.0	15.02	15.15	9.04	224.21
	3	0.50	4.50	1.45	1.88	1.97	**0.450**	**200.0**	**6.33**	**0.69**	**0.57**	**207.59**
	4	0.50	5.00	1.60	2.30	3.31	0.500	215.0	2.49	0.02	0.02	217.54
	5	0.50	5.50	1.74	2.76	4.93	0.550	230.0	0.94	0.00	0.00	230.94
	6	0.50	6.00	1.89	3.26	6.75	0.600	245.0	0.35	0.00	0.00	245.35
	7	0.50	6.50	2.03	3.81	8.73	0.650	260.0	0.13	0.00	0.00	260.13
II	8	1.00	3.50	1.31	1.28	0.59	0.350	185.0	14.99	77.00	41.56	318.55
	9	1.00	4.00	1.45	1.64	1.39	**0.400**	**200.0**	**6.33**	**5.42**	**3.82**	**215.57**
	10	1.00	4.50	1.60	2.03	2.51	0.450	215.0	2.49	0.19	0.20	217.88
	11	1.00	5.00	1.74	2.47	3.89	0.500	230.0	0.94	0.00	0.01	230.95
	12	1.00	5.50	1.89	2.96	5.50	0.550	245.0	0.35	0.00	0.00	245.35
	13	1.00	6.00	2.03	3.48	7.29	0.600	260.0	0.13	0.00	0.00	260.13
	14	1.00	6.50	2.18	4.05	9.21	0.650	275.0	0.05	0.00	0.00	275.05
III	15	1.50	3.50	1.45	1.37	0.86	0.350	200.0	6.35	42.71	25.67	274.72
	16	1.50	4.00	1.60	1.75	1.75	**0.400**	**215.0**	**2.49**	**2.21**	**1.94**	**221.64**
	17	1.50	4.50	1.74	2.17	2.91	0.450	230.0	0.94	0.06	0.09	231.09
	18	1.50	5.00	1.89	2.63	4.31	0.500	245.0	0.35	0.00	0.00	245.35
	19	1.50	5.50	2.03	3.13	5.89	0.550	260.0	0.13	0.00	0.00	260.13
	20	1.50	6.00	2.18	3.68	7.63	0.600	275.0	0.05	0.00	0.00	275.05
	21	1.50	6.50	2.32	4.27	9.49	0.650	290.0	0.02	0.00	0.00	290.02
VI	22	2.00	3.50	1.60	1.45	1.08	0.350	215.0	2.50	26.45	18.49	262.45
	23	2.00	4.00	1.74	1.85	2.02	**0.400**	**230.0**	**0.94**	**1.05**	**1.23**	**233.22**
	24	2.00	4.50	1.89	2.29	3.19	0.450	245.0	0.35	0.02	0.06	245.43
	25	2.00	5.00	2.03	2.77	4.56	0.500	260.0	0.13	0.00	0.00	260.13
	26	2.00	5.50	2.18	3.29	6.11	0.550	275.0	0.05	0.00	0.00	275.05
	27	2.00	6.00	2.32	3.86	7.79	0.600	290.0	0.02	0.00	0.00	290.02
	28	2.00	6.50	2.47	4.47	9.60	0.650	305.0	0.01	0.00	0.00	305.01
V	29	2.50	3.50	1.74	1.50	1.23	0.350	230.0	0.94	18.82	15.95	265.71
	30	2.50	4.00	1.89	1.92	2.18	**0.400**	**245.0**	**0.35**	**0.59**	**1.00**	**246.94**
	31	2.50	4.50	2.03	2.38	3.34	0.450	260.0	0.13	0.01	0.06	260.19
	32	2.50	5.00	2.18	2.88	4.68	0.500	275.0	0.05	0.00	0.01	275.05
	33	2.50	5.50	2.32	3.43	6.18	0.550	290.0	0.02	0.00	0.00	290.02
	34	2.50	6.00	2.47	4.02	7.82	0.600	305.0	0.01	0.00	0.00	305.01
	35	2.50	6.50	2.61	4.64	9.56	0.650	320.0	0.00	0.00	0.00	320.00
VI	36	3.00	3.50	1.89	1.53	1.30	0.350	245.0	0.35	15.62	16.59	277.56
	37	3.00	4.00	2.03	1.97	2.24	**0.400**	**260.0**	**0.13**	**0.40**	**1.07**	**261.59**
	38	3.00	4.50	2.18	2.45	3.38	0.450	275.0	0.05	0.01	0.08	275.13
	39	3.00	5.00	2.32	2.98	4.69	0.500	290.0	0.02	0.00	0.01	290.03
	40	3.00	5.50	2.47	3.54	6.14	0.550	305.0	0.01	0.00	0.00	305.01
	41	3.00	6.00	2.61	4.15	7.72	0.600	320.0	0.00	0.00	0.00	320.00
	42	3.00	6.50	2.76	4.80	9.41	0.650	335.0	0.00	0.00	0.00	335.00
	43	**0.75**	**4.60**	**1.55**	**2.04**	**2.51**	**0.460**	**210.5**	**3.32**	**0.17**	**0.17**	**214.17**

Table 6.7 Selection of Optimum Design for 20 ft High Wall

η		
Sliding	Over	Bear
1	5	3

Group No.	Case No.	t	B	S.F.			B/H	C	P_f * CF			Total Cost
				Sliding	Over	Bear			Sliding	Over	Bear	
I	1	1.00	7.00	1.16	1.16	0.26	0.350	680.0	128.7	592.5	491.3	1892.55
	2	1.00	8.00	1.31	1.50	0.91	0.400	740.0	60.1	60.5	82.9	943.48
	3	1.00	9.00	1.45	1.88	1.96	**0.450**	**800.0**	**25.3**	**2.8**	**7.7**	**835.82**
	4	1.00	10.00	1.60	2.30	3.39	0.500	860.0	10.0	0.1	0.5	870.59
	5	1.00	11.00	1.74	2.76	5.12	0.550	920.0	3.8	0.0	0.0	923.82
	6	1.00	12.00	1.89	3.26	7.11	0.600	980.0	1.4	0.0	0.0	981.39
	7	1.00	13.00	2.03	3.81	9.30	0.650	1040.0	0.5	0.0	0.0	1040.51
II	8	1.50	7.00	1.23	1.22	0.39	0.350	710.0	89.3	425.6	392.2	1617.06
	9	1.50	8.00	1.38	1.57	1.12	0.400	770.0	39.4	35.8	58.6	903.74
	10	1.50	9.00	1.53	1.96	2.24	**0.450**	**830.0**	**16.0**	**1.4**	**5.2**	**852.62**
	11	1.50	10.00	1.67	2.39	3.69	0.500	890.0	6.1	0.0	0.4	896.58
	12	1.50	11.00	1.82	2.86	5.44	0.550	950.0	2.3	0.0	0.0	952.34
	13	1.50	12.00	1.96	3.37	7.41	0.600	1010.0	0.8	0.0	0.0	1010.85
	14	1.50	13.00	2.11	3.93	9.57	0.650	1070.0	0.3	0.0	0.0	1070.31
III	15	2.00	7.00	1.31	1.28	0.51	0.350	740.0	60.1	308.1	319.1	1427.25
	16	2.00	8.00	1.45	1.64	1.32	0.400	800.0	25.3	21.7	43.2	890.22
	17	2.00	9.00	1.60	2.03	2.48	**0.450**	**860.0**	**10.0**	**0.8**	**3.7**	**874.48**
	18	2.00	10.00	1.74	2.47	3.96	0.500	920.0	3.8	0.0	0.3	924.11
	19	2.00	11.00	1.89	2.96	5.70	0.550	980.0	1.4	0.0	0.0	981.43
	20	2.00	12.00	2.03	3.48	7.65	0.600	1040.0	0.5	0.0	0.0	1040.51
	21	2.00	13.00	2.18	4.05	9.78	0.650	1100.0	0.2	0.0	0.0	1100.19
VI	22	2.50	7.00	1.38	1.33	0.64	0.350	770.0	39.4	226.8	266.5	1302.71
	23	2.50	8.00	1.53	1.70	1.50	**0.400**	**830.0**	**16.0**	**13.6**	**33.5**	**893.10**
	24	2.50	9.00	1.67	2.10	2.69	0.450	890.0	6.2	0.4	2.9	899.50
	25	2.50	10.00	1.82	2.56	4.18	0.500	950.0	2.3	0.0	0.3	952.59
	26	2.50	11.00	1.96	3.05	5.91	0.550	1010.0	0.8	0.0	0.0	1010.88
	27	2.50	12.00	2.11	3.58	7.84	0.600	1070.0	0.3	0.0	0.0	1070.31
	28	2.50	13.00	2.25	4.16	9.94	0.650	1130.0	0.1	0.0	0.0	1130.11
V	29	3.00	7.00	1.45	1.37	0.76	0.350	800.0	25.3	170.8	229.9	1225.99
	30	3.00	8.00	1.60	1.75	1.65	**0.400**	**860.0**	**10.0**	**8.8**	**27.4**	**906.17**
	31	3.00	9.00	1.74	2.17	2.87	0.450	920.0	3.8	0.2	2.5	926.48
	32	3.00	10.00	1.89	2.63	4.35	0.500	980.0	1.4	0.0	0.3	981.67
	33	3.00	11.00	2.03	3.13	6.07	0.550	1040.0	0.5	0.0	0.0	1040.55
	34	3.00	12.00	2.18	3.68	7.98	0.600	1100.0	0.2	0.0	0.0	1100.19
	35	3.00	13.00	2.32	4.27	10.04	0.650	1160.0	0.1	0.0	0.0	1160.07
VI	36	3.50	7.00	1.53	1.41	0.86	0.350	830.0	16.0	132.3	205.5	1183.79
	37	3.50	8.00	1.67	1.80	1.78	**0.400**	**890.0**	**6.2**	**6.0**	**23.6**	**925.74**
	38	3.50	9.00	1.82	2.23	3.01	0.450	950.0	2.3	0.1	2.3	954.69
	39	3.50	10.00	1.96	2.70	4.49	0.500	1010.0	0.8	0.0	0.3	1011.12
	40	3.50	11.00	2.11	3.22	6.19	0.550	1070.0	0.3	0.0	0.1	1070.35
	41	3.50	12.00	2.25	3.77	8.07	0.600	1130.0	0.1	0.0	0.0	1130.12
	42	3.50	13.00	2.40	4.37	10.10	0.650	1190.0	0.0	0.0	0.0	1190.04
	43	**1.50**	**9.20**	**1.55**	**2.04**	**2.50**	**0.460**	**842.0**	**13.3**	**0.7**	**3.1**	**859.07**

Table 6.8 Selection of Optimum Design for 30 ft High Wall

η		
Sliding	Over	Bear
1	5	3

Group No.	Case No.	t	B	S.F.			B/H	C	P_f * CF			Total Cost
				Sliding	Over	Bear			Sliding	Over	Bear	
I	1	1.0	11.0	1.16	1.23	0.29	0.367	1530.0	289.9	908.6	1361.2	4089.7
	2	1.0	12.0	1.26	1.45	0.72	0.400	1620.0	176.6	195.8	537.9	2530.3
	3	1.0	13.0	1.36	1.69	1.36	0.433	1710.0	102.3	29.0	170.8	2012.1
	4	1.0	14.0	1.45	1.95	2.22	**0.467**	**1800.0**	**56.9**	**3.2**	**48.6**	**1908.8**
	5	1.0	15.0	1.55	2.23	3.26	0.500	1890.0	30.8	0.3	13.9	1934.9
	6	1.0	16.0	1.65	2.53	4.48	0.533	1980.0	16.3	0.0	4.3	2000.6
	7	1.0	17.0	1.74	2.85	5.86	0.567	2070.0	8.5	0.0	1.5	2080.0
II	8	1.5	11.0	1.21	1.27	0.38	0.367	1575.0	227.9	693.1	1194.3	3690.3
	9	1.5	12.0	1.31	1.50	0.85	0.400	1665.0	135.1	136.2	451.4	2387.7
	10	1.5	13.0	1.40	1.75	1.54	0.433	1755.0	76.6	18.7	140.4	1990.8
	11	1.5	14.0	1.50	2.01	2.43	**0.467**	**1845.0**	**42.0**	**2.0**	**40.3**	**1929.2**
	12	1.5	15.0	1.60	2.30	3.49	0.500	1935.0	22.4	0.2	11.9	1969.4
	13	1.5	16.0	1.69	2.60	4.73	0.533	2025.0	11.8	0.0	3.8	2040.6
	14	1.5	17.0	1.79	2.92	6.10	0.567	2115.0	6.1	0.0	1.4	2122.5
III	15	2.0	11.0	1.26	1.31	0.47	0.367	1620.0	176.6	529.9	1055.2	3381.7
	16	2.0	12.0	1.36	1.55	0.99	0.400	1710.0	102.3	95.6	384.2	2292.1
	17	2.0	13.0	1.45	1.80	1.71	0.433	1800.0	56.9	12.3	117.9	1987.1
	18	2.0	14.0	1.55	2.07	2.62	**0.467**	**1890.0**	**30.8**	**1.2**	**34.2**	**1956.2**
	19	2.0	15.0	1.65	2.36	3.70	0.500	1980.0	16.3	0.1	10.4	2006.8
	20	2.0	16.0	1.74	2.67	4.94	0.533	2070.0	8.5	0.0	3.5	2081.9
	21	2.0	17.0	1.84	2.99	6.32	0.567	2160.0	4.4	0.0	1.3	2165.6
VI	22	2.5	11.0	1.31	1.35	0.56	0.367	1665.0	135.1	407.3	941.0	3148.4
	23	2.5	12.0	1.40	1.59	1.12	0.400	1755.0	76.6	67.9	332.4	2231.9
	24	2.5	13.0	1.50	1.85	1.87	0.433	1845.0	42.0	8.2	101.2	1996.4
	25	2.5	14.0	1.60	2.12	2.80	**0.467**	**1935.0**	**22.4**	**0.8**	**29.8**	**1988.0**
	26	2.5	15.0	1.69	2.42	3.90	0.500	2025.0	11.8	0.1	9.3	2046.1
	27	2.5	16.0	1.79	2.73	5.14	0.533	2115.0	6.1	0.0	3.2	2124.3
	28	2.5	17.0	1.89	3.06	6.51	0.567	2205.0	3.1	0.0	1.2	2209.3
V	29	3.0	11.0	1.36	1.39	0.66	0.367	1710.0	102.3	315.4	848.3	2976.0
	30	3.0	12.0	1.45	1.64	1.24	0.400	1800.0	56.9	48.8	292.5	2198.2
	31	3.0	13.0	1.55	1.90	2.02	**0.433**	**1890.0**	**30.8**	**5.5**	**88.8**	**2015.1**
	32	3.0	14.0	1.65	2.18	2.96	0.467	1980.0	16.3	0.5	26.6	2023.4
	33	3.0	15.0	1.74	2.47	4.06	0.500	2070.0	8.5	0.0	8.5	2087.0
	34	3.0	16.0	1.84	2.79	5.31	0.533	2160.0	4.4	0.0	3.0	2167.3
	35	3.0	17.0	1.94	3.13	6.67	0.567	2250.0	2.2	0.0	1.1	2253.4
VI	36	3.5	11.0	1.40	1.43	0.75	0.367	1755.0	76.6	246.8	774.3	2852.7
	37	3.5	12.0	1.50	1.68	1.36	0.400	1845.0	42.0	35.6	262.0	2184.5
	38	3.5	13.0	1.60	1.94	2.15	**0.433**	**1935.0**	**22.4**	**3.8**	**79.6**	**2040.9**
	39	3.5	14.0	1.69	2.23	3.11	0.467	2025.0	11.8	0.3	24.3	2061.3
	40	3.5	15.0	1.79	2.53	4.21	0.500	2115.0	6.1	0.0	7.9	2129.0
	41	3.5	16.0	1.89	2.85	5.45	0.533	2205.0	3.1	0.0	2.8	2210.9
	42	3.5	17.0	1.99	3.19	6.82	0.567	2295.0	1.6	0.0	1.1	2297.7
	43	**2.5**	**13.7**	**1.57**	**2.04**	**2.50**	**0.457**	**1908.0**	**27.2**	**1.6**	**43.2**	**1980.0**

limit state is estimated by multiplying the probability of failure (P_f) by the cost of failure. Finally, the total cost is obtained by summing the construction cost and the probable failure cost ($P_f * CF$). The combination of t and B that yields the least total cost is considered as the reliabilistic optimum design.

6.3.1 Effect of Relative Cost Factors, (η_i)

Since the relative cost factors, (η_i) for each limit state can be different from one situation to another, five different combinations of η values were examined in this study. The combinations considered for the relative cost factors for sliding, overturning, bearing limit states are 1:5:3, 1:3:5, 1:1:1, 3:3:3 and 5:5:5, respectively. Figures 6.5 to 6.8 present the estimated total costs of each height of the wall using all five combinations of η values. As observed in the figures, the relative cost factors (η_i) influence the total costs significantly in the cases where the probability of failures are high. However, the cases that produce the low total costs appear to be almost independent from the relative cost factors (η_i). Since the change of η_i values did not affect the conclusion of this study, 1:5:3 ratio is used for the purpose of presentation, and the results are summarized in Tables 6.5 to 6.8 given previously.

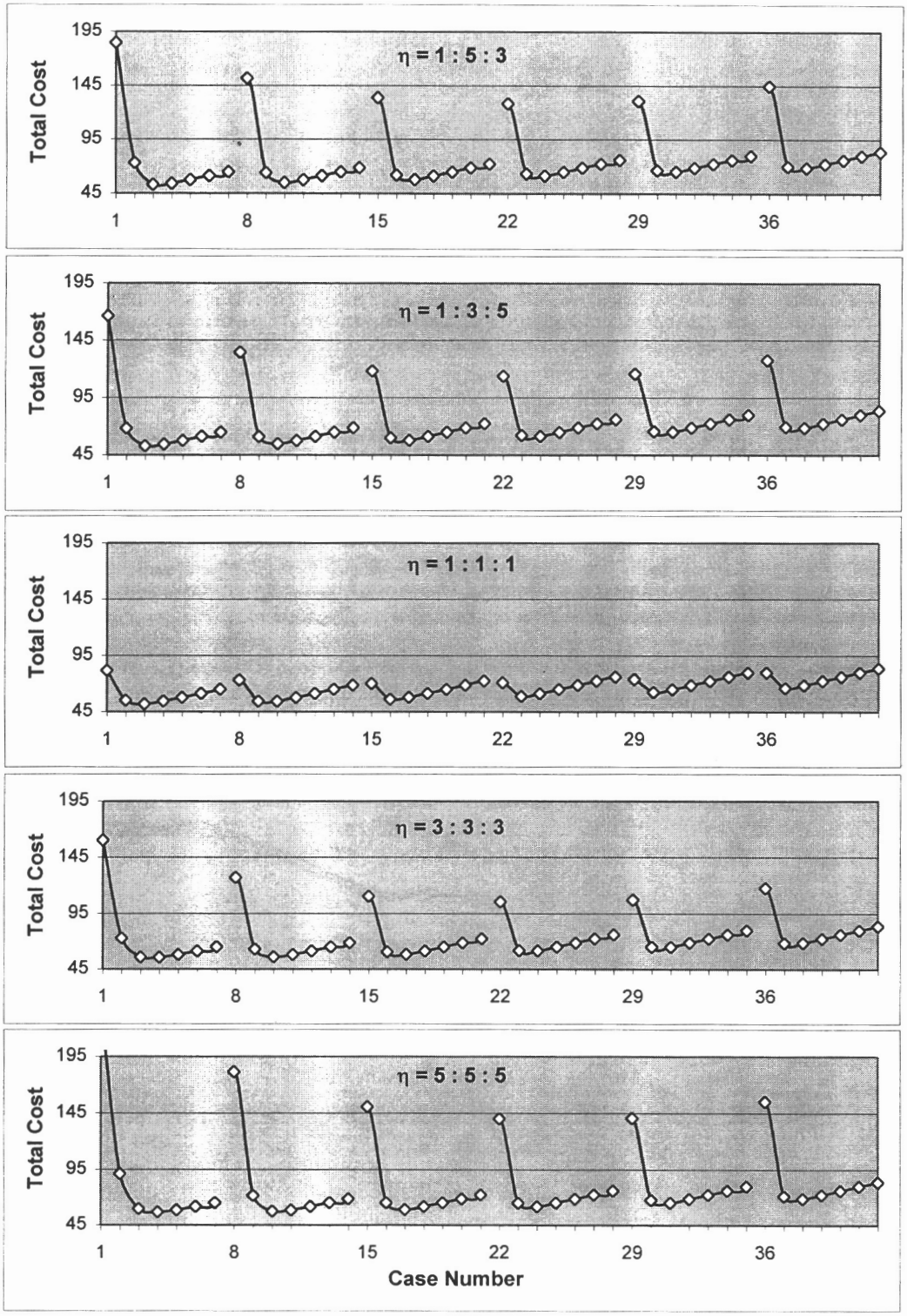

Figure 6.5 Total Cost of 5 ft Wall with Various η Ratios

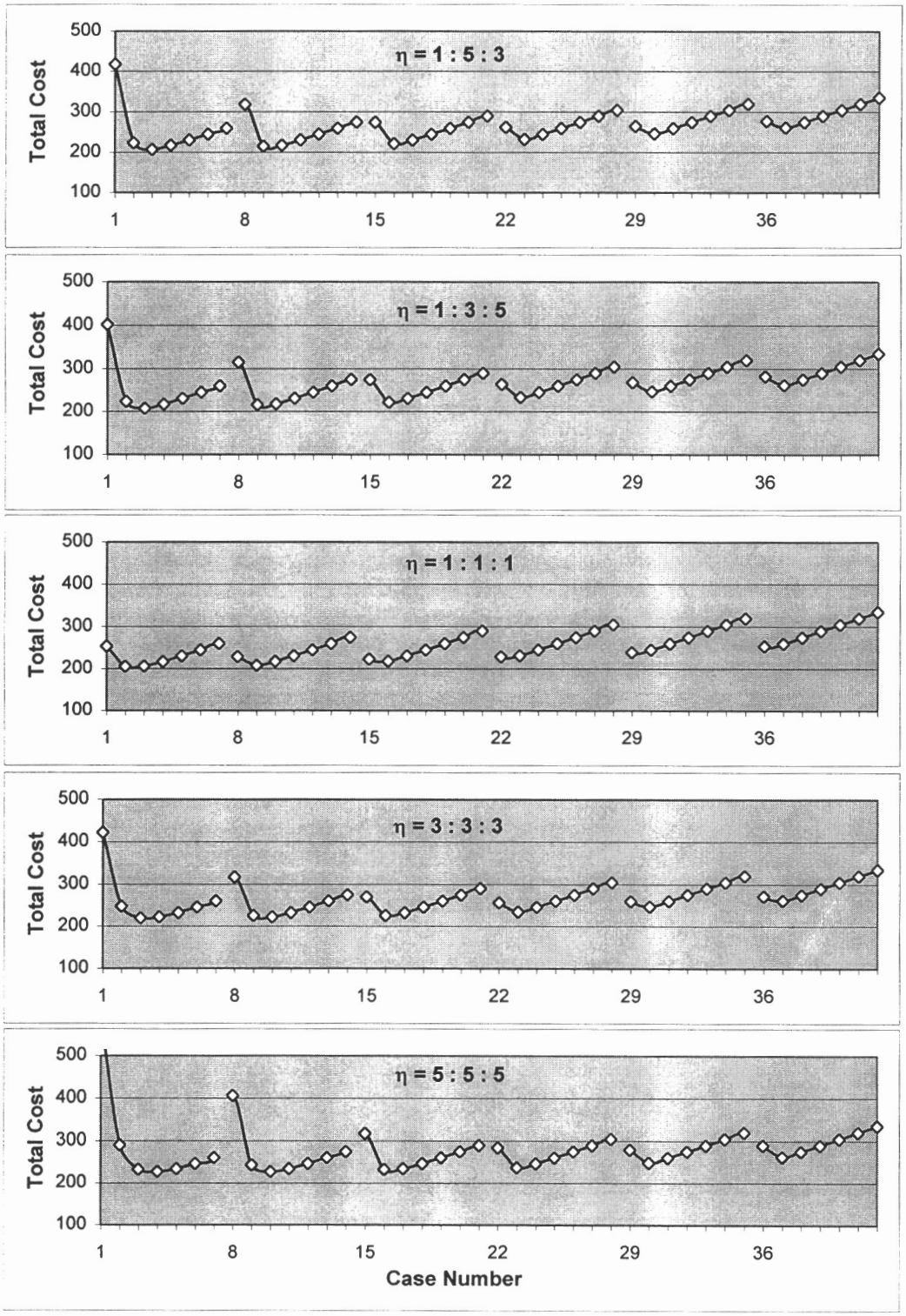

Figure 6.6 Total Cost of 10 ft Wall with Various η Ratios

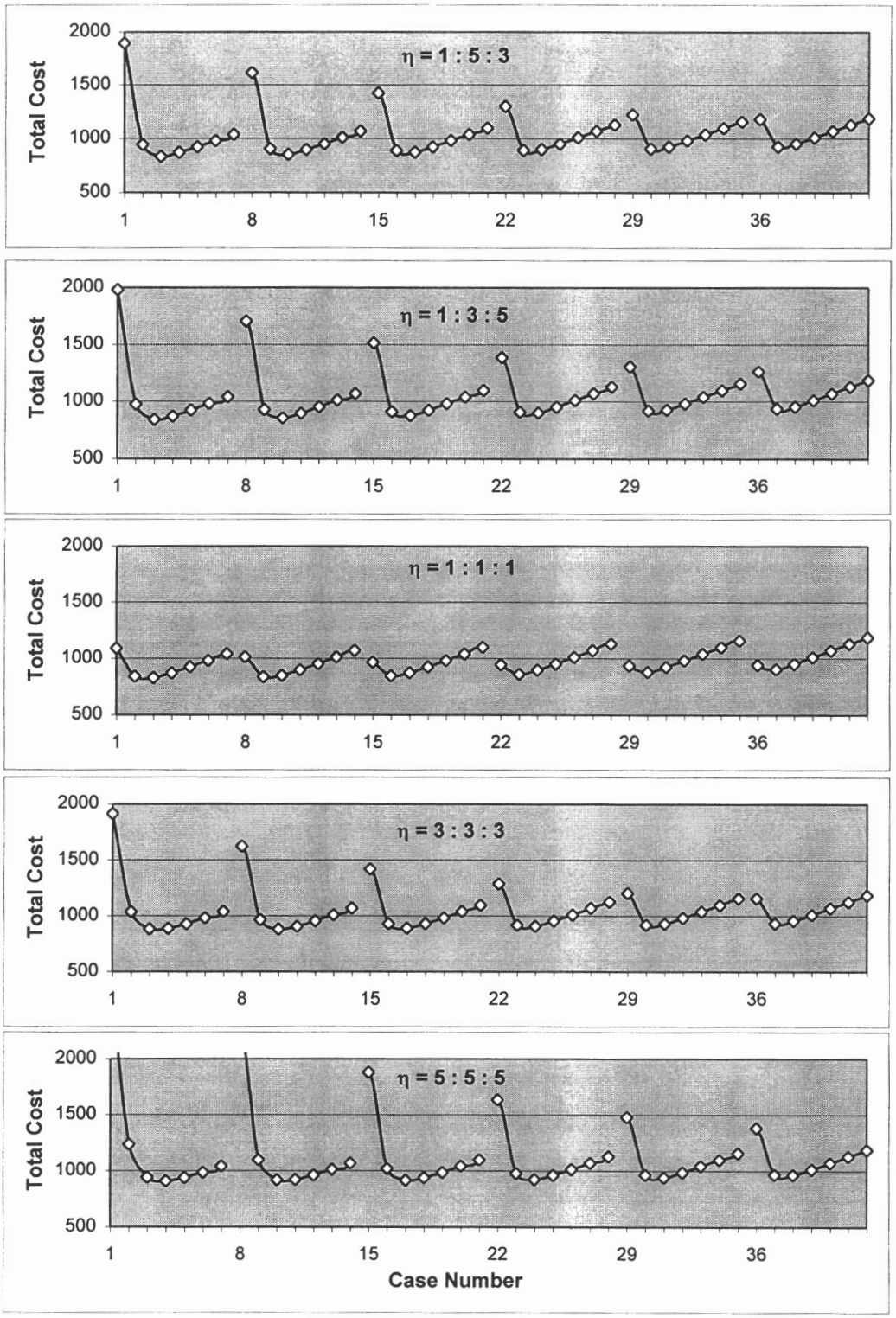

Figure 6.7 Total Cost of 20 ft Wall with Various η Ratios

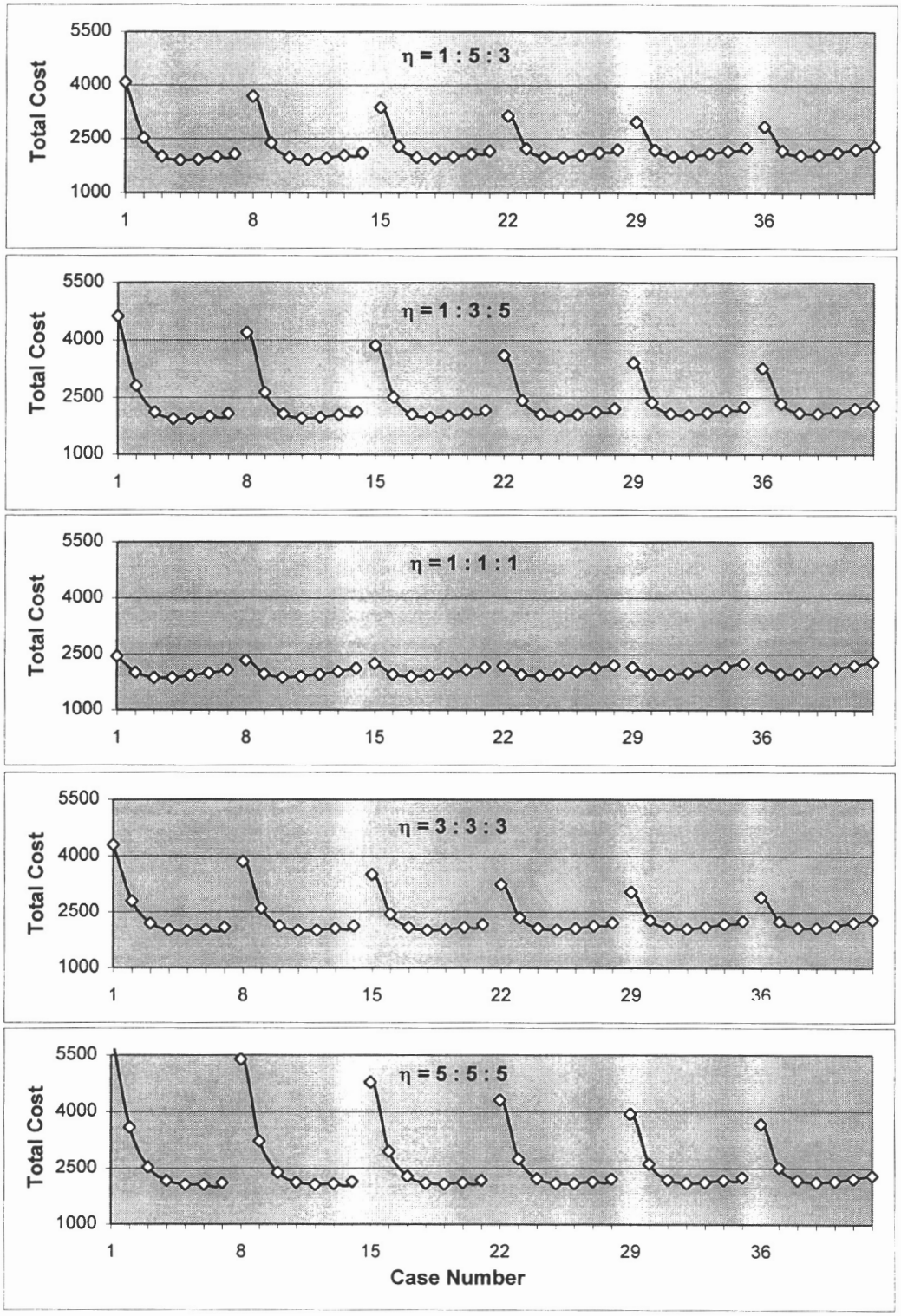

Figure 6. 8 Total Cost of 30 ft Wall with Various η Ratios

6.3.2 Optimum Design

Tables 6.5 to 6.8 presented earlier require additional explanation. They consist of six large groups classified by the top widths. Each group contains seven cases that have different base widths varied with a fixed increment. The shaded and bolded cases in the tables indicate the combinations of t and B which produce the lowest total cost in each group. The shaded and non-bolded cases in each group are those which produce the lowest total cost, while satisfying all the conventional design (ASD) criteria.

An interesting comparison can be made between Case 2, 3 and 4 in Group I of Table 6.7 for a 20 ft wall, which is a typical example. Even though the construction cost of Case 2 is lower than the other two cases, it produces the highest total cost. The probable failure cost ($P_f * CF$) of Case 4 is smaller than the other two, but the case yields higher total cost than Case 3 due to the higher construction cost. Case 3 has the lowest total cost, and therefore it is selected as the reliabilistic optimum design.

Through a similar procedure, it is found that the base widths that produce the optimum design for each wall height range from 0.4H to 0.5H. For example, the

optimum base width of 5 ft wall is 0.4H (2.0 ft) for all top widths, and the optimum base width of 30 ft wall is about 0.47H (14 ft). Table 6.9 summarizes the top widths and the base widths of the optimum design for all heights of the wall and for all relative cost factors.

The change of the top width was shown not to significantly affect the total cost. Even though the case with the narrowest top width generated the lowest total cost, the minimum top width of H/12 should be used for construction purpose in actual design of the wall. The top width in Case 43 in each height of the wall is close to H/12, i.e., 0.42 ft for 5 ft wall, 0.75 ft for 10 ft wall, 1.5 ft for 20 ft wall and 2.5 ft for 30 ft wall.

6.4 SUMMARIES

Forty-two cases with various combinations of top and base widths for four different wall heights (total 168 walls) have been evaluated to find the probabilistically optimized design. Analysis results were tabulated and graphed to observe the influence of the wall dimensions to the safety factor and the safety index. The base width proved to be very influential while the top width almost not at all. As the base width increases, the safety factors and the safety indices

Table 6.9 B/H Ratio of the Optimum Design

H (ft)	Group No.	t (ft)	B/H				
			η = 1:5:3	η = 1:3:5	η = 1:1:1	η = 3:3:3	η = 5:5:5
5	I	0.50	**0.40**	0.40	0.40	0.40	0.45
	II	0.75	**0.40**	0.40	0.40	0.40	0.40
	III	1.00	**0.40**	0.40	0.35	0.40	0.40
	IV	1.25	**0.40**	0.40	0.35	0.40	0.40
	V	1.50	**0.40**	0.40	0.35	0.35	0.40
	VI	1.75	**0.40**	0.40	0.35	0.35	0.40
10	I	0.50	**0.45**	0.45	0.40	0.45	0.50
	II	1.00	**0.40**	0.40	0.40	0.45	0.45
	III	1.50	**0.40**	0.40	0.40	0.40	0.40
	IV	2.00	**0.40**	0.40	0.35	0.40	0.40
	V	2.50	**0.40**	0.40	0.35	0.40	0.40
	VI	3.00	**0.40**	0.40	0.35	0.40	0.40
20	I	1.00	**0.45**	0.45	0.45	0.45	0.50
	II	1.50	**0.45**	0.45	0.40	0.45	0.45
	III	2.00	**0.45**	0.45	0.40	0.45	0.45
	IV	2.50	**0.40**	0.45	0.40	0.45	0.45
	V	3.00	**0.40**	0.40	0.40	0.40	0.45
	VI	3.50	**0.40**	0.40	0.40	0.40	0.45
30	I	1.00	**0.467**	0.467	0.467	0.500	0.500
	II	1.50	**0.467**	0.467	0.433	0.467	0.500
	III	2.00	**0.467**	0.467	0.433	0.467	0.500
	IV	2.50	**0.467**	0.467	0.433	0.467	0.467
	V	3.00	**0.433**	0.467	0.433	0.467	0.467
	VI	3.50	**0.433**	0.467	0.400	0.433	0.467

increase. However, it was observed that there was no direct relationship between the safety factor and the safety index.

The effect of the relative cost factors (η_i) was examined by using five different combinations of the factor. It was revealed that these factors did not significantly affect the total costs of the optimum design, because the probability of failure of the optimum design is generally low and accordingly the probable failure cost becomes relatively small.

The ratios of the base width to the wall height (B/H) which produce the optimum design range from 0.4 to 0.47. This compares well with the range from 0.42 to 0.58 as shown in Fig. 2.21 (Clayton and Militisky, 1986).

As mentioned in Section 6.2, the widths of t and B in Case 43 were determined to closely meet the ASD criteria. It is observed that the total cost of Case 43 is very close to that of the case which gives the reliabilistic optimum design. From this, one may draw a conclusion that the conventionally optimized design results in the probabilistically optimized design, as far as this study is concerned.

Chapter 7
CONCLUSIONS

7.1 GENERAL

A retaining wall is subject to various limit states such as sliding, overturning and bearing capacity limit states, and it can fail by any one of them. Since a great deal of uncertainty is involved in the analysis of the limit states, the use of deterministic conventional safety factors may produce a misleading result.

The main objective of this study is to develop a procedure for the optimum design of a retaining wall by using the reliability theory. Four typical gravity retaining walls with different heights were selected in this study. The walls were designed first to satisfy the conventional design criteria, and later the safety indices inherent in the walls were computed by using Advanced First Order Second Moment method. With the safety indices, the probabilities of failure for the three limit states were estimated and the probabilistic optimized design could be achieved using the probability of failure. The influence of the coefficient of variation on the probability of failure was investigated. The ratios of base width to height of the wall which lead to the optimum design were obtained through a parametric study.

7.2 NEW FINDINGS

This section will briefly summarize the new findings achieved through this study. The new findings include a new trend in the wall failure modes revealed in the survey, the safety indices inherent in the conventional design, the concept of probabilistic optimum design employing the probable cost of failure, and the ratio of base width to height of the wall for the optimum design.

7.2.1 Survey on Highway Bridges

A survey was conducted in 1945 by Peck et al (1948) to obtain information on unsatisfactory performance of railroad bridge abutments and retaining walls. Forty-eight years later a survey for this study was distributed to the departments of transportation of fifty states and the District of Columbia to gather similar type of information on highway bridge abutments and retaining walls

The survey conducted by Peck et al (1945) received about 52 percent of responses and the survey conducted for this study in 1993 received 73 percent of replies. The average height of the walls in the railroad survey is 25 ft and the one in highway survey is 15 ft. The ratios of tolerable movement to wall height in the railroad survey and the highway survey are closely matched as $\Delta/H = 0.01$.

All of the failures reported in the 1945 survey were associated with clay soil. However, the 1993 survey indicated an almost equal percentage of unsatisfactory behavior in granular and clay soils. This phenomenon can be explained in two ways. First, designers may have been aware, since the railroad survey, that the safety margin was larger in sand than in clay and took measures to reduce the conservatism. On the other hand, the safety factor in clay soils may have been considered insufficient and it might have been increased. In any case, the 1993 survey result showed that more unsatisfactory behavior in sand, gravel and rock was reported than in the 1945 survey.

7.2.2 Inherent Safety Indices in the Conventional Design of Wall

Safety indices inherent in gravity retaining walls were investigated. The three limit states of sliding, overturning and bearing capacity were included in the analysis for the walls with different heights of 5 ft, 10 ft, 20 ft and 30 ft. The walls were initially designed according to a conventional method (ASD) and then analyzed by the reliability method (Advanced FOSM) to estimate the inherent safety indices.

A detailed illustration was provided on the procedure for obtaining the safety indices using Advanced FOSM method. The inherent safety indices for the sliding limit state and the overturning limit state were consistent throughout the various wall heights. The estimated safety index of the sliding limit state was about 2.15 for a safety factor of 1.55, and the safety index of the overturning was 3.59 for a safety factor of 2.0. However, the inherent safety indices for the bearing capacity limit state varied from 3.75 (H = 30 ft) to 2.43 (H = 5 ft) for a safety factor of 2.5. The reason why the different safety indices were obtained is that different mean values and standard deviation values of the friction angle of the foundation soil were used to closely match all ASD criteria simultaneously.

7.2.3 Probabilistic Optimum Design

The primary goal in the conventional optimum design is to minimize the initial construction cost. Since the conventional design method does not directly reflect the randomness of design parameters, a more rational optimum method which employed the probability concept was introduced. The probable cost of failure was included in the total expected cost of the wall to find the probabilistic optimum design.

A parametric study was conducted to investigate the effect of various COV values of the design parameters. Three COV values of 0.05, 0.10 and 0.15 were used in the study, because the typical COV values recommended by many researchers for the design parameters employed in this study fell within the range. The overturning limit state appeared to be the most sensitive to the change of COV values and the sliding limit state proved to be the least sensitive. The internal friction angles of the backfill and the foundation soil were found to be the most influential random variables which affected the probability of failure.

Three design cases were presented to illustrate the procedure of the probabilistic optimum design. The total expected cost is the sum of construction cost and the probable cost of failure of each limit state. The relative costs of failure for sliding, overturning and bearing were assumed to be one, five and three times the cost of construction, respectively. The illustration proved that the design which produced the minimum construction cost did not necessarily yield the minimum total expected cost. With a more precise set of the relative costs of failure for each limit state, a designer can achieve a more reasonable probabilistic optimum designs.

7.2.4 B/H Ratio for Optimum Design

A total of 168 walls with various combinations of top and base widths were examined to find the B/H ratio that produces the reliabilistic optimum design. The sensitivity of the dimension change to the safety factor and the safety index was investigated. The change in the top width was found to be less influential to the optimum design than the base width change. As the base width changes, the safety factor and the safety index increase. However, the rate of increase of the two values were found to be different from one limit state to another, which implies that there is no direct mathematical relationship between the two quantities.

The influence of the relative cost factors (η_i) was studied by employing five different combinations of the factor. These factors were found not to affect the total costs of the optimum design due to their relatively small probable failure costs.

The ratios of the base width to the wall height (B/H) for the optimum design were discovered to be between 0.4 and 0.5. It should be pointed out that the ratios of B/H for the reliabilistic optimum design happen to be very close to those of the conventionally optimized design.

7.3 FUTURE STUDY

A gravity retaining wall was employed in this study because there is general agreement in the analysis to estimate the earth pressure applied to the structure. The application of the probabilistic procedure to find an optimum design can be extended to more complicated structures such as a cantilever retaining wall or an innovative wall.

The B/H ratios which lead to the optimum design were found to range from 0.4 to 0.47. It may be interesting to check whether a different optimum B/H ratio would be obtained when different mean values and COV values of the design parameters are used.

The slope stability limit state may have to be included in order to make this design optimization complete. The inclusion of actual case histories would add to the practicality of the results.

Since the probabilistic approach requires a large number of computations and a considerable knowledge on the reliability theory, many engineers are reluctant to take advantage of it. It is wished that this study may stimulate further research on the application of the reliability-based design.

REFERENCES

American Association of State Highway and Transportation Officials (1989) "Standard Specifications for Highway Bridges," Fourteen Edition, AASHTO, Washington, D.C.

Barker, R.M., Duncan, J.M., Rojiani, K.B., Ooi, P.S.K., Tan, C.K. and Kim, S.G. (1991), "Manuals for the Design of Bridge Foundations," NCHRP Report 343, Transportation Research Board, Washington, D.C.

Bowles, J.E. (1975) "Spread Footings," Chapter 15 in Foundation Engineering Handbook Edited by Winterkorn H. and Fang H.Y., Van Nostrand Reinhold Co., New York, pp 481-503.

Bowles, J.E. (1988) "Foundation Analysis and Design," Fourth Edition, McGraw-Hill Publication Co., pp 304-579.

Brown, W.G. (1964) "Difficulties Associated with Predicting Depth of Freeze or Thaw," Canadian Geotechnical Journal, Vol. 1, No. 4, pp 215-226.

Canadian Geotechnical Society (1985) "Canadian Foundation Engineering Manual", 2nd Edition, Bitech Publishers Ltd., 460 pp.

Caquot, A. and Kerisel, J. (1948) "Tables for the Calculation of Passive Pressure, Active Pressure and Bearing Capacity of Foundations," Gauthier-Villars, Imprimeur-Libraire, Libraire du Bureau des Longitudes, de L'Ecole Polytechnique, Paris, 120 pp.

Carroll, R.G., Jr., and Murphy, J.C. (1985) "Drainage Objective: Prefabricated Drainage Composites," Geotechnical Fabrics Report, Vol 3, NO. 3, pp 14-18.

Clausen, C.J.F. and Johansen, S. (1972) "Earth Pressures Measured Against a Section of a Basement Wall," Proceeding, 5th European Conference on SMFE, Madrid, pp 515-516.

Clayton, C.R.I. and Milititsky, J. (1986) "Earth Pressure and Earth-Retaining Structures," Surrey University Press, Glasgow, 300 pp.

Clough, G.W. and Duncan, J.M. (1971) "Finite Element Analyses of Retaining Wall Behavior," Journal of Soil Mechanics and Foundations Division, ASCE, Vol. 97, SM12, pp 1657-1673.

Clough, G.W. and Duncan, J.M. (1991) "Foundation Engineering Handbook" 2nd Edition, edited by H.Y. Fang, Van Nostrand Reinhold, New York, NY, pp 223-235.

Danish Geotechnical Institute (1978) "Code of Practice for Foundation Engineering", Danish Geotechnical Institute, Copenhagen, Denmark, Bulletin No. 32, p 52.

D'Appolonia, Inc. (1989) "Recommended Specifications for the Design of Foundations, Retaining Walls and Substructures," Drafted Report for NCHRP 12-35, Prepared for Transportation Research Board, Washington, D.C.

Duncan, J.M., Clough, G.W. and Ebeling, R.M. (1990) "Behavior and Design of Gravity Earth Retaining Structures," Proceeding of Conference on Design and Performance of Earth Retaining Structures, ASCE, Cornell University, Ithaca, New York, pp 251-277.

Elms, D.G. and Martin, G.R. (1979) "Factors involved in the Seismic Design of Bridge Abutments," Applied Technology Council Workshop on Earthquake Resistance of Highway Bridges, ATC-6-1, pp 230-252.

Elms, D.G. and Richards, R. (1990) "Seismic Design of Retaining Walls," Proceeding of Conference on Design and Performance of Earth Retaining Structures, ASCE, Cornell University, Ithaca, New York, pp 854-871.

Esteva and Rosenblueth (1972) "Use of Reliability Theory in Building Codes", Statistics and Probability in Civil Engineering, Hong Kong University Press, distributed by Oxford University Press, London.

Geotechnical Control Office (1982) "Guide to Retaining Wall Design," Geoguide 1, Engineering Development Department, Hong Kong. Available from: U.S. Army Engineer Waterways experiment Station, P.O. Box 631, Vicksburg, MS 39180.

Grivas, D.A. and Souflis, C. (1982) "Probabilistic Safety Analysis of Earth Retaining Structures During Earthquakes," Report No. NSF/CEE-82030, National Science Foundation, Washington, DC, July, 136 pp.

Harr, M.E. (1977) "Mechanics of Particulate Media, A Probabilistic Approach," McGraw-Hill, Inc., New York.

Höeg, K. and Murarka, R.P. (1974) "Probabilistic Analysis and Design of a Retaining Wall," Journal of the Geotechnical Engineering Division, ASCE, Vol. 100, GT3, March, pp 349-366.

Holtz, W.G. and Gibbs, H.J. (1956) "Engineering Properties of Expansive Clays", Transactions, ASCE, Vol. 120.

Huntington, W.C. (1957) "Earth Pressures and Retaining Walls," John Willey and Sons, Inc. New York, 534 pp.

Jaky, J. (1944) "The Coefficient of Earth Pressure At-Rest," Journal for Society of Hungarian Architects and Engineers, Budapest, Hungary, Oct., pp 355-358.

Kulhawy, F.H., Trautmann, C.H., Beech, J.F., O'Rourke, T.D., and McGuire, W. (1983) "Transmission Line Structure Foundations for Uplift-Compression Loading", EPRI Report EL-2870, Electric Power Research Institute.

Laursen, E.W. and Toch, A. (1956) "Scour around Bridge Piers and Abutments," Iowa Highway Research Board, Bulletin 4.

Mayne, P.W. and Kulhawy, F.H. (1982) "K_O-OCR Relationships in Soils," Journal of the Geotechnical Engineering, ASCE, Vol. 108, No. GT6, June, pp 851-872.

Meyerhof, G.G. (1953) "The Ultimate Bearing Capacity of Foundations under Eccentric and Inclined Loads", Proc., 3rd International Conference on Soil Mechanics and Foundation Engineering, Zurich, Vol. 1, pp 440-445.

Meyerhof, G.G. (1970) "Safety Factors in Soil Mechanics," Canadian Geotechnical Journal, Toronto, Ontario, Canada, Vol. 7, No. 4, Nov., pp 349-355.

Meyerhof, G.G. (1984) "Safety Factors and Limit States Analysis in Geotechnical Engineering," Canadian Geotechnical Journal, Toronto, Ontario, Canada, Vol. 21, pp 1-7.

Munfakh, G.A. (1990) "Innovative Earth Retaining Structures: Selection, Design & Performance," Proceeding of Conference on Design and Performance of Earth Retaining Structures, ASCE, Cornell University, Ithaca, New York, June, pp 85-118.

Newman, M. (1976) "Standard Cantilever, Retaining Walls," McGraw-Hill Publication Co., 648 pp.

New Zealand Ministry of Works and Development (1979) "Retaining Wall Design Notes," Wellington, New Zealand, July, 43 pp.

Peck, R.B., Hansen, W.E. and Thornburn, T.H. (1974) "Foundation Engineering," Second Edition, John Wiley and Sons Inc., NY, 514 pp.

Schnore, A.R. (1990) "Selecting Retaining Wall Type and Specifying Proprietary Retaining Walls in NYSDOT Practice," Proceeding of Conference on Design and Performance of Earth Retaining Structures, ASCE, Cornell University, Ithaca, New York, June, pp 119-124.

Schultze, E (1972) "Frequency Distributions and Correlations of Soil Properties," Statistics and Probability in Civil Engineering, Hong Kong University Press (Hong Kong International Conference), distributed by Oxford University Press, London.

Seed, H.B. and Whitman, R.V. (1970) "Design of Earth Retaining Structures for Dynamic Loads," ASCE Speciality Conference on Lateral Stresses in the Ground and Earth Retaining Structures, Cornell University, pp 103-147.

Seelye, E.E. (1956) "Foundations: Design and Practice," John Wiley and Sons, Inc., NY.

Sherif, M.A., Ishibashi, I. and Lee, C.D. (1982) "Earth Pressures Against Rigid Retaining Walls," Journal of Geotechnical Engineering Division, ASCE, Vol. 108, GT5, pp 679-695.

Sibley, E.A. (1967) "Backfill Adjacent to Structures," Proceedings of the Montana Conference on Soil Mechanics and Foundation Engineering, Department of Civil Engineering, Montana State University, Bozeman, MT. Available from: U.S. Army Engineer Waterways experiment Station, P.O. Box 631, Vicksburg, MS 39180.

Singh, A (1972) "How Reliable is the Factor of Safety in Foundation Engineering?" International Conference of Statistics and Probability in Civil Engineering, Hong Kong University Press (Hong Kong International Conference), distributed by Oxford University Press, London.

Skempton, A.W. (1951) "The Bearing Capacity of Clays", Proc. of the Building Research Congress, London, England, Vol. 1, pp 180-189.

Snyder, R. and Moses, F. (1978) "Load Factor Design for Substructures and Retaining Walls," FHWA Report No. 79-S0862, Nov, 153 pp.

Sowers, G.F. (1962) "Shallow Foundations," Chapter 6 in Foundation Engineering edited by Leonards, G.A., McGraw-Hill Publication Co., pp 525-632.

Tschebotarioff, G.P. (1962) "Retaining Structures," Chapter 5 in Foundation Engineering edited by Leonards, G.A., McGraw-Hill Publication Co., pp 438-524.

Terzaghi, K. (1934) "Retaining Wall Design for Fifteen-Mile Falls Dam," Eng. News Record, May, pp 632-636.

Terzaghi, K. and Peck, R.B. (1967) "Soil Mechanics in Engineering Practice," John Wiley and Sons Inc., NY, pp 729.

U.S. Army Corps of Engineers (1949) "Report on Frost Penetration," Addendum No. 1, 1945-47, Corps of Engineers, US Army, New England Division, Boston,.

U.S. Army Corps of Engineers (1989) "Engineering and Design Retaining and Flood Walls," Manual EM No. 1110-2-2502, Washington, D.C. Sept.

U.S. Dept. of Navy (1982) "NAVFAC DM7.1, Soil Mechanics," Naval Facilities Engineering Command, VA, May, 348 pp.

U.S. Dept. of Navy (1982) "NAVFAC DM7.2, Foundations and Earth Structures," Naval Facilities Engineering Command, VA, May, 244 pp.

Wu, T.H. (1975) "Retaining Walls," Chapter 12 in Foundation Engineering Handbook Edited by Winterkorn H. and Fang H.Y., Van Nostrand Reinhold Co., New York, pp 402-417.

APPENDIX

(First Letter)

Virginia Tech
VIRGINIA POLYTECHNIC INSTITUTE
AND STATE UNIVERSITY

The Charles Edward Via, Jr.
Department of Civil Engineering

Blacksburg, Virginia 24061-0105
(703) 231-6635 Fax: (703) 231-7532
Telex: (910) 333-1861

Mr. Steve Bradford
Chief Bridge Engineer
Dept. of Transp. & Public Facilities
3132 Channel Drive
Juneau, AK 99811

Dear Mr. Bradford:

I recently served as a principal investigator for the AASHTO-sponsored National Cooperative Highway Research Program (NCHRP) Project 24-4, "Load Factor Design Criteria for Highway Structure Foundations." The results of this project have been published in NCHRP Report 343, Manual for Design of Bridge Foundations, December 1991.

Since the completion of that study, a number of questions have been raised concerning retaining walls and abutments and their failure modes. The primary question is, "Do they ever fail?" (where failure is defined as no longer able to perform its intended function). And if they do fail, "How do they fail? Sliding? Overturning? Bearing? Slope Stability? Drainage? Structural? Movement?"

It would be most helpful in preparing design specifications to know the problem areas, if any, so that attention can be focused in the direction of most importance. For the information to be of benefit to the largest audience, I believe it must reflect the collective experience of bridge engineers across the United States, and not be just one person's opinion. Therefore, we (I admit I have a graduate student working with me) need your input and would appreciate your completing the enclosed questionnaire, or refer it to the person in your organization who would best answer it. Results of this survey will be sent to the person identified as the respondent at the tip of the questionnaire.

If you have any questions, or if you need more information, please do not hesitate to let me know. You can reach me by phone at (703) 231-7143.

Truly yours,

RM Barker

Richard M. Barker
Professor of Civil Engineering

RETAINING WALL AND ABUTMENT QUESTIONNAIRE

Name of Respondent _____

Mailing Address _____

_____

_____

_____

Telephone _____

Please answer the following questions to the best of your ability.

1.a: How many bridges are there in your jurisdiction ? _____

b: Approximately how many retaining walls, not associated with abutments, are there ?

_____

2. In the historical records of your department (going back to 19____), how many bridge abutments or retaining walls in the following categories have exhibited unsatisfactory behavior ? (For a description of types of unsatisfactory behavior, see next page)

	Abutments	Retaining Walls
Gravity		
Cantilever		
Mechanically Stabilized Earth		
Crib		
Gabion		
Other		

3. For as many of the above abutments and walls as you have information, please complete the next page.

4. Could we call you if we need more information on your response ? Yes ___ No ___
If yes, please include telephone number above.

Please return this questionnaire and survey sheets to:

Professor Richard M. Barker
Department of Civil Engineering
200 Patton Hall
Virginia Polytechnic Institute and State University
Blacksburg, VA 24061-0105
Telephone: (703) 552-0540 Fax: (703) 231-7532

Retaining wall and abutment questionnaire

Note: If more than seven cases, the following form should be duplicated.

Case No. (A-xx for abutment, W-xx for wall)	Year built	Year out of service	Wall height (ft)	Type of unsatisfactory behavior (check all that apply)						
				Movement soon after construction; stable afterward	Progressive outward or tilting movement	Settlement of backfill	Complete failure		Other (describe on extra sheet)	Earth-quake related ?
							Overturned	Structure broken		yes / no

Case No.	Observed movement of top of abutment or wall (inches)				Foundation type			
	Horizontal		Vertical		Spread footing	Pile	Drilled Shaft	Other
	forward	backward	downward	upward				

Case No.	Backfill material			Foundation material			
	Sand, gravel	Clay	Unknown	Sand, gravel	Rock	Clay	Unknown

A sketch of the failed wall or abutment would be helpful in interpreting this data.

If you would not mind including one for as many cases as you can, it would certainly be appreciated. Thank you.

-RMB-

(Follow-up Letter)

Virginia Tech
VIRGINIA POLYTECHNIC INSTITUTE
AND STATE UNIVERSITY

The Charles Edward Via, Jr.
Department of Civil Engineering

Blacksburg, Virginia 24061-0105
(703) 231-6635 Fax: (703) 231-7532
Telex: (910) 333-1861

August 19, 1993

Mr. Steve Bradford
Chief Bridge Engineer
Dept. of Transp. & Public Facilities
3132 Channel Drive
Juneau, AK 99811

Dear Mr. Bradford:

Earlier in the summer, a questionnaire on abutments and retaining walls was mailed to all of the state bridge engineers. We have received responses from over one-half of the states, but would like to make the survey as complete as possible. Therefore, we are enclosing another copy of the questionnaire and asking that it be completed to the best of your knowledge.

If your agency has not experienced any problems with abutments or retaining walls, that is important information, too, and all you need to do is return the first page of the questionnaire. If the second page does not fit your circumstances, feel free to respond in whatever manner you are comfortable with.

Realizing that summer is a busy time for bridge engineers, we have extended the deadline for response to the questionnaire to 17 September 1993. If you have any questions, you can reach me at 703-231-7143. Thank you.

Truly yours,

RM Barker

Richard M. Barker
Professor of Civil Engineering

RMB/ac

VITA

John Sang Kim was born in Chonbuk, South Korea on Feb. 4, 1961. He started his college education at Han Yang University in Seoul, Korea where he received a Bachelor of Science in Architectural Engineering in March, 1983. A few months later, he came to the United States to continue his education and entered California Polytechnic State University in Pomona. He majored in Civil Engineering specializing structures and received a Master's degree in June of 1986.

He wanted to pursue the doctoral degree and was admitted to Virginia Polytechnic Institute and State University in Blacksburg. During his study at VA Tech, he was involved in a NCHRP Project 24-4 as a research assistant and a few industrial projects as a personal consultant to Dr. Richard M. Barker. Currently, he is employed to Virginia Department of Transportation, where he had a summer internship in 1989 and rejoined as a full-time bridge designer in July, 1994.

He is happily married to Eunice Kim who likes to cook and enjoys playing organ at Blacksburg Baptist Church as an organist. The author also has a son who never spares the heart-melting smile to his dad.